UNIVERSIDADE FEDERAL DO PARANÁ

BEATRIZ DE CARVALHO PATO VILA

ELECTRICAL AND MECHANICAL CARDIAC CONDUCTION TIMES AND DYSYNCHRONY IN DOGS WITH MYXOMATOUS MITRAL VALVE DISEASE AND HEALTHY DOGS

CURITIBA
2024

BEATRIZ DE CARVALHO PATO VILA

ELECTRICAL AND MECHANICAL CARDIAC CONDUCTION TIMES AND DYSYNCHRONY IN DOGS WITH MYXOMATOUS MITRAL VALVE DISEASE AND HEALTHY DOGS

Tese apresentada ao Programa de Pós-graduação em Ciências Veterinárias, setor de Ciências Agrárias, Universidade Federal do Paraná, como requisito parcial à obtenção do título de doutor em Ciências Veterinárias.

Orientador: Prof. Dr. Marlos Gonçalves Sousa

CURITIBA
2024

DADOS INTERNACIONAIS DE CATALOGAÇÃO NA PUBLICAÇÃO (CIP)
UNIVERSIDADE FEDERAL DO PARANÁ
SISTEMA DE BIBLIOTECAS – BIBLIOTECA DE CIÊNCIAS AGRÁRIAS

Vila, Beatriz de Carvalho Pato
Electrical and mechanical cardiac conduction times and dysynchrony in dogs with myxomatous mitral valve disease and healthy dogs / Beatriz de Carvalho Pato Vila. – Curitiba, 2024.
1 recurso online: PDF.

Tese (Doutorado) – Universidade Federal do Paraná, Setor de Ciências Agrárias, Programa de Pós-Graduação em Ciências Veterinárias.
Orientador: Prof. Dr. Marlos Gonçalves Sousa

1. Cardiologia veterinária. 2. Cães - Doenças. 3. Insuficiência cardíaca. 4. Arritmia. I. Sousa, Marlos Gonçalves. II. Universidade Federal do Paraná. Programa de Pós-Graduação em Ciências Veterinárias. III. Título.

Bibliotecária: Ana Camila Quaresma Moura CRB-9/2212

TERMO DE APROVAÇÃO

Os membros da Banca Examinadora designada pelo Colegiado do Programa de Pós-Graduação CIÊNCIAS VETERINÁRIAS da Universidade Federal do Paraná foram convocados para realizar a arguição da tese de Doutorado de **BEATRIZ DE CARVALHO PATO VILA** intitulada: **ELECTRICAL AND MECHANICAL CARDIAC CONDUCTION TIMES AND DYSYNCHRONY IN DOGS WITH MYXOMATOUS MITRAL VALVE DISEASE AND HEALTHY DOGS**, sob orientação do Prof. Dr. MARLOS GONÇALVES SOUSA, que após terem inquirido a aluna e realizada a avaliação do trabalho, são de parecer pela sua APROVAÇÃO no rito de defesa.

A outorga do título de doutora está sujeita à homologação pelo colegiado, ao atendimento de todas as indicações e correções solicitadas pela banca e ao pleno atendimento das demandas regimentais do Programa de Pós-Graduação.

CURITIBA, 08 de Outubro de 2024.

Assinatura Eletrônica
09/10/2024 08:26:10.0
MARLOS GONÇALVES SOUSA
Presidente da Banca Examinadora

Assinatura Eletrônica
10/10/2024 17:31:19.0
MATHEUS MATIOLI MANTOVANI
Avaliador Externo (UNIVERSIDADE FEDERAL DE UBERLÂNDIA)

Assinatura Eletrônica
09/10/2024 09:35:49.0
AFONSO CASSA REIS
Avaliador Externo (CENTRO UNIVERSITARIO MAURICIO DE NASSAU)

Assinatura Eletrônica
09/10/2024 09:37:53.0
RUTHNÉA APARECIDA LÁZARO MUZZI
Avaliador Externo (UNIVERSIDADE FEDERAL DE LAVRAS)

Assinatura Eletrônica
09/10/2024 07:57:06.0
GUSTAVO LENCI MARQUES
Avaliador Externo (UNIVERSIDADE FEDERAL DO PARANÁ - UFPR)

AGRADECIMENTOS

À Deus, por me dar saúde, por me cercar de pessoas iluminadas, e por permitir que eu seguisse meu sonho.

Aos meus pais e meu irmão - José Antonio, Sonia e Guilherme - por permanecerem ao meu lado nos melhores e piores momentos, por me ensinarem a acreditar em mim mesma desde pequena, por me apoiarem em todas as situações e por me darem todo o amor do mundo. Devo tudo à vocês.

Ao meu orientador, professor Marlos, por todas oportunidades que já me deu, por acreditar no meu potencial, e sempre me dar um empurrãozinho pra eu ir além do que eu achava que conseguiria. Serei eternamente grata por todo conhecimento, paciência, incentivo e acolhimento.

Aos meus avós - Teresinha, Aloísio, Alice e Atilio – por serem a base de tudo, por terem lutado tanto pela nossa família, e por me guiarem sempre.

Ao meu padrinho e à minha madrinha, Waldir e Glauce, por serem ombro amigo, suporte e por me darem força em todas as vezes que precisei.

Aos membros da minha banca de qualificação e de defesa do doutorado, pela gentileza em terem aceitado o nosso convite, e pela disponibilidade de tempo e energia em nos ajudar a lapidar esta tese. Com certeza a bagagem de conhecimento de vocês vai aprimorar nosso trabalho.

A todos os meus cardiofriends queridos, por não me deixarem desistir, por me presentearem com alegria, leveza, amizade verdadeira, empatia, cafés, conversas e carinho.

Aos tutores e pacientes que participaram do meu projeto, pela confiança no meu trabalho e por fazerem parte deste sonho.

A todos os membros do Laboratório de Cardiologia Comparada da Universidade Federal do Paraná pelo companheirismo, parceria e ensinamentos.

“Acredite que você pode, assim você já está no meio do caminho.”

(Theodore Roosevelt)

RESUMO

A avaliação da heterogeneidade de ativação cardíaca é de importância crucial para a compreensão e manejo de doenças cardiovasculares, pois alterações na ativação elétrica e mecânica do coração podem sinalizar a progressão de condições patológicas e influenciar o prognóstico dos pacientes. Em humanos, alguns índices de ativação têm se mostrado preditores significativos de mortalidade e da resposta à terapia de ressincronização cardíaca, destacando seu valor na prática clínica. No entanto, o conhecimento sobre a aplicação desses conceitos na espécie canina é ainda limitado e necessita de mais investigação, especialmente considerando a alta prevalência de doenças cardíacas como a degeneração mixomatosa da valva mitral (DMVM) em cães. Esta tese visa avaliar parâmetros de ativação elétrica e mecânica nos átrios e ventrículos de cães com DMVM e cães saudáveis, buscando identificar marcadores diagnósticos não invasivos que possam ser usados para avaliar a progressão da doença, identificar arritmias e monitorar o remodelamento cardíaco. O primeiro artigo investigou marcadores de ativação atrial, utilizando eletrocardiografia e ecocardiografia para medir tempos de condução e associá-los com arritmias, remodelamento e insuficiência cardíaca. Os resultados mostraram que índices de condução elétrica e mecânica foram eficazes na identificação de alterações cardíacas decorrentes da progressão da DMVM, revelando a utilidade desses marcadores na prática clínica para a avaliação de cães com esta doença. Apesar de alguns índices apresentarem áreas sob a curva (AUC) elevadas, outros mostraram menor relevância clínica, o que enfatiza a necessidade de uma avaliação criteriosa dos marcadores em diferentes contextos. O segundo artigo focou nos marcadores de dissincronia e tempo de ativação ventricular, analisando como esses marcadores variam com os estágios da doença, remodelamento cardíaco, insuficiência cardíaca e arritmias. Os dados mostraram que, com a progressão da DMVM, houve um aumento nos tempos de ativação ventricular e na heterogeneidade mecânica, refletindo alterações significativas na condução elétrica e mecânica do coração. Alguns índices foram identificados como adequados para o diagnóstico de arritmias e para a identificação de corações dilatados ou com insuficiência cardíaca, oferecendo novos insights para a prática clínica veterinária. Em conclusão, a avaliação da heterogeneidade de ativação cardíaca em cães com DMVM revelou-se uma ferramenta valiosa para o monitoramento da progressão da doença e para a identificação de alterações estruturais e hemodinâmicas no coração. A integração de marcadores eletrocardiográficos e ecocardiográficos pode contribuir significativamente para a prática clínica e para o manejo de doenças cardiovasculares na espécie canina.

Palavras-chave: Atraso de condução; Índices eletromecânicos; Heterogeneidade de ativação; Arritmias; Insuficiência cardíaca

ABSTRACT

The assessment of cardiac activation heterogeneity is crucial for understanding and managing cardiovascular diseases, as changes in both electrical and mechanical activation of the heart can indicate the progression of pathological conditions and influence patient prognosis. In humans, certain activation indices have proven to be significant predictors of mortality and response to cardiac resynchronization therapy, highlighting their clinical value. However, knowledge about the application of these concepts to canines is still limited and requires further investigation, particularly considering the high prevalence of cardiac diseases such as myxomatous mitral valve degeneration (MMVD) in dogs. This thesis aims to evaluate electrical and mechanical activation parameters in the atria and ventricles of dogs with MMVD and healthy dogs, seeking to identify non-invasive diagnostic markers that can be used to assess disease progression, identify arrhythmias, and monitor cardiac remodeling. The first paper investigated atrial activation markers using electrocardiography and echocardiography to measure conduction times and correlate them with cardiac remodeling and heart failure (HF). The results showed that indices of mechanical and electrical atrial activation were effective in identifying cardiac abnormalities caused by the progression of MMVD, demonstrating the utility of these markers in clinical practice for evaluating dogs with this disease. While some indices presented high areas under the curve (AUC), others showed lower clinical relevance, emphasizing the need for a thorough evaluation of markers in different contexts. The second paper focused on ventricular activation time and dyssynchrony markers, analyzing how these markers vary with disease stages, cardiac remodeling, HF, and arrhythmias. The data revealed that with the progression of MMVD, there was an increase in ventricular activation times and mechanical heterogeneity, reflecting significant changes in both electrical and mechanical conduction of the heart. Some indices were identified as suitable for diagnosing arrhythmias and for identifying dilated hearts or those with HF, providing new insights for veterinary clinical practice. In conclusion, the assessment of cardiac activation heterogeneity in dogs with MMVD proved to be a valuable tool for monitoring disease progression and identifying structural and hemodynamic changes in the heart. The integration of electrocardiographic and echocardiographic markers can significantly contribute to clinical practice and the management of cardiovascular diseases in canines.

Keywords: Conduction delay; Electromechanical indices; Activation heterogeneity; Arrhythmias; Heart failure

SUMMARY

INTRODUCTION 11

REFERENCES 16

CHAPTER 1 – ATRIAL CONDUCTION TIMES IN HEALTHY DOGS AND DOGS WITH MYXOMATOUS MITRAL VALVE DISEASE* 25

ABSTRACT 26

INTRODUCTION/OBJECTIVES 28

ANIMALS, MATERIALS AND METHODS 30

RESULTS 36

DISCUSSION 41

LIMITATIONS 46

CONCLUSIONS 46

REFERENCES 47

FIGURE LEGENDS 83

SUPPLEMENTARY MATERIAL TABLES 92

CHAPTER 2 - VENTRICULAR ELECTRICAL AND MECHANICAL ACTIVATION TIMES AND DYSSYNCHRONY IN DOGS WITH MYXOMATOUS MITRAL VALVE DISEASE* 102

ABSTRACT 103

INTRODUCTION/OBJECTIVES 105

ANIMALS, MATERIALS AND METHODS 107

RESULTS 114

DISCUSSION 119

LIMITATIONS 124

CONCLUSION 125

REFERENCES 126

FIGURE LEGENDS 158

SUPPLEMENTARY MATERIAL TABLES 172
FINAL CONSIDERATIONS 180
VITA 182
REFERENCES 183
ANNEX 1 – CERTIFICATE FROM THE COMMITTEE ON ETHICS IN THE USE AND EXPERIMENTATION OF ANIMALS.....189

INTRODUCTION

The normal heart functions through a coordinated process that includes stimulation, excitation, conduction, contraction, and relaxation. Myocardial contraction, driven by myocardial excitation via electromechanical coupling, allows the heart to perform its pumping function. For this function to be effective, the heart relies on rhythmically synchronized contractions and relaxations. When myocardial lesions are present, they can cause electrical and/or mechanical dyssynchrony, leading to a decrease in ventricular pumping efficiency (Bristow et al., 2004).A synchronous cardiac activation sequence is required to maintain normal cardiac pump function. Cardiac synchrony applies to various anatomical levels: between the atria (interatrial), within the atria (intra-atrial), between the atria and ventricles (atrioventricular), between the ventricles (interventricular), and mainly within the ventricle (intraventricular) (Sweeney & Prinzen, 2006). Interventricular and intraventricular dyssynchrony have a relatively greater effect on ventricular pump function (Spartalis et al., 2017). In people, dyssynchrony is a significant contributor to heart failure (HF), a prognostic factor, and a powerful predictor of mortality in patients with HF (Bleeker et al., 2004; Dhingra et al., 2006; Spragg & Kass, 2006; Vernooy et al., 2003). However, in veterinary medicine there is still little information about cardiac dyssynchrony, especially when it comes to evaluating these indices as prognostic markers.

Electrical dyssynchrony and ventricular activation times can be interrogated by electrocardiography (ECG). A simple and easy example is the duration and morphology of QRS complex, which can be used as a prognostic marker. In a Doberman Pinscher population affected by dilated cardiomyopathy, a QRS >60 ms was associated with shorter survival times (Pedro et al., 2011). Similarly, in a study of dogs with rapid pacing-induced HF, increased QRS duration (≥ 100 ms) predicted an unsatisfactory recovery (Y. Wang et al., 2011). In symptomatic people with HF and reduced ejection fraction, the association of QRS with increased duration and a morphology of left bundle branch block represents an indication for cardiac resynchronization therapy (Glikson et al., 2021). However, the duration of QRS can neither distinguish between right- or left-sided conduction abnormalities nor between inter- and intraventricular dyssynchrony, which can be more accurately detected using precordial leads.

In people, precordial leads are extremely important for the diagnosis of bundle branch blocks and are also useful for studying right and left ventricle activation times.

In particular, R peak time (RPT) analysis in precordial leads is commonly used to differentiate right from left bundle blocks (Surawicz et al., 2009). This parameter is obtained by measuring the time between the beginning of the QRS complex (Q or R-wave) to the apex or peak of the R or R' wave on the 12-lead electrocardiogram, thus reflecting the electrical activation time that occurs from the endocardium to the epicardium (Pérez-Riera, de Abreu, Barbosa-Barros, Nikus, et al., 2016). In people and dogs presenting right bundle branch block, RPT is normal in left precordial leads and prolonged in right precordial leads. On the contrary, in left bundle branch block the RPT is prolonged in the left precordial leads (Battaia et al., 2022; Pérez-Riera, de Abreu, Barbosa-Barros, Nikus, et al., 2016).

The interventricular dyssynchrony index (IDI), recently proposed in human and veterinary medicine, is based on the values of left and right precordial RPT (Battaia et al., 2022; Vereckei et al., 2018). This index determines the presence of dyssynchrony and, therefore, predicts the clinical response to cardiac resynchronization therapy in people (Vereckei et al., 2018). The rationale behind this index is that the RPT in leads V1 and V5 reflect approximately the time elapsed from the beginning of ventricular activation until right and left ventricle activation are completed, since leads V1 and V5 reflect the electrical activation potentials of the right and left ventricle, respectively (Pérez-Riera, de Abreu, Barbosa-Barros, Nikus, et al., 2016). In people, in addition to patients with left bundle branch block, IDI appears to have great value in selecting patients with nonspecific intraventricular conduction disorder and duration of borderline QRS who might benefit from cardiac resynchronization therapy. According to current guidelines, the indication for cardiac resynchronization therapy is questionable in these patients (Ponikowski et al., 2016; Vereckei et al., 2018). Although there are currently no clinical indications for cardiac resynchronization therapy in dogs, analysis of IDI in dogs with heart diseases that can lead to electrical heterogeneity of the ventricles might provide interesting prognostic information in the future.

It is recognized that the demonstration of electrical dyssynchrony evidenced by the electrocardiogram alone may not be sufficient for the discrimination of people with advanced HF who will respond satisfactorily to therapy with the implantation of biventricular pacemaker (Bax et al., 2004; Bristow et al., 2004; Lane, 2004; Rodrigues et al., 2006; Vieira et al., 2005). Although conduction abnormalities are common, this is not always the case and patients with HF may present left ventricle dyssynchrony in the absence of regionally delayed electrical activation. Interestingly, the prevalence of

mechanical dyssynchrony ranges from 30 to 50% in people with HF and narrow QRS complex (Bleeker et al., 2005; Haghjoo et al., 2007; Yu, 2003). Delayed relaxation and dyssynchrony can be induced by abnormal loading of the heart. In healthy dogs, clamping the aorta to increase afterload resulted in regional desynchronization, as well as prolongation of relaxation time (Yano et al., 1994). These findings are supported by another study, which documented improvement in dyssynchrony and relaxation in people with HF once vasodilators and diuretics were given(Wang et al., 2007). Abnormal myocardial load, which is characteristic in patients with HF, may by itself contribute to dyssynchrony, and this type of dyssynchrony may not be amenable to electrical resynchronization (Cheng et al., 2009).

Mechanical dyssynchrony is detected mainly by echocardiography. One of the methods that have been used for the evaluation of ventricular mechanical activation times is Tissue Doppler Imaging (TDI). By placing the gate in a myocardial segment, two different time intervals can be acquired: the electromechanical delay, which is measured from the beginning of the QRS complex to the beginning of the S wave (Bader et al., 2004; Lafitte et al., 2004), and the electrosystolic delay, from the beginning of the QRS complex to the peak of S wave (Bax et al., 2003). In people, the delay of more than 40 ms between the opposite LV walls in any of those measurements is indicative of dyssynchrony, while values of approximately 20 ms are normal (Bader et al., 2004). In dogs, the maximal systolic time difference between LV segments lower than 30 ms was considered normal (Griffiths et al., 2011)

The presence of interventricular dyssynchrony is also easily assessed by measuring the difference between the left and right pre-ejection intervals. These intervals are measured from the beginning of the QRS complex to the beginning of the corresponding Doppler ejection signal. Considering that values of 20±10 ms were measured in healthy people, values of interventricular electromechanical delay >40 ms and values of left ventricle pre-ejection period >140 ms in people are considered pathological and indicative of intervention(Gorcsan et al., 2012; Gorcsan & Tayal, 2015; van Everdingen et al., 2016). In healthy dogs, the normal range of interventricular synchrony assessed by the right and the left ventricle pre-ejection period is extremely small, and the normal interventricular electromechanical delay can vary between -10.2 and 12.6 ms (Griffiths et al., 2011). In spite of the usual variation in cardiac cycle length in dogs, this technique does not appear to be significantly affected by beat-to-beat variability (Griffiths et al., 2011).

Although ventricular dyssynchrony is more harmful to the performance of the heart pump than atrial dyssynchrony, the assessment of the heterogeneity of atrial activation is also important for determining the risk of supraventricular arrhythmias, especially atrial fibrillation(Akamatsu et al., 2020; Jagannatha et al., 2024; Müller et al., 2021; Neves et al., 2018; Pessoa, 2019). The duration and the morphology of the P-wave are simple methods that reflect the electrophysiological properties of the atrial myocardium. In conventional electrocardiography, P-wave duration below 40 ms in dogs and 120 ms in people is considered normal (LL et al., 2013; Santilli, Moïse, et al., 2019). Prolonged duration, and/or the bifid morphology of the P-wave may indicate the presence of fibrosis, anoxia, myocarditis, and abnormalities in the conduction within or between the atria in dogs (Santilli, Moïse, et al., 2019).

P-wave dispersion (Pd) is an electrocardiographic index that has already been studied in human and veterinary cardiology (Dilaveris & Gialafos, 2001; Dittrich et al., 2018; Duru et al., 2006; Falchi et al., 2014; Irdem et al., 2016; Kosar et al., 2008; Noszczyk-Nowak, 2012; Noszczyk-Nowak et al., 2008, 2011; Özer et al., 2000; Seyfeli et al., 2006). This index is defined as the difference between the maximum and minimum duration of the P-wave recorded in different electrocardiographic leads. As electrical activity of the heart muscle displayed on the electrocardiogram is closely related to the conduction of specific areas of the atrium, regional depolarization disorders can lead to variation in P-wave duration in different electrocardiographic leads (Dilaveris & Gialafos, 2001; Noszczyk-Nowak et al., 2008; Villani et al., 1996). Changes in Pd may reflect disturbances in inter- and intra-atrial conduction and the inhomogeneous propagation of sinus impulses. It is not clear whether only the conduction heterogeneity of the atria (local effect) or also the various projections of the single depolarization vector in different electrocardiographic leads (projection phenomenon) play a role in the variation of P-wave duration between the leads (Ndrepepa et al., 2000; Spach et al., 1981).

Also, the mechanical aspect of atrial activation can be assessed, especially using echocardiography. In a study conducted in dogs with different types of heart disease, TDI was able to predict the future onset of atrial fibrillation (Neves et al., 2018). Interestingly, the time between the onset of the P-wave on the electrocardiogram and the peak of the last diastolic wave recorded by TDI in the mitral annulus was significantly higher in dogs that developed atrial fibrillation in the following 6 months as compared to those that did not (Neves et al., 2018). A similar result was documented

in people. Using the same TDI measurement in the left atrial wall, a study proposed a cutoff of 190 ms to identify people at increased risk for atrial fibrillation (De Vos et al., 2009).

It is undeniable that dyssynchrony impairs cardiac performance and adds severity to the pathological process. While this topic has been extensively explored in humans, the information available in veterinary medicine is still limited, leaving room for further investigation in animals. This thesis aims to evaluate cardiac activation heterogeneity in dogs with MMVD. The focus is to identify non-invasive diagnostic markers that can be used to monitor disease progression and assess cardiac remodeling. The document is divided in two chapters, each one corresponding to a different manuscript. The first chapter covers the analysis of atrial activation parameters through electrocardiography and echocardiography. This chapter evaluates how atrial conduction times correlate with cardiac remodeling and HF, seeking to determine the effectiveness of these markers in veterinary clinical practice. The second chapter focuses on investigating ventricular activation parameters, and how disease stage, cardiac remodeling, HF, and arrhythmias interfere with myocardial electromechanical parameters. The goal of this chapter is to provide a detailed understanding of ventricular activation and assess the utility of these markers as surrogates for MMVD severity and prognosis. Each chapter is designed to offer an in-depth analysis of the respective topics and their implications for veterinary clinical practice, allowing for a clear understanding of the conducted studies and their applications in the context of MMVD in dogs.

REFERENCES

Abdellah, A. T., & El-Nagary, M. (2018). Prevalence of P wave dispersion and interatrial block in patients with systolic heart failure and their relationship with functional status, hospitalization and one year mortality. *The Egyptian Heart Journal*, *70*(3), 181–187. https://doi.org/10.1016/j.ehj.2018.02.006

Aiken, A. V., Goldhaber, J. I., & Chugh, S. S. (2022). Delayed intrinsicoid deflection: Electrocardiographic harbinger of heart disease. *Annals of Noninvasive Electrocardiology*, *27*(3). https://doi.org/10.1111/anec.12940

Akamatsu, K., Ito, T., Miyamura, M., Kanzaki, Y., Sohmiya, K., & Hoshiga, M. (2020). Usefulness of tissue Doppler-derived atrial electromechanical delay for identifying patients with paroxysmal atrial fibrillation. *Cardiovascular Ultrasound*, *18*(1), 22. https://doi.org/10.1186/s12947-020-00205-2

Bader, H., Garrigue, S., Lafitte, S., Reuter, S., Jaïs, P., Haïssaguerre, M., Bonnet, J., Clementy, J., & Roudaut, R. (2004). Intra-left ventricular electromechanical asynchrony. *Journal of the American College of Cardiology*, *43*(2), 248–256. https://doi.org/10.1016/j.jacc.2003.08.038

BaronToaldo, M., Guglielmini, C., Diana, A., Sarcinella, F., & Cipone, M. (2014). Feasibility and reproducibility of echocardiographic assessment of regional left atrial deformation and synchrony by tissue Doppler ultrasonographic imaging in healthy dogs. *American Journal of Veterinary Research*, *75*(1), 59–66. https://doi.org/10.2460/ajvr.75.1.59

Battaia, S., Perego, M., Perciballi, C., Cavallini, D., & Santilli, R. (2022). Noninvasive electrocardiographic parameters to assess interventricular dyssynchrony in dogs with bundle branch blocks. *Journal of Veterinary Cardiology*, *41*, 134–144. https://doi.org/10.1016/j.jvc.2022.02.005

Bax, J. J., Ansalone, G., Breithardt, O. A., Derumeaux, G., Leclercq, C., Schalij, M. J., Sogaard, P., St. John Sutton, M., & Nihoyannopoulos, P. (2004). Echocardiographic evaluation of cardiac resynchronization therapy: ready for routine clinical use? *Journal of the American College of Cardiology*, *44*(1), 1–9. https://doi.org/10.1016/j.jacc.2004.02.055

Bax, J. J., Molhoek, S. G., van Erven, L., Voogd, P. J., Somer, S., Boersma, E., Steendijk, P., Schalij, M. J., & Van der Wall, E. E. (2003). Usefulness of myocardial tissue Doppler echocardiography to evaluate left ventricular dyssynchrony before and after biventricular pacing in patients with idiopathic dilated cardiomyopathy. *The American Journal of Cardiology*, *91*(1), 94–97. https://doi.org/10.1016/S0002-9149(02)03009-6

Bayam, E., Yıldırım, E., Kalçık, M., Karaduman, A., Kalkan, S., Güner, A., Küp, A., Kahyaoğlu, M., Yılmaz, Y., Selcuk, M., & Uyan, C. (2021). Relationship between P wave peak time and coronary artery disease severity in non-ST elevation acute coronary syndrome. *Herz*, *46*(2), 188–194. https://doi.org/10.1007/s00059-019-04859-1

Bleeker, G. B., Schalij, M. J., Molhoek, S. G., Holman, E. R., Verwey, H. F., Steendijk, P., van der Wall, E. E., & Bax, J. J. (2005). Frequency of left ventricular dyssynchrony in patients with heart failure and a narrow QRS complex. *The American Journal of Cardiology*, *95*(1), 140–142. https://doi.org/10.1016/j.amjcard.2004.08.082

Bleeker, G. B., Schalij, M. J., Molhoek, S. G., Verwey, H. F., HOLMAN, E. R., BOERSMA, E., STEENDIJK, P., VAN DER WALL, E. E., & BAX, J. J. (2004). Relationship Between QRS Duration and Left Ventricular Dyssynchrony in

Patients with End-Stage Heart Failure. *Journal of Cardiovascular Electrophysiology*, *15*(5), 544–549. https://doi.org/10.1046/j.1540-8167.2004.03604.x

Boon, J. A. (2011). *Veterinary echocardiography* (J. A. Boon, Ed.). Wiley-Blackwell.

Bristow, M. R., Saxon, L. A., Boehmer, J., Krueger, S., Kass, D. A., De Marco, T., Carson, P., DiCarlo, L., DeMets, D., White, B. G., DeVries, D. W., & Feldman, A. M. (2004). Cardiac-Resynchronization Therapy with or without an Implantable Defibrillator in Advanced Chronic Heart Failure. *New England Journal of Medicine*, *350*(21), 2140–2150. https://doi.org/10.1056/NEJMoa032423

Cekirdekci, E. I., Unal Evren, E., Evren, H., & Bugan, B. (2019). R-peak time: A novel marker of depolarization in patients with Human Immunodeficiency Virus. *Journal of Electrocardiology*, *55*, 133–137. https://doi.org/10.1016/j.jelectrocard.2019.05.016

Celik, Y., Yıldırım, N., Demir, V., Alp, C., Sahin, O., & Tolga Doğru, M. (2021). Atrial electromechanical delay and p wave dispersion associated with severity of chronic obstructive pulmonary disease. *African Health Sciences*, *21*(1), 140–149. https://doi.org/10.4314/ahs.v21i1.19

Chan, Y. H. (2003). Biostatistics 104: correlational analysis. *Singapore Medical Journal*, *44*(12), 614–619.

Cheng, A., Helm, R. H., & Abraham, T. P. (2009). Pathophysiological mechanisms underlying ventricular dyssynchrony. *Europace*, *11*(Supplement 5), v10–v14. https://doi.org/10.1093/europace/eup272

Cinier, G., Yilmaz, A. S., Tekkesin, A. I., & Cetin, M. (2021). Predictors for the prolonged R wave peak time among patients with arterial hypertension. *Turk Kardiyoloji Dernegi Arsivi-Archives of the Turkish Society of Cardiology*, *49*(5), 387–394. https://doi.org/10.5543/tkda.2021.80540

Cornell, C. C., Kittleson, M. D., Della Torre, P., Häggström, J., Lombard, C. W., Pedersen, H. D., Vollmar, A., & Wey, A. (2004). Allometric scaling of M-mode cardiac measurements in normal adult dogs. *Journal of Veterinary Internal Medicine*, *18*(3), 311–321. https://doi.org/10.1892/0891-6640(2004)18<311:asomcm>2.0.co;2

Crosara, S., Borgarelli, M., Perego, M., Häggström, J., La Rosa, G., Tarducci, A., & Santilli, R. A. (2010). Holter monitoring in 36 dogs with myxomatous mitral valve disease. *Australian Veterinary Journal*, *88*(10), 386–392. https://doi.org/10.1111/j.1751-0813.2010.00628.x

Darouian, N., Narayanan, K., Aro, A. L., Reinier, K., Uy-Evanado, A., Teodorescu, C., Gunson, K., Jui, J., & Chugh, S. S. (2016). Delayed intrinsicoid deflection of the QRS complex is associated with sudden cardiac arrest. *Heart Rhythm*, *13*(4), 927–932. https://doi.org/10.1016/j.hrthm.2015.12.022

De Vos, C. B., Weijs, B., Crijns, H. J. G. M., Cheriex, E. C., Palmans, A., Habets, J., Prins, M. H., Pisters, R., Nieuwlaat, R., & Tieleman, R. G. (2009). Atrial tissue Doppler imaging for prediction of new-onset atrial fibrillation. *Heart*, *95*(10), 835–840. https://doi.org/10.1136/hrt.2008.148528

Dhingra, R., Pencina, M. J., Wang, T. J., Nam, B.-H., Benjamin, E. J., Levy, D., Larson, M. G., Kannel, W. B., D'Agostino, R. B., & Vasan, R. S. (2006). Electrocardiographic QRS Duration and the Risk of Congestive Heart Failure. *Hypertension*, *47*(5), 861–867. https://doi.org/10.1161/01.HYP.0000217141.20163.23

Dilaveris, P. E., & Gialafos, J. E. (2001). P-Wave Dispersion: A Novel Predictor of Paroxysmal Atrial Fibrillation. *Annals of Noninvasive Electrocardiology*, *6*(2),

159–165. https://doi.org/10.1111/j.1542-474X.2001.tb00101.x
Dittrich, G., Campos, G. M. V. der B., Sousa, M. G., & Oliveira, S. T. (2018). P wave dispersion in obese dogs with and without mitral valve disease. *Ciência Rural*, *48*(10). https://doi.org/10.1590/0103-8478cr20180047
Duru, M., Seyfeli, E., Kuvandik, G., Kaya, H., & Yalcin, F. (2006). Effect of Weight Loss on P Wave Dispersion in Obese Subjects*. *Obesity*, *14*(8), 1378–1382. https://doi.org/10.1038/oby.2006.156
Erbay, A. R., Turhan, H., Yasar, A. S., Bicer, A., Senen, K., Sasmaz, H., Sabah, I., & Yetkin, E. (2005). Effects of long-term beta-blocker therapy on P-wave duration and dispersion in patients with rheumatic mitral stenosis. *International Journal of Cardiology*, *102*(1), 33–37. https://doi.org/10.1016/j.ijcard.2004.03.079
Estes, E. H. (2017). Commentary on Electrocardiographic Time to Intrinsicoid Deflection and Heart Failure: the Multi-Ethnic Study of Atherosclerosis. *Clinical Cardiology*, *40*(1), 53–53. https://doi.org/10.1002/clc.22629
Falchi, A. G., Grecchi, I., Muggia, C., & Tinelli, C. (2014). Weight loss and P wave dispersion: a preliminary study. *Obesity Research & Clinical Practice*, *8*(6), e614–e617. https://doi.org/10.1016/j.orcp.2014.08.005
Glikson, M., Nielsen, J. C., Kronborg, M. B., Michowitz, Y., Auricchio, A., Barbash, I. M., Barrabés, J. A., Boriani, G., Braunschweig, F., Brignole, M., Burri, H., Coats, A. J. S., Deharo, J. C., Delgado, V., DIller, G. P., Israel, C. W., Keren, A., Knops, R. E., Kotecha, Di., … Tolosana, J. M. (2021). 2021 ESC Guidelines on cardiac pacing and cardiac resynchronization therapy. In *European Heart Journal* (Vol. 42, Issue 35, pp. 3427–3520). Oxford University Press. https://doi.org/10.1093/eurheartj/ehab364
Gorcsan, J., Marek, J. J., & Onishi, T. (2012). The Contemporary Role of Echocardiography in Improving Patient Response to Cardiac Resynchronization Therapy. In *Current Cardiovascular Imaging Reports* (Vol. 5, Issue 6, pp. 462–472). Current Medicine Group LLC 1. https://doi.org/10.1007/s12410-012-9172-2
Gorcsan, J., & Tayal, B. (2015). Newer Echocardiographic Techniques in Cardiac Resynchronization Therapy. In *Cardiac Electrophysiology Clinics* (Vol. 7, Issue 4, pp. 609–618). W.B. Saunders. https://doi.org/10.1016/j.ccep.2015.08.013
Griffiths, L. G., Fransioli, J. R., & Chigerwe, M. (2011). Echocardiographic assessment of interventricular and intraventricular mechanical synchrony in normal dogs. *Journal of Veterinary Cardiology*, *13*(2), 115–126. https://doi.org/10.1016/j.jvc.2011.02.001
Guglielmini, C., Goncalves Sousa, M., Baron Toaldo, M., Valente, C., Bentivoglio, V., Mazzoldi, C., Bergamin, I., Drigo, M., & Poser, H. (2020). Prevalence and risk factors for atrial fibrillation in dogs with myxomatous mitral valve disease. *Journal of Veterinary Internal Medicine*, *34*(6), 2223–2231. https://doi.org/10.1111/jvim.15927
Guntekin, U., Gunes, Y., Tuncer, M., Gunes, A., Sahin, M., & Simsek, H. (2008). Long-term Follow-up of P-wave Duration and Dispersion in Patients with Mitral Stenosis. *Pacing and Clinical Electrophysiology*, *31*(12), 1620–1624. https://doi.org/10.1111/j.1540-8159.2008.01235.x
Haghjoo, M., Bagherzadeh, A., Fazelifar, A. F., Haghighi, Z. O., Esmaielzadeh, M., Alizadeh, A., Emkanjoo, Z., Sadeghpour, A., Samiei, N., Farahani, M. M., Sadr-Ameli, M. A., Maleki, M., & Noohi, F. (2007). Prevalence of Mechanical Dyssynchrony in Heart Failure Patients with Different QRS Durations. *Pacing and Clinical Electrophysiology*, *30*(5), 616–622. https://doi.org/10.1111/j.1540-8159.2007.00722.x

Hansson, K., Häggström, J., Kvart, C., & Lord, P. (2002). LEFT ATRIAL TO AORTIC ROOT INDICES USING TWO-DIMENSIONAL AND M-MODE ECHOCARDIOGRAPHY IN CAVALIER KING CHARLES SPANIELS WITH AND WITHOUT LEFT ATRIAL ENLARGEMENT. *Veterinary Radiology & Ultrasound*, *43*(6), 568–575. https://doi.org/10.1111/j.1740-8261.2002.tb01051.x

Irdem, A., Aydın Sahin, D., Kervancioglu, M., Baspinar, O., Sucu, M., Keskin, M., & Kilinc, M. (2016). Evaluation of P-Wave Dispersion, Diastolic Function, and Atrial Electromechanical Conduction in Pediatric Patients with Subclinical Hypothyroidism. *Echocardiography*, *33*(9), 1397–1401. https://doi.org/10.1111/echo.13255

Jagannatha, G. N. P., Antara, I. M. P. S., Kosasih, A. M., Kamardi, S., & Pradnyana, I. W. A. S. (2024). P-wave peak time and P-wave dispersion in surface electrocardiography as initial predictors of new-onset atrial fibrillation in early-onset hypertension. *Hypertension Research*, *47*(1), 137–148. https://doi.org/10.1038/s41440-023-01357-0

Janus, I., Noszczyk-Nowak, A., Nowak, M., Ciaputa, R., Kandefer-Gola, M., & Pasławska, U. (2016). A comparison of the histopathologic pattern of the left atrium in canine dilated cardiomyopathy and chronic mitral valve disease. *BMC Veterinary Research*, *12*(1), 3. https://doi.org/10.1186/s12917-015-0626-z

Keene, B. W., Atkins, C. E., Bonagura, J. D., Fox, P. R., Häggström, J., Fuentes, V. L., Oyama, M. A., Rush, J. E., Stepien, R., & Uechi, M. (2019). ACVIM consensus guidelines for the diagnosis and treatment of myxomatous mitral valve disease in dogs. *Journal of Veterinary Internal Medicine*, *33*(3), 1127–1140. https://doi.org/10.1111/jvim.15488

Kirk, J. A., & Kass, D. A. (2013). Electromechanical Dyssynchrony and Resynchronization of the Failing Heart. *Circulation Research*, *113*(6), 765–776. https://doi.org/10.1161/CIRCRESAHA.113.300270

Koo, T. K., & Li, M. Y. (2016). A Guideline of Selecting and Reporting Intraclass Correlation Coefficients for Reliability Research. *Journal of Chiropractic Medicine*, *15*(2), 155–163. https://doi.org/10.1016/j.jcm.2016.02.012

Korovesis, T. G., Koutrolou-Sotiropoulou, P., & Katritsis, D. G. (2022). Arrhythmogenic Mitral Valve Prolapse. *Arrhythmia & Electrophysiology Review*, *11*. https://doi.org/10.15420/aer.2021.28

Kosar, F., Aksoy, Y., Ari, F., Keskin, L., & Sahin, I. (2008). P-Wave Duration and Dispersion in Obese Subjects. *Annals of Noninvasive Electrocardiology*, *13*(1), 3–7. https://doi.org/10.1111/j.1542-474X.2007.00194.x

Lafitte, S., Garrigue, S., Perron, J.-M., Bordachar, P., Reuter, S., Jaïs, P., Haïssaguerre, M., Clementy, J., & Roudaut, R. (2004). Improvement of left ventricular wall synchronization with multisite ventricular pacing in heart failure: a prospective study using Doppler tissue imaging. *European Journal of Heart Failure*, *6*(2), 203–212. https://doi.org/10.1016/j.ejheart.2003.10.008

Lane, R. E. (2004). Selection and optimisation of biventricular pacing: the role of echocardiography. *Heart*, *90*(suppl_6), vi10–vi16. https://doi.org/10.1136/hrt.2004.043000

Lee, J., Mizuno, M., Mizuno, T., Harada, K., & Uechi, M. (2015). Pathologic Manifestations on Surgical Biopsy and Their Correlation with Clinical Indices in Dogs with Degenerative Mitral Valve Disease. *Journal of Veterinary Internal Medicine*, *29*(5), 1313–1321. https://doi.org/10.1111/jvim.13587

LL, T., SG, T., & KK, P. (2013). ECG P wave abnormalities. *Singapore Medical Journal*, *54*(1), 4–5. https://doi.org/10.11622/smedj.2013002

Mano, H., Okumura, Y., Watanabe, I., Ohta, M., Kogawa, R., Sasaki, N., Nakai, T., Ohkubo, K., Kofune, M., Nagashima, K., Sonoda, K., Haruta, H., & Hirayama, A. (2014). Changes over time in echocardiographic variables and atrial electromechanical intervals after ablation for atrial fibrillation. *Journal of Arrhythmia*, *30*(6), 466–472. https://doi.org/10.1016/j.joa.2014.01.005

Mateos Pañero, M., Battaia, S., Ramera, L., Perego, M., & Santilli, R. A. (2021). R-peak time in clinically healthy dogs with different thoracic conformations. *Veterinary Journal*, *268*. https://doi.org/10.1016/j.tvjl.2020.105592

Müller, P., Weijs, B., Bemelmans, N. M. A. A., Mügge, A., Eckardt, L., Crijns, H. J. G. M., Bax, J. J., Linz, D., & den Uijl, D. W. (2021). Echocardiography-derived total atrial conduction time (PA-TDI duration): risk stratification and guidance in atrial fibrillation management. *Clinical Research in Cardiology*, *110*(11), 1734–1742. https://doi.org/10.1007/s00392-021-01917-9

Ndrepepa, G., Zrenner, B., Deisenhofer, I., Karch, M., Schneider, M., Schreieck, J., & Schmitt, C. (2000). Relationship between surface electrocardiogram characteristics and endocardial activation sequence in patients with typical atrial flutter. *Zeitschrift Für Kardiologie*, *89*(6), 527–537. https://doi.org/10.1007/s003920070225

Neves, J., Pedro, B., Christley, R., & Dukes-McEwan, J. (2018). Usefulness of pulsed-wave tissue Doppler imaging at the mitral annulus for prediction of new-onset atrial fibrillation in dogs. *Journal of Veterinary Cardiology*, *20*(6), 425–437. https://doi.org/10.1016/j.jvc.2018.10.002

Noszczyk-Nowak, A. (2012). P-Wave Dispersion in Prediction of Maintenance of Sinus Rhythm After an Electrical Cardioversion of Atrial Fibrillation in Dogs. *Bulletin of the Veterinary Institute in Pulawy*, *56*(1), 99–102. https://doi.org/10.2478/v10213-012-0018-0

Noszczyk-Nowak, A., Paslawska, U., Szalas, A., & Nicpon, J. (2008). P-WAVE DISPERSION IN HEALTHY DOGS. A PRELIMINARY STUDY. *Bulletin of the Veterinary Institute in Pulawy*, *52*, 683–688.

Noszczyk-Nowak, A., Szałas, A., Pasławska, U., & Nicpoń, J. (2011). Comparison of P-wave dispersion in healthy dogs, dogs with chronic valvular disease and dogs with disturbances of supraventricular conduction. *Acta Veterinaria Scandinavica*, *53*(1), 18. https://doi.org/10.1186/1751-0147-53-18

Ogawa, M., Ogi, H., Miyakawa, H., Hsu, H.-H., Miyagawa, Y., & Takemura, N. (2022). Evaluation of the association between electrocardiogram parameters and left cardiac remodeling in dogs with myxomatous mitral valve disease. *Veterinary World*, 2072–2083. https://doi.org/10.14202/vetworld.2022.2072-2083

Okutucu, S., Aytemir, K., & Oto, A. (2016). P-wave dispersion: What we know till now? *JRSM Cardiovascular Disease*, *5*, 204800401663944. https://doi.org/10.1177/2048004016639443

O'Neal, W. T., Mazur, M., Bertoni, A. G., Bluemke, D. A., Al-Mallah, M. H., Lima, J. A. C., Kitzman, D., & Soliman, E. Z. (2017). Electrocardiographic Predictors of Heart Failure With Reduced Versus Preserved Ejection Fraction: The Multi-Ethnic Study of Atherosclerosis. *Journal of the American Heart Association*, *6*(6). https://doi.org/10.1161/JAHA.117.006023

O'Neal, W. T., Qureshi, W. T., Nazarian, S., Kawel-Boehm, N., Bluemke, D. A., Lima, J. A. C., & Soliman, E. Z. (2016). Electrocardiographic Time to Intrinsicoid Deflection and Heart Failure: The Multi-Ethnic Study of Atherosclerosis. *Clinical Cardiology*, *39*(9), 531–536. https://doi.org/10.1002/clc.22561

Özer, N., Aytemir, K., Atalar, E., Sade, E., Aksöyek, S., Övünç, K., Açýl, T., Nazlý, N.,

Özmen, F., Oto, A., & Kes, S. (2000). P Wave Dispersion in Hypertensive Patients with Paroxysmal Atrial Fibrillation. *Pacing and Clinical Electrophysiology*, *23*(11P2), 1859–1862. https://doi.org/10.1111/j.1540-8159.2000.tb07038.x

Özer, N., Yavuz, B., Can, I., Atalar, E., Aksöyek, S., Övünç, K., Özmen, F., & Kes, S. (2005). Doppler tissue evaluation of intra-atrial and interatrial electromechanical delay and comparison with P-wave dispersion in patients with mitral stenosis. *Journal of the American Society of Echocardiography*, *18*(9), 945–948. https://doi.org/10.1016/j.echo.2005.01.015

Pedro, B. M., Alves, J. V., Cripps, P. J., Stafford Johnson, M. J., & Martin, M. W. S. (2011). Association of QRS duration and survival in dogs with dilated cardiomyopathy: A retrospective study of 266 clinical cases. *Journal of Veterinary Cardiology*, *13*(4), 243–249. https://doi.org/10.1016/j.jvc.2011.09.003

Pérez-Riera, A. R., de Abreu, L. C., Barbosa-Barros, R., Grindler, J., Fernandes-Cardoso, A., & Baranchuk, A. (2016). P-wave dispersion: an update. *Indian Pacing and Electrophysiology Journal*, *16*(4), 126–133. https://doi.org/10.1016/j.ipej.2016.10.002

Pérez-Riera, A. R., de Abreu, L. C., Barbosa-Barros, R., Nikus, K. C., & Baranchuk, A. (2016). R-Peak Time: An Electrocardiographic Parameter with Multiple Clinical Applications. *Annals of Noninvasive Electrocardiology*, *21*(1), 10–19. https://doi.org/10.1111/anec.12323

Perry, R., De Pasquale, C. G., Chew, D. P., McGavigan, A. D., & Joseph, M. X. (2011). Tissue Doppler Derived Mechanical Dyssynchrony Does Not Change after Cardiac Resynchronization Therapy. *Echocardiography*, *28*(9), 961–967. https://doi.org/10.1111/j.1540-8175.2011.01498.x

Pessoa, R. B. (2019). *Mensuração do Tempo de Condução Atrial Total por meio da ecocardiografia tecidual em cães normais e em cães com Valvopatia Mitral Mixomatosa* [Universidade de São Paulo]. https://doi.org/10.11606/D.10.2019.tde-21112018-122807

Piccirillo, G., Moscucci, F., Mezzadri, M., Caltabiano, C., Di Diego, I., Carnovale, M., Corrao, A., Stefano, S., Scinicariello, C., Giuffrè, M., De Santis, V., Sciomer, S., Rossi, P., & Magrì, D. (2023). Electrocardiographic and other Noninvasive Hemodynamic Markers in Decompensated CHF Patients. *Journal of Cardiovascular Development and Disease*, *10*(3), 125. https://doi.org/10.3390/jcdd10030125

Ponikowski, P., Voors, A. A., Anker, S. D., Bueno, H., Cleland, J. G. F., Coats, A. J. S., Falk, V., González-Juanatey, J. R., Harjola, V.-P., Jankowska, E. A., Jessup, M., Linde, C., Nihoyannopoulos, P., Parissis, J. T., Pieske, B., Riley, J. P., Rosano, G. M. C., Ruilope, L. M., Ruschitzka, F., … van der Meer, P. (2016). 2016 ESC Guidelines for the diagnosis and treatment of acute and chronic heart failure. *European Heart Journal*, *37*(27), 2129–2200. https://doi.org/10.1093/eurheartj/ehw128

Pozios, I., Vouliotis, A. I., Dilaveris, P., & Tsioufis, C. (2023). Electro-Mechanical Alterations in Atrial Fibrillation: Structural, Electrical, and Functional Correlates. *Journal of Cardiovascular Development and Disease*, *10*(4), 149. https://doi.org/10.3390/jcdd10040149

Risum, N. (2014). Assessment of mechanical dyssynchrony in cardiac resynchronization therapy. *Dan Med J* , *61*(12), B4981.

Rodrigues, A. C. T., Tsutsui, J. M., & Mathias Jr, W. (2006). Avaliação de dissincronia cardíaca pelo ecocardiograma: estratégias para um resultado

adequado Cardiac dyssynchrony in patients with heart failure: strategies for an adequate echocardiographic assessment. *Revista Brasileira de Ecocardiografia*, *19*(3), 46–51.

Rudski, L. G., Lai, W. W., Afilalo, J., Hua, L., Handschumacher, M. D., Chandrasekaran, K., Solomon, S. D., Louie, E. K., & Schiller, N. B. (2010). Guidelines for the Echocardiographic Assessment of the Right Heart in Adults: A Report from the American Society of Echocardiography. *Journal of the American Society of Echocardiography*, *23*(7), 685–713. https://doi.org/10.1016/j.echo.2010.05.010

Russo, V., Rago, A., Di Meo, F., Papa, A. A., Ciardiello, C., Cristiano, A., Calabrò, R., Russo, M. G., & Nigro, G. (2015). Atrial Septal Aneurysms and Supraventricular Arrhythmias: The Role of Atrial Electromechanical Delay. *Echocardiography*, *32*(10), 1504–1514. https://doi.org/10.1111/echo.12908

Salem, A. S., Abazeed, S. H., Elhawary, A., & Abdelmonem, A. H. (2021). Correlation Between Left Ventricular Electromechanical Delay and Body Mass Index. *European Heart Journal Supplements*, *23*(Supplement_D). https://doi.org/10.1093/eurheartj/suab069.004

Santilli, R. A., Moïse, N. S., Pariaut, R., & Perego, M. (2019). *Electrocardiography of the dog and cat: diagnosis of arrhythmias* (R. A. Santilli, N. S. Moïse, R. Pariaut, & M. Perego, Eds.). Edra.

Santilli, R. A., Porteiro Vázquez, D. M., Gerou-Ferriani, M., Lombardo, S. F., & Perego, M. (2019). Development and assessment of a novel precordial lead system for accurate detection of right atrial and ventricular depolarization in dogs with various thoracic conformations. *American Journal of Veterinary Research*, *80*(4), 358–368. https://doi.org/10.2460/ajvr.80.4.358

Seyfeli, E., Duru, M., Kuvandık, G., Kaya, H., & Yalcin, F. (2006). Effect of obesity on P-wave dispersion and QT dispersion in women. *International Journal of Obesity*, *30*(6), 957–961. https://doi.org/10.1038/sj.ijo.0803233

Simpson, K. E., Devine, B. C., Woolley, R., Corcoran, BrendamM., & French, A. T. (2008). TIMING OF LEFT HEART BASE DESCENT IN DOGS WITH DILATED CARDIOMYOPATHY AND NORMAL DOGS. *Veterinary Radiology & Ultrasound*, *49*(3), 287–294. https://doi.org/10.1111/j.1740-8261.2008.00359.x

Sivri, F., Şencan, M., Ceyhan, B. Ö., Içen, Y. K., Coskun, M., & Aksoy, F. (2023). Prognostic value of R wave peak time in COVID-19 pneumonia. *Journal of Electrocardiology*, *80*, 91–95. https://doi.org/10.1016/j.jelectrocard.2023.05.005

Spach, M. S., Miller, W. T., Geselowitz, D. B., Barr, R. C., Kootsey, J. M., & Johnson, E. A. (1981). The discontinuous nature of propagation in normal canine cardiac muscle. Evidence for recurrent discontinuities of intracellular resistance that affect the membrane currents. *Circulation Research*, *48*(1), 39–54. https://doi.org/10.1161/01.RES.48.1.39

Spartalis, M., Tzatzaki, E., Spartalis, E., Damaskos, C., Athanasiou, A., Livanis, E., & Voudris, V. (2017). Pathophysiology and Current Evidence for Detection of Dyssynchrony. *Cardiology Research*, *8*(5), 179–183. https://doi.org/10.14740/cr598w

Spragg, D. D., & Kass, D. A. (2006). Pathobiology of Left Ventricular Dyssynchrony and Resynchronization. *Progress in Cardiovascular Diseases*, *49*(1), 26–41. https://doi.org/10.1016/j.pcad.2006.05.001

Surawicz, B., Childers, R., Deal, B. J., & Gettes, L. S. (2009). AHA/ACCF/HRS Recommendations for the Standardization and Interpretation of the Electrocardiogram. *Journal of the American College of Cardiology*, *53*(11), 976–

981. https://doi.org/10.1016/j.jacc.2008.12.013
Sweeney, M. O., & Prinzen, F. W. (2006). A New Paradigm for Physiologic Ventricular Pacing. *Journal of the American College of Cardiology*, *47*(2), 282–288. https://doi.org/10.1016/j.jacc.2005.09.029
Tapia-Orihuela, R. K., Gharacholou, S. M., Asirvatham, S. J., & Munoz, F. D.-C. (2022). Electrocardiographic markers of cardiac resynchronization therapy response: delayed time to intrinsicoid deflection onset in lateral leads. *Journal of Geriatric Cardiology : JGC*, *19*(1), 21–30. https://doi.org/10.11909/j.issn.1671-5411.2022.01.009
Tidholm, A., Ljungvall, I., HÃ¶glund, K., Westling, A. B., & HÃ¤ggstrÃ¶m, J. (2009). Tissue Doppler and Strain Imaging in Dogs with Myxomatous Mitral Valve Disease in Different Stages of Congestive Heart Failure. *Journal of Veterinary Internal Medicine*, *23*(6), 1197–1207. https://doi.org/10.1111/j.1939-1676.2009.0403.x
Trikhun, P., Surachetpong, S. D., Sutayatram, S., & Buranakarl, C. (2020). Left ventricular systolic function in dogs with pulmonic stenosis. *Veterinary World*, *13*(11), 2436–2442. https://doi.org/10.14202/vetworld.2020.2436-2442
Turhan, H., Yetkin, E., Senen, K., Yilmaz, M. B., Ileri, M., Atak, R., Cehreli, S., & Kutuk, E. (2002). Effects of percutaneous mitral balloon valvuloplasty on P-wave dispersion in patients with mitral stenosis. *The American Journal of Cardiology*, *89*(5), 607–609. https://doi.org/10.1016/S0002-9149(01)02307-4
van Everdingen, W. M., Schipper, J. C., Van 'T Sant, J., Misier, K. R., Meine, M., & Cramer, M. J. (2016). Echocardiography and cardiac resynchronisation therapy, friends or foes? In *Netherlands Heart Journal* (Vol. 24, Issue 1, pp. 25–38). Bohn Stafleu van Loghum. https://doi.org/10.1007/s12471-015-0769-3
Vereckei, A., Szelényi, Z., Kutyifa, V., Zima, E., Szénási, G., Kiss, M., Katona, G., Karádi, I., & Merkely, B. (2018). Novel electrocardiographic dyssynchrony criteria improve patient selection for cardiac resynchronization therapy. *EP Europace*, *20*(1), 97–103. https://doi.org/10.1093/europace/euw326
Vernooy, K., Verbeek, X. A. A. M., Paschar, M., & Prinzen, F. W. (2003). Relation Between Abnormal Ventricular Impulse Conduction and Heart Failure. *Journal of Interventional Cardiology*, *16*(6), 557–562. https://doi.org/10.1046/j.1540-8183.2003.01061.x
Vieira, M. L. C., Maddukuri, P. V., Phang, R. S., Pandian, N. G., Mathias Júnior, W., & Ramires, J. A. F. (2005). Demonstração do mecanismo da terapia de ressincronização ventricular com ecocardiografia tridimensional em tempo real em paciente com insuficiência cardíaca. *Arquivos Brasileiros de Cardiologia*, *85*(5). https://doi.org/10.1590/S0066-782X2005001800006
Vila, B. de C. P., Camacho, A. A., & Sousa, M. G. (2021). T-wave peak-end interval and ratio of T-wave peak-end and QT intervals: novel arrhythmogenic and survival markers for dogs with myxomatous mitral valve disease. *Journal of Veterinary Cardiology*, *35*, 25–41. https://doi.org/10.1016/j.jvc.2021.02.004
Villani, G. Q., Piepoli, M., Rosi, A., & Capucci, A. (1996). P-wave dispersion index: a marker of patients with paroxysmal atrial fibrillation. *International Journal of Cardiology*, *55*(2), 169–175. https://doi.org/10.1016/0167-5273(96)02677-0
Wang, J., Kurrelmeyer, K. M., Torre-Amione, G., & Nagueh, S. F. (2007). Systolic and Diastolic Dyssynchrony in Patients With Diastolic Heart Failure and the Effect of Medical Therapy. *Journal of the American College of Cardiology*, *49*(1), 88–96. https://doi.org/10.1016/j.jacc.2006.10.023
Yano, M., Kohno, M., Konishi, M., Takahashi, T., Seki, K., & Matsuzaki, M. (1994).

Influence of left ventricular regional nonuniformity on afterload-dependent relaxation in intact dogs. *American Journal of Physiology-Heart and Circulatory Physiology*, *267*(1), H148–H154. https://doi.org/10.1152/ajpheart.1994.267.1.H148

Yu, C.-M. (2003). High prevalence of left ventricular systolic and diastolic asynchrony in patients with congestive heart failure and normal QRS duration. *Heart*, *89*(1), 54–60. https://doi.org/10.1136/heart.89.1.54

Zhu, T., Lei, M., Wang, Z., Zhang, R., Zhang, Y., Jin, W., Yu, C., Huang, C. L.-H., Liu, D., Zheng, W., Liu, Y., Quan, X., Kong, L., Liang, S., & Zhang, X. (2021). A Comparative Study of Systolic and Diastolic Mechanical Synchrony in Canine, Primate, and Healthy and Failing Human Hearts. *Frontiers in Cardiovascular Medicine*, *8*. https://doi.org/10.3389/fcvm.2021.750067

CHAPTER 1 – ATRIAL CONDUCTION TIMES IN HEALTHY DOGS AND DOGS WITH MYXOMATOUS MITRAL VALVE DISEASE*

Running head: Atrial conduction times in dogs with myxomatous mitral valve disease

* Manuscript will be submitted to the Journal of Veterinary Cardiology (Online ISSN: 1875-0834). Written in accordance with the guidelines available at https://www.sciencedirect.com/journal/journal-of-veterinary-cardiology/publish/guide-for-authors

ABSTRACT

Introduction/Objectives: Myxomatous mitral valve disease (MMVD) can lead to heterogeneous mechanical and electrical atrial activity, and a higher risk of atrial fibrillation. The aim of this study was to assess indices of atrial conduction times in dogs with MMVD and in healthy dogs.

Animals: This cross-sectional study in two veterinary institutions included dogs diagnosed with MMVD, and healthy dogs.

Methods: The times between the beginning of the P-wave in electrocardiography and the beginning or the peak of A'-wave in tissue Doppler were measured in the lateral mitral, septal, and lateral tricuspid annulus. Echocardiographic intra-left atrial (LA) or interatrial conduction delay were defined as the difference between the septal and the lateral measurements, or the tricuspid and the mitral measurements, respectively. In electrocardiography, P-wave duration was measured in 12 leads. The difference between longest and shortest P-wave durations was defined as P-wave dispersion (Pd).

Results: Were recruited 207 dogs, but 139 of them were included (42 control, 50 B1, 19 B2 and 28 C MMVD dogs). Most markers of atrial conduction times changed with the progression of MMVD. Some electrical and mechanical markers showed an AUC>0.7 for the identification of cardiac remodeling, heart failure and/or arrhythmias, especially Pd, P-wave durations in bipolar and unipolar leads, and left atrium mechanical conduction times.

Conclusions: Electrocardiographic and echocardiographic indices of atrial conduction heterogeneity change with the progression of MMVD, and are noninvasive markers of arrhythmias, cardiac dilation and heart failure. Furthermore, this is the first paper describing L-PAb, S-PAb, S-PAp, R-PAb and R-PAp values in healthy dogs and

in MMVD dogs.

KEYWORDS: P-wave dispersion; dyssynchrony; electromechanical activation; arrhythmia; heart failure.

ABBREVIATION TABLE

AF	Atrial flutter
Interatrial-b	Interatrial conduction delay, calculated as the difference between the R-PAb and L-PAb times
Interatrial-p	Interatrial conduction delay, calculated as the difference between the R-PAp and L-PAp times
Intra-LAb	Intra-left atrial conduction delay, calculated as the difference between the S-PAb and L-PAb times
Intra-LAp	Intra-left atrial conduction delay, calculated as the difference between the S-PAp and L-PAp times
LA	Left atrial
L-PAb	The atrial electromechanical delay in lateral mitral annulus
L-PAp	The atrial electrosystolic delay in lateral mitral annulus
LV	Left ventricle
MMVD	Myxomatous mitral valve disease
NPV	Negative predictive value
PAb	The atrial electromechanical delay, defined as the time between the beginning of the P-wave in ECG and the beginning of A' wave in tissue Doppler traces
PAp	The atrial electrosystolic delay, defined as the time between the beginning of the P-wave in ECG and the peak of A' wave in tissue Doppler traces
Pd	P-wave dispersion
Pmax	The longest P-wave duration within 12 leads
Pmin	The shortest P-wave duration within 12 leads
PPV	Positive predictive value
R-PAb	The atrial electromechanical delay in lateral tricuspid annulus
R-PAp	The atrial electrosystolic delay in lateral tricuspid annulus
S-PAb	The atrial electromechanical delay in septal annulus
S-PAp	The atrial electrosystolic delay in septal annulus
TDI	Tissue Doppler Imaging

INTRODUCTION/OBJECTIVES

Atrial conduction disorders are frequent in both people and dogs with mitral valve disease (Crosara et al., 2010; Korovesis et al., 2022). The progressive increase in mitral insufficiency leads to left atrial (LA) dilation and, consequently, predisposes to the development of arrhythmias, which are present in more than 70% of dogs with

myxomatous mitral valve disease (MMVD) (Crosara et al., 2010). Electrophysiological and electromechanical abnormalities associated with increased heterogeneous atrial electrical activity pose a higher risk of atrial fibrillation (AF) and flutter (Irdem et al., 2016).

Timing of electrical events has mostly relied on electrocardiographic (ECG) and invasive electrophysiologic procedures. P-wave dispersion (Pd) is defined as the difference between the maximum (Pmax) and the minimum (Pmin) P-wave duration recorded from multiple different-surface ECG leads. It has been known that increased P-wave duration and Pd reflect prolongation of intraatrial and interatrial conduction time and the inhomogeneous propagation of sinus impulses, which are well-known electrophysiologic characteristics related to atrial arrhythmias (Okutucu et al., 2016). In previous studies it has been shown that Pd is increased in people with mitral stenosis (Erbay et al., 2005; Guntekin et al., 2008; Okutucu et al., 2016; Özer et al., 2005; Turhan et al., 2002) and in dogs with MMVD (Dittrich et al., 2018; Noszczyk-Nowak et al., 2011). However, its association with echocardiographic variables of atrial conduction times in dogs with MMVD has never been investigated.

Determination of electromechanical incidents via transthoracic echocardiography may be helpful for a better understanding of atrial conduction times. Atrial electromechanical delay can be calculated as the time between the beginning of the P-wave in single lead surface ECG and the beginning or the peak of atrial contraction determined via tissue Doppler imaging (TDI) echocardiography (Celik et al., 2021; Mano et al., 2014; Müller et al., 2021; Neves et al., 2018; Özer et al., 2005; Pozios et al., 2023; Russo et al., 2015). The evaluation of atrial conduction delays using TDI measurements might serve as a non-invasive atrial substrate assessment method (Celik et al., 2021). Indeed, some indices of atrial conduction delay have already been

indicated as a predictor of AF in both dogs and people (Akamatsu et al., 2020; Müller et al., 2021; Neves et al., 2018; Pessoa, 2019). However, some indices, such as the time between the beginning of the P-wave in ECG and the beginning of atrial contraction in TDI have never been studied in dogs.

Since both electrical and mechanical changes occur in atrial tissue with the progression of MMVD (Guglielmini et al., 2020), we hypothesize that atrial heterogeneity indices assessed by electrocardiogram and echocardiogram increase in the more advanced stages of the disease. We also believe that dogs with arrhythmias, cardiac remodeling, or heart failure (HF) have greater atrial conduction delay. Therefore, the aim of this study was (1) to assess electrocardiographic and echocardiographic indices of atrial conduction times in dogs with MMVD and in a control group; (2) to investigate if those variables change along the progression of the disease; (3) to check whether they can differentiate dogs with arrythmias from those with sinus rhythms; (4) to evaluate whether cardiac remodeling and HF interfere with these indices; and (5) and to test their reproducibility.

ANIMALS, MATERIALS AND METHODS

This was a cross-sectional observational study, conducted at a Veterinary Teaching facility and at a private Cardiology Service. The study was approved by the institutional Animal Care and Use Committee (protocol 047/2022) and complied with the National Institutes of Health Guide for the Use and Care of Laboratory Animals.

Animals

We included dogs admitted to both institutions between Dezember 2022 and May 2024. Inclusion criteria were dogs weighing less than 15 kg of body weight with a diagnosis of naturally occurring DMVM confirmed by echocardiographic examination, with a good quality ECG tracing, regardless of breed, age or sex. Myxomatous mitral

116 valve disease dogs were classified according to the stage of the disease as outlined in
117 the American College of Veterinary Internal Medicine consensus statement (Keene et
118 al., 2019). Although thoracic radiography was not performed in all dogs, the
119 identification of CHF in MMVD dogs in stage C was performed through clinical
120 evaluation (history of previous pulmonary edema, pulmonary crepitation with high-
121 intensity murmur in the mitral focus, clinical signs associated with heart disease) and
122 echocardiographic findings (increased indices of pulmonary venous congestion,
123 dilation of pulmonary veins, pulmonary B lines). Patients weighing 15 kg or more, who
124 had been diagnosed with congenital heart disease, other acquired cardiovascular
125 disease or any significant systemic disease, or those who received antiarrhythmic
126 treatment, were not admitted to this investigation. For the control group, clinically
127 healthy dogs weighing less than 15 kg admitted for elective procedures that did not
128 present any echocardiographic abnormalities and that were not receiving any
129 medication for cardiovascular disease were selected.

130 **Transthoracic echocardiography**

131 In both Cardiology Services, echocardiographic evaluation was performed by
132 experienced veterinary cardiologists using echocardiographic machines[a,b] equipped
133 with a range of phased-array transducers, which were selected according to the patient
134 size. A simultaneous single-lead electrocardiogram was acquired with the images.
135 Standard echocardiographic views were obtained as previously described (Boon,
136 2011), with the dogs in the right and left lateral recumbencies. Recordings were stored
137 as still frames or cine loops for the offline analysis either in the equipment or using a
138 DICON software[c]. None of the dogs were sedated.

139 The parameters included in the study were: cross-sectional left atrium diameter
140 (LA), aortic root diameter (Ao), LA-to-Ao ratio (LA:Ao) (Hansson et al., 2002), LV

internal dimension at end diastole (LVIDd) and at end-systole (LVIDs), and both of them normalized for body weight (LVIDdN, and LVIDsN) (Cornell et al., 2004), fractional shortening (FS), peak velocity of early (E) and of late (A) diastolic transmitral flow, ratio of early to late transmitral flow (E:A). Isovolumic relaxation time (IVRT) was defined as the time (in milliseconds) from the onset of the aortic valve closure spike artifact to the onset of the mitral valve opening spike artifact, obtained from the apical five-chamber view by aligning the Doppler beam midway between the LV inflow and the LV. Accordingly, ratio of early transmitral flow to IVRT (E:IVRT) was also calculated.

The tissue Doppler spectral images were obtained by placing the pulsed-wave tissue Doppler at the left ventricle lateral mitral annulus, septal mitral annulus and right ventricle lateral tricuspid annulus in apical 4-chambers images. Once the image was obtained, the first negative myocardial diastolic velocity wave was named as E’ wave (after ECG’s T wave), whereas the second negative myocardial diastolic velocity was named as A’ wave (after ECG’s P wave). The E’ wave was formed at the rapid ventricular filling phase, whereas, the A’ wave was produced during the atrial contraction. The first positive low amplitude myocardial systolic velocity was the isovolumic contraction wave; the second long wave with a positive high amplitude was called myocardial systolic velocity (S') (Rudski et al., 2010).

Echocardiographic assessment of atrial conduction times

The time between the beginning of the P-wave in ECG and the beginning of A' wave in tissue Doppler images was defined as the atrial electromechanical delay (PAb) (Celik et al., 2021; Özer et al., 2005; Russo et al., 2015). The time between the beginning of the P-wave in ECG and the peak of A' wave in tissue Doppler traces was defined as the atrial electrosystolic delay (PAp) (Mano et al., 2014; Müller et al., 2021;

Neves et al., 2018; Pozios et al., 2023).

Both PAb and PAp were measured in three points: lateral mitral annulus (L-PAb, L-PAp), septal mitral annulus (S-PAb, S-PAp), and lateral tricuspid annulus (R-PAb, R-PAp). The difference between the S-PAb and L-PAb times, and between S-PAp and L-PAp times was defined as the mechanical intra-LA conduction delay (Intra-LAb and Intra-LAp). The difference between the R-PAb and L-PAb times, and between R-PAp and L-PAp times was defined as the mechanical interatrial conduction delay (Interatrial-b and Interatrial-p, respectively). Those measurements are shown in Figure 1.

Measurement results were calculated using the average of measurements in three beats. Also, to reduce bias, the single trained operator (BCPV) that performed those measurements was blinded to the patient's clinical and electrocardiographic condition.

Electrocardiographic analyses

Good quality computer-based ECG recordings[d,e] were used for measurements. All ECG tracings were recorded continuously for at least 3 minutes, and followed recommendations described elsewhere [24]. Precordial leads had to be positioned according to Wilson's precordial lead system modified by Santilli et al., in which V1 is positioned at the first right intercostal space at the level of the costochondral junction and the sixth intercostal space used for all left side leads (V2-V6) [25].

In lead II, the following ECG variables were obtained: cardiac rhythm; minimum, maximum and mean heart rate (HR) (bpm); PQ interval; and QRS complex duration (ms).

Electrocardiographic assessment of atrial conduction times

The beginning of the P-wave was accepted as the point where the first deflection of the P-wave dismisses the isoelectric line, and the end of the P-wave was accepted

as the point where the P-wave re-intersected with the isoelectric line. P-wave duration was measured in all 12 leads. Pmax and Pmin were defined as the longest and the shortest P-wave durations within 12 leads, respectively. The difference between Pmax and Pmin was calculated as Pd.

Once again, measurement results were considered as the average of three consecutive waves examined in each lead. To reduce bias, the single trained operator (BCPV) that performed those measurements was blinded to the patient's clinical and echocardiographic condition.

Statistical analysis

All data underwent the Shapiro-Wilk normality test. Kruskal-Wallis test followed by either Dunn's *post hoc* test or an analysis of variance (ANOVA) followed by Tukey's multiple comparison test was performed to check for differences in age, body weight, HR, electrocardiographic and echocardiographic variables, and markers of atrial conduction times between controls and MMVD dogs. Chi-square test was used to evaluate association between groups and nominal categorical variables, such as sex, and presence of arrhythmias.

Student's t-test or Mann-Whitney test was performed to access the differences in markers of atrial conduction times between (a) dogs with arrhythmias and dogs with sinus rhythms; (b) dogs with supraventricular arrhythmias and dogs with sinus rhythms; (c) dogs with ventricular arrhythmias and dogs with sinus rhythms; (d) MMVD dogs with cardiac remodeling (stages B2 and C (Keene et al., 2019)) and MMVD dogs with normal sized hearts (stage B1 (Keene et al., 2019)); (e) MMVD dogs in HF (stage C (Keene et al., 2019)) and asymptomatic MMVD animals (stages B1 and B2 (Keene et al., 2019)). Of note, the arrhythmias that were included in the statistics were only those related to the pathophysiology of MMVD, such as supraventricular or ventricular

ectopies (isolated or organized), or intra- or interatrial or interventricular conduction delays (such as bifid P wave or QRS complex with bundle branch block morphology). The atrioventricular blocks observed in this study were described but were not included in the statistics.

Spearman's test was used to investigate correlations between ECG and echocardiographic surrogates of atrial conduction times, as well as to check if they correlated with epidemiological, electrocardiographic and echocardiographic variables. For the interpretation of the Spearman correlation magnitude, the following classification was adopted: correlation coefficients <0.3 (poor), 0.3 to 0.5 (fair), 0.6 to 0.8 (moderately strong) and >0.8 (very strong) [26].

Receiver operating characteristic (ROC) curves were constructed to evaluate sensitivity and specificity of markers of atrial conduction times to differentiate (a) dogs with arrhythmias identified during electrocardiography from those without rhythm disturbances; (b) dogs with supraventricular arrhythmias from those with sinus rhythm; (c) dogs with ventricular arrhythmias from those with sinus rhythm; (d) MMVD dogs with dilated hearts from those without remodeling; and (e) to distinguish MMVD dogs in HF from the asymptomatic MMVD animals.

An area under the curve (AUC) >0.7 was used as the cut-off criteria for acceptable sensitivity and specificity [27]. Youden index was used to select the two results with the best combination of sensitivity and specificity. True positive (TP), true negative (TN), false positive and false negative values were used to calculate probability variables. Positive predictive value (PPV) was calculated as TP/(TP+ false positive). Negative predictive value (NPV) was calculated as TN/(false negative +TN). Accuracy was calculated as (TP+TN)/(TP+TN+ false positive + false negative). Odds ratio was calculated as (positive likelihood ratio) / (negative likelihood ratio).

Logistic regression analyses were performed to identify predictors of (a) cardiac remodeling, (b) heart failure, (c) arrhythmias, (d) supraventricular arrhythmias, and (e) ventricular arrhythmias. Variables were selected for inclusion in the models based on a univariate analysis with a ROC curve showing an area under the curve (AUC) >0.7 and $p < 0.05$. For each logistic regression model, odds ratios with 95% confidence intervals (CI) were calculated to determine the strength of association between predictors and outcomes. Model performance was assessed using AUC, Akaike Information Criterion (AIC), classification accuracy, and Hosmer-Lemeshow goodness-of-fit test. Variables with $p > 0.05$ in the multivariable model were excluded iteratively to achieve the final models. If only one variable met the selection criteria for a given outcome, the ROC curve analysis alone was reported without regression modeling.

Lastly, to access intra-observer variability of the measurements of ventricular activation times variables, 15% of the ECG tracings or the echocardiographic images were randomly selected, and the same investigator (B.C.P.V) repeated the measurements. Bland-Altman plots were performed to analyze bias between repeated measurements. Student's t-test or Mann-Whitney test was performed to access the differences in the measurements made by the same observer. All analyzes were performed using statistical softwares[f] with default settings. Statistical significance was defined as $P < 0.05$.

RESULTS

Animals

A total of 207 dogs were evaluated, but 68 of them were excluded due to body weight of 15 kg or greater. Thus, 139 healthy and MMVD dogs met the inclusion criteria and were recruited for this study. Among them, 42/139 (30.2%) dogs were included in

the control group, 50/139 (36%) were classified as stage B1, 19/139 (13.7%) as stage B2 and 28/139 (20.1%) as stage C. Although mixed breed dogs (n=38) formed the majority of cases, several breeds were represented, including French Bulldog (n=15), Poodle, Lhasa Apso (n=14 each), Shih tzu (n=11), Yorkshire (n=10), Dachshund (n=7), Maltese (n=6), Pug, German Spitz (n=5 each), Pinscher (n=3), Chihuahua, Cocker, Beagle, Schnauzer, Whippet (n=2 each), as well as Pekingese (n=1 each).

There were 75/139 (54%) females and 64/139 (46%) males. Although no statistical difference existed between healthy and MMVD groups with regard to sex and body weight, in the advanced stages of the disease, dogs were older (Table 1).

Electrocardiographic and echocardiographic features

Left atrium, LA:Ao, LVIDd, LVIDs, LVIDdN, LVIDsN, FS, E wave, E:A, E:IVRT, E:E', maximum and mean heart rate, and duration of P-wave and QRS complex differed between groups (Table 1). Even though the presence of arrhythmias was observed in all groups, including the controls, an association existed between the severity of MMVD and the number of arrhythmias ($P < 0.0001$).

Supraventricular arrhythmias were observed in three control dogs (3.33%) (one dog with ectopic atrial rhythm, one dog with bifid P-wave and first degree atrioventricular block [AVB], and one dog with first degree atrioventricular block), three (4.76%) stage B1 dogs (one with atrial premature complex [APC], one with junctional scape beats, one with Mobitz I second degree AVB), four (17.39%) B2 dogs (three with bifid P-wave, and one with APCs), nine (31.03%) C dogs (one with first degree AVB, seven with APCs, one with APCs and bifid P-wave). Ventricular arrhythmias were observed in one (1.09%) control animal (one with ventricular premature complex [VPC]), one (1.59%) B1 animals (one with right bundle branch block), two (8.7%) B2 animals (both with VPCs) and three (10.34%) C animals (all of them with VPCs).

Markers of atrial conduction times *vs* disease stages

Tables 2 and 3 show ECG and echocardiographic markers of atrial conduction times obtained in healthy and MMVD dogs. Except for P V2, P V3, P V4, Pmin, R-PAp, intra-LAb, intra-LAp, interatrial-b, and R-PAp, all markers of atrial conduction times changed along the progression of the disease. In the advanced stages, both electrical and mechanical indices were more delayed, and the interatrial conduction delay was more pronounced (Figures 2 and 3).

Markers of atrial conduction times *vs* cardiac remodeling

All indices differed between dogs with and without cardiac remodeling, with the exception of Intra-LAb and Interatrial-b (Table 4). For the identification of cardiac remodeling, the indices that presented adequate AUC were P DII, S-PAp, P aVF, S-PAb, P aVR, P max, P V6, L-PAp, Pd, , P V5, P DI, P V1, P DIII, L-PAb and R-PAb. ROC curves of selected atrial conduction markers are shown in Figure 4. Cut-off values for each marker of atrial conduction time and its respective AUC value, p value, sensitivity, specificity and positive likelihood ratio for detecting cardiac remodeling are listed in Table 5.

Two logistic regression models were evaluated for predicting remodeling (Table 6). The first model included Pd and SPAp, both statistically significant ($p<0.05$), with odds ratios of 1.203 (95% CI: 1.074–1.387) and 1.174 (95% CI: 1.097–1.288), respectively. The model showed excellent discriminative ability (AUC=0.93, 95% CI: 0.8668–0.9911) and good fit, as indicated by a significant reduction in AIC (60.77) compared to the null model (110.9). Overall accuracy was 84.81%, with PPV of 87.50% and NPV of 82.98%. The Hosmer-Lemeshow test ($p=0.4658$) confirmed good fit.

The second model included P DII, Pd, and SPAp, with P DII being the only variable significantly associated with remodeling ($p<0.05$, OR = 1.405, 95% CI: 1.168–1.796).

316 Despite slight performance improvement (AUC=0.96, 95% CI: 0.9140–0.9968), the
317 model presented increased complexity and included non-significant variables (Pd and
318 SPAp, p>0.05). The AIC was marginally lower (46.63), and the Hosmer-Lemeshow
319 test (p=0.2674) also indicated good fit. Overall accuracy was 89.87%, with PPV of
320 93.75% and NPV of 87.23%. While the first model offered ease of use and
321 interpretation, the second model provided better predictive performance and
322 robustness, particularly when higher accuracy is required.

323 **Markers of atrial conduction times *vs* heart failure**

324 All indices differed between dogs with and without cardiac remodeling, with the
325 exception of R-PAb, R-PAp and Intra-LAb (Table 7). The variables with AUC > 0.7 for
326 the identification of dogs with HF were P DII, PDIII, P V6, P avR, Pmax, P avF, S-PAp,
327 P V5, P V1, S-PAb, P DI, Interatrial PAp, P min, P avL, P V3, P V2, L-PAp, Pd and P
328 V2 (Table 8 and Figure 5).

329 The final logistic regression model for predicting HF (Table 9) included SPAp and
330 P DII, both statistically significant ($p < 0.05$). The odds ratios were 1.060 (95% CI: 1.020
331 to 1.109) for SPAp and 1.198 (95% CI: 1.094 to 1.348) for P DII, indicating a positive
332 association with ICC. The model showed excellent discrimination (AUC = 0.8932, 95%
333 CI: 0.8200 to 0.9664) and good fit (AIC = 62.52; Hosmer-Lemeshow test, $p = 0.7589$).
334 Overall accuracy was 78.48%, with a PPV of 58.82% and an NPV of 83.87%.

335 **Markers of atrial conduction times *vs* arrhythmias**

336 <u>All arrhythmias</u>

337 For the investigation of arrhythmias, P avF presented the highest accuracy,
338 followed by P avR, P DII, Interatrial-b, Pd, Pmax, P DI, S-PAb, P V1, P avR, L-PAb, P
339 V6 (Table 10). Other variables such as L-PAp, S-PAb differed between dogs with
340 arrhythmias and dogs with sinus rhythms (Table 11), however presented a low

sensitivity and specificity.

The final logistic regression model for predicting arrhythmias included P aVF and Pd (Table 12), both statistically significant ($p < 0.05$). P aVF (OR = 1.188, 95% CI: 1.056 to 1.385) and Pd (OR = 1.116, 95% CI: 1.002 to 1.266) were positively associated with the likelihood of arrhythmias. The model showed excellent discrimination (AUC = 0.8951, 95% CI: 0.8208 to 0.9694), good fit (AIC = 57.15, Hosmer-Lemeshow p = 0.6527), and strong classification performance with 86.75% accuracy, 75% PPV, and 88% NPV.

Supraventricular arrhythmias

Most indices differed between dogs with supraventricular arrhythmias and dogs with sinus rhythms (Table 13). As shown in Table 14, the indices that showed the highest AUC for the identification of supraventricular arrhythmias were Pd, P avF, P DII, P avR, Pmax, P DI, P V6, P V5, P V1, P DIII, S-PAb, S-PAp, and L-PAb (Figure 6).

The final logistic regression model for predicting supraventricular arrhythmias included P DII and Pd (Table 14), both statistically significant ($p < 0.05$). P DII had an odds ratio of 1.125 (95% CI: 1.028 to 1.252), and Pd had an odds ratio of 1.135 (95% CI: 1.017 to 1.288), indicating positive associations with supraventricular arrhythmias. The model showed excellent discrimination (AUC = 0.8954, 95% CI: 0.8063 to 0.9846), good fit (AIC = 57.34), and strong classification performance with 91.23% accuracy, 66.67% PPV, and 92.59% NPV.

Ventricular arrhythmias

For the detection of ventricular arrhythmias, only Pd showed adequate results: AUC 0.8; P 0.0238). When applying the cut-off values of >20.67 ms and >17.17 ms, dogs with ventricular arrhythmias may be identified with 60% (23,07% to 92,89%) and 80%

(37,55% to 98,97%) sensitivity, 87,7% (78,74% to 93,15%) and 72,8% (62,28% to 81,33%) specificity, positive likelihood ratio of 4,9 and 3, PPV of 0.2 and 0.2, NPV of 1 and 1, accuracy of 86,1% and 73,3%, and odds ratio of 10,7 and 10,7, respectively. As shown in Table 15, dogs with ventricular arrhythmias also presented prolonged P wave measured in aVF, when compared to dog with sinus rhythm; however, this parameter did not show an adequate AUC.

Since only one parameter (Pd) was significant for predicting ventricular arrhythmias, logistic regression was not necessary. The ROC curve analysis was sufficient to evaluate its discriminative performance and determine the optimal cutoff point.

Correlation between markers of atrial conduction times *vs.* each other, or other variables

Although we observed correlation between echocardiographic and electrocardiographic variables of atrial activation time, no very strong correlations were found. Only a few moderately strong correlations were found between atrial activation indices and echocardiographic parameters such as P DII, P avR, P V6 and Pmax with moderately strong positive correlation with LA, LVIDd and LVIDdN (supplementary material tables A and B).

Intra-observer analyses

Atrial activation time measurements were repeated to assess intra-observer variability. They did not differ from the first measurement. P-wave dispersion showed the lowest bias and Interatrial-p showed the highest bias, as shown in Table 16.

DISCUSSION

We evaluated electrocardiographic and echocardiographic indices of atrial

391 conduction heterogeneity in dogs and investigated their behavior in different stages of
392 MMVD. We confirmed the hypothesis that these indices change with the progression
393 of the disease, and that they behave differently in dogs with arrhythmias, cardiac
394 remodeling and HF.

395 The duration and the morphology of the P-wave are straightforward methods that
396 reflect the electrophysiological properties of the atrial muscle [24]. Except for V2, P-
397 wave measured in all ECG leads increased with the progression of the MMVD (Table
398 2). In addition, P-wave durations also could adequately identify dogs with remodeled
399 hearts and dogs with HF (Tables 5 and 8). A recent paper also showed correlation
400 between P-wave duration and left cardiac remodeling indicators in dogs with MMVD
401 [28]. Although Pmin differed between groups, Pmax showed a greater increase in
402 advanced stages, therefore the difference between these indices (Pd) increased
403 progressively with the worsening of the disease. Despite the lack of good correlation
404 between Pd and the degree of LA dilation in our study and in others [9,29], our results
405 point that a Pd>13.2 ms increases 8 times the odds of having a dilated heart. The
406 findings of this study underline the importance of recognizing electrophysiological
407 markers such as Pd for their role in identifying dogs with significant cardiac remodeling.
408 The sensitivity and specificity achieved in the logistic regression model further support
409 the integration of these indices in clinical decision-making. In humans, Pd has also
410 been shown to be an indicator of HF and has been associated with frequent
411 hospitalizations and higher mortality rates [30].

412 In people, the normal value of Pd is 29 ± 9 ms [31]. The healthy dogs in this study
413 showed Pd values of 9.3 (7; 16.3) ms, which is more similar to the results also obtained
414 in dogs by Dittrich et al. (2018) (7.3 ± 2.2). Our results showed that dogs with Pd>17.2
415 ms are 15.6 or 10.7 times more likely to present supraventricular or ventricular

arrhythmias, respectively. The application of logistic regression also identified Pd and P DII as independent risk markers for supraventricular arrhythmias.These results highlight the potential of Pd as a non-invasive marker for early risk stratification in MMVD. Similar findings were reported in a previous study that documented higher Pd in dogs with mitral regurgitation and dogs with supraventricular conduction disorders as compared to healthy dogs [29]. In a recent study that evaluated people with early-onset hypertension, Pd was recognized as a good predictor of new-onset AF when using a cutoff of ≥ 35.5 ms [32]. Since Pd reflects the electrical heterogeneity of atrial tissue, the identification of dogs with ventricular rhythm disorders using this index may be related to the higher prevalence of this type of arrhythmia in the more advanced stages of MMVD, which also presents with increased Pd. In addition, the microscopic changes that occur with the worsening of the disease develop in both the atria and ventricles, which may increase the risk for electrical disorders. Valve regurgitation leads to the enlargement of the belonging atria, annulus fibrosus and ventricle. Microscopic cardiac changes include myocardial fatty replacement, immune cell infiltration, endocardial and atrial muscle fibrosis, intraparietal infarcts, and changes in arterial vessels. These processes lead to the inhomogeneous propagation of impulses in the atria which, together with the dilation of the atria, impacts on the increase of the dispersion of the P-wave [29,33,34].

In addition to electrocardiographic indices, this study also revealed that echocardiographic evaluation of atrial electromechanical activation time changes over the progression of MMVD. We found that interatrial dyssynchrony as well as all indices of LA conduction time increase with the progression of the disease, and are surrogates for cardiac remodeling and HF. This is the first study evaluating L-PAb, S-PAb, S-PAp, R-PAb and R-PAp in dogs. The only variable that has already been studied in dogs is

L-PAp, evaluated by pulsed-wave TDI (Neves et al., 2018) and color TDI [17,35]. In our study, the healthy dogs presented L-PAp similar (42.3 [37; 48.3] ms) to a previous report (47.3 ± 9.1 ms), which had also demonstrated a significant increase with the progression of MMVD (Pessoa, 2019). The present study showed that dogs with L-PAp higher than 57.3 ms or 57.8 ms may identify dogs with dilated heart or HF with an accuracy of 74.7% or 71.6% (Tables 5 and 8). As these measurements indicate the time that the electrical impulse takes to travel between the sinus node and the walls of the LA, the volume overload and dilation of this chamber associated with tissue fibrosis eventually results in a longer time for electrical propagation.

We showed that LA mechanical times are more prolonged in dogs with arrhythmias of supraventricular origin. The only two previous papers that investigated L-PAp in dogs used color TDI and concluded that it was useful for predicting the future onset of AF (Neves et al., 2018; Pessoa, 2019). Neves et al. (2018) showed that dogs with any cardiac disease that developed AF in the following six months had higher L-PAp (89.4 ± 12.5 ms) than those that did not (66.8 ± 14 ms). In the same way, Pessoa (2019) showed that MMVD dogs that developed AF in the following 2 years presented higher L-PAp (64.22 ± 16.99) in comparison to the dogs that did not (51.9 ± 9.8). Such results are consistent with a similar study with people, that proposed L-PAp as a marker of AF risk in people [36]. Although this variable was significantly more prolonged in dogs with arrhythmias than in dogs with sinus rhythms in our study, L-PAb, S-PAb and S-PAp proved to be more sensitive and specific for the identification of dogs with supraventricular arrythmias. Interestingly, another investigation also showed that L-PAb was a good predictor of paroxysmal AF in people, and presented a higher AUC in comparison with S-PAb (Akamatsu et al., 2020).

For the identification of dogs with ventricular arrhythmias, Pd emerged as the only

significant predictor. Dogs with Pd > 20.67 ms had a 10.7-fold increased likelihood of presenting with ventricular arrhythmias. A potential hypothesis to explain this finding is that both increased Pd and the frequency of ventricular arrhythmias are more commonly observed in the same population of dogs—those in more advanced stages of MMVD. This overlap may reflect the progressive electrical and structural remodeling that occurs as the disease advances, linking prolonged atrial conduction times with the increased susceptibility to ventricular electrical instability. These results further emphasize the importance of Pd as a marker for identifying dogs at higher risk of ventricular arrhythmias in the context of MMVD.

The application of logistic regression in this study was instrumental in distinguishing the independent contributions of echocardiographic and ECG variables to cardiac remodeling, HF and arrhythmias. While ROC analysis demonstrated diagnostic performance for individual variables, regression models allowed us to evaluate their predictive power after adjusting for the influence of other factors. For example, even among multiple indices with significant ROC values, logistic regression identified S-PAp and Pd as the most robust predictors of cardiac remodeling, as well as S-PAp and P DII as HF predictors, highlighting their independent association with structural heart changes in MMVD. These findings emphasize the significant role of atrial conduction disturbances in reflecting structural heart changes.

Although we observed similar results between the electrocardiographic and echocardiographic indices of atrial conduction times, we did not observe a strong correlation between them. We hypothesize that this finding might be explained by the fact that, even with the development of structural abnormalities and electrical disturbances in the atrial tissue owing to the progression of MMVD, they are not likely to occur in parallel and homogeneously. Structural remodeling encounters alterations

in atrial tissue properties, size, and cellular ultrastructure that underline the pathophysiological basis of AF. Electrical correlates of conduction disturbances include relative abnormalities in electrocardiographic or electrophysiological characteristics of vulnerability to AF (Pozios et al., 2023). Therefore, despite both processes being observed in this disease, the inhomogeneous propagation of sinus impulses detected by the ECG may not increase in the same rate as the delay in atrial electromechanical activation detected by echocardiography.

LIMITATIONS

As MMVD is a degenerative disease that is mainly seen in older dogs, group differences related to age are the main limitations of this study. Although there was no correlation between the indices studied and age, we do not know whether this difference between the groups may have influenced the investigation. Although we used the same protocol, the dogs were evaluated in two different locations, with different echocardiogram and electrocardiogram equipment. Therefore, we suggest that future studies be carried out standardizing only one piece of equipment for performing the echocardiogram and one piece of equipment for performing the electrocardiogram. Radiographic examination was not included in the standard protocol and therefore not performed in all dogs. Not using 24-hour Holter analysis for the exclusion of AF and other arrhythmias is another limitation. It was a cross-sectional study, without case follow-up, which implies the loss of information about the prognostic power of the evaluated indices.

CONCLUSIONS

Electrocardiographic and echocardiographic indices of atrial conduction heterogeneity change with the progression of MMVD. Also, selected indices are

noninvasive surrogates for the development of arrhythmias, cardiac dilation and HF. This is the first paper describing L-PAb, S-PAb, R-PAb and R-PAp values in healthy dogs and in dogs with MMVD, which may serve as a cornerstone for future investigations.

Footnotes

[a] - Philips Affiniti 50 ultrasound system equipped with 2-4, 3-8 and 4-12 MHz phased-array transducers, Andover, MA, USA.

[b] – Siemens Acuson P500 ultrasound system equipped with 2-4 and 4-8 MHz phased-array transducers, Issaquah, Washington, USA.

[c] - RadiAnt DICOM Viewer - Poznan, Wielkopolskie , Poland.

[d] – INPulse – INCardio ICV2.1 - Florianópolis, Brazil

[e] - TEB ECG PC - Tecnologia Eletrônica Brasileira, São Paulo, Brazil.

[f] - Graphpad prism 5.0 Software

REFERENCES

Abdellah, A. T., & El-Nagary, M. (2018). Prevalence of P wave dispersion and interatrial block in patients with systolic heart failure and their relationship with functional status, hospitalization and one year mortality. *The Egyptian Heart Journal*, *70*(3), 181–187. https://doi.org/10.1016/j.ehj.2018.02.006

Aiken, A. V., Goldhaber, J. I., & Chugh, S. S. (2022). Delayed intrinsicoid deflection: Electrocardiographic harbinger of heart disease. *Annals of Noninvasive Electrocardiology*, *27*(3). https://doi.org/10.1111/anec.12940

Akamatsu, K., Ito, T., Miyamura, M., Kanzaki, Y., Sohmiya, K., & Hoshiga, M. (2020). Usefulness of tissue Doppler-derived atrial electromechanical delay for identifying patients with paroxysmal atrial fibrillation. *Cardiovascular Ultrasound*, *18*(1), 22. https://doi.org/10.1186/s12947-020-00205-2

Bader, H., Garrigue, S., Lafitte, S., Reuter, S., Jaïs, P., Haïssaguerre, M., Bonnet, J., Clementy, J., & Roudaut, R. (2004). Intra-left ventricular electromechanical asynchrony. *Journal of the American College of Cardiology*, *43*(2), 248–256. https://doi.org/10.1016/j.jacc.2003.08.038

BaronToaldo, M., Guglielmini, C., Diana, A., Sarcinella, F., & Cipone, M. (2014). Feasibility and reproducibility of echocardiographic assessment of regional left atrial deformation and synchrony by tissue Doppler ultrasonographic imaging in healthy dogs. *American Journal of Veterinary Research*, *75*(1), 59–66. https://doi.org/10.2460/ajvr.75.1.59

Battaia, S., Perego, M., Perciballi, C., Cavallini, D., & Santilli, R. (2022). Noninvasive

electrocardiographic parameters to assess interventricular dyssynchrony in dogs with bundle branch blocks. *Journal of Veterinary Cardiology*, *41*, 134–144. https://doi.org/10.1016/j.jvc.2022.02.005

Bax, J. J., Ansalone, G., Breithardt, O. A., Derumeaux, G., Leclercq, C., Schalij, M. J., Sogaard, P., St. John Sutton, M., & Nihoyannopoulos, P. (2004). Echocardiographic evaluation of cardiac resynchronization therapy: ready for routine clinical use? *Journal of the American College of Cardiology*, *44*(1), 1–9. https://doi.org/10.1016/j.jacc.2004.02.055

Bax, J. J., Molhoek, S. G., van Erven, L., Voogd, P. J., Somer, S., Boersma, E., Steendijk, P., Schalij, M. J., & Van der Wall, E. E. (2003). Usefulness of myocardial tissue Doppler echocardiography to evaluate left ventricular dyssynchrony before and after biventricular pacing in patients with idiopathic dilated cardiomyopathy. *The American Journal of Cardiology*, *91*(1), 94–97. https://doi.org/10.1016/S0002-9149(02)03009-6

Bayam, E., Yıldırım, E., Kalçık, M., Karaduman, A., Kalkan, S., Güner, A., Küp, A., Kahyaoğlu, M., Yılmaz, Y., Selcuk, M., & Uyan, C. (2021). Relationship between P wave peak time and coronary artery disease severity in non-ST elevation acute coronary syndrome. *Herz*, *46*(2), 188–194. https://doi.org/10.1007/s00059-019-04859-1

Bleeker, G. B., Schalij, M. J., Molhoek, S. G., Holman, E. R., Verwey, H. F., Steendijk, P., van der Wall, E. E., & Bax, J. J. (2005). Frequency of left ventricular dyssynchrony in patients with heart failure and a narrow QRS complex. *The American Journal of Cardiology*, *95*(1), 140–142. https://doi.org/10.1016/j.amjcard.2004.08.082

Bleeker, G. B., Schalij, M. J., Molhoek, S. G., Verwey, H. F., HOLMAN, E. R., BOERSMA, E., STEENDIJK, P., VAN DER WALL, E. E., & BAX, J. J. (2004). Relationship Between QRS Duration and Left Ventricular Dyssynchrony in Patients with End-Stage Heart Failure. *Journal of Cardiovascular Electrophysiology*, *15*(5), 544–549. https://doi.org/10.1046/j.1540-8167.2004.03604.x

Boon, J. A. (2011). *Veterinary echocardiography* (J. A. Boon, Ed.). Wiley-Blackwell.

Bristow, M. R., Saxon, L. A., Boehmer, J., Krueger, S., Kass, D. A., De Marco, T., Carson, P., DiCarlo, L., DeMets, D., White, B. G., DeVries, D. W., & Feldman, A. M. (2004). Cardiac-Resynchronization Therapy with or without an Implantable Defibrillator in Advanced Chronic Heart Failure. *New England Journal of Medicine*, *350*(21), 2140–2150. https://doi.org/10.1056/NEJMoa032423

Cekirdekci, E. I., Unal Evren, E., Evren, H., & Bugan, B. (2019). R-peak time: A novel marker of depolarization in patients with Human Immunodeficiency Virus. *Journal of Electrocardiology*, *55*, 133–137. https://doi.org/10.1016/j.jelectrocard.2019.05.016

Celik, Y., Yıldırım, N., Demir, V., Alp, C., Sahin, O., & Tolga Doğru, M. (2021). Atrial electromechanical delay and p wave dispersion associated with severity of chronic obstructive pulmonary disease. *African Health Sciences*, *21*(1), 140–149. https://doi.org/10.4314/ahs.v21i1.19

Chan, Y. H. (2003). Biostatistics 104: correlational analysis. *Singapore Medical Journal*, *44*(12), 614–619.

Cheng, A., Helm, R. H., & Abraham, T. P. (2009). Pathophysiological mechanisms underlying ventricular dyssynchrony. *Europace*, *11*(Supplement 5), v10–v14. https://doi.org/10.1093/europace/eup272

Cinier, G., Yilmaz, A. S., Tekkesin, A. I., & Cetin, M. (2021). Predictors for the prolonged R wave peak time among patients with arterial hypertension. *Turk Kardiyoloji Dernegi Arsivi-Archives of the Turkish Society of Cardiology*, *49*(5), 387–394. https://doi.org/10.5543/tkda.2021.80540

Cornell, C. C., Kittleson, M. D., Della Torre, P., Häggström, J., Lombard, C. W., Pedersen, H. D., Vollmar, A., & Wey, A. (2004). Allometric scaling of M-mode cardiac measurements in normal adult dogs. *Journal of Veterinary Internal Medicine*, *18*(3), 311–321. https://doi.org/10.1892/0891-6640(2004)18<311:asomcm>2.0.co;2

Crosara, S., Borgarelli, M., Perego, M., Häggström, J., La Rosa, G., Tarducci, A., & Santilli, R. A. (2010). Holter monitoring in 36 dogs with myxomatous mitral valve disease. *Australian Veterinary Journal*, *88*(10), 386–392. https://doi.org/10.1111/j.1751-

0813.2010.00628.x
Darouian, N., Narayanan, K., Aro, A. L., Reinier, K., Uy-Evanado, A., Teodorescu, C., Gunson, K., Jui, J., & Chugh, S. S. (2016). Delayed intrinsicoid deflection of the QRS complex is associated with sudden cardiac arrest. *Heart Rhythm*, *13*(4), 927–932. https://doi.org/10.1016/j.hrthm.2015.12.022
De Vos, C. B., Weijs, B., Crijns, H. J. G. M., Cheriex, E. C., Palmans, A., Habets, J., Prins, M. H., Pisters, R., Nieuwlaat, R., & Tieleman, R. G. (2009). Atrial tissue Doppler imaging for prediction of new-onset atrial fibrillation. *Heart*, *95*(10), 835–840. https://doi.org/10.1136/hrt.2008.148528
Dhingra, R., Pencina, M. J., Wang, T. J., Nam, B.-H., Benjamin, E. J., Levy, D., Larson, M. G., Kannel, W. B., D'Agostino, R. B., & Vasan, R. S. (2006). Electrocardiographic QRS Duration and the Risk of Congestive Heart Failure. *Hypertension*, *47*(5), 861–867. https://doi.org/10.1161/01.HYP.0000217141.20163.23
Dilaveris, P. E., & Gialafos, J. E. (2001). P-Wave Dispersion: A Novel Predictor of Paroxysmal Atrial Fibrillation. *Annals of Noninvasive Electrocardiology*, *6*(2), 159–165. https://doi.org/10.1111/j.1542-474X.2001.tb00101.x
Dittrich, G., Campos, G. M. V. der B., Sousa, M. G., & Oliveira, S. T. (2018). P wave dispersion in obese dogs with and without mitral valve disease. *Ciência Rural*, *48*(10). https://doi.org/10.1590/0103-8478cr20180047
Duru, M., Seyfeli, E., Kuvandik, G., Kaya, H., & Yalcin, F. (2006). Effect of Weight Loss on P Wave Dispersion in Obese Subjects*. *Obesity*, *14*(8), 1378–1382. https://doi.org/10.1038/oby.2006.156
Erbay, A. R., Turhan, H., Yasar, A. S., Bicer, A., Senen, K., Sasmaz, H., Sabah, I., & Yetkin, E. (2005). Effects of long-term beta-blocker therapy on P-wave duration and dispersion in patients with rheumatic mitral stenosis. *International Journal of Cardiology*, *102*(1), 33–37. https://doi.org/10.1016/j.ijcard.2004.03.079
Estes, E. H. (2017). Commentary on Electrocardiographic Time to Intrinsicoid Deflection and Heart Failure: the Multi-Ethnic Study of Atherosclerosis. *Clinical Cardiology*, *40*(1), 53–53. https://doi.org/10.1002/clc.22629
Falchi, A. G., Grecchi, I., Muggia, C., & Tinelli, C. (2014). Weight loss and P wave dispersion: a preliminary study. *Obesity Research & Clinical Practice*, *8*(6), e614–e617. https://doi.org/10.1016/j.orcp.2014.08.005
Glikson, M., Nielsen, J. C., Kronborg, M. B., Michowitz, Y., Auricchio, A., Barbash, I. M., Barrabés, J. A., Boriani, G., Braunschweig, F., Brignole, M., Burri, H., Coats, A. J. S., Deharo, J. C., Delgado, V., DIller, G. P., Israel, C. W., Keren, A., Knops, R. E., Kotecha, Di., … Tolosana, J. M. (2021). 2021 ESC Guidelines on cardiac pacing and cardiac resynchronization therapy. In *European Heart Journal* (Vol. 42, Issue 35, pp. 3427–3520). Oxford University Press. https://doi.org/10.1093/eurheartj/ehab364
Gorcsan, J., Marek, J. J., & Onishi, T. (2012). The Contemporary Role of Echocardiography in Improving Patient Response to Cardiac Resynchronization Therapy. In *Current Cardiovascular Imaging Reports* (Vol. 5, Issue 6, pp. 462–472). Current Medicine Group LLC 1. https://doi.org/10.1007/s12410-012-9172-2
Gorcsan, J., & Tayal, B. (2015). Newer Echocardiographic Techniques in Cardiac Resynchronization Therapy. In *Cardiac Electrophysiology Clinics* (Vol. 7, Issue 4, pp. 609–618). W.B. Saunders. https://doi.org/10.1016/j.ccep.2015.08.013
Griffiths, L. G., Fransioli, J. R., & Chigerwe, M. (2011). Echocardiographic assessment of interventricular and intraventricular mechanical synchrony in normal dogs. *Journal of Veterinary Cardiology*, *13*(2), 115–126. https://doi.org/10.1016/j.jvc.2011.02.001
Guglielmini, C., Goncalves Sousa, M., Baron Toaldo, M., Valente, C., Bentivoglio, V., Mazzoldi, C., Bergamin, I., Drigo, M., & Poser, H. (2020). Prevalence and risk factors for atrial fibrillation in dogs with myxomatous mitral valve disease. *Journal of Veterinary Internal Medicine*, *34*(6), 2223–2231. https://doi.org/10.1111/jvim.15927
Guntekin, U., Gunes, Y., Tuncer, M., Gunes, A., Sahin, M., & Simsek, H. (2008). Long-term Follow-up of P-wave Duration and Dispersion in Patients with Mitral Stenosis. *Pacing and Clinical Electrophysiology*, *31*(12), 1620–1624. https://doi.org/10.1111/j.1540-

8159.2008.01235.x
Haghjoo, M., Bagherzadeh, A., Fazelifar, A. F., Haghighi, Z. O., Esmaielzadeh, M., Alizadeh, A., Emkanjoo, Z., Sadeghpour, A., Samiei, N., Farahani, M. M., Sadr-Ameli, M. A., Maleki, M., & Noohi, F. (2007). Prevalence of Mechanical Dyssynchrony in Heart Failure Patients with Different QRS Durations. *Pacing and Clinical Electrophysiology*, *30*(5), 616–622. https://doi.org/10.1111/j.1540-8159.2007.00722.x
Hansson, K., Häggström, J., Kvart, C., & Lord, P. (2002). LEFT ATRIAL TO AORTIC ROOT INDICES USING TWO-DIMENSIONAL AND M-MODE ECHOCARDIOGRAPHY IN CAVALIER KING CHARLES SPANIELS WITH AND WITHOUT LEFT ATRIAL ENLARGEMENT. *Veterinary Radiology & Ultrasound*, *43*(6), 568–575. https://doi.org/10.1111/j.1740-8261.2002.tb01051.x
Irdem, A., Aydın Sahin, D., Kervancioglu, M., Baspinar, O., Sucu, M., Keskin, M., & Kilinc, M. (2016). Evaluation of P-Wave Dispersion, Diastolic Function, and Atrial Electromechanical Conduction in Pediatric Patients with Subclinical Hypothyroidism. *Echocardiography*, *33*(9), 1397–1401. https://doi.org/10.1111/echo.13255
Jagannatha, G. N. P., Antara, I. M. P. S., Kosasih, A. M., Kamardi, S., & Pradnyana, I. W. A. S. (2024). P-wave peak time and P-wave dispersion in surface electrocardiography as initial predictors of new-onset atrial fibrillation in early-onset hypertension. *Hypertension Research*, *47*(1), 137–148. https://doi.org/10.1038/s41440-023-01357-0
Janus, I., Noszczyk-Nowak, A., Nowak, M., Ciaputa, R., Kandefer-Gola, M., & Pasławska, U. (2016). A comparison of the histopathologic pattern of the left atrium in canine dilated cardiomyopathy and chronic mitral valve disease. *BMC Veterinary Research*, *12*(1), 3. https://doi.org/10.1186/s12917-015-0626-z
Keene, B. W., Atkins, C. E., Bonagura, J. D., Fox, P. R., Häggström, J., Fuentes, V. L., Oyama, M. A., Rush, J. E., Stepien, R., & Uechi, M. (2019). ACVIM consensus guidelines for the diagnosis and treatment of myxomatous mitral valve disease in dogs. *Journal of Veterinary Internal Medicine*, *33*(3), 1127–1140. https://doi.org/10.1111/jvim.15488
Kirk, J. A., & Kass, D. A. (2013). Electromechanical Dyssynchrony and Resynchronization of the Failing Heart. *Circulation Research*, *113*(6), 765–776. https://doi.org/10.1161/CIRCRESAHA.113.300270
Koo, T. K., & Li, M. Y. (2016). A Guideline of Selecting and Reporting Intraclass Correlation Coefficients for Reliability Research. *Journal of Chiropractic Medicine*, *15*(2), 155–163. https://doi.org/10.1016/j.jcm.2016.02.012
Korovesis, T. G., Koutrolou-Sotiropoulou, P., & Katritsis, D. G. (2022). Arrhythmogenic Mitral Valve Prolapse. *Arrhythmia & Electrophysiology Review*, *11*. https://doi.org/10.15420/aer.2021.28
Kosar, F., Aksoy, Y., Ari, F., Keskin, L., & Sahin, I. (2008). P-Wave Duration and Dispersion in Obese Subjects. *Annals of Noninvasive Electrocardiology*, *13*(1), 3–7. https://doi.org/10.1111/j.1542-474X.2007.00194.x
Lafitte, S., Garrigue, S., Perron, J.-M., Bordachar, P., Reuter, S., Jaïs, P., Haïssaguerre, M., Clementy, J., & Roudaut, R. (2004). Improvement of left ventricular wall synchronization with multisite ventricular pacing in heart failure: a prospective study using Doppler tissue imaging. *European Journal of Heart Failure*, *6*(2), 203–212. https://doi.org/10.1016/j.ejheart.2003.10.008
Lane, R. E. (2004). Selection and optimisation of biventricular pacing: the role of echocardiography. *Heart*, *90*(suppl_6), vi10–vi16. https://doi.org/10.1136/hrt.2004.043000
Lee, J., Mizuno, M., Mizuno, T., Harada, K., & Uechi, M. (2015). Pathologic Manifestations on Surgical Biopsy and Their Correlation with Clinical Indices in Dogs with Degenerative Mitral Valve Disease. *Journal of Veterinary Internal Medicine*, *29*(5), 1313–1321. https://doi.org/10.1111/jvim.13587
LL, T., SG, T., & KK, P. (2013). ECG P wave abnormalities. *Singapore Medical Journal*, *54*(1), 4–5. https://doi.org/10.11622/smedj.2013002
Mano, H., Okumura, Y., Watanabe, I., Ohta, M., Kogawa, R., Sasaki, N., Nakai, T., Ohkubo,

715 K., Kofune, M., Nagashima, K., Sonoda, K., Haruta, H., & Hirayama, A. (2014).
716 Changes over time in echocardiographic variables and atrial electromechanical intervals
717 after ablation for atrial fibrillation. *Journal of Arrhythmia*, *30*(6), 466–472.
718 https://doi.org/10.1016/j.joa.2014.01.005
719 Mateos Pañero, M., Battaia, S., Ramera, L., Perego, M., & Santilli, R. A. (2021). R-peak time
720 in clinically healthy dogs with different thoracic conformations. *Veterinary Journal*, *268*.
721 https://doi.org/10.1016/j.tvjl.2020.105592
722 Müller, P., Weijs, B., Bemelmans, N. M. A. A., Mügge, A., Eckardt, L., Crijns, H. J. G. M.,
723 Bax, J. J., Linz, D., & den Uijl, D. W. (2021). Echocardiography-derived total atrial
724 conduction time (PA-TDI duration): risk stratification and guidance in atrial fibrillation
725 management. *Clinical Research in Cardiology*, *110*(11), 1734–1742.
726 https://doi.org/10.1007/s00392-021-01917-9
727 Ndrepepa, G., Zrenner, B., Deisenhofer, I., Karch, M., Schneider, M., Schreieck, J., &
728 Schmitt, C. (2000). Relationship between surface electrocardiogram characteristics and
729 endocardial activation sequence in patients with typical atrial flutter. *Zeitschrift Für*
730 *Kardiologie*, *89*(6), 527–537. https://doi.org/10.1007/s003920070225
731 Neves, J., Pedro, B., Christley, R., & Dukes-McEwan, J. (2018). Usefulness of pulsed-wave
732 tissue Doppler imaging at the mitral annulus for prediction of new-onset atrial fibrillation
733 in dogs. *Journal of Veterinary Cardiology*, *20*(6), 425–437.
734 https://doi.org/10.1016/j.jvc.2018.10.002
735 Noszczyk-Nowak, A. (2012). P-Wave Dispersion in Prediction of Maintenance of Sinus
736 Rhythm After an Electrical Cardioversion of Atrial Fibrillation in Dogs. *Bulletin of the*
737 *Veterinary Institute in Pulawy*, *56*(1), 99–102. https://doi.org/10.2478/v10213-012-0018-
738 0
739 Noszczyk-Nowak, A., Paslawska, U., Szalas, A., & Nicpon, J. (2008). P-WAVE DISPERSION
740 IN HEALTHY DOGS. A PRELIMINARY STUDY. *Bulletin of the Veterinary Institute in*
741 *Pulawy*, *52*, 683–688.
742 Noszczyk-Nowak, A., Szałas, A., Pasławska, U., & Nicpoń, J. (2011). Comparison of P-wave
743 dispersion in healthy dogs, dogs with chronic valvular disease and dogs with
744 disturbances of supraventricular conduction. *Acta Veterinaria Scandinavica*, *53*(1), 18.
745 https://doi.org/10.1186/1751-0147-53-18
746 Ogawa, M., Ogi, H., Miyakawa, H., Hsu, H.-H., Miyagawa, Y., & Takemura, N. (2022).
747 Evaluation of the association between electrocardiogram parameters and left cardiac
748 remodeling in dogs with myxomatous mitral valve disease. *Veterinary World*, 2072–
749 2083. https://doi.org/10.14202/vetworld.2022.2072-2083
750 Okutucu, S., Aytemir, K., & Oto, A. (2016). P-wave dispersion: What we know till now? *JRSM*
751 *Cardiovascular Disease*, *5*, 204800401663944.
752 https://doi.org/10.1177/2048004016639443
753 O'Neal, W. T., Mazur, M., Bertoni, A. G., Bluemke, D. A., Al-Mallah, M. H., Lima, J. A. C.,
754 Kitzman, D., & Soliman, E. Z. (2017). Electrocardiographic Predictors of Heart Failure
755 With Reduced Versus Preserved Ejection Fraction: The Multi-Ethnic Study of
756 Atherosclerosis. *Journal of the American Heart Association*, *6*(6).
757 https://doi.org/10.1161/JAHA.117.006023
758 O'Neal, W. T., Qureshi, W. T., Nazarian, S., Kawel-Boehm, N., Bluemke, D. A., Lima, J. A.
759 C., & Soliman, E. Z. (2016). Electrocardiographic Time to Intrinsicoid Deflection and
760 Heart Failure: The Multi-Ethnic Study of Atherosclerosis. *Clinical Cardiology*, *39*(9),
761 531–536. https://doi.org/10.1002/clc.22561
762 Özer, N., Aytemir, K., Atalar, E., Sade, E., Aksöyek, S., Övünç, K., Açýl, T., Nazlý, N.,
763 Özmen, F., Oto, A., & Kes, S. (2000). P Wave Dispersion in Hypertensive Patients with
764 Paroxysmal Atrial Fibrillation. *Pacing and Clinical Electrophysiology*, *23*(11P2), 1859–
765 1862. https://doi.org/10.1111/j.1540-8159.2000.tb07038.x
766 Özer, N., Yavuz, B., Can, I., Atalar, E., Aksöyek, S., Övünç, K., Özmen, F., & Kes, S. (2005).
767 Doppler tissue evaluation of intra-atrial and interatrial electromechanical delay and
768 comparison with P-wave dispersion in patients with mitral stenosis. *Journal of the*
769 *American Society of Echocardiography*, *18*(9), 945–948.

https://doi.org/10.1016/j.echo.2005.01.015
Pedro, B. M., Alves, J. V., Cripps, P. J., Stafford Johnson, M. J., & Martin, M. W. S. (2011). Association of QRS duration and survival in dogs with dilated cardiomyopathy: A retrospective study of 266 clinical cases. *Journal of Veterinary Cardiology*, *13*(4), 243–249. https://doi.org/10.1016/j.jvc.2011.09.003
Pérez-Riera, A. R., de Abreu, L. C., Barbosa-Barros, R., Grindler, J., Fernandes-Cardoso, A., & Baranchuk, A. (2016). P-wave dispersion: an update. *Indian Pacing and Electrophysiology Journal*, *16*(4), 126–133. https://doi.org/10.1016/j.ipej.2016.10.002
Pérez-Riera, A. R., de Abreu, L. C., Barbosa-Barros, R., Nikus, K. C., & Baranchuk, A. (2016). R-Peak Time: An Electrocardiographic Parameter with Multiple Clinical Applications. *Annals of Noninvasive Electrocardiology*, *21*(1), 10–19. https://doi.org/10.1111/anec.12323
Perry, R., De Pasquale, C. G., Chew, D. P., McGavigan, A. D., & Joseph, M. X. (2011). Tissue Doppler Derived Mechanical Dyssynchrony Does Not Change after Cardiac Resynchronization Therapy. *Echocardiography*, *28*(9), 961–967. https://doi.org/10.1111/j.1540-8175.2011.01498.x
Pessoa, R. B. (2019). *Mensuração do Tempo de Condução Atrial Total por meio da ecocardiografia tecidual em cães normais e em cães com Valvopatia Mitral Mixomatosa* [Universidade de São Paulo]. https://doi.org/10.11606/D.10.2019.tde-21112018-122807
Piccirillo, G., Moscucci, F., Mezzadri, M., Caltabiano, C., Di Diego, I., Carnovale, M., Corrao, A., Stefano, S., Scinicariello, C., Giuffrè, M., De Santis, V., Sciomer, S., Rossi, P., & Magrì, D. (2023). Electrocardiographic and other Noninvasive Hemodynamic Markers in Decompensated CHF Patients. *Journal of Cardiovascular Development and Disease*, *10*(3), 125. https://doi.org/10.3390/jcdd10030125
Ponikowski, P., Voors, A. A., Anker, S. D., Bueno, H., Cleland, J. G. F., Coats, A. J. S., Falk, V., González-Juanatey, J. R., Harjola, V.-P., Jankowska, E. A., Jessup, M., Linde, C., Nihoyannopoulos, P., Parissis, J. T., Pieske, B., Riley, J. P., Rosano, G. M. C., Ruilope, L. M., Ruschitzka, F., … van der Meer, P. (2016). 2016 ESC Guidelines for the diagnosis and treatment of acute and chronic heart failure. *European Heart Journal*, *37*(27), 2129–2200. https://doi.org/10.1093/eurheartj/ehw128
Pozios, I., Vouliotis, A. I., Dilaveris, P., & Tsioufis, C. (2023). Electro-Mechanical Alterations in Atrial Fibrillation: Structural, Electrical, and Functional Correlates. *Journal of Cardiovascular Development and Disease*, *10*(4), 149. https://doi.org/10.3390/jcdd10040149
Risum, N. (2014). Assessment of mechanical dyssynchrony in cardiac resynchronization therapy. *Dan Med J* , *61*(12), B4981.
Rodrigues, A. C. T., Tsutsui, J. M., & Mathias Jr, W. (2006). Avaliação de dissincronia cardíaca pelo ecocardiograma: estratégias para um resultado adequado Cardiac dyssynchrony in patients with heart failure: strategies for an adequate echocardiographic assessment. *Revista Brasileira de Ecocardiografia*, *19*(3), 46–51.
Rudski, L. G., Lai, W. W., Afilalo, J., Hua, L., Handschumacher, M. D., Chandrasekaran, K., Solomon, S. D., Louie, E. K., & Schiller, N. B. (2010). Guidelines for the Echocardiographic Assessment of the Right Heart in Adults: A Report from the American Society of Echocardiography. *Journal of the American Society of Echocardiography*, *23*(7), 685–713. https://doi.org/10.1016/j.echo.2010.05.010
Russo, V., Rago, A., Di Meo, F., Papa, A. A., Ciardiello, C., Cristiano, A., Calabrò, R., Russo, M. G., & Nigro, G. (2015). Atrial Septal Aneurysms and Supraventricular Arrhythmias: The Role of Atrial Electromechanical Delay. *Echocardiography*, *32*(10), 1504–1514. https://doi.org/10.1111/echo.12908
Salem, A. S., Abazeed, S. H., Elhawary, A., & Abdelmonem, A. H. (2021). Correlation Between Left Ventricular Electromechanical Delay and Body Mass Index. *European Heart Journal Supplements*, *23*(Supplement_D). https://doi.org/10.1093/eurheartj/suab069.004
Santilli, R. A., Moïse, N. S., Pariaut, R., & Perego, M. (2019). *Electrocardiography of the dog and cat: diagnosis of arrhythmias* (R. A. Santilli, N. S. Moïse, R. Pariaut, & M. Perego,

Eds.). Edra.
Santilli, R. A., Porteiro Vázquez, D. M., Gerou-Ferriani, M., Lombardo, S. F., & Perego, M. (2019). Development and assessment of a novel precordial lead system for accurate detection of right atrial and ventricular depolarization in dogs with various thoracic conformations. *American Journal of Veterinary Research*, *80*(4), 358–368. https://doi.org/10.2460/ajvr.80.4.358
Seyfeli, E., Duru, M., Kuvandık, G., Kaya, H., & Yalcin, F. (2006). Effect of obesity on P-wave dispersion and QT dispersion in women. *International Journal of Obesity*, *30*(6), 957–961. https://doi.org/10.1038/sj.ijo.0803233
Simpson, K. E., Devine, B. C., Woolley, R., Corcoran, BrendamM., & French, A. T. (2008). TIMING OF LEFT HEART BASE DESCENT IN DOGS WITH DILATED CARDIOMYOPATHY AND NORMAL DOGS. *Veterinary Radiology & Ultrasound*, *49*(3), 287–294. https://doi.org/10.1111/j.1740-8261.2008.00359.x
Sivri, F., Şencan, M., Ceyhan, B. Ö., Içen, Y. K., Coskun, M., & Aksoy, F. (2023). Prognostic value of R wave peak time in COVID-19 pneumonia. *Journal of Electrocardiology*, *80*, 91–95. https://doi.org/10.1016/j.jelectrocard.2023.05.005
Spach, M. S., Miller, W. T., Geselowitz, D. B., Barr, R. C., Kootsey, J. M., & Johnson, E. A. (1981). The discontinuous nature of propagation in normal canine cardiac muscle. Evidence for recurrent discontinuities of intracellular resistance that affect the membrane currents. *Circulation Research*, *48*(1), 39–54. https://doi.org/10.1161/01.RES.48.1.39
Spartalis, M., Tzatzaki, E., Spartalis, E., Damaskos, C., Athanasiou, A., Livanis, E., & Voudris, V. (2017). Pathophysiology and Current Evidence for Detection of Dyssynchrony. *Cardiology Research*, *8*(5), 179–183. https://doi.org/10.14740/cr598w
Spragg, D. D., & Kass, D. A. (2006). Pathobiology of Left Ventricular Dyssynchrony and Resynchronization. *Progress in Cardiovascular Diseases*, *49*(1), 26–41. https://doi.org/10.1016/j.pcad.2006.05.001
Surawicz, B., Childers, R., Deal, B. J., & Gettes, L. S. (2009). AHA/ACCF/HRS Recommendations for the Standardization and Interpretation of the Electrocardiogram. *Journal of the American College of Cardiology*, *53*(11), 976–981. https://doi.org/10.1016/j.jacc.2008.12.013
Sweeney, M. O., & Prinzen, F. W. (2006). A New Paradigm for Physiologic Ventricular Pacing. *Journal of the American College of Cardiology*, *47*(2), 282–288. https://doi.org/10.1016/j.jacc.2005.09.029
Tapia-Orihuela, R. K., Gharacholou, S. M., Asirvatham, S. J., & Munoz, F. D.-C. (2022). Electrocardiographic markers of cardiac resynchronization therapy response: delayed time to intrinsicoid deflection onset in lateral leads. *Journal of Geriatric Cardiology : JGC*, *19*(1), 21–30. https://doi.org/10.11909/j.issn.1671-5411.2022.01.009
Tidholm, A., Ljungvall, I., HÃ¶glund, K., Westling, A. B., & HÃ¤ggstrÃ¶m, J. (2009). Tissue Doppler and Strain Imaging in Dogs with Myxomatous Mitral Valve Disease in Different Stages of Congestive Heart Failure. *Journal of Veterinary Internal Medicine*, *23*(6), 1197–1207. https://doi.org/10.1111/j.1939-1676.2009.0403.x
Trikhun, P., Surachetpong, S. D., Sutayatram, S., & Buranakarl, C. (2020). Left ventricular systolic function in dogs with pulmonic stenosis. *Veterinary World*, *13*(11), 2436–2442. https://doi.org/10.14202/vetworld.2020.2436-2442
Turhan, H., Yetkin, E., Senen, K., Yilmaz, M. B., Ileri, M., Atak, R., Cehreli, S., & Kutuk, E. (2002). Effects of percutaneous mitral balloon valvuloplasty on P-wave dispersion in patients with mitral stenosis. *The American Journal of Cardiology*, *89*(5), 607–609. https://doi.org/10.1016/S0002-9149(01)02307-4
van Everdingen, W. M., Schipper, J. C., Van 'T Sant, J., Misier, K. R., Meine, M., & Cramer, M. J. (2016). Echocardiography and cardiac resynchronisation therapy, friends or foes? In *Netherlands Heart Journal* (Vol. 24, Issue 1, pp. 25–38). Bohn Stafleu van Loghum. https://doi.org/10.1007/s12471-015-0769-3
Vereckei, A., Szelényi, Z., Kutyifa, V., Zima, E., Szénási, G., Kiss, M., Katona, G., Karádi, I., & Merkely, B. (2018). Novel electrocardiographic dyssynchrony criteria improve patient

selection for cardiac resynchronization therapy. *EP Europace*, *20*(1), 97–103. https://doi.org/10.1093/europace/euw326

Vernooy, K., Verbeek, X. A. A. M., Paschar, M., & Prinzen, F. W. (2003). Relation Between Abnormal Ventricular Impulse Conduction and Heart Failure. *Journal of Interventional Cardiology*, *16*(6), 557–562. https://doi.org/10.1046/j.1540-8183.2003.01061.x

Vieira, M. L. C., Maddukuri, P. V., Phang, R. S., Pandian, N. G., Mathias Júnior, W., & Ramires, J. A. F. (2005). Demonstração do mecanismo da terapia de ressincronização ventricular com ecocardiografia tridimensional em tempo real em paciente com insuficiência cardíaca. *Arquivos Brasileiros de Cardiologia*, *85*(5). https://doi.org/10.1590/S0066-782X2005001800006

Vila, B. de C. P., Camacho, A. A., & Sousa, M. G. (2021). T-wave peak-end interval and ratio of T-wave peak-end and QT intervals: novel arrhythmogenic and survival markers for dogs with myxomatous mitral valve disease. *Journal of Veterinary Cardiology*, *35*, 25–41. https://doi.org/10.1016/j.jvc.2021.02.004

Villani, G. Q., Piepoli, M., Rosi, A., & Capucci, A. (1996). P-wave dispersion index: a marker of patients with paroxysmal atrial fibrillation. *International Journal of Cardiology*, *55*(2), 169–175. https://doi.org/10.1016/0167-5273(96)02677-0

Wang, J., Kurrelmeyer, K. M., Torre-Amione, G., & Nagueh, S. F. (2007). Systolic and Diastolic Dyssynchrony in Patients With Diastolic Heart Failure and the Effect of Medical Therapy. *Journal of the American College of Cardiology*, *49*(1), 88–96. https://doi.org/10.1016/j.jacc.2006.10.023

Yano, M., Kohno, M., Konishi, M., Takahashi, T., Seki, K., & Matsuzaki, M. (1994). Influence of left ventricular regional nonuniformity on afterload-dependent relaxation in intact dogs. *American Journal of Physiology-Heart and Circulatory Physiology*, *267*(1), H148–H154. https://doi.org/10.1152/ajpheart.1994.267.1.H148

Yu, C.-M. (2003). High prevalence of left ventricular systolic and diastolic asynchrony in patients with congestive heart failure and normal QRS duration. *Heart*, *89*(1), 54–60. https://doi.org/10.1136/heart.89.1.54

Zhu, T., Lei, M., Wang, Z., Zhang, R., Zhang, Y., Jin, W., Yu, C., Huang, C. L.-H., Liu, D., Zheng, W., Liu, Y., Quan, X., Kong, L., Liang, S., & Zhang, X. (2021). A Comparative Study of Systolic and Diastolic Mechanical Synchrony in Canine, Primate, and Healthy and Failing Human Hearts. *Frontiers in Cardiovascular Medicine*, *8*. https://doi.org/10.3389/fcvm.2021.750067

Table 1. Demographic, echocardiographic and electrocardiographic features of healthy dogs and dogs with myxomatous mitral valve disease.

	Control (n=42)	B1 (n=50)	B2 (n=19)	C (n=28)	P
Age (years)	2 (2; 5)[a]	8 (4; 11)[b]	11.2 (±2.4)[bc]	12.2 (±2.3)[c]	<0.0001**
Body weight (kg)	8.5 (±2.9)[a]	7.2 (4.7; 10)[b]	7.3 (5.3; 8;3)[b]	7.5 (±2.8)[b]	0.3172**
Females (N [%])	23 (54.8)	27 (54)	11 (57.9)	14 (50)	0.9589*
HR min (bpm)	97.9 (±26.5)[a]	90.1 (±26.9)[abc]	71.1 (±23.2)[b]	100.6 (±29.6)[c]	0.0073***
HR max (bpm)	154.8 (±30.4)	154 (140; 188)	168.9 (±49.4)	186.1 (±52.8)	0.1106**
HR med (bpm)	133 (±30.7)[ab]	122.7 (±25.3)[a]	127.8 (±35.4)[ab]	150.7 (±28.6)[b]	0.0034**
PQ interval (ms)	80 (70; 87)[a]	83 (76; 93.8)[ac]	95.7 (±16.6)[bc]	97.5 (±18.7)[b]	<0.0001**
QRS complex (ms)	54 (50; 60)[a]	55(±5.1)[a]	57.3 (±5.5)[ab]	62.5 (54; 70)[b]	<0.0001**
LA (mm)	1.9 (±0.3)[a]	1.9 (±0.3)[a]	2.6 (2.4; 3)[b]	3 (±0.5)[b]	<0.0001**
LA:Ao	1.3 (±0.1)[a]	1.3 (1.2; 1.4)[a]	2 (±0.3)[b]	2.4 (±0.4)[c]	<0.0001**
LVIDd (mm)	2.5 (±0.5)[a]	2.4 (2.2; 3)[a]	3.2 (3.1; 3.5)[b]	3.7 (3.4; 3.8)[c]	<0.0001**
LVIDs (mm)	1.5 (1.3; 1.8)[ab]	1.5 (±0.4)[a]	1.7 (±0.4)[ab]	1.8 (±0.4)[b]	0.0153**
LVIDdN	1.3 (1.2; 1.5)[a]	1.5 (±0.2)[b]	1.9 (±0.2)[c]	2 (±0.3)[d]	<0.0001***
LVIDsN	0.8 (0.7; 0.9)	0.8 (±0.1)	0.9 (±0.2)	0.9 (±0.2)	0.3796**
FS (%)	40 (±8.3)[a]	43.1 (±8.1)[a]	50 (±6.7)[b]	51.2 (±7.8)[b]	<0.0001***
E (cm/s)	71.2 (±14)[a]	64.1 (±14.2)[a]	98 (±20.2)[b]	132.9 (±23.8)[c]	<0.0001***
E:A	1.3 (1.1; 1.7)[a]	1.1 (0.8; 1.4)[b]	1.1(±0.4)[ab]	1.3 (1.1; 2.1)[a]	0.0012**
E:IVRT	1.2 (±0.4)[a]	0.9 (±0.3)[b]	1.5 (±0.6)[ac]	2.2 (1.9; 2.5)[c]	<0.0001**
E:E'	7.4 (±2.1)[ab]	6.8 (5.7; 7.8)[a]	8.9 (±3)[bc]	10.8 (8.4; 13.2)[c]	<0.0001**

Results are presented as mean ± standard deviation or median (interquartile interval). Values followed by the same letter do not differ from each other by Dunn's test or Tukey's multiple comparison test (P>0.05).

*: Chi-square test; **: Kruskal-Wallis test and Dunn test; ***: Tukey's multiple comparison test; E: Peak velocity of early diastolic transmitral flow; E:A: Ratio of early-to-late transmitral flow peak velocities; E:IVRT: ratio of early transmitral flow to isovolumetric relaxation time; E:E': Ratio of early transmitral flow peak velocity to the early mitral annulus tissue peak velocity; FS: Fractional

shortening; LA:Ao: Ratio of the left atrial dimensions to the aortic annulus dimension; LVIDdN: left ventricular end diastolic diameter normalized for body weight; LVIDsN: left ventricular end systolic diameter normalized for body weight.

Table 2. Electrical atrial conduction times in healthy dogs and dogs with myxomatous mitral valve disease.

	Control	B1	B2	C	P
P DI (ms)	43.6 (±4.9)[ab]	42.6 (±4.5)[a]	48 (±7)[bc]	50.2 (±7.3)[c]	<0.0001**
P DII (ms)	42.7 (±4.6)[a]	44.9 (±4)[ab]	50.8 (±6.9)[bc]	56 (±8.5)[c]	<0.0001**
P DIII (ms)	45.6 (±6.9)[a]	43.7 (±5.1)[a]	44.5 (±7.12)[a]	51.2 (±8.4)[b]	0.0005**
P avR (ms)	43.1 (±4.5)[a]	44 (42; 46.4)[a]	50 (±6.6)[b]	53.8 (±7.8)[b]	<0.0001*
P avL (ms)	45.2 (±7.3)[ab]	42.4 (±4.9)[a]	44.7 (±6.1)[ab]	50.3 (±10.3)[b]	0.0035**
P avF (ms)	42.1 (±4.5)[a]	44.5 (±4.4)[ab]	48.1 (±6)[bc]	53.1 (±9.3) [c]	<0.0001**
P V1 (ms)	40.2 (± 4.5)[a]	39.3 (±5)[a]	43.1 (±5.6)[ab]	47.9 (±9.4)[b]	0.0009**
P V2 (ms)	47.2 (±6.6)	46.4 (±5.5)	47.7 (39.8; 55.7)	52.8 (46.7; 58)	0.0569*
P V3 (ms)	46 (±6.2)	46.3 (±5.5)	46 (40; 51.7)	51.9 (±8.9)	0.0437*
P V4 (ms)	44.7 (±4.9)[ab]	44.8 (±5.1)[a]	46 (41.2; 49.2)[ab]	50.1 (± 8.8)[b]	0.0319*
P V5 (ms)	43.7 (±4.4)[a]	42.8 (±3.9)[a]	46 (42; 49.2)[ab]	50.4 (±7.7)[b]	0.0002*
P V6 (ms)	42 (±4.4)[a]	43 (±3.8)[a]	46.1 (±6.5)[ab]	50.6 (±6.5)[b]	<0.0001**
P min (ms)	38.5 (±3.8) [ab]	37.4 (±3.2) [a]	38.9 (±3.9) [ab]	43 (±7.9) [b]	0.0162*
P max (ms)	49.5 (±6.2)[a]	48.9 (±5)[a]	53.3 (48.2; 61.2)[ab]	60.1 (±9.7) [b]	<0.0001*
Pd (ms)	9.3 (7; 16.3)[a]	10.7 (7.7; 13.5)[a]	14.3 (9.3; 22)[ab]	17.1 (±6.2)[b]	0.0016*

Results are presented as mean ± standard deviation or median (interquartile interval). Values followed by the same letter do not differ from each other by Dunn's test or Tukey's multiple comparison test (P>0.05).

*: Kruskal-Wallis test and Dunn test; **: Tukey's multiple comparison test; Pd: P-wave dispersion; Pmax: The longest P-wave duration within 12 leads; Pmin: The shortest P-wave duration within 12 leads

Table 3. Mechanical atrial conduction times in healthy dogs and dogs with myxomatous mitral valve disease.

	Control	B1	B2	C	P
L-PAb (ms)	16.3 (11.8; 16.25)[a]	24.3 (±11.3)[a]	35 (27.7; 40.7)[b]	36.2 (±13.2) [b]	<0.0001*
L-PAp (ms)	42.3 (37; 48.3)[a]	48.4 (±10.5)[a]	61.4 (±14.9)[b]	59.9 (±14.3)[b]	<0.0001*
S-PAb (ms)	12 (5; 18.3)[a]	15.8 (±8.5)[a]	26.7 (±11.1)[b]	30.1 (±12.9)[b]	<0.0001*
S-PAp (ms)	39.89 (33.2; 45.9)[a]	44.3 (±9.8)[a]	59.9 (±18.5)[b]	62.3 (±13.4)[b]	<0.0001*
R-PAb (ms)	6 (2; 15.7)[a]	15.3 (4.3; 22.7)[ab]	24 (16.4; 26.5)[b]	20.8 (±9.4)[b]	0.0001*
R-PAp (ms)	43.8 (38.1; 49.9) [a]	48.2 (±9.7) [a]	56 (52; 61.8) [b]	48.5 (±14.5) [a]	0.1134*
Intra-LAb (ms)	-3.5 (±7.7)	-8.7 (±8.9)	-9.6 (±9.4)	-6.2 (±11.5)	0.0461**
Intra-LAp (ms)	-2 (±8.3)	-4.3 (-12.6; 0) [a]	-3.2 (±13.1) [b]	1.3 (±12.7) [a]	0.1534*
Interatrial-b (ms)	-8 (-12; -0.7)	-8.7 (-15; -4)	-12 (±9.4)	-16.7 (±12.7)	0.0185*
Interatrial-p (ms)	3 (-7.7; 12.7)[a]	0 (±11)[a]	-4.3 (-11; 6.8)[ab]	-12.7 (±14.8)[b]	<0.0001*

Results are presented as mean ± standard deviation or median (interquartile interval). Values followed by the same letter do not differ from each other by Dunn's test or Tukey's multiple comparison test (P>0.05).

*Kruskal-Wallis test and Dunn test; **Tukey's multiple comparison test; Interatrial-b: Interatrial conduction delay, calculated as the difference between the R-PAb and L-PAb times; Interatrial-p: Interatrial conduction delay, calculated as the difference between the R-PAp and L-PAp times; Intra-LAb: Intra-left atrial conduction delay, calculated as the difference between the S-PAb and L-PAb times; Intra-LAp: Intra-left atrial conduction delay, calculated as the difference between the S-PAp and L-PAp times; L-PAb: The time between the beginning of the P-wave in ECG and the beginning of A' wave in tissue Doppler traces in lateral mitral annulus; L-PAp: The time between the beginning of the P-wave in ECG and the peak of A' wave in tissue Doppler traces in lateral mitral annulus; R-PAb:The time between the beginning of the P-wave in ECG and the beginning of A' wave in tissue Doppler traces in lateral tricuspid annulus; R-PAp: The time between the beginning of the P-wave in ECG and the peak of A' wave in tissue Doppler traces in lateral tricuspid annulus; S-PAb: The time between the beginning of the P-wave in ECG and the beginning of A' wave in tissue Doppler traces in mitral septal annulus; S-PAp: The time between the beginning of the P-wave in ECG and the peak of A' wave in tissue Doppler traces in mitral septal annulus.

Table 4. Markers of atrial conduction times in dogs with normal size hearts and in dogs with dilated hearts.

	Normal size heart	Dilated heart	P
L-PAb (ms)	23.9 (±11.1)	36 (±12.6)	<0.0001**
L-PAp (ms)	47.8 (±9.9)	60.5 (±14.4)	<0.0001**
S-PAb (ms)	15.7 (±8.5)	24 (21.7; 37.5)	<0.0001*
S-PAp (ms)	44 (±9.7)	60.9 (±15.7)	<0.0001*
R-PAb (ms)	15 (4; 22.3)	23 (14.8; 27.5)	0.0015*
R-PAp (ms)	57.72 (±9.2)	54 (46; 61)	0.0208 *
Intra-LAb (ms)	-8.5 (±8.9)	-7.8 (±10.6)	0.7459**
Intra-LAp (ms)	-4 (-12.3; 0)	-0.7 (±12.9)	0.0245*
Interatrial-b (ms)	-8.8 (-15.2; -3.9)	-14.4 (±11.3)	0.0586*
Interatrial-p (ms)	0 (±11.3)	-8 (±14.2)	0.0058**
Pd (ms)	10.7 (7.7; 13.5)	15 (12; 22)	0.0007*
P DI (ms)	42.6 (±4.5)	49.3 (±7.1)	0.0001 **
P DII (ms)	44.9 (±4)	53.9 (±8.2)	<0.0001**
P DIII (ms)	42.6 (±4.5)	47.8 (±8.5)	0.0040**
P avR (ms)	43.8 (±4)	50.7 (44.8; 56.4)	<0.0001*
P avL (ms)	42.4 (±4.9)	48 (±9.2)	0.0047**
P avF (ms)	44.5 (±4.4)	51.1 (±8.4)	0.0003**
P V1 (ms)	39.3 (±5)	44.7 (40; 50.5)	0.0001*
P V2 (ms)	46.4 (±5.5)	51 (43.8; 57.5)	0.0295*
P V3 (ms)	46.3 (±5.5)	50.4 (±9.6)	0.0437**
P V4 (ms)	45.7 (±5.5)	48 (44; 53.3)	0.0316*
P V5 (ms)	42.8 (±3.9)	48 (43.3; 53)	<0.0001**
P V6 (ms)	42 (±3.8)	48.8 (±6.8)	<0.0001**
P min (ms)	37.4 (±3.2)	41.4 (±6.8)	0.0048**
P max (ms)	48.9 (±5)	56 (50.2; 56)	<0.0001*

Results are presented as mean ± standard deviation or median (interquartile interval). (P>0.05). *Mann-Whitney test; **Unpaired t test; Interatrial-b: Interatrial conduction delay, calculated as the difference between the R-PAb and L-PAb times; Interatrial-p: Interatrial conduction delay, calculated as the difference between the R-PAp and L-PAp times; Intra-LAb: Intra-left atrial conduction delay, calculated as the difference between the S-PAb and L-PAb times; Intra-LAp: Intra-left atrial conduction delay, calculated as the difference between the S-PAp and L-PAp times; L-PAb: The time between the beginning of the P-wave in ECG and the beginning of A' wave in tissue Doppler traces in lateral mitral annulus; L-PAp : The time between the beginning of the P-wave in ECG and the peak of A' wave in tissue Doppler traces in lateral mitral annulus; R-PAb:The time between the beginning of the P-wave in ECG and the beginning of A' wave in tissue Doppler traces in lateral tricuspid annulus; R-PAp: The time between the beginning of the P-wave in ECG and the peak of A' wave in tissue Doppler traces in lateral tricuspid annulus; S-PAb: The time between the beginning of the P-wave in ECG and the beginning of A' wave in tissue Doppler traces in mitral septal annulus; S-PAp: The time between the beginning of the P-wave in ECG and the peak of A' wave in tissue Doppler traces in mitral septal annulus; Pd: P-wave dispersion; Pmax: The longest P-wave duration within 12 leads; Pmin: The shortest P-

wave duration within 12 leads

Table 5. Cut-off values for each marker of atrial conduction time and its respective AUC value, P value, sensitivity, specificity, PPV, NPV, accuracy and odds ratio for detecting cardiac remodeling

Index	AUC	p	Cutoff (ms)	Sensitivity (%)	95% CI	Specificity (%)	95% CI	Positive likelihood ratio	PPV	NPV	Accuracy (%)	Odds Ratio
P DII	0.85	<0.0001	> 47.67	77.5	62.50% to 87.68%	82.8	65.45% to 92.40%	4.5	0.86	0.73	79.7	16.5
P DII	0.85	<0.0001	> 46.33	82.5	68.05% to 91.25%	75.9	57.89% to 87.78%	3.4	0.83	0.76	79.7	14.8
P avF	0.79	<0.0001	> 45.83	82.5	68.05% to 91.25%	72.4	54.28% to 85.30%	3.0	0.80	0.75	78.3	12.4
S-PAp	0.83	<0.0001	> 54.58	66.7	51.55% to 78.99%	87.0	74.33% to 93.88%	5.1	0.84	0.74	78.3	15.2
S-PAb	0.82	<0.0001	> 21.33	76.9	61.66% to 87.35%	78.6	64.06% to 88.29%	3.6	0.79	0.77	77.7	12.1
S-PAp	0.83	<0.0001	> 49.33	78.6	64.06% to 88.29%	73.9	59.74% to 84.40%	3.0	0.76	0.79	77.2	11.7
P avR	0.84	<0.0001	> 48.17	65.0	49.51% to 77.87%	89.7	73.61% to 96.42%	6.3	0.90	0.65	75.4	16.1
P avR	0.84	<0.0001	> 45.83	72.5	57.17% to 83.89%	79.3	61.61% to 90.15%	3.5	0.83	0.68	75.4	10.1
P max	0.80	<0.0001	> 49.33	85.0	70.93% to 92.94%	62.1	44.00% to 77.31%	2.2	0.76	0.75	75.4	9.3
P V6	0.81	<0.0001	> 42.33	87.2	73.29% to 94.40%	58.6	40.74% to 74.49%	2.1	0.74	0.77	75.0	9.6
L-PAp	0.79	<0.0001	> 57.33	65.9	51.14% to 78.12%	84.1	70.63% to 92.07%	4.1	0.82	0.70	74.7	10.2
S-PAb	0.82	<0.0001	> 20.67	76.9	61.66% to 87.35%	71.4	56.43% to 82.83%	2.7	0.73	0.75	74.1	8.3
P V6	0.81	<0.0001	> 46.83	61.5	45.90% to 75.11%	89.7	73.61% to 96.42%	5.9	0.89	0.63	73.5	13.9
Pd	0.74	0.0009	> 11.67	80.0	65.24% to 89.50%	62.1	44.00% to 77.31%	2.1	0.74	0.69	72.5	6.6

P avF	0.79	<0.0001	> 48.33	62.5	47.03% to 75.78%	86.2	69.44% to 94.50%	4.5	0.86	0.63	72.5	10.4
L-PAb	0.76	<0.0001	> 32.83	64.3	49.17% to 77.01%	81.0	66.70% to 90.02%	3.4	0.78	0.68	72.4	7.7
P V5	0.77	0.0001	> 45.00	71.8	56.22% to 83.46%	72.4	54.28% to 85.30%	2.6	0.78	0.66	72.1	6.7
P V5	0.77	0.0001	> 44.33	74.4	58.92% to 85.43%	69.0	50.77% to 82.72%	2.4	0.76	0.67	72.1	6.4
L-PAp	0.79	<0.0001	> 54.67	72.7	58.15% to 83.65%	70.5	55.78% to 81.84%	2.5	0.72	0.70	71.4	6.2
Pd	0.74	0.0009	> 13.17	67.5	52.02% to 79.92%	75.9	57.89% to 87.78%	2.8	0.79	0.63	71.0	6.5
P DI	0.78	<0.0001	> 47.17	60.0	44.60% to 73.65%	86.2	69.44% to 94.50%	4.4	0.86	0.61	71.0	9.4
P V1	0.77	0.0002	> 42.17	65.0	49.51% to 77.87%	79.3	61.61% to 90.15%	3.1	0.81	0.62	71.0	7.1
P max	0.80	<0.0001	> 53.00	62.5	47.03% to 75.78%	82.8	65.45% to 92.40%	3.6	0.83	0.62	71.0	8.0
P DI	0.78	<0.0001	> 43.67	82.5	68.05% to 91.25%	51.7	34.43% to 68.61%	1.7	0.70	0.68	69.6	5.1
P DIII	0.70	0.0039	> 46.17	57.5	42.20% to 71.49%	86.2	69.44% to 94.50%	4.2	0.85	0.60	69.6	8.5
P DIII	0.70	0.0039	> 43.17	72.5	57.17% to 83.89%	65.5	47.35% to 80.06%	2.1	0.74	0.63	69.6	5.0
P V1	0.77	0.0002	> 41.17	70.0	54.57% to 81.93%	69.0	50.77% to 82.72%	2.3	0.76	0.63	69.6	5.2
L-PAb	0.76	<0.0001	> 29.83	69.1	53.97% to 80.93%	69.1	53.97% to 80.93%	2.2	0.70	0.67	69.0	4.9
R-PAb	0.71	0.0018	> 23.83	48.7	33.45% to 64.11%	82.9	68.74% to 91.47%	2.8	0.72	0.61	64.2	4.0
R-PAb	0.71	0.0018	> 9.750	91.9	78.70% to 97.20%	39.0	25.66% to 54.27%	1.5	0.59	0.80	64.2	5.8

Pd: P-wave dispersion; Pmax: The longest P-wave duration within 12 leads; L-PAb: The time between the beginning of the P-wave in ECG and the beginning of A' wave in tissue Doppler traces in lateral mitral annulus; L-PAp: The time between the beginning

of the P-wave in ECG and the peak of A' wave in tissue Doppler traces in lateral mitral annulus; R-PAb: The time between the beginning of the P-wave in ECG and the beginning of A' wave in tissue Doppler traces in lateral tricuspid annulus S-PAb: The time between the beginning of the P-wave in ECG and the beginning of A' wave in tissue Doppler traces in mitral septal annulus; S-PAp: The time between the beginning of the P-wave in ECG and the peak of A' wave in tissue Doppler traces in mitral septal annulus; R-PAb:The time between the beginning of the P-wave in ECG and the beginning of A' wave in tissue Doppler traces in lateral tricuspid annulus; PPV: Positive predictive value; NPV: Negative predictive value; AUC: area under the curve.

Table 6. Comparison between the simple model (Pd + SPAp) and the complete model (P DII + Pd + SPAp) for predicting remodeling.

Variable	Estimate (β)	Standard Error	95% CI	Odds Ratio (95% CI)
Model 1				
Intercept	-10.85	2.329	-16.21 to -6.912	—
Pd	0.1847	0.06412	0.07144 to 0.3271	1.203 (1.074 to 1.387)
SPAp	0.1607	0.04039	0.09275 to 0.2531	1.174 (1.097 to 1.288)
Model 2				
Intercept	-26.61	6.975	-43.61 to -15.51	—
P DII	0.3398	0.107	0.1552 to 0.5856	1.405 (1.168 to 1.796)
Pd	0.06345	0.07778	-0.09331 to 0.2268	1.066 (0.9109 to 1.255)
SPAp	0.188	0.05748	0.09658 to 0.3275	1.207 (1.101 to 1.388)

PPV: Positive predictive value; NPV: Negative predictive value; AUC: area under the curve; AIC: Akaike information criterion; Pd: P-wave dispersion; S-PAp: The time between the beginning of the P-wave in ECG and the peak of A' wave in tissue Doppler traces in mitral septal annulus.

Table 7. Markers of atrial conduction times in dogs with heart failure and asymptomatic dogs.

	No HF	HF	P
L-PAb (ms)	29 (19; 35)	36.2 (±13.2)	0.0060*
L-PAp (ms)	52 (43; 60)	59.9 (±14.2)	0.0026*
S-PAb (ms)	19.2 (11.4; 24)	30.1 (±12.9)	0.0003*
S-PAp (ms)	46.7 (38; 55.7)	62.3 (±13.4)	<0.0001*
R-PAb (ms)	18.3 (9; 24)	20.8 (±9.4)	0.1286*
R-PAp (ms)	50 (45.7; 55.9)	48.5 (±14.5)	0.4190*
Intra-LAb (ms)	-8.8 (±9)	-6.2 (±11.5)	0.2961**
Intra-LAp (ms)	-4.1 (±11.7)	1.3 (±12.7)	0.0703**
Interatrial-b (ms)	-10.7 (±9.6)	-16.7 (±12.7)	0.0354**
Interatrial-p (ms)	-0.7 (±11.3)	-12.7 (±14.8)	0.0003**
Pd (ms)	11.3 (8.3; 15.5)	17.1 (±6.2)	0.0060*
P DI (ms)	44.7 (40.3; 47.2)	50.2 (±7.3)	0.0018*
P DII (ms)	45.7 (43; 49.7)	56 (±8.5)	<0.0001*
P DIII (ms)	42.7 (39.2; 45.7)	50.7 (±8.2)	<0.0001*
P avR (ms)	44 (42.8; 48.7)	53.5 (±7.9)	<0.0001*
P avL (ms)	43.2 (±5.4)	50.3 (±10.3)	0.0004**
P avF (ms)	45.8 (±5.3)	53.1 (±9.3)	<0.0001**
P V1 (ms)	40 (37.3; 43.3)	47.9 (±9.4)	0.0002*
P V2 (ms)	47.3 (41.7; 50.8)	52.8 (46.7; 58)	0.0071*
P V3 (ms)	45.3 (42; 50)	51.9 (±8.9)	0.0038*
P V4 (ms)	44.7 (41.3; 49.2)	50.1 (±8.8)	0.0078*
P V5 (ms)	43.3 (40.3; 47.5)	49.3 (45.7; 53.3)	0.0001*
P V6 (ms)	42.7 (40; 46.7)	50.6 (±6.5)	<0.0001*
P min (ms)	38 (±3.5)	43 (±7.9)	0.0004**
P max (ms)	48.7 (46; 54.7)	60.1 (±9.7)	<0.0001*

Results are presented as mean ± standard deviation or median (interquartile interval). (P>0.05).

*Mann-Whitney test; **Unpaired t test; Interatrial-b: Interatrial conduction delay, calculated as the difference between the R-PAb and L-PAb times; Interatrial-p: Interatrial conduction delay, calculated as the difference between the R-PAp and L-PAp times; Intra-LAb: Intra-left atrial conduction delay, calculated as the difference between the S-PAb and L-PAb times; Intra-LAp: Intra-left atrial conduction delay, calculated as the difference between the S-PAp and L-PAp times; L-PAb: The time between the beginning of the P-wave in ECG and the beginning of A' wave in tissue Doppler traces in lateral mitral annulus; L-PAp : The time between the beginning of the P-wave in ECG and the peak of A' wave in tissue Doppler traces in lateral mitral annulus; R-PAb:The time between the beginning of the P-wave in ECG and the beginning of A' wave in tissue Doppler traces in lateral tricuspid annulus; R-PAp: The time between the beginning of the P-wave in ECG and the peak of A' wave in tissue Doppler traces in lateral tricuspid annulus; S-PAb: The time between the beginning of the P-wave in ECG and the beginning of A' wave in tissue Doppler traces in mitral septal annulus; S-PAp: The time between the beginning of the P-wave in ECG and the peak of A' wave in tissue Doppler traces in mitral septal annulus; Pd: P-wave

dispersion; Pmax: The longest P-wave duration within 12 leads; Pmin: The shortest P-wave duration within 12 leads; HF: heart failure.

Table 8. Cut-off values for each marker of atrial conduction time and its respective AUC value, P value, sensitivity, specificity, PPV, NPV, accuracy and odds ratio for detecting dogs with heart failure.

Index	AUC	p	Cutoff (ms)	Sensitivity (%)	95% CI	Specificity (%)	95% CI	Positive likelihood ratio	PPV	NPV	Accuracy (%)	Odds Ratio
S-PAp (ms)	0.79	<0.0001	> 61.50	62.5	42.71% to 78.84%	89.1	79.10% to 94.60%	5.7	0.68	0.86	81.8	13.6
P DIII (ms)	0.81	<0.0001	> 46.17	79.2	59.53% to 90.76%	82.2	68.67% to 90.71%	4.5	0.70	0.88	81.2	17.6
P min (ms)	0.71	0.0042	> 43.67	54.2	35.07% to 72.11%	95.6	85.17% to 99.21%	12.2	0.87	0.80	81.2	25.4
P DIII (ms)	0.81	<0.0001	> 45.67	83.3	64.15% to 93.32%	75.6	61.33% to 85.76%	3.4	0.65	0.89	78.3	15.5
P DI (ms)	0.73	0.0022	> 49.17	62.5	42.71% to 78.84%	84.4	71.22% to 92.25%	4.0	0.68	0.81	76.8	9.1
P DII (ms)	0.83	<0.0001	> 48.83	83.3	64.15% to 93.32%	73.3	58.96% to 84.04%	3.1	0.63	0.89	76.8	13.8
P avR (ms)	0.8	<0.0001	> 49.17	70.8	50.83% to 85.09%	80.0	66.18% to 89.10%	3.5	0.65	0.84	76.8	9.7
Pmax (ms)	0.8	<0.0001	> 56.17	62.5	42.71% to 78.84%	84.4	71.22% to 92.25%	4.0	0.68	0.81	76.8	9.1
P V5 (ms)	0.77	0.0002	> 49.17	52.2	32.96% to 70.76%	88.9	76.50% to 95.16%	4.7	0.71	0.78	76.5	8.7
P V6 (ms)	0.81	<0.0001	> 46.83	73.9	53.53% to 87.45%	77.8	63.73% to 87.46%	3.3	0.63	0.85	76.5	9.9
P DII (ms)	0.83	<0.0001	> 49.67	75.0	55.10% to 88.00%	75.6	61.33% to 85.76%	3.1	0.62	0.85	75.4	9.3
P avF (ms)	0.8	<0.0001	> 48.33	75.0	55.10% to 88.00%	75.6	61.33% to 85.76%	3.1	0.62	0.85	75.4	9.3
P V1 (ms)	0.76	0.0003	> 44.00	66.7	46.71% to 82.03%	80.0	66.18% to 89.10%	3.3	0.64	0.82	75.4	8.0
P DI (ms)	0.73	0.0022	> 47.17	70.8	50.83% to 85.09%	75.6	61.33% to 85.76%	2.9	0.61	0.83	73.9	7.5
Interatrial PAp (ms)	0.73	0.0017	< -7.167	61.9	40.88% to 79.25%	77.1	65.09% to 85.81%	2.7	0.48	0.85	73.2	5.5

P avL (ms)	0.71	0.0046	> 45.83	70.8	50.83% to 85.09%	74.4	59.76% to 85.07%	2.8	0.61	0.82	73.1	7.1
P avF (ms)	0.8	<0.0001	> 46.83	83.3	64.15% to 93.32%	66.7	52.07% to 78.64%	2.5	0.57	0.88	72.5	10.0
P V2 (ms)	0.7	0.0077	> 51.50	58.3	38.83% to 75.53%	80.0	66.18% to 89.10%	2.9	0.61	0.78	72.5	5.6
P V6 (ms)	0.81	<0.0001	> 45.00	82.6	62.86% to 93.02%	66.7	52.07% to 78.64%	2.5	0.56	0.88	72.1	9.5
L-PAp (ms)	0.7	0.003	> 57.83	68.0	48.41% to 82.79%	73.0	60.97% to 82.42%	2.5	0.50	0.85	71.6	5.8
P V1 (ms)	0.76	0.0003	> 42.17	75.0	55.10% to 88.00%	68.9	54.34% to 80.47%	2.4	0.56	0.84	71.0	6.6
P V3 (ms)	0.71	0.0043	> 49.17	70.8	50.83% to 85.09%	71.1	56.63% to 82.27%	2.5	0.57	0.82	71.0	6.0
S-PAb (ms)	0.76	0.0004	> 22.67	66.7	45.37% to 82.81%	71.7	59.23% to 81.49%	2.4	0.45	0.86	70.4	5.1
P avR (ms)	0.8	<0.0001	> 45.83	79.2	59.53% to 90.76%	64.4	49.84% to 76.78%	2.2	0.54	0.85	69.6	6.9
Pd (ms)	0.7	0.0066	> 16.50	54.2	35.07% to 72.11%	77.8	63.73% to 87.46%	2.4	0.57	0.76	69.6	4.1
P V5 (ms)	0.77	0.0002	> 45.50	78.3	58.10% to 90.34%	64.4	49.84% to 76.78%	2.2	0.53	0.85	69.1	6.5
P avL (ms)	0.71	0.0046	> 45.17	70.8	50.83% to 85.09%	67.4	52.52% to 79.51%	2.2	0.55	0.81	68.7	5.0
Interatrial PAp (ms)	0.73	0.0017	< -5.250	71.4	50.04% to 86.19%	67.2	54.72% to 77.66%	2.2	0.43	0.87	68.3	5.1
P V2 (ms)	0.7	0.0077	> 49.33	70.8	50.83% to 85.09%	66.7	52.07% to 78.64%	2.1	0.53	0.81	68.1	4.9
P V3 (ms)	0.71	0.0043	> 48.83	70.8	50.83% to 85.09%	66.7	52.07% to 78.64%	2.1	0.53	0.81	68.1	4.9
S-PAb (ms)	0.76	0.0004	> 21.33	81.0	60.00% to 92.33%	63.3	50.68% to 74.38%	2.2	0.44	0.90	67.9	7.3
Pmax (ms)	0.8	<0.0001	> 49.33	95.8	79.76% to 99.79%	51.1	37.00% to 65.04%	2.0	0.51	0.96	66.7	24.1

L-PAp (ms)	0.7	0.003	> 56.33	68.0	48.41% to 82.79%	65.1	52.75% to 75.67%	1.9	0.44	0.84	65.9	4.0
S-PAp (ms)	0.79	<0.0001	> 61.50	79.2	59.53% to 90.76%	59.4	47.15% to 70.54%	1.9	0.42	0.88	64.8	5.6
P min (ms)	0.71	0.0042	> 39.17	66.7	46.71% to 82.03%	62.2	47.63% to 74.89%	1.8	0.48	0.78	63.8	3.3
Pd (ms)	0.7	0.0066	> 11.67	87.5	69.00% to 95.66%	51.1	37.00% to 65.04%	1.8	0.49	0.88	63.8	7.3

Interatrial-p: Interatrial conduction delay, calculated as the difference between the R-PAp and L-PAp times; L-PAb: The time between the beginning of the P-wave in ECG and the beginning of A' wave in tissue Doppler traces in lateral mitral annulus; L-PAp: The time between the beginning of the P-wave in ECG and the peak of A' wave in tissue Doppler traces in lateral mitral annulus; S-PAb: The time between the beginning of the P-wave in ECG and the beginning of A' wave in tissue Doppler traces in mitral septal annulus; S-PAp: The time between the beginning of the P-wave in ECG and the peak of A' wave in tissue Doppler traces in mitral septal annulus; PPV: Positive predictive value; NPV: Negative predictive value; AUC: area under the curve.

Table 9. Logistic regression model for HF prediction in dogs with MMVD

Variable	Estimate (β)	Standard Error	95% CI	Odds Ratio (95% CI)
Intercept	-13.42	3.018	-20.33 to -8.262	—
SPAp	0.05873	0.02073	0.02026 to 0.1035	1.060 (1.020 to 1.109)
P DII	0.1803	0.05263	0.08968 to 0.2989	1.198 (1.094 to 1.348)

S-PAp: The time between the beginning of the P-wave in ECG and the peak of A' wave in tissue Doppler traces in mitral septal annulus.

Table 10. Cut-off values for each marker of atrial conduction time and its respective AUC value, P value, sensitivity, specificity, PPV, NPV, accuracy and odds ratio for detecting dogs with arrhythmia.

Index	AUC	p	Cutoff (ms)	Sensitivity (%)	95% CI	Specificity (%)	95% CI	Positive likelihood ratio	PPV	NPV	Accuracy (%)	Odds Ratio
P avF	0.85	<0.0001	> 53.67	60.0	35.75% to 80.18%	94.1	85.83% to 97.69%	10.2	0.69	0.91	88.0	24.0
P DII	0.84	<0.0001	> 52.83	73.3	48.05% to 89.10%	88.4	78.75% to 94.01%	6.325	0.27	0.94	85.7	21.0
P avR	0.81	0.0002	> 53.33	60.0	35.75% to 80.18%	91.3	82.30% to 95.95%	6.9	0.60	0.91	85.7	15.8
Interatrial-b	0.74	0.0058	< -18.08	61.5	35.52% to 82.29%	88.0	79.85% to 93.19%	5.147	0.42	0.94	84.8	11.8
Pd	0.88	<0.0001	> 17.17	86.7	62.12% to 97.63%	82.6	72.02% to 89.76%	4.983	0.52	0.97	83.3	30.9
Pd	0.88	<0.0001	> 17.83	73.3	48.05% to 89.10%	85.5	75.34% to 91.93%	5.06	0.52	0.94	83.3	16.2
P max	0.82	0.0001	> 58.83	60.0	35.75% to 80.18%	87.0	77.03% to 92.98%	4.6	0.50	0.91	82.1	10.0
P DI	0.79	0.0006	> 49.67	66.7	41.71% to 84.82%	84.1	73.67% to 90.86%	4.182	0.48	0.92	81.0	10.6
S-PAp	0.70	0.0115	> 55.83	68.8	44.40% to 85.84%	81.1	72.65% to 87.44%	3.644	0.35	0.95	79.5	9.5
Interatrial-b	0.74	0.0058	< -15.75	69.2	42.37% to 87.32%	78.3	68.79% to 85.46%	3.185	0.31	0.95	77.1	8.1
P max	0.82	0.0001	> 55.00	80.0	54.81% to 92.95%	75.4	64.04% to 84.01%	3.247	0.41	0.95	76.2	12.2
L-PAb	0.7	0.0176	> 33.17	71.4	45.35% to 88.28%	76.2	67.07% to 83.48%	3.006	0.29	0.95	75.7	8.0
P V1	0.71	0.0099	> 44.50	66.7	41.71% to 84.82%	76.5	65.14% to 84.97%	2.833	0.38	0.91	74.7	6.5
P DI	0.79	0.0006	> 46.83	80.0	54.81% to 92.95%	69.6	57.92% to 79.15%	2.629	0.36	0.94	71.4	9.1
P avR	0.81	0.0002	> 48.17	73.3	48.05% to 89.10%	71.0	59.43% to 80.38%	2.53	0.35	0.92	71.4	6.7

S-PAp	0.70	0.0115	> 51.17	75.0	50.50% to 89.82%	70.8	61.49% to 78.57%	2.565	0.28	0.95	71.3	7.3
P avF	0.85	<0.0001	> 47.17	86.7	62.12% to 97.63%	67.7	55.84% to 77.56%	2.679	0.37	0.96	71.1	13.6
L-PAb	0.7	0.0176	> 30.67	71.4	45.35% to 88.28%	70.3	60.77% to 78.33%	2.405	0.25	0.95	70.4	5.9
P V6	0.70	0.0222	> 47.17	57.1	32.59% to 78.62%	72.5	60.95% to 81.61%	2.075	0.30	0.89	69.9	3.5
P DII	0.84	<0.0001	> 47.67	86.7	62.12% to 97.63%	63.8	51.98% to 74.10%	2.392	0.34	0.96	67.9	11.4
P V1	0.71	0.0099	> 42.17	80.0	54.81% to 92.95%	64.7	52.84% to 75.00%	2.267	0.33	0.94	67.5	7.3
P V6	0.70	0.0222	> 45.00	78.6	52.41% to 92.43%	62.3	50.52% to 72.82%	2.085	0.30	0.93	65.1	6.1

S-PAp: The time between the beginning of the P-wave in ECG and the peak of A' wave in tissue Doppler traces in mitral septal annulus; Pd: P-wave dispersion; Pmax: The longest P-wave duration within 12 leads; PPV: Positive predictive value; NPV: Negative predictive value; AUC: area under the curve.

Table 11. Markers of atrial conduction times in dogs with arrhythmias and dogs with sinus rhythms.

	No arrhythmia	Arrhythmia	P
L-PAb (ms)	24 (14.8; 32.8)	33.9 (±16.3)	0.0166*
L-PAp (ms)	47 (39.9; 57)	62.2 (39.5; 69.3)	0.0499*
S-PAb (ms)	17 (10.7; 24)	23.6 (±13.1)	0.0781*
S-PAp (ms)	44.7 (36.3; 54)	57.4 (±22.5)	0.0107*
R-PAb (ms)	14 (4.7; 24)	15.3 (±8.8)	0.9386*
R-PAp (ms)	48 (40.8; 54)	51.1 (±16.3)	0.3736*
Intra-LAb (ms)	-6.3 (±9.4)	-11.4 (±7.9)	0.0633**
Intra-LAp (ms)	-2.7 (-8; 3.8)	0 (±16.2)	0.9140*
Interatrial-b (ms)	-9.2 (-15; -3.4)	-19.8 (±13.6)	0.0049*
Interatrial-p (ms)	-0.9 (-8.4; 6.7)	-5.6 (±21.2)	0.5770*
Pd (ms)	11.3 (8; 15)	20 (17.3; 23.3)	<0.0001*
P DI (ms)	44.5 (±5.6)	52.1 (±8.3)	<0.0001**
P DII (ms)	45.7 (42.3; 50.3)	57.7 (±9.5)	<0.0001*
P DIII (ms)	45.4 (±6.6)	49 (±9.6)	0.042**
P avR (ms)	45.7 (±5.5)	55.1 (±9)	0.0015**
P avL (ms)	44.8 (±7.3)	49 (±10.2)	0.0717**
P avF (ms)	45.2 (±5.7)	55 (±8.4)	<0.0001**
P V1 (ms)	41.1 (±5.3)	47.8 (±10.3)	0.0005**
P V2 (ms)	47.7 (42; 52.8)	53.6 (±14.6)	0.1366*
P V3 (ms)	47.4 (±6.9)	51.2 (±11.6)	0.0960**
P V4 (ms)	44.7 (42; 49.7)	50.4 (±10.9)	0.1175*
P V5 (ms)	44.3 (41.3; 48)	49.2 (±10)	0.0988*
P V6 (ms)	43 (40; 47.5)	49.2 (±8.1)	0.0288*
P min (ms)	38.9 (±4.5)	39 (34.7; 44)	0.6748*
P max (ms)	50 (46; 55.2)	62.4 (±11.4)	<0.0001*

Results are presented as mean ± standard deviation or median (interquartile interval). (P>0.05).

*Mann-Whitney test; **Unpaired t test; Interatrial-b: Interatrial conduction delay, calculated as the difference between the R-PAb and L-PAb times; Interatrial-p: Interatrial conduction delay, calculated as the difference between the R-PAp and L-PAp times; Intra-LAb: Intra-left atrial conduction delay, calculated as the difference between the S-PAb and L-PAb times; Intra-LAp: Intra-left atrial conduction delay, calculated as the difference between the S-PAp and L-PAp times; L-PAb: The time between the beginning of the P-wave in ECG and the beginning of A' wave in tissue Doppler traces in lateral mitral annulus; L-PAp : The time between the beginning of the P-wave in ECG and the peak of A' wave in tissue Doppler traces in lateral mitral annulus; R-PAb:The time between the beginning of the P-wave in ECG and the beginning of A' wave in tissue Doppler traces in lateral tricuspid annulus; R-PAp: The time between the beginning of the P-wave in ECG and the peak of A' wave in tissue Doppler traces in lateral tricuspid annulus; S-PAb: The time between the beginning of the P-wave in ECG and the beginning of A' wave in tissue Doppler traces in mitral septal annulus; S-PAp: The time between the beginning of the P-wave in ECG and the peak of A' wave in tissue Doppler traces in mitral septal annulus; Pd: P-wave

dispersion; Pmax: The longest P-wave duration within 12 leads; Pmin: The shortest P-wave duration within 12 leads.

Table 12. Logistic regression model for arrhythmia prediction in dogs.

Variable	Estimate (β)	Standard Error	95% CI	Odds Ratio (95% CI)
Intercept	-11.76	3.268	-19.23 to -6.301	—
P aVF	0.1719	0.06885	0.05469 to 0.3256	1.188 (1.056 to 1.385)
Pd	0.1099	0.05869	0.001530 to 0.2357	1.116 (1.002 to 1.266)

Pd: P-wave dispersion

Table 13. Markers of atrial conduction times in dogs with supraventricular arrhythmia and dogs with sinus rhythm.

	No arrhythmia	Arrhythmia	P
L-PAb (ms)	25 (15.7; 33.5)	35.4 (±15.4)	0.0078*
L-PAp (ms)	50 (42.3; 60)	57.7 (±17.8)	0.0591*
S-PAb (ms)	15.8 (8.7; 24)	26.3 (±11.2)	0.004*
S-PAp (ms)	45.3 (38; 54.8)	57.2 (±19)	0.0027*
R-PAb (ms)	13.3 (3.3; 23.7)	18.1 (±8.7)	0.1659*
R-PAp (ms)	50 (44.7; 60.5)	52.6 (±17.2)	0.8727*
Intra-LAb (ms)	-7.9 (±10.2)	-8.4 (±8.5)	0.85**
Intra-LAp (ms)	-4.7 (±11.4)	-4.8 (-13.7; 5)	0.99*
Interatrial-b (ms)	-11.1 (±10)	-17 (±15.7)	0.055**
Interatrial-p (ms)	0.1 (±12.4)	-5.8(±22.2)	0.0985**
Pd (ms)	11.3 (8; 15)	22.4 (±7.4)	<0.0001*
P DI (ms)	44.6 (± 5.5)	53.4 (±7.5)	<0.0001**
P DII (ms)	46.6 (±5.7)	60.2 (±9.6)	<0.0001**
P DIII (ms)	43.8 (±6)	52.5 (±10.9)	0.0002**
P avR (ms)	44.3 (42.8; 49)	56.8 (±9.3)	<0.0001*
P avL (ms)	44 (39.3; 49.7)	50.5 (±11.3)	0.1402*
P avF (ms)	45.3 (±5.6)	56.8 (±8.9)	<0.0001**
P V1 (ms)	40 (37.8; 44.1)	49.6 (±11.4)	0.0075*
P V2 (ms)	48 (48; 84.3)	54.8 (±16.4)	0.1632*
P V3 (ms)	47.3 (42.7; 51.7)	52.8 (±12.2)	0.1334*
P V4 (ms)	44.7 (42; 49.7)	52.1 (±11.8)	0.0404*
P V5 (ms)	44.7 (41.3; 48)	52.3 (±10.1)	0.0047*
P V6 (ms)	43.3 (40; 47.5)	52.3 (±6.9)	0.0006*
P min (ms)	38.9 (±4.5)	42.4 (±9.8)	0.0547**
P max (ms)	50 (46; 55.2)	64.8 (±12.3)	0.0001*

Results are presented as mean ± standard deviation or median (interquartile interval). (P>0.05).

*Mann-Whitney test; **Unpaired t test; Interatrial-b: Interatrial conduction delay, calculated as the difference between the R-PAb and L-PAb times; Interatrial-p: Interatrial conduction delay, calculated as the difference between the R-PAp and L-PAp times; Intra-LAb: Intra-left atrial conduction delay, calculated as the difference between the S-PAb and L-PAb times; Intra-LAp: Intra-left atrial conduction delay, calculated as the difference between the S-PAp and L-PAp times; L-PAb: The time between the beginning of the P-wave in ECG and the beginning of A' wave in tissue Doppler traces in lateral mitral annulus; L-PAp : The time between the beginning of the P-wave in ECG and the peak of A' wave in tissue Doppler traces in lateral mitral annulus; R-PAb:The time between the beginning of the P-wave in ECG and the beginning of A' wave in tissue Doppler traces in lateral tricuspid annulus; R-PAp: The time between the beginning of the P-wave in ECG and the peak of A' wave in tissue Doppler traces in lateral tricuspid annulus; S-PAb: The time between the beginning of the P-wave in ECG and the beginning of A' wave in tissue Doppler traces in mitral septal annulus; S-PAp: The time between the beginning of the P-wave in ECG and the peak of A' wave in tissue Doppler traces in mitral septal annulus; Pd: P-wave

dispersion; Pmax: The longest P-wave duration within 12 leads; Pmin: The shortest P-wave duration within 12 leads.

Table 14. Cut-off values for each marker of atrial conduction time and its respective AUC value. P value. sensitivity. specificity. PPV. NPV. accuracy and odds ratio for detecting dogs with supraventricular arrhythmias.

Index	AUC	p	Cutoff (ms)	Sensitivity (%)	95% CI	Specificity (%)	95% CI	Positive likelihood ratio	PPV	NPV	Accuracy (%)	Odds Ratio
P avF	0.88	<0.0001	> 53.67	72.7	43.44% to 90.25%	94.1	85.83% to 97.69%	12.4	0.57	0.96	89.4	30.2
P max	0.84	0.0003	> 61.67	63.6	35.38% to 84.83%	94.2	86.02% to 97.72%	11.0	0.47	0.93	85.2	12.5
Pd	0.89	<0.0001	> 17.83	81.8	52.30% to 96.77%	85.5	75.34% to 91.93%	5.6	0.41	0.95	81.5	13.2
P DII	0.88	<0.0001	> 53.67	81.8	52.30% to 96.77%	89.9	80.51% to 95.00%	8.1	0.50	0.97	81.2	33.0
P DIII	0.74	0.0109	> 50.67	54.6	28.01% to 78.73%	84.6	73.94% to 91.42%	3.5	0.35	0.92	80.5	6.6
P DI	0.83	0.0005	> 49.67	72.7	43.44% to 90.25%	84.1	73.67% to 90.86%	4.6	0.36	0.95	80.2	11.6
P avR	0.85	0.0002	> 50.67	72.7	43.44% to 90.25%	84.1	73.67% to 90.86%	4.6	0.36	0.95	80.2	11.6
Pd	0.89	<0.0001	> 17.17	90.9	62.26% to 99.53%	82.6	72.02% to 89.76%	5.2	0.39	0.96	79.6	15.6
P avF	0.88	<0.0001	> 49.33	81.8	52.30% to 96.77%	79.4	68.36% to 87.32%	4.0	0.35	0.97	77.7	15.1
S-PAp	0.72	0.0068	> 55.83	71.4	45.35% to 88.28%	79.3	72.29% to 84.82%	3.4	0.25	0.96	76.9	7.1
P V5	0.77	0.006	> 48.33	70.0	39.68% to 89.22%	76.8	65.60% to 85.19%	3.0	0.29	0.95	76.5	8.0
P DII	0.88	<0.0001	> 51.00	81.8	52.30% to 96.77%	76.8	65.60% to 85.19%	3.5	0.32	0.97	75.6	13.3
P avR	0.85	0.0002	> 49.17	81.8	52.30% to 96.77%	76.8	65.60% to 85.19%	3.5	0.32	0.97	75.6	13.3
P DI	0.83	0.0005	> 47.83	81.8	52.30% to 96.77%	75.4	64.04% to 84.01%	3.3	0.31	0.96	74.4	12.4

P V1	0.75	0.0088	> 44.50	72.7	43.44% to 90.25%	76.5	65.14% to 84.97%	3.1	0.30	0.95	74.1	7.7
L-PAb	0.71	0.0138	> 33.17	75.0	46.77% to 91.11%	75.5	68.06% to 81.67%	3.1	0.23	0.96	73.7	7.5
P V5	0.77	0.006	> 47.67	80.0	49.02% to 96.45%	71.0	59.43% to 80.38%	2.8	0.28	0.96	72.9	10.3
L-PAb	0.71	0.0138	> 32.83	75.0	46.77% to 91.11%	74.8	67.36% to 81.08%	3.0	0.22	0.96	72.8	7.1
P V6	0.82	0.0011	> 47.83	70.0	39.68% to 89.22%	78.3	67.18% to 86.36%	3.2	0.25	0.93	70.1	4.4
P max	0.84	0.0003	> 55.00	81.8	52.30% to 96.77%	75.4	64.04% to 84.01%	3.3	0.28	0.94	69.4	6.1
S-PAp	0.72	0.0068	> 51.25	78.6	52.41% to 92.43%	67.3	59.67% to 74.10%	2.4	0.20	0.96	67.8	6.1
P DIII	0.74	0.0109	> 45.67	72.7	43.44% to 90.25%	66.2	54.04% to 76.47%	2.1	0.24	0.94	65.9	4.9
P V1	0.75	0.0088	> 42.33	81.8	52.30% to 96.77%	66.2	54.34% to 76.29%	2.4	0.24	0.96	64.7	7.4
P V6	0.82	0.0011	> 45.83	90.0	59.58% to 99.49%	63.8	51.98% to 74.10%	2.5	0.24	0.96	61.7	8.3
S-PAb	0.72	0.0092	> 18.50	84.6	57.77% to 97.27%	57.6	49.47% to 65.41%	2.0	0.16	0.96	55.1	4.9
S-PAb	0.72	0.0092	> 22.67	69.2	42.37% to 87.32%	71.5	63.67% to 78.26%	2.4	0.10	0.88	15.6	0.8

L-PAb: The time between the beginning of the P-wave in ECG and the beginning of A' wave in tissue Doppler traces in lateral mitral annulus; S-PAb: The time between the beginning of the P-wave in ECG and the beginning of A' wave in tissue Doppler traces in mitral septal annulus; S-PAp: The time between the beginning of the P-wave in ECG and the peak of A' wave in tissue Doppler traces in mitral septal annulus; Pd: P-wave dispersion; Pmax: The longest P-wave duration within 12 leads; PPV: Positive predictive value; NPV: Negative predictive value; AUC: area under the curve.

Table 15. Markers of atrial conduction times in dogs with ventricular arrhythmia and dogs with sinus rhythm.

	No arrhytmia	Arrhytmia	P
L-PAb (ms)	25 (15.9; 35)	35.1 (±20.6)	0.2231*
L-PAp (ms)	47.8 (40.4; 59)	61.1 (±14.4)	0.0802*
S-PAb (ms)	18.7 (11.3; 25)	20.6 (±15.1)	0.7177*
S-PAp (ms)	45.7 (±37.2)	60.5 (±23.8)	0.1072**
R-PAb (ms)	14.2 (5.3; 24)	15.5 (±10.6)	0.9776*
R-PAp (ms)	48.3 (40.8; 54.5)	55.1 (±12.3)	0.2838*
Intra-left atrial PAb (ms)	-6.6 (±9.4)	-14.5 (±6.4)	0.0998**
Intra-left atrial PAp (ms)	-2.7 (-9.1; -2.7)	-0.6 (±15)	0.687*
Interatrial PAb (ms)	-9.3 (-16; -3.7)	-19.6 (±12.4)	0.0962*
Interatrial PAp (ms)	-0.8 (-9.5; 6.7)	-6.4 (±12.8)	0.5558*
Pd (ms)	12 (8.7; 17.5)	19.2 (±3.5)	0.0206*
P DI (ms)	44.7 (41; 49.3)	49.6 (±9.4)	0.1826*
P DII (ms)	46 (42.7; 51.7)	54.9 (±9.8)	0.3322*
P DIII (ms)	44.7 (±7.1)	49.3 (±12.3)	0.1815**
P avR (ms)	44.7 (43.2; 50)	53.7 (±9.9)	0.1833*
P avL (ms)	44.47 (39.3; 50)	47.9 (±8.8)	0.2885*
P avF (ms)	46.6 (±7)	55.2 (±12.2)	0.0135**
P V1 (ms)	41 (38; 45.5)	45.9 (±7.7)	0.212*
P V2 (ms)	48 (42.3; 53.3)	50.7 (±7.6)	0.8325*
P V3 (ms)	47.7 (42.7; 52)	48.3 (±9.2)	0.9409*
P V4 (ms)	46 (42; 50)	47.7 (±7.5)	0.9715*
P V5 (ms)	45.3 (41.3; 49)	44 (±6.7)	0.2436*
P V6 (ms)	44.2 (40; 48)	45 (±9.2)	0.7751*
P min (ms)	38.7 (35.5; 41.7)	40.9 (±7.2)	0.9234*
P max (ms)	50.7 (47.2; 57.2)	60.1 (±10)	0.0718*

*Mann-Whitney test; **Unpaired t test; Interatrial-b: Interatrial conduction delay, calculated as the difference between the R-PAb and L-PAb times; Interatrial-p: Interatrial conduction delay, calculated as the difference between the R-PAp and L-PAp times; Intra-

LAb: Intra-left atrial conduction delay, calculated as the difference between the S-PAb and L-PAb times; Intra-LAp: Intra-left atrial conduction delay, calculated as the difference between the S-PAp and L-PAp times; L-PAb: The time between the beginning of the P-wave in ECG and the beginning of A' wave in tissue Doppler traces in lateral mitral annulus; L-PAp : The time between the beginning of the P-wave in ECG and the peak of A' wave in tissue Doppler traces in lateral mitral annulus; R-PAb:The time between the beginning of the P-wave in ECG and the beginning of A' wave in tissue Doppler traces in lateral tricuspid annulus; R-PAp: The time between the beginning of the P-wave in ECG and the peak of A' wave in tissue Doppler traces in lateral tricuspid annulus; S-PAb: The time between the beginning of the P-wave in ECG and the beginning of A' wave in tissue Doppler traces in mitral septal annulus; S-PAp: The time between the beginning of the P-wave in ECG and the peak of A' wave in tissue Doppler traces in mitral septal annulus; Pd: P-wave dispersion; Pmax: The longest P-wave duration within 12 leads; Pmin: The shortest P-wave duration within 12 leads

Table 16. Intra-observer bias and difference in markers of atrial conduction times in dogs.

	Bias	SD of Bias	95% Limits of Agreement	P
Intra-LAb (ms)	0.4769	6.558	-11.27 to 14.43	0.4769**
Intra-LAp (ms)	-0.644	6.635	-13.65 to 12.36	0.6569*
Interatrial-b (ms)	0.4417	8.156	-15.54 to 16.43	0.5793*
Interatrial-p (ms)	-1.039	10.52	-21.65 to 19.58	0.6676**
Pd (ms)	0.1935	4.906	-9.42 to 9.809	0.7616*

*Mann-Whitney test; **Unpaired t test; Interatrial-b: Interatrial conduction delay, calculated as the difference between the R-PAb and L-PAb times; Interatrial-p: Interatrial conduction delay, calculated as the difference between the R-PAp and L-PAp times; Intra-LAb: Intra-left atrial conduction delay, calculated as the difference between the S-PAb and L-PAb times; Intra-LAp: Intra-left atrial conduction delay, calculated as the difference between the S-PAp and L-PAp times; Pd: P-wave dispersion; SD: standard deviation

FIGURE LEGENDS

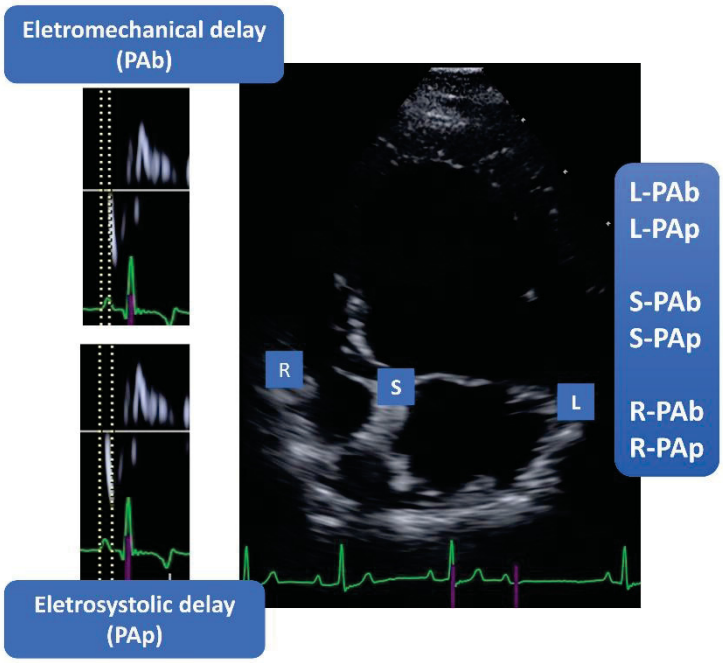

Mechanical delay in left intra-atrial conduction

Intra-LAb = (S-PAb) – (L-PAb)

Intra-LAp = (S-PAp) – (L-PAp)

Mechanical delay in interatrial conduction

Interatrial-b = (R-PAb) - (L-PAb)

Interatrial-p = (R-PAp) - (L-PAp)

Figure 1. The time between the beginning of the P-wave in ECG and the beginning or the peak of A' wave in tissue Doppler images were defined as the atrial electromechanical delay (PAb) or the atrial electrosystolic delay (PAp). Both PAb and PAp were measured in three points: lateral mitral annulus (L-PAb, L-PAp), septal mitral annulus (S-PAb, S-PAp), and lateral tricuspid annulus (R-PAb, R-PAp). The difference between the S-PAb and L-PAb times, and between S-PAp and L-PAp times was defined as the mechanical intra-left atrial conduction delay (Intra-LAb and Interatrial-p). The difference between the R-PAb and L-PAb times, and between R-PAp and L-PAp times was defined as the mechanical interatrial conduction delay (Interatrial-b and Interatrial-p, respectively).

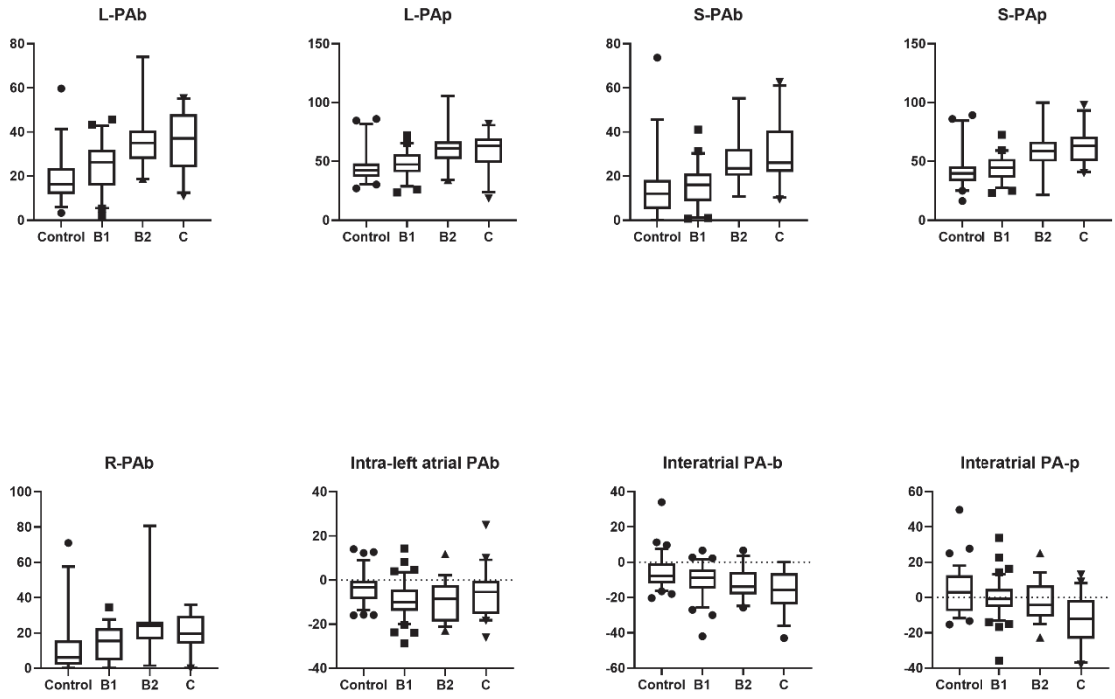

Figure 2. Echocardiographic indices of atrial conduction times in healthy dogs and dogs in different stages of myxomatous mitral valve disease. Results are presented in milliseconds. L-PAb: time between the beginning of the P-wave in ECG and the beginning of A' wave in tissue Doppler images obtained at the lateral mitral annulus; L-PAp: time between the beginning of the P-wave in ECG and the peak of A' wave in tissue Doppler images obtained in lateral mitral annulus; S-PAb: time between the beginning of the P-wave in ECG and the beginning of A' wave in tissue Doppler images obtained in mitral septal annulus; S-PAp: time between the beginning of the P-wave in ECG and the peak of A' wave in tissue Doppler images obtained in mitral septal annulus; R-PAb: The time between the beginning of the P-wave in ECG and the beginning of A' wave in tissue Doppler traces in lateral tricuspid annulus; Interatrial-b: Interatrial conduction delay, calculated as the difference between the R-PAb and L-PAb times; Interatrial-p: Interatrial conduction delay, calculated as the difference between the R-PAp and L-PAp times; Intra-LAb: Intra-left atrial conduction delay, calculated as the difference between the S-PAb and L-PAb times.

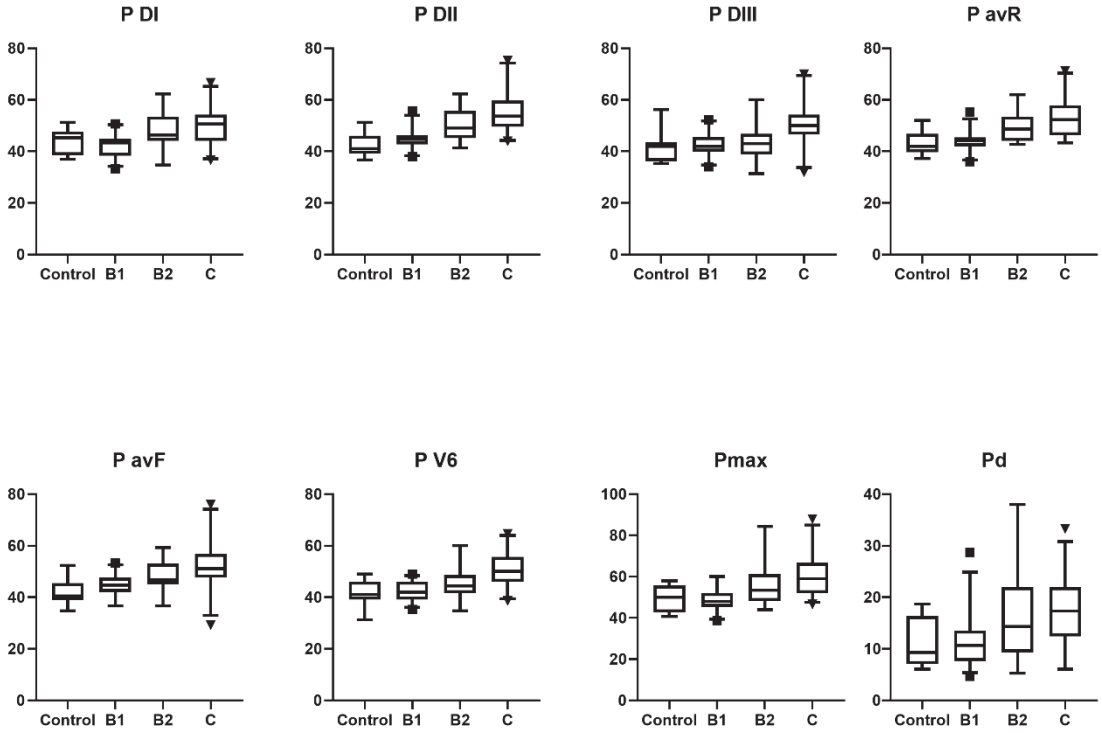

Figure 3. Electrocardiographic indices of atrial conduction times in healthy dogs and dogs in different stages of myxomatous mitral valve disease. Results are presented in milliseconds. Pd: P-wave dispersion; Pmax: The longest P-wave duration within 12 leads.

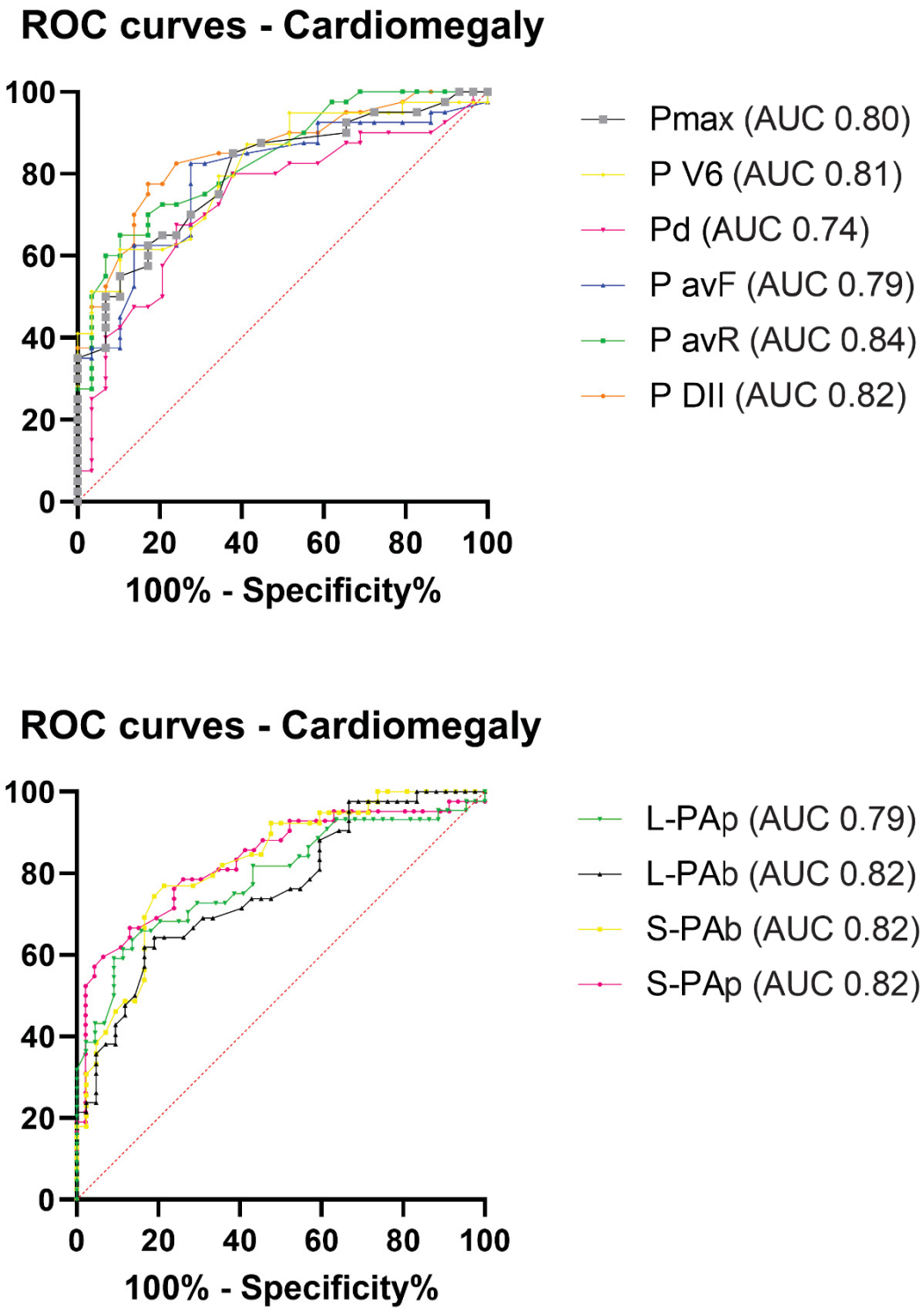

Figure 4. Receiver operating characteristic curves constructed to assess sensitivity and specificity of atrial conduction heterogeneity markers for differentiation of dogs presenting cardiomegaly and dogs with normal sized hearts. ROC: Receiver operating characteristic curve; L-PAb: time between the beginning of the P-wave in ECG and the beginning of A' wave in tissue Doppler images obtained at the lateral mitral annulus; L-PAp: time between the beginning of the P-wave in ECG and the peak of A' wave in tissue Doppler images obtained in lateral mitral annulus; obtained in lateral mitral

annulus; S-PAb: time between the beginning of the P-wave in ECG and the beginning of A' wave in tissue Doppler images obtained in mitral septal annulus; S-PAp: time between the beginning of the P-wave in ECG and the peak of A' wave in tissue Doppler images obtained in mitral septal annulus; Pd: P-wave dispersion; Pmax: The longest P-wave duration within 12 leads; AUC: area under the curve.

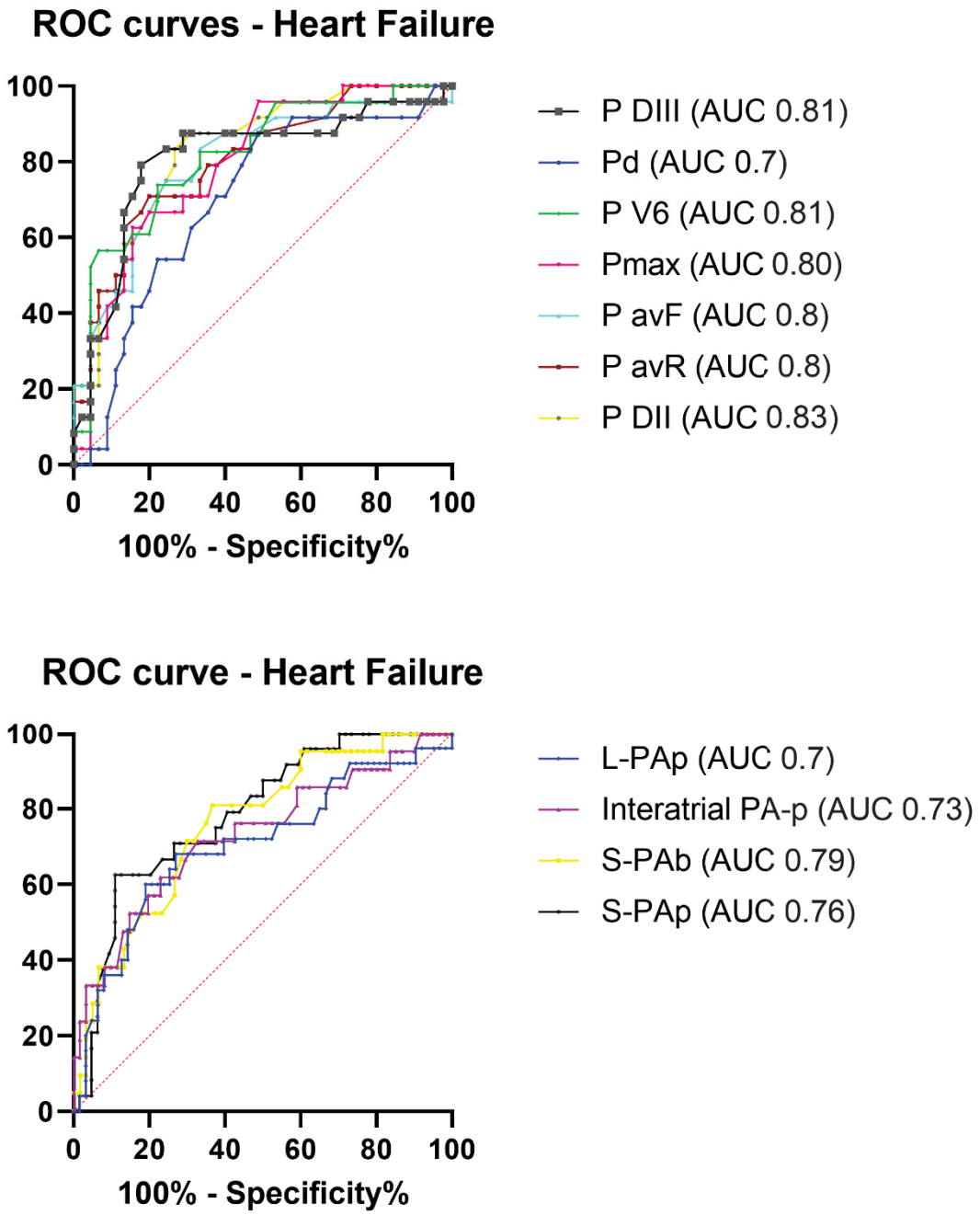

Figure 5. Receiver operating characteristic curves constructed to assess sensitivity and specificity of atrial conduction heterogeneity markers for differentiation of dogs presenting heart failure and asymptomatic dogs. ROC: Receiver operating characteristic curve; L-PAp: time between the beginning of the P-wave in ECG and the peak of A' wave in tissue Doppler images obtained in lateral mitral annulus; obtained in lateral mitral annulus; S-PAb: time between the beginning of the P-wave in ECG and the beginning of A' wave in tissue Doppler images obtained in mitral septal annulus; S-PAp: time between the beginning of the P-wave in ECG and the peak of A' wave in tissue Doppler images obtained in mitral septal annulus; Interatrial-p: Interatrial conduction delay, calculated as the difference between the R-PAp and L-PAp times;

Pmax: The longest P-wave duration within 12 leads; Pd: P-wave dispersion; AUC: area under the curve.

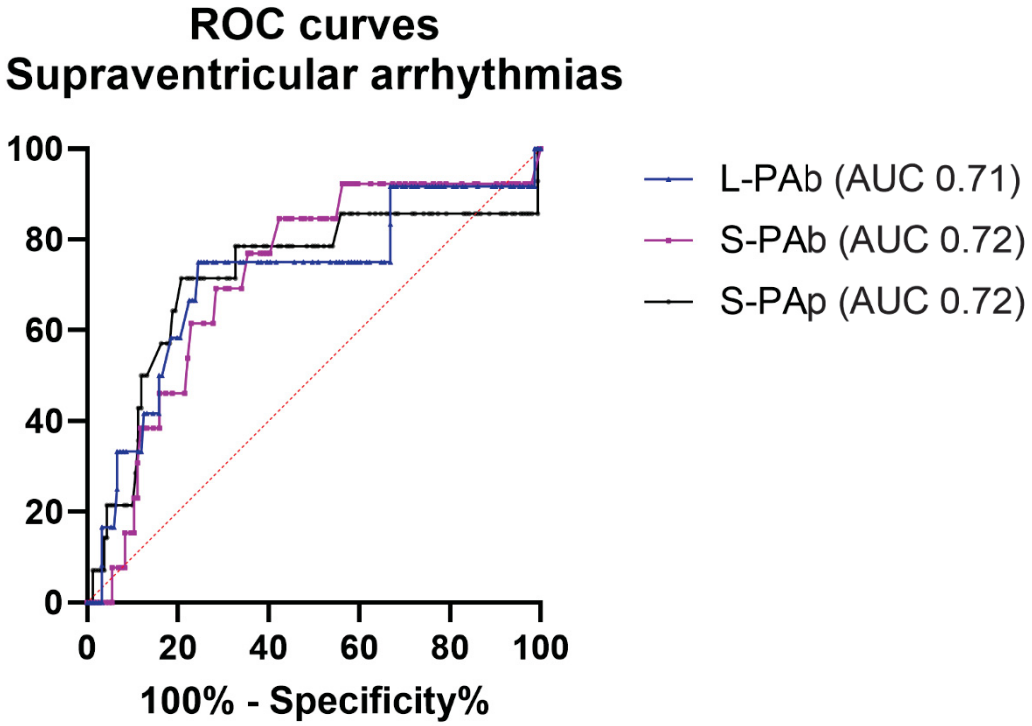

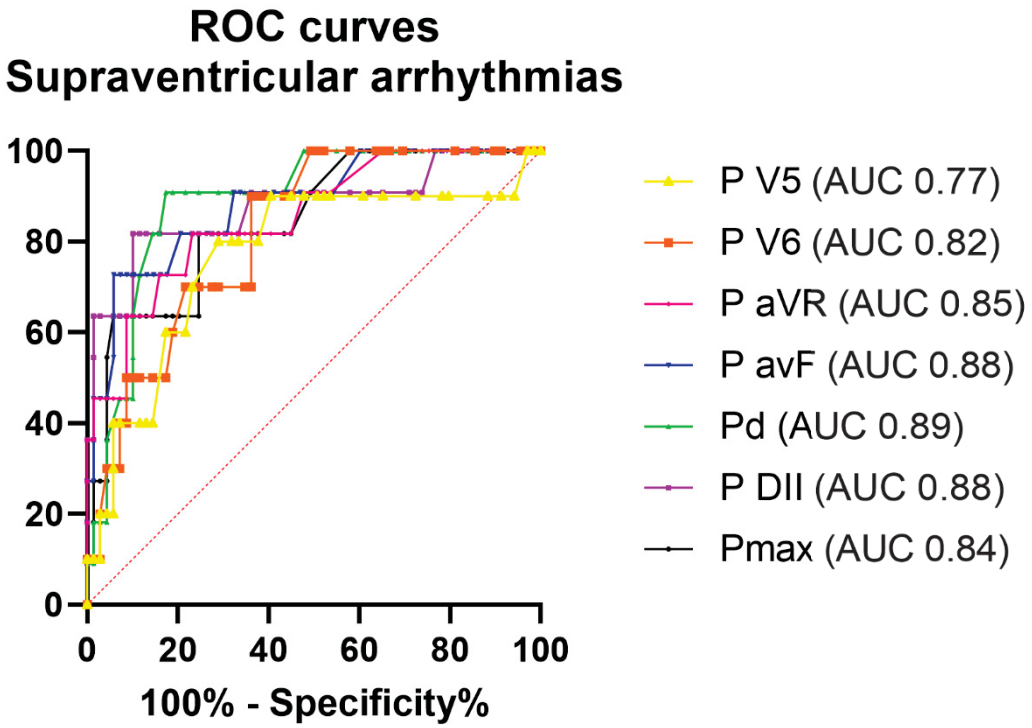

Figure 6. Receiver operating characteristic curves constructed to assess sensitivity and specificity of atrial conduction heterogeneity markers for differentiation of dogs presenting supraventricular arrhythmias and dogs with rhythms of sinus origin. ROC:

Receiver operating characteristic curve; L-PAb: time between the beginning of the P-wave in ECG and the beginning of A' wave in tissue Doppler images obtained at the lateral mitral annulus; S-PAb: time between the beginning of the P-wave in ECG and the beginning of A' wave in tissue Doppler images obtained in mitral septal annulus; S-PAp: time between the beginning of the P-wave in ECG and the peak of A' wave in tissue Doppler images obtained in mitral septal annulus; Pd: P-wave dispersion; Pmax: The longest P-wave duration within 12 leads.

SUPPLEMENTARY MATERIAL TABLES

Supplementary material table A. Rho-values obtained by Spearman's test to investigate correlations between markers ECG and echocardiographic of atrial conduction times, as well as to check correlation with epidemiological, electrocardiographic and echocardiographic variables.

	L-PAb	L-PAp	S-PAb	S-PAp	R-PAb	R-PAp	Intra-LAb	Intra-PAp	Interatrial-b	Interatrial-p	PDI	PDII	PDIII	PaVR	PaVL	PaVF	PV1	PV2	PV3	PV4	PV5	PV6	Pmin	Pmax	Pd
Age (years	0.59	0.52	0.60	0.52	0.57	0.29	-0.14	0.04	-0.16	-0.25	0.210	0.440	0.31	0.35	0.10	0.43	0.310	0.100	0.110	0.180	0.240	0.290	0.25	0.17	0.050
Weight	-0.05	0.03	-0.11	-0.01	-0.05	0.29	-0.06	-0.07	-0.03	0.23	.120	.130	0.20	0.20	0.22	0.21	.280	.290	.260	.250	.200	.220	0.21	0.28	0.180
LA	0.43	0.44	0.43	0.46	0.34	0.36	-0.08	0.05	-0.21	-0.20	0.530	.640	0.47	0.65	0.45	0.56	.560	.410	.400	.390	.530	.620	0.44	0.62	.470
Ao	-0.17	-0.08	-0.25	-0.16	-0.14	0.26	-0.04	-0.12	0.03	0.23	.120	.070	0.12	0.10	0.19	0.12	.250	.240	.200	.160	.090	.130	0.26	0.15	0.050
LA/Ao	0.53	0.46	0.60	0.52	0.39	0.09	-0.05	0.11	-0.25	-0.39	.370	.540	0.36	0.50	0.27	0.44	.350	.210	.240	.260	.400	.450	0.23	0.45	0.390
LVIDd	0.36	0.42	0.35	0.38	0.27	0.33	-0.12	-0.05	-0.21	-0.19	.530	.670	0.52	0.64	0.44	0.59	.550	.410	.380	.380	.520	.630	0.44	0.66	.510
LVIDs	0.09	0.18	0.09	0.13	0.06	0.25	-0.07	-0.07	-0.10	-0.01	.420	.430	0.35	0.45	0.39	0.39	.460	.370	.380	.360	.430	.530	0.38	0.55	.430
LVIDdN	0.41	0.44	0.41	0.40	0.33	0.21	-0.11	-0.05	-0.19	-0.33	.530	.720	0.52	0.63	0.38	0.59	.500	.370	.360	.350	.530	.640	0.41	0.63	.520
LVIDsN	0.14	0.22	0.17	0.18	0.11	0.17	-0.06	-0.05	-0.10	-0.11	.470	.500	0.39	0.45	0.37	0.41	.460	.340	.380	.360	.450	.560	0.38	0.57	.470
FS	0.38	0.29	0.33	0.30	0.27	-0.07	-0.15	0.03	-0.19	-0.37	-0.03	-0.19	0.14	0.15	0.02	0.16	-0.030	-0.090	-0.120	-0.070	0.01	0.01	-0.03	0.00	-0.030
E	0.34	0.31	0.37	0.26	0.20	0.01	0.00	-0.02	-0.23	-0.35	.510	.580	0.38	0.57	0.40	0.47	.430	.360	.370	.360	.440	.550	0.32	0.58	.500

A	0.46	0.44	0.53	0.43	0.52	0.21	-0.10	0.12	-0.12	-0.30	0.14	0.35	0.11	0.26	-0.07	0.28	0.06	-0.09	-0.110	-0.050	0.12	0.21	-0.02	0.11	0.11
E/A	-0.20	-0.15	-0.22	-0.24	-0.34	-0.14	0.12	-0.19	-0.05	0.01	0.32	0.16	0.20	0.24	0.39	0.14	0.36	0.40	-0.420	0.32	0.26	0.26	0.32	0.41	0.32
IVRT	0.12	0.18	0.04	0.17	0.24	0.38	-0.18	-0.07	0.08	0.16	-0.160	-0.140	-0.18	-0.18	-0.11	-0.10	-0.150	-0.140	-0.090	-0.020	-0.080	-0.050	-0.03	-0.23	-0.210
E/IVRT	0.19	0.16	0.25	0.11	0.04	-0.18	0.09	0.01	-0.20	-0.37	-0.460	-0.510	0.41	0.52	0.37	0.42	-0.400	-0.330	-0.330	-0.270	-0.410	-0.450	0.27	0.55	-0.470
E/E'lat	0.14	0.20	0.09	0.12	-0.05	-0.10	-0.10	-0.03	-0.26	-0.27	-0.300	-0.340	0.31	0.30	0.26	0.29	-0.230	-0.240	-0.250	-0.240	-0.330	-0.410	0.16	0.40	-0.370
E/E'sep	-0.21	-0.12	-0.12	-0.04	-0.28	-0.09	0.19	0.07	-0.07	-0.08	-0.360	-0.330	0.34	0.37	0.36	0.35	-0.340	-0.330	-0.430	-0.410	-0.450	-0.520	0.34	0.46	-0.310
E'	0.29	0.17	0.34	0.19	0.33	0.04	0.04	0.01	0.00	-0.18	-0.220	-0.250	0.07	0.30	0.25	0.17	-0.200	-0.160	-0.180	-0.160	-0.120	-0.190	0.17	0.22	-0.160
A'	0.57	0.48	0.57	0.46	0.61	0.31	-0.19	0.07	-0.07	-0.23	-0.110	-0.150	-0.03	0.13	0.03	0.12	-0.030	-0.140	-0.150	-0.050	-0.020	-0.120	0.05	-0.04	-0.120
E'/A'	-0.39	-0.37	-0.33	-0.31	-0.43	-0.26	0.24	-0.04	0.04	0.10	-0.120	-0.060	0.04	0.13	0.14	0.00	-0.160	-0.280	-0.310	-0.170	-0.080	-0.020	0.10	0.26	-0.270
S'	0.50	0.44	0.53	0.47	0.45	0.18	-0.06	0.05	-0.14	-0.33	-0.250	-0.390	0.18	0.42	0.20	0.30	-0.280	-0.030	-0.040	-0.150	-0.240	-0.260	0.21	0.24	-0.140
L-PAb	1.00	0.86	0.77	0.71	0.67	0.42	-0.48	-0.10	-0.53	-0.46	-0.300	-0.400	0.21	0.33	0.18	0.32	-0.240	-0.050	-0.100	-0.180	-0.240	-0.310	0.19	0.24	-0.190
L-PAp	0.86	1.00	0.65	0.66	0.59	0.42	-0.42	-0.25	-0.46	-0.59	-0.330	-0.410	0.24	0.37	0.21	0.36	-0.320	-0.060	-0.090	-0.190	-0.270	-0.360	0.27	0.27	-0.170
S-PAb	0.77	0.65	1.00	0.83	0.70	0.42	0.13	0.28	-0.18	-0.23	0.20	0.29	0.12	0.27	0.17	0.21	0.28	-0.110	-0.070	0.04	0.17	0.24	0.16	0.12	0.06
S-PAp	0.71	0.66	0.83	1.00	0.62	0.45	0.03	0.49	-0.20	-0.21	0.23	0.39	0.22	0.32	0.10	0.33	0.24	-0.	0.02	0.10	0.22	0.33	0.16	0.22	0.16

R-PAb	0.67	0.59	0.70	0.62	1.00	0.63	-0.11	0.13	0.22	-0.04	-0.01	0.09	-0.07	0.04	-0.02	0.08	0.08	01	-0.26	-0.26	-0.20	-0.01	0.03	0.04	-0.17	-0.25
R-PAp	0.42	0.42	0.42	0.45	0.63	1.00	-0.08	0.12	0.08	0.39	0.08	0.15	0.05	0.10	-0.05	0.18	0.17	-0.09	-0.08	-0.03	0.07	0.16	0.10	0.00	-0.06	
Intra-LAb	-0.48	-0.42	0.13	0.03	-0.11	-0.08	1.00	0.49	0.56	0.36	-0.15	-0.16	-0.15	-0.10	0.00	-0.18	0.04	-0.06	-0.13	-0.14	-0.03	-0.06	-0.01	-0.12	-0.13	
Intra-PAp	-0.10	-0.25	0.28	0.49	0.13	0.12	0.49	1.00	0.22	0.41	-0.20	-0.06	-0.03	-0.11	-0.20	-0.09	-0.15	-0.13	-0.19	-0.20	-0.12	-0.06	-0.18	-0.14	-0.06	
Interatrial-b	-0.53	-0.46	-0.18	-0.20	0.22	0.08	0.56	0.22	1.00	0.51	-0.40	-0.40	-0.34	-0.36	-0.23	-0.30	-0.20	-0.29	-0.39	-0.39	-0.29	-0.36	-0.15	-0.50	-0.54	
Interatrial-p	-0.46	-0.59	-0.23	-0.21	-0.04	0.39	0.36	0.41	0.51	1.00	-0.300	-0.320	-0.14	-0.32	-0.23	-0.19	-0.190	-0.120	-0.140	-0.130	-0.180	-0.200	-0.16	-0.30	-0.250	
HRmin	-0.30	-0.30	-0.24	-0.20	-0.30	-0.41	0.17	0.05	0.08	-0.10	-0.20	-0.16	0.19	0.25	0.26	0.18	-0.11	-0.16	-0.12	-0.08	-0.16	-0.12	0.09	0.26	-0.23	
HRmax	0.33	0.21	0.33	0.27	0.26	-0.05	-0.10	0.02	-0.02	-0.26	0.00	-0.11	0.08	0.14	0.22	0.06	-0.02	-0.07	-0.19	-0.11	-0.15	-0.08	0.08	-0.12	-0.15	
HRmed	-0.07	-0.04	0.02	0.00	-0.23	-0.36	0.14	0.13	-0.19	-0.28	0.11	-0.18	0.19	0.23	0.13	0.08	0.01	-0.04	-0.09	-0.04	-0.13	-0.13	0.07	0.08	0.06	
QRS axis	-0.03	-0.04	0.03	0.03	0.00	0.18	0.04	0.03	0.05	0.23	0.02	-0.05	0.14	0.03	0.01	0.15	-0.04	-0.15	-0.08	-0.04	0.06	-0.01	0.01	-0.08	-0.11	
P (mV)	0.30	0.27	0.39	0.37	0.32	-0.09	0.04	0.13	-0.04	-0.35	0.06	-0.27	0.29	0.19	0.04	0.25	0.08	0.03	0.04	0.04	0.14	0.14	0.20	0.04	-0.100	
P (ms)	0.19	0.26	0.11	0.21	0.02	0.07	-0.18	-0.11	-0.22	-0.22	0.54	0.71	0.56	0.70	0.35	0.72	0.52	0.35	0.34	0.36	0.48	0.58	0.42	0.58	0.40	

P-R (ms)	0.27	0.31	0.26	0.30	0.20	0.44	-0.04	0.00	-0.11	0.04	0.410	0.470	0.35	0.41	0.31	0.43	0.400	0.390	0.370	0.360	0.410	0.510	0.30	0.50	0.410
QRS (mV)	0.39	0.33	0.43	0.39	0.31	0.20	-0.07	0.09	-0.17	-0.19	0.220	0.470	0.37	0.34	0.19	0.39	0.210	0.060	0.060	0.120	0.340	0.350	0.19	0.26	0.190
QRS (ms)	0.09	0.16	0.15	0.15	0.05	0.10	-0.01	-0.04	-0.09	-0.10	0.39	0.45	0.42	0.43	0.34	0.44	0.46	0.17	0.23	0.18	0.23	0.35	0.33	0.43	0.29
S-T	0.17	0.04	0.03	0.01	0.07	-0.001	-0.20	0.03	-0.14	-0.01	-0.180	-0.080	-0.07	-0.13	-0.23	-0.06	-0.17	0.08	0.07	0.04	-0.100	-0.170	-0.17	-0.11	-0.050
QT (ms)	0.16	0.19	0.09	0.16	0.10	0.25	-0.13	-0.08	-0.09	0.09	0.040	-0.110	0.25	0.02	0.16	0.13	0.250	0.160	0.180	0.200	0.230	0.210	0.18	0.19	0.070
T (mV)	-0.18	-0.19	-0.16	-0.15	-0.19	-0.15	0.07	0.02	0.03	0.08	-0.091	-0.110	-0.11	-0.06	0.09	-0.20	-0.010	-0.020	-0.010	-0.070	-0.120	-0.170	0.00	-0.07	-0.070
PDI	0.30	0.33	0.20	0.23	-0.01	0.08	-0.15	-0.20	-0.40	-0.30	0.000	-0.731	0.45	0.83	0.58	0.64	0.650	0.490	0.510	0.560	0.660	0.720	0.58	0.78	0.550
PDII	0.40	0.41	0.29	0.39	0.09	0.15	-0.16	-0.06	-0.40	-0.32	0.730	-0.000	0.71	0.89	0.44	0.88	0.680	0.490	0.480	0.520	0.660	0.750	0.58	0.78	0.580
PDIII	0.21	0.24	0.12	0.22	-0.07	0.05	-0.15	-0.03	-0.34	-0.14	0.450	-0.710	1.00	0.61	0.40	0.80	0.560	0.490	0.510	0.570	0.660	0.680	0.64	0.62	0.340
PaVR	0.33	0.37	0.27	0.32	0.04	0.10	-0.10	-0.11	-0.36	-0.32	0.830	-0.890	0.61	1.00	0.52	0.82	0.720	0.460	0.460	0.530	0.700	0.770	0.63	0.77	0.520
PaVL	0.18	0.21	0.17	0.10	-0.02	-0.05	0.00	-0.20	-0.23	-0.23	0.580	-0.440	0.40	0.52	1.00	0.38	0.500	0.490	0.490	0.530	0.580	0.540	0.66	0.62	0.330
PaVF	0.32	0.36	0.21	0.33	0.08	0.18	-0.18	-0.09	-0.30	-0.19	0.640	-0.880	0.80	0.82	0.38	1.00	0.691	0.530	0.510	0.560	0.690	0.760	0.60	0.75	0.510
PV1	0.24	0.32	0.28	0.24	0.08	0.17	0.04	-0.15	-0.20	-0.19	0.650	-0.680	0.56	0.72	0.50	0.69	0.000	0.451	0.440	0.470	0.600	0.660	0.79	0.67	0.300
PV2	0.05	0.06	-0.11	-0.01	-0.26	-0.09	-0.06	-0.13	-0.29	-0.12	0.490	-0.490	0.49	0.46	0.49	0.53	0.450	0.001	0.880	0.810	0.700	0.610	0.54	0.73	0.540

PV3	0.10	0.09	-0.07	0.02	-0.26	-0.08	-0.13	-0.19	-0.39	-0.14	0.510	0.480	0.51	0.46	0.49	0.51	0.440	0.880	1.000	0.901	0.740	0.640	0.51	0.74	0.560
PV4	0.18	0.19	0.04	0.10	-0.20	-0.03	-0.14	-0.20	-0.39	-0.13	0.560	0.520	0.57	0.53	0.53	0.56	0.470	0.810	0.900	1.000	0.801	0.700	0.60	0.70	0.460
PV5	0.24	0.27	0.17	0.22	-0.01	0.07	-0.03	-0.12	-0.29	-0.18	0.660	0.660	0.66	0.70	0.58	0.69	0.600	0.700	0.740	0.800	1.000	0.861	0.68	0.75	0.470
PV6	0.31	0.36	0.24	0.33	0.03	0.16	-0.06	-0.06	-0.36	-0.20	0.720	0.750	0.68	0.77	0.54	0.76	0.660	0.610	0.640	0.700	0.860	1.000	0.68	0.76	0.490
Pmin	0.19	0.27	0.16	0.16	0.04	0.10	-0.01	-0.18	-0.15	-0.16	0.580	0.580	0.64	0.63	0.66	0.60	0.790	0.540	0.510	0.600	0.680	0.680	1.00	0.54	0.040
Pmax	0.24	0.27	0.12	0.22	-0.17	0.00	-0.12	-0.14	-0.50	-0.30	0.780	0.780	0.62	0.77	0.62	0.75	0.670	0.730	0.740	0.700	0.750	0.760	0.54	1.00	0.841
Pd	0.19	0.17	0.06	0.16	-0.25	-0.06	-0.13	-0.06	-0.54	-0.25	0.555	0.558	0.34	0.52	0.33	0.51	0.300	0.544	0.556	0.446	0.447	0.449	0.04	0.84	1.000

Interatrial-b: Interatrial conduction delay, calculated as the difference between the R-PAb and L-PAb times; Interatrial-p: Interatrial conduction delay, calculated as the difference between the R-PAp and L-PAp times; Intra-LAb: Intra-left atrial conduction delay, calculated as the difference between the S-PAb and L-PAb times; Intra-LAp: Intra-left atrial conduction delay, calculated as the difference between the S-PAp and L-PAp times; L-PAb: The time between the beginning of the P-wave in ECG and the beginning of A' wave in tissue Doppler traces in lateral mitral annulus; L-PAp: The time between the beginning of the P-wave in ECG and the peak of A' wave in tissue Doppler traces in lateral mitral annulus; R-PAb:The time between the beginning of the P-wave in ECG and the beginning of A' wave in tissue Doppler traces in lateral tricuspid annulus; R-PAp: The time between the beginning of the P-wave in ECG and the peak of A' wave in tissue Doppler traces in lateral tricuspid annulus; S-PAb: The time between the beginning of the P-wave in ECG and the beginning of A' wave in tissue Doppler traces in mitral septal annulus; S-PAp: The time between the beginning of the P-wave in ECG and the peak of A' wave in tissue Doppler traces in mitral septal annulus; Pd: P-wave dispersion; Pmax: The longest P-wave duration within 12 leads; Pmin: The shortest P-wave duration within 12 leads; E: Peak velocity of early diastolic transmitral flow; E:A: Ratio of early-to-late transmitral flow peak velocities; E:IVRT: ratio of early transmitral flow to isovolumetric relaxation time; E:E': Ratio of early transmitral flow peak velocity to the early mitral annulus tissue peak velocity; FS: Fractional shortening; LA:Ao: Ratio of the left atrial dimensions to the aortic annulus dimension; LVIDdN: left ventricular end diastolic diameter normalized for body weight; LVIDsN: left ventricular end systolic diameter normalized for body weight.

Supplementary material table B. P-values obtained by Spearman's test to investigate correlations between markers ECG and echocardiographic of atrial conduction times, as well as to check correlation with epidemiological, electrocardiographic and echocardiographic variables.

	L-PAb	L-PAp	S-PAb	S-PAp	R-PAb	R-PAp	Intra-LAb	Intra-PAp	Interatrial-b	Interatrial-p	PDI	PDI I	PDI II	PaVR	PaVL	PaVF	PV1	PV2	PV3	PV4	PV5	PV6	Pmin	Pmax	Pd
Age (years)	1.7E-12	2.87E-10	1.49E-12	3.57E-10	7.64E-11	0.001391	0.139994	0.679498	0.096857	0.005527	0.055194	3.12E-05	0.004401	0.001067	0.39526	4.16E-05	0.00458	0.386783	0.315095	0.092225	0.02621	0.007698	0.023732	0.130325	0.668913
Weight	0.590451	0.711055	0.243534	0.886475	0.591056	0.001302	0.54482	0.428252	0.780376	0.013853	0.258838	0.238379	0.067077	0.064595	0.045951	0.050518	0.00875	0.007369	0.016996	0.018061	0.071073	0.043863	0.049062	0.009422	0.091387
LA	1.44E-06	3.1E-07	1.63E-06	7.06E-08	0.000231	4.28E-05	0.413993	0.603068	0.028259	0.032271	1.38E-07	3.7E-11	1.01E-05	1.76E-11	2.29E-05	1.85E-08	2.68E-08	8.53E-05	0.000117	0.00021	1.91E-07	2.82E-10	2.51E-05	2.94E-10	4.13E-06
Ao	0.068179	0.37284	0.006765	0.078438	0.132893	0.003511	0.6612	0.196765	0.779511	0.011791	0.274451	0.524948	0.284198	0.336565	0.088306	0.263587	0.022363	0.028337	0.064118	0.149905	0.432178	0.244037	0.015801	0.15835	0.634482
LA/Ao	4.24E-10	7.01E-08	1.1E-12	3.15E-10	2.18E-05	0.311655	0.601193	0.251535	0.009107	1.17E-05	0.000494	1.03E-07	0.000835	7.4E-07	0.013254	2.39E-05	0.00099	0.05628	0.025101	0.015931	0.000124	1.83E-05	0.037248	1.2E-05	0.000173
LVIDd	6.41E-05	1.03E-06	0.000128	9.03E-06	0.003584	0.000189	0.209234	0.595246	0.029441	0.042953	2.07E-07	1.68E-12	5.55E-07	2.52E-11	3.19E-05	2.1E-09	6.43E-08	8.12E-05	0.000308	0.000257	3.61E-07	8.3E-11	2.42E-05	5.31E-12	4.89E-07
LVIDs	0.334683	0.039372	0.344206	0.146043	0.553228	0.005156	0.470881	0.442302	0.284366	0.912905	6.26E-05	4.4E-05	0.001257	1.44E-05	0.000316	0.000201	7.49E-06	0.000399	0.000268	0.000588	4.06E-05	1.98E-07	0.000314	3.74E-08	3E-05

LVIDdN	3.43E-06	2.37E-07	6.55E-06	3.77E-06	0.00049	0.022591	0.236887	0.559605	0.050451	0.000247	1.31E-07	8.67E-15	5.61E-07	6.82E-11	0.000486	2.86E-09	9.83E-07	0.00054	0.000646	0.000891	1.44E-07	4.77E-11	0.000108	5.27E-11	3.67E-07
LVIDsN	0.120295	0.01375	0.062918	0.049791	0.233465	0.066399	0.559394	0.584597	0.315912	0.238214	4.67E-06	1.05E-06	0.000291	1.1E-05	0.000682	0.000102	7.97E-06	0.001231	0.000306	0.000608	1.41E-05	1.98E-08	0.000265	1.2E-08	5.52E-06
FS	3.05E-05	0.001288	0.000344	0.000787	0.00488	0.451804	0.125605	0.7736	0.054792	4.33E-05	0.820721	0.075696	0.203408	0.160952	0.83699	0.146322	0.815602	0.414347	0.262762	0.546773	0.896098	0.925738	0.821403	0.986461	0.819571
E	0.000153	0.000411	3.76E-05	0.00379	0.031873	0.932219	0.966607	0.85937	0.015309	8.69E-05	6.35E-07	5.35E-09	0.00047	8.9E-09	0.000227	5.06E-06	4.14E-05	0.000787	0.000426	0.000678	2.08E-05	5.55E-08	0.002946	3.48E-09	1.11E-06
A	1.22E-07	3.03E-07	1.04E-09	4.56E-07	5.84E-09	0.019307	0.307154	0.193031	0.208108	0.001153	0.202748	0.000954	0.333346	0.015871	0.54387	0.010605	0.587893	0.396574	0.297797	0.633094	0.258637	0.051517	0.886637	0.317097	0.328747
E/A	0.029349	0.098777	0.020662	0.007023	0.000201	0.116177	0.21032	0.042217	0.632557	0.900315	0.003169	0.141953	0.070363	0.026268	0.000313	0.20319	0.000874	0.000172	6.13E-05	0.002673	0.015765	0.016803	0.002439	8.01E-05	0.003133
IVRT	0.203713	0.05344	0.690949	0.069687	0.014249	1.69E-05	0.068303	0.475907	0.416713	0.093887	0.154768	0.224847	0.12646	0.107741	0.329187	0.372066	0.189535	0.218213	0.411414	0.884705	0.486665	0.690179	0.825076	0.039893	0.057216
E/IVRT	0.037758	0.081685	0.008912	0.23079	0.670281	0.047377	0.373299	0.89829	0.036445	5.6E-05	1.58E-05	1.43E-06	0.000226	1.12E-06	0.001184	0.000146	0.000304	0.002812	0.00283	0.018176	0.00194	3.28E-05	0.015401	1.46E-07	1.45E-05
E/E'lat	0.121	0.023	0.344	0.174	0.610	0.287	0.310	0.780	0.005999	0.002881	0.004	0.001	0.005	0.006	0.020	0.007	0.032	0.029	0.021	0.029	0.002	0.000	0.148	0.000	0.000

	859	499	457	187	439	533	014	478			964	382	258	08	425	313	843	184	675	843	049	145	441	14	463
E/E' sep	0.033678	0.227954	0.223438	0.646845	0.004698	0.3658	0.049182	0.483722	0.494536	0.426382	0.002124	0.005774	0.005117	0.001652	0.002909	0.003469	0.00465	0.004902	0.0002	0.000548	0.000105	4.86E-06	0.004854	8.16E-05	0.008627
E'	0.001439	0.059324	0.000199	0.030653	0.000386	0.636136	0.709271	0.88503	0.980791	0.046737	0.04296	0.020489	0.551391	0.005327	0.028387	0.119559	0.065474	0.149437	0.109455	0.136954	0.292909	0.088463	0.129671	0.041072	0.149384
A'	1.22E-11	1.81E-08	7.76E-11	8.6E-08	2.06E-12	0.000469	0.050001	0.460374	0.473853	0.013744	0.33044	0.166183	0.80653	0.259441	0.787936	0.288738	0.774775	0.193889	0.17655	0.641278	0.8919	0.298097	0.671598	0.695839	0.284144
E'/A'	1.39E-05	2.79E-05	0.000395	0.000508	2.56E-06	0.004738	0.011918	0.655519	0.704915	0.262245	0.272253	0.573671	0.728874	0.22546	0.222717	0.973852	0.140319	0.011552	0.004332	0.128087	0.472474	0.856224	0.351429	0.018473	0.01456
S'	5.14E-08	2.13E-06	1.03E-08	5.28E-07	3.47E-06	0.062319	0.549388	0.629016	0.161949	0.000694	0.034363	0.000985	0.134169	0.00035	0.10114	0.012433	0.021315	0.787569	0.741501	0.222528	0.047459	0.032931	0.076022	0.042339	0.261558
L-P Ab		4.95E-36	1.46E-23	1.44E-18	2.28E-15	4.1E-06	9.88E-08	0.300863	3.66E-09	3.58E-07	0.008183	0.000284	0.075542	0.002927	0.117418	0.004317	0.033972	0.664856	0.368888	0.11338	0.038307	0.007052	0.102853	0.038185	0.090637
L-P Ap	4.95E-36		4.62E-15	1.31E-16	9.9E-12	1.45E-06	3.58E-06	0.006314	6.28E-07	1.39E-12	0.002325	0.000117	0.033311	0.000708	0.06057	0.001131	0.003263	0.577191	0.399057	0.095572	0.013077	0.000935	0.013212	0.013813	0.129981
S-P Ab	1.46E-23	4.62E-15		2.49E-30	2.67E-17	3.95E-06	0.1621	0.002813	0.067691	0.016835	0.100554	0.014913	0.338542	0.022768	0.152146	0.07525	0.019809	0.343507	0.582708	0.749882	0.146674	0.039115	0.17005	0.295849	0.644768

S-PAp	1.44E-18	1.31E-16	2.49E-30		3.93E-13	1.77E-07	0.769864	8.82E-09	0.041578	0.02361	0.040869	0.000459	0.056811	0.003507	0.409717	0.003208	0.031319	0.958661	0.894822	0.381319	0.054368	0.00343	0.155512	0.054827	0.164374
R-PAb	2.28E-15	9.9E-12	2.67E-17	3.93E-13		6.02E-14	0.272893	0.183772	0.021219	0.658906	0.917823	0.477507	0.558144	0.763595	0.858332	0.493345	0.528253	0.030596	0.02854	0.099863	0.958125	0.817664	0.758155	0.154881	0.032466
R-PAp	4.1E-06	1.45E-06	3.95E-06	1.77E-07	6.02E-14		0.380733	0.204927	0.38035	1.41E-05	0.499685	0.181908	0.652901	0.36844	0.660797	0.127805	0.14182	0.441023	0.49539	0.799892	0.526392	0.161613	0.364125	0.985032	0.579234
Intra-LAb	9.88E-08	3.58E-06	0.1621	0.769864	0.272893	0.380733		3.42E-08	2.97E-10	9.83E-05	0.198292	0.183733	0.214011	0.415632	0.968189	0.126925	0.747935	0.621442	0.294726	0.241868	0.832813	0.62347	0.936503	0.333294	0.289254
Intra-PAp	0.300863	0.006314	0.002813	8.82E-09	0.183772	0.204927	3.42E-08		0.024234	3.11E-06	0.083617	0.629367	0.788112	0.330359	0.08495	0.440604	0.190433	0.252059	0.096429	0.084331	0.304944	0.592201	0.122533	0.238228	0.626182
Interatrial-b	3.66E-09	6.28E-07	0.067691	0.041578	0.021219	0.38035	2.97E-10	0.024234		1.24E-08	0.000548	0.000474	0.004248	0.001823	0.053097	0.010282	0.088898	0.013546	0.000836	0.000637	0.01197	0.002098	0.222782	8.72E-06	1.06E-06
Interatrial-p	3.58E-07	1.39E-12	0.016835	0.02361	0.658906	1.41E-05	9.83E-05	3.11E-06	1.24E-08		0.008455	0.00421	0.224566	0.005023	0.047122	0.094403	0.103122	0.300725	0.21911	0.258175	0.116895	0.087135	0.168981	0.009076	0.025966
HRmin	0.002891	0.002776	0.021872	0.044303	0.003573	3.15E-05	0.107493	0.629331	0.463559	0.34595	0.078739	0.167501	0.111796	0.027643	0.024862	0.118994	0.346964	0.179627	0.293475	0.472668	0.179306	0.294662	0.426391	0.022429	0.047207
HRmax	0.001	0.034	0.001	0.007	0.012	0.596	0.334	0.818	0.830127	0.01	0.977	0.369	0.490	0.240	0.068	0.624	0.872	0.542	0.102	0.331	0.203	0.474	0.476	0.299	0.206

HR med	0790.541808	6670.720076	5430.885322	6240.982837	6650.003545	5890.000363	4730.195413	4180.226547	0.0860887	0.0008606	6040.368808	0430.128488	2520.110243	4320.005180	53	0.285563	8220.502901	6220.900361	4290.733587	4640.448477	9760.753698	972	0.254833	18	0.266756	944	0.536667	3190.522638	9220.593829

Interatrial-b: Interatrial conduction delay, calculated as the difference between the R-PAb and L-PAb times; Interatrial-p: Interatrial conduction delay, calculated as the difference between the R-PAp and L-PAp times; Intra-LAb: Intra-left atrial conduction delay, calculated as the difference between the S-PAb and L-PAb times; Intra-LAp: Intra-left atrial conduction delay, calculated as the difference between the S-PAp and L-PAp times; L-PAb: The time between the beginning of the P-wave in ECG and the beginning of A' wave in tissue Doppler traces in lateral mitral annulus; L-PAp: The time between the beginning of the P-wave in ECG and the peak of A' wave in tissue Doppler traces in lateral mitral annulus; R-PAb:The time between the beginning of the P-wave in ECG and the beginning of A' wave in tissue Doppler traces in lateral tricuspid annulus; R-PAp: The time between the beginning of the P-wave in ECG and the peak of A' wave in tissue Doppler traces in lateral tricuspid annulus; S-PAb: The time between the beginning of the P-wave in ECG and the beginning of A' wave in tissue Doppler traces in mitral septal annulus; S-PAp: The time between the beginning of the P-wave in ECG and the peak of A' wave in tissue Doppler traces in mitral septal annulus; Pd: P-wave dispersion; Pmax: The longest P-wave duration within 12 leads; Pmin: The shortest P-wave duration within 12 leads; E: Peak velocity of early diastolic transmitral flow; E:A: Ratio of early-to-late transmitral flow peak velocities; E:IVRT: ratio of early transmitral flow to isovolumetric relaxation time; E:E': Ratio of early transmitral flow peak velocity to the early mitral annulus tissue peak velocity; FS: Fractional shortening; LA:Ao: Ratio of the left atrial dimensions to the aortic annulus dimension; LVIDdN: left ventricular end diastolic diameter normalized for body weight; LVIDsN: left ventricular end systolic diameter normalized for body weight.

CHAPTER 2 - VENTRICULAR ELECTRICAL AND MECHANICAL ACTIVATION TIMES AND DYSSYNCHRONY IN DOGS WITH MYXOMATOUS MITRAL VALVE DISEASE*

Running head: Ventricular activation times and dyssynchrony in dogs with myxomatous mitral valve disease

* Manuscript will be submitted to the Journal of Veterinary Cardiology (Online ISSN: 1875-0834). Written in accordance with the guidelines available at https://www.sciencedirect.com/journal/journal-of-veterinary-cardiology/publish/guide-for-authors

ABSTRACT

Introduction/Objectives: Myxomatous mitral valve disease (MMVD) can lead to heart failure (HF), and arrhythmias. People with HF frequently develop ventricular dyssynchrony, which worsens mortality. This study aimed to evaluate electrocardiographic and echocardiographic markers of ventricular activation and dyssynchrony in dogs with MMVD, offering insights into their progression and clinical implications.

Animals: This cross-sectional study in two veterinary institutions included dogs diagnosed with MMVD, and healthy dogs.

Methods: The time from the beginning of the QRS complex to the beginning of the pulmonic flow (RPulm) and the aortic flow were measured, and their difference was defined as mechanical interventricular dyssynchrony. The time from the beginning of the QRS complex to the beginning or the peak of S'-wave in tissue Doppler were measured in lateral mitral, septal, and lateral tricuspid annulus, and mechanical intra-left ventricle (LV) and interventricular conduction delay were calculated. R-peak time (RPT) was measured in precordial leads from the onset of the QRS complex to the peak of the R-wave. Interventricular dyssynchrony index was defined as: (RPT V5 – RPT V1) / QRS duration.

Results: Were recruited 207 dogs, but 139 of them were included (42 control, 50 B1, 19 B2 and 28 C MMVD dogs). With the advance of MMVD, LV activation times prolonged, and mechanical interventricular and intraventricular dyssynchrony increased. Some indices adequately identified cardiomegaly, HF, and arrhythmias, especially left ventricle mechanical and electrical indices.

Conclusions: Ventricular activation times were significantly prolonged, and mechanical dyssynchrony progressively worsened as MMVD advanced. Both electrical

and mechanical ventricular activation times were markers of arrhythmias, cardiomegaly and HF.

KEYWORDS: R-Peak Time; Arrhythmia; Interventricular dyssynchrony index; Heart Failure; Canine

ABBREVIATION TABLE

BBB	Bundle branch blocks
ECG	Electrocardiography
HF	Heart failure
IDI	Interventricular dyssynchrony index
Inter-Vb	Mechanical interventricular conduction delay using the beginning of the S' wave
Inter-Vp	Mechanical interventricular conduction delay using the peak of the S' wave
Intra-LVb	Mechanical intra-left ventricle conduction delay using the beginning of the S' wave
Intra-LVp	Mechanical intra-left ventricle conduction delay using the peak of the S' wave
L-RSb	Electromechanical delay measured in lateral mitral annulus
L-RSp	Electrosystolic delay measured in lateral mitral annulus
LV	Left ventricle
MMVD	Myxomatous mitral valve disease
NPV	Negative predictive value
PPV	Positive predictive value
Pulm-Ao	Mechanical interventricular dyssynchrony
RAo	Time intervals from the start of the QRS complex to the beginning of the aortic flow
RPT	R-peak time
RPulm	Time intervals from the start of the QRS complex to the beginning of the pulmonic flow
R-RSb	Electromechanical delay measured in lateral tricuspid annulus
R-RSp	Electrosystolic delay measured in lateral tricuspid annulus
S-RSb	Electromechanical delay measured septal mitral annulus
S-RSp	Electrosystolic delay measured septal mitral annulus

INTRODUCTION/OBJECTIVES

Myxomatous mitral valve disease (MMVD) is the most common cardiac disease in dogs, and can lead to consequences such as heart failure (HF), and arrhythmias (Crosara et al., 2010; Keene et al., 2019; Vila et al., 2021). It is well known that people with HF frequently develop uncoordinated contraction due to ventricle electrical activation delay. Often termed dyssynchrony, this further depresses systolic function and chamber efficiency, and worsens morbidity and mortality (Kirk & Kass, 2013).

Ventricular dyssynchrony is categorized into electrical and mechanical types, with analyses focusing on either interventricular or intraventricular regions depending on the area of interest (Spartalis et al., 2017). The time it takes for the ventricles to be electrically or mechanically activated can be assessed in several different ways. Intrinsicoid deflection time, which is also known as ventricular activation time or R-Peak Time (RPT), is a surface electrocardiography (ECG) index that expresses the time from the beginning of the QRS complex to the peak of the R wave and shows the conduction time from the endocardium to the epicardium of the ventricle (Aiken et al., 2022). Based on this principle, RPT can estimate the electrical activation delay, and is currently a useful electrocardiographic marker for the diagnosis and prognosis of both structural and electrical cardiac abnormalities in people (Pérez-Riera, de Abreu, Barbosa-Barros, Nikus, et al., 2016), also being used as a predictor for cardiac resynchronization therapy response (Tapia-Orihuela et al., 2022). The interventricular dyssynchrony index (IDI) is a simple tool based on the values of left (V1) and right (V5) precordial RPT, which can determine the presence of dyssynchrony and, therefore, predicts the clinical response to cardiac resynchronization therapy in people (Pérez-Riera, de Abreu, Barbosa-Barros, Nikus, et al., 2016; Vereckei et al., 2018). There is little information regarding RPT and IDI in veterinary literature. There is only one paper describing RPT in healthy dogs (Mateos Pañero et al., 2021), and another paper describing both indices in dogs with bundle branch blocks (BBB) (Battaia et al., 2022). Neither of these two parameters has been studied in dogs with MMVD before.

Mechanical ventricular activation times and dyssynchrony can be interrogated using echocardiography. The time from the beginning of QRS complex to the systolic wave is a noninvasive marker of ventricular electromechanical delay (Salem et al., 2021). In people, the delay of more than 40 ms between the opposite left ventricle (LV)

walls in any of those measurements is indicative of dyssynchrony, while values of approximately 20 ms are normal (Bader et al., 2004). In dogs with MMVD, Tidholm et al. observed that the time difference between the systolic velocity of the LV free wall and the interventricular septum were longer compared to healthy dogs (Tidholm et al., 2009). Myocardial dyssynchrony, therefore, was considered an early sign of MMVD in dogs (Tidholm et al., 2009).

Since both electrical and mechanical changes occur in the heart of dogs with MMVD (Tidholm et al., 2009; Vila et al., 2021), we hypothesize that ventricular heterogeneity indices assessed by electrocardiogram and echocardiogram increase in the more advanced stages of the disease. We also believe that dogs with arrhythmias, cardiac remodeling, or HF exhibit significantly greater ventricular conduction delays compared to those without these conditions. Therefore, the aim of this study was: (1) to assess electrocardiographic and echocardiographic indices of ventricle activation times in dogs with MMVD and in a control group; (2) to investigate if those variables change with the progression of the disease; (3) to check if whether they can differentiate dogs with arrythmias from those with sinus rhythms, (4) to evaluate whether cardiac remodeling and HF interfere with these indices; and (5) and to test their reproducibility.

ANIMALS, MATERIALS AND METHODS

This was a cross-sectional observational study, conducted at a Veterinary Teaching facility and at a private Cardiology Service. The study was approved by the institutional Animal Care and Use Committee (protocol 047/2022) and complied with the National Institutes of Health Guide for the Use and Care of Laboratory Animals.

Animals

We included dogs admitted to both institutions between December 2022 and May 2024. Inclusion criteria encompassed dogs weighing less than 15 kg, diagnosed with naturally occurring MMVD confirmed via echocardiographic examination, and presenting high-quality ECG tracings, irrespective of breed, age, or sex. Myxomatous mitral valve disease dogs were classified according to the stage of the disease as outlined in the American College of Veterinary Internal Medicine consensus statement [20]. Although thoracic radiography was not performed in all dogs, the identification of CHF in MMVD dogs in stage C was performed through clinical evaluation (history of previous pulmonary edema, pulmonary crepitation with high-intensity murmur in the mitral focus, clinical signs associated with heart disease) and echocardiographic findings (increased indices of pulmonary venous congestion, dilation of pulmonary veins, pulmonary B lines). Patients weighing 15 kg or more, who had been diagnosed with congenital heart disease, other acquired cardiovascular disease or any significant systemic disease, or those who received antiarrhythmic treatment, were not admitted to this investigation. For the control group, clinically healthy dogs weighing less than 15 kg admitted for elective procedures that did not present any echocardiographic abnormalities and that were not receiving any medication for cardiovascular disease were selected.

Transthoracic echocardiography

In both Cardiology Services, echocardiographic evaluation was performed by experienced veterinary cardiologists using echocardiographic machines[a,b] equipped with a range of phased-array transducers, which were selected according to the patient size. A simultaneous single-lead electrocardiogram was acquired with the images. Standard echocardiographic views were obtained as previously described (Boon, 2011), with the dogs in the right and left lateral recumbencies. Recordings were stored

as still frames or cine loops for the offline analysis either in the equipment or using a DICON software[c]. None of the dogs were sedated.

The parameters included in the study were: cross-sectional left atrium diameter (LA), aortic root diameter (Ao), LA-to-Ao ratio (LA:Ao) (Hansson et al., 2002), LV internal dimension at end diastole (LVIDd) and at end-systole (LVIDs), and both of them normalized for body weight (LVIDdN, and LVIDsN) (Cornell et al., 2004), fractional shortening (FS), peak velocity of early (E) and of late (A) diastolic transmitral flow, ratio of early to late transmitral flow (E:A). Isovolumic relaxation time (IVRT) was defined as the time (in milliseconds) from the onset of the aortic valve closure spike artifact to the onset of the mitral valve opening spike artifact, obtained from the apical five-chamber view by aligning the Doppler beam midway between the LV inflow and the LV. Accordingly, ratio of early transmitral flow to IVRT (E:IVRT) was also calculated.

The tissue Doppler spectral images were obtained by placing the pulsed-wave tissue Doppler at the left ventricle lateral mitral annulus, septal mitral annulus and right ventricle lateral tricuspid annulus in apical 4-chambers images. Once the image was obtained, the first negative myocardial diastolic velocity wave was named as E' wave (after ECG's T wave), whereas the second negative myocardial diastolic velocity was named as A' wave (after ECG's P wave). The E' wave was formed at the rapid ventricular filling phase, whereas, the A' wave was produced during the atrial contraction. The first positive low amplitude myocardial systolic velocity was the isovolumic contraction wave; the second long wave with a positive high amplitude was called myocardial systolic velocity (S') (Rudski et al., 2010).

Assessment of ventricular mechanical activation times

163 The aortic flow was recorded from the apical 5-chamber view using pulsed-wave
164 Doppler, and the pulmonic flow was obtained either from the right cranial parasternal
165 short axis view or the left cranial parasternal view, whichever optimized alignment with
166 the pulmonary trunk and outflow, using pulsed-wave Doppler. From the spectral
167 Doppler traces, the time intervals in milliseconds from the start of the QRS complex on
168 the simultaneously acquired ECG to the beginning of the pulmonic flow (Rpulm) and
169 to the beginning of the aortic flow (Rao) were measured. The difference between
170 RPulm and Rao was defined as mechanical interventricular dyssynchrony (Figure 1).

171 The time between the beginning of the QRS complex in ECG and the beginning
172 of S' wave in tissue Doppler traces was defined as the electromechanical delay (RSb)
173 wave (Bader et al., 2004; Lafitte et al., 2004). The time between the beginning of the
174 QRS complex in ECG and the peak of S' wave in tissue Doppler traces was defined as
175 the electrosystolic delay (RSp) (Bax et al., 2003). Both RSb and RSp were measured
176 in three points: lateral mitral anulus (L-RSb, L-RSp), septal mitral anulus (S-RSb, S-
177 RSp), and lateral tricuspid annulus (R-RSb, R-RSp). The difference between the S-
178 RSb and L-RSb times, and between S-RSp and L-RSp times was defined as the
179 mechanical intra-left ventricle conduction delay (Intra-LVb and Intra-LVp). The
180 difference between the R-RSb and L-RSb times, and between R-RSp and L-RSp
181 times was defined as the mechanical interventricular conduction delay (Inter-Vb and
182 Inter-Vp, respectively). Those measurements are shown in Figure 2.

183 Measurement results were calculated using the average of measurements in
184 three beats. To reduce bias, the single trained operator (BCPV) that performed those
185 measurements was blinded to the patient's clinical and electrocardiographic condition.

186 **Electrocardiographic analyses**

Good quality computer-based ECG recordings[d,e] were used for measurements. All ECG tracings were recorded continuously for at least 3 minutes, and followed recommendations described elsewhere (Santilli, Moïse, et al., 2019). Precordial leads had to be positioned according to Wilson's precordial lead system modified by Santilli et al., in which V1 is positioned at the first right intercostal space at the level of the costochondral junction and the sixth intercostal space used for all left side leads (V2-V6) (Santilli, Porteiro Vázquez, et al., 2019).

In lead II, the following ECG variables were obtained: cardiac rhythm; minimum, maximum and mean heart rate (HR) (bpm); PQ interval; and QRS complex duration (ms).

Assessment of ventricular electrical activation times

R-peak time was measured in each precordial lead as previously described, from the earliest onset of the QRS complex, determined by multiple simultaneously recorded leads, to the peak of the R wave or, if present, R' wave (Figure 3) (Battaia et al., 2022; Mateos Pañero et al., 2021; Pérez-Riera, de Abreu, Barbosa-Barros, Nikus, et al., 2016). This measurement was performed in three subsequent heartbeats, and the mean was calculated and used for analysis purposes.

The IDI was determined, by calculating the absolute value of the difference between RPT in leads V5 and V1, reflecting left and right ventricular electrical potentials, divided by the QRS duration (Figure 3). After careful evaluation in all leads, the longest QRS duration was chosen for calculation, from the lead where the limits of the QRS complex were most clearly visible (Battaia et al., 2022).

To reduce bias, the single trained operator (BCPV) that performed those measurements was blinded to the patient's clinical and echocardiographic condition.

Statistical analysis

All data underwent the Shapiro-Wilk normality test. Kruskal-Wallis test followed by either Dunn's *post hoc* test or an analysis of variance (ANOVA) followed by Tukey's multiple comparison test was performed to check for differences in age, body weight, HR, electrocardiographic and echocardiographic variables, and markers of ventricular heterogeneity between controls and MMVD dogs. Chi-square test was used to evaluate association between groups and nominal categorical variables, such as sex, and presence of arrhythmias.

Student's t-test or Mann-Whitney test was performed to access the differences in markers of ventricular heterogeneity between (a) dogs with arrhythmias identified during electrocardiography from those without rhythm disturbances; (b) dogs with supraventricular arrhythmias from those with sinus rhythm; (c) dogs with ventricular arrhythmias from those with sinus rhythm; (d) MMVD dogs with dilated hearts (stages B2 and C (Keene et al., 2019)) from those without remodeling (stage B1 (Keene et al., 2019)); and (e) to distinguish MMVD dogs in HF (stage C (Keene et al., 2019)) from the asymptomatic MMVD animals (stages B1 and B2 (Keene et al., 2019)). Of note, the arrhythmias that were included in the statistics were only those related to the pathophysiology of MMVD, such as supraventricular or ventricular ectopies (isolated or organized), or intra- or interatrial or interventricular conduction delays (such as bifid P wave or QRS complex with BBB morphology). The atrioventricular blocks observed in this study were described but were not included in the statistics.

Spearman's test was used to investigate correlations between ECG and echocardiographic surrogates of ventricular conduction times, as well as to check if they correlated with epidemiological, electrocardiographic and echocardiographic variables. For the interpretation of the Spearman correlation magnitude, the following

236 classification was adopted: correlation coefficients <0.3 (poor), 0.3 to 0.5 (fair), 0.6 to
237 0.8 (moderately strong) and >0.8 (very strong) (Chan, 2003).

238 Receiver operating characteristic (ROC) curves were constructed to evaluate
239 sensitivity and specificity of markers of ventricular heterogeneity to differentiate (a)
240 dogs with arrhythmias identified during ECG from those without rhythm disturbances;
241 (b) dogs with supraventricular arrhythmias from those without this type of arrhythmia;
242 (c) dogs with ventricular arrhythmias from those without this type of arrhythmia; (d)
243 dogs with dilated hearts from those without remodeling; and (e) to distinguish dogs in
244 HF from the asymptomatic animals.

245 An area under the curve (AUC) >0.7 was used as the cut-off criteria for
246 acceptable sensitivity and specificity (Koo & Li, 2016). Youden index was used to select
247 the two results with the best combination of sensitivity and specificity. True positive
248 (TP), true negative (TN), false positive and false negative values were used to calculate
249 probability variables. Positive predictive value (PPV) was calculated as TP/(TP+ false
250 positive). Negative predictive value (NPV) was calculated as TN/(false negative +TN).
251 Accuracy was calculated as (TP+TN)/(TP+TN+ false positive + false negative). Odds
252 ratio was calculated as (positive likelihood ratio) / (negative likelihood ratio).

253 Logistic regression models were applied to identify predictors of ventricular
254 remodeling, heart failure, and arrhythmias (general, supraventricular, and ventricular)
255 based on ventricular indices. Variables with diagnostic performance (AUC > 0.7) in
256 receiver operating characteristic (ROC) curve analyses were considered for inclusion.
257 The Youden index was used to determine optimal sensitivity and specificity cutoffs.
258 Logistic regression models were built using a forward stepwise method, retaining
259 variables with $P < 0.05$. Odds ratios (OR) and 95% confidence intervals (CI) were
260 calculated, and model fit was assessed with the Hosmer-Lemeshow test. Model

discrimination was evaluated using AUC values. Diagnostic metrics, including positive PPV, NPV, and accuracy, were calculated from TP, TN, FP, and FN values.

Lastly, to access intra-observer variability of the measurements of ventricular activation times variables, 15% of the ECG tracings or the echocardiographic images were randomly selected, and the same investigator (B.C.P.V) repeated the measurements. Intraclass correlation coefficient estimates were calculated based on a mean-rating (k = 2), absolute-agreement, 2-way mixed-effects model. Bland-Altman plots were performed to analyze bias between repeated measurements. Student's t-test or Mann-Whitney test was performed to access the differences in the measurements made by the same observer. All analyzes were performed using statistical softwares[f] with default settings. Statistical significance was defined as $P < 0.05$.

RESULTS

Animals

A total of 207 dogs were evaluated, but 68 of them were excluded due to body weight of 15 kg or greater. Thus, 139 healthy and MMVD dogs met the inclusion criteria and were recruited for this study. Among them, 42/139 (30.2%) dogs were included in the control group, 50/139 (36%) were classified as stage B1, 19/139 (13.7%) as stage B2 and 28/139 (20.1%) as stage C. Although mixed breed dogs (n=38) formed the majority of cases, several breeds were represented, including French Bulldog (n=15), Poodle, Lhasa Apso (n=14 each), Shih tzu (n=11), Yorkshire (n=10), Dachshund (n=7), Maltese (n=6), Pug, German Spitz (n=5 each), Pinscher (n=3), Chihuahua, Cocker, Beagle, Schnauzer, Whippet (n=2 each), as well as Pekingese (n=1 each).

There were 75/139 (54%) females and 64/139 (46%) males. Although no statistical

difference existed between healthy and MMVD groups with regard to sex and body weight, in the advanced stages of the disease, dogs were older (Table 1).

Echocardiographic and electrocardiographic features

Left atrium, LA:Ao, LVIDd, LVIDs, LVIDdN, LVIDsN, FS, E wave, E:A, E:IVRT, E:E', maximum and mean heart rate, and duration of P-wave and QRS complex differed between groups (Table 1). Even though the presence of arrhythmias was observed in all groups, including the controls, an association existed between the severity of MMVD and the number of arrhythmias ($P < 0.0001$).

Supraventricular arrhythmias were observed in three control dogs (3.33%) (one dog with ectopic atrial rhythm, one dog with bifid P-wave and first degree atrioventricular block [AVB], and one dog with first degree atrioventricular block), three (4.76%) stage B1 dogs (one with atrial premature complex [APC], one with junctional scape beats, one with Mobitz I second degree AVB), four (17.39%) B2 dogs (three with bifid P-wave, and one with APCs), nine (31.03%) C dogs (one with first degree AVB, seven with APCs, one with APCs and bifid P-wave). Ventricular arrhythmias were observed in one (1.09%) control animal (one with ventricular premature complex [VPC]), one (1.59%) B1 animals (one with right BBB [RBBB]), two (8.7%) B2 animals (both with VPCs) and three (10.34%) C animals (all of them with VPCs).

Markers of ventricular activation time *vs* disease stages

Tables 2 and 3 show ECG and echocardiographic markers of ventricular heterogeneity obtained in healthy and MMVD dogs. Except for RPT V1, IDI, S-RSb, S-RSp, R-RSp, RAo, and intra-LVb, all markers of ventricular heterogeneity changed along the progression of the disease. There was a greater delay in L-RSb, L-RSp, and RPT measured in leads V2, V3, V4, V5 and V6 in the more advanced stages of the

309 disease (Figures 4 and 5). On the other hand, R-RSb was shown to be less delayed in
310 these patients. In addition, in those groups there was also an increase in mechanical
311 intra-left and interventricular conduction delay, with Intra-LVp, Inter-Vb, Inter-Vp
312 showing more negative values (Figure 6).

313 Interventricular mechanical dyssynchrony also changed with the worsening of
314 MMVD. In healthy dogs, RAo exhibited greater delays compared to RPulm. As MMVD
315 progressed, RPulm became increasingly prolonged, culminating in a reversal of the
316 Pulm-Ao pattern in stage C (Figures 5 and 6).

317 **Markers of ventricular activation time *vs* cardiac remodeling**

318 With the exception of RPT V1, IDI, S-RSb, R-RSp and Rao, all parameters
319 studied showed difference between dogs with normal and dilated hearts (Table 4). For
320 the identification of cardiac remodeling, The indices that presented the highest
321 accuracy for the identification of cardiac remodeling were RPT V6, Inter-Vb, RPT V4,
322 L-RSp, L-RSp, L-RSb, RPT V3 and RPT V5 (Table 5; Figure 7).

323 The logistic regression model for predicting ventricular remodeling included L-
324 RSp, RPT V4, and RPT V6 (Table 6), all statistically significant ($p < 0.05$). Odds ratios
325 indicated that higher values of L-RSp (OR = 1.068; 95% CI: 1.038 to 1.104), RPT V4
326 (OR = 1.220; 95% CI: 1.031 to 1.504), and RPT V6 (OR = 1.335; 95% CI: 1.084 to
327 1.693) were associated with an increased likelihood of remodeling. The model
328 demonstrated excellent discrimination with an AUC of 0.8805 (95% CI: 0.8184 to
329 0.9426). It achieved an overall classification accuracy of 79.09%, with a PPV of 71.43%
330 and a NPV of 82.67%. The Hosmer-Lemeshow test ($p = 0.9251$) indicated good model
331 fit, supporting the robustness of these parameters in predicting ventricular remodeling.

332 **Markers of ventricular activation time *vs* heart failure**

The variables that different between dogs with heart failure and asymptomatic dogs were: RPT measured in V3, V4, V5 and V6, as well as RPulm and Pulm-Ao (Table 7). The parameters that showed adequate specificity and sensitivity for the identification of dogs with HF were: RPulm, RPT V4, RPT V5, and RPT V6 (Table 8; Figure 8).

The logistic regression model for predicting HF included RPT V4 and RPT V6 as significant predictors (Table 9). Higher values of RPT V4 (OR = 1.360; 95% CI: 1.132 to 1.753) and RPT V6 (OR = 1.242; 95% CI: 1.000 to 1.550) were associated with an increased likelihood of HF. The model demonstrated good discrimination with an AUC of 0.8557 (95% CI: 0.7713 to 0.9401). It achieved an overall classification accuracy of 82.64%, with a NPV of 84.55% and a PPV of 63.64%. The Hosmer-Lemeshow test (p = 0.4389) indicated an adequate model fit. These results highlight the potential of RPT V4 and RPT V6 as important markers for identifying HF.

Markers of ventricular activation time *vs* arrhythmias

Arrhythmias

With the exception of RPT V5, IDI, S-RSp, S-RSb, R-RSp, Rao, Pulm-Ao, Intra-LVb and Intra-LVp, all indices showed difference between dogs with arrhythmias and dogs with sinus rhythms (Table 10). For the identification of dogs with arrhythmias, RPT V6, L-RSb, RPT V3, L-RSp, RPT V1, RPT V2 and Inter-Vb showed adequate AUC (Table 11; Figure 9).

As shown in table 12, logistic regression analysis identified two independent predictors of arrhythmias: L-RSp (OR = 1.022, 95% CI: 1.001–1.048, p = 0.047) and RPT V6 (OR = 1.450, 95% CI: 1.212–1.788, p < 0.001). The model demonstrated good predictive performance, with an AUC of 0.8019 (95% CI: 0.7120–0.8918, p < 0.0001).

The Hosmer-Lemeshow test indicated no significant lack of fit (p = 0.8090), supporting the adequacy of the model. The final model correctly classified 81.82% of cases, with a negative predictive power of 84.00% and a positive predictive power of 60.00%.

Supraventricular arrhythmias

Table 13 shows the parameters studied in dogs with supraventricular arrhythmias and in dogs with sinus rhythms. The indices that showed the highest AUC for the identification of dogs with supraventricular arrhythmias were L-RSp, RPT V6, L-RSb, RPT V2, RPulm, RPT V1, RPT V4 , and R-RSp (Table 14; Figure 10).

The logistic regression model for supraventricular arrhythmias identified L-RSb and V6 as significant predictors (Table 15). The model demonstrated good discrimination (AUC = 0.8583, 95% CI: 0.7352–0.9814, p = 0.0001) and an acceptable fit (Hosmer-Lemeshow test: p = 0.5468). Negative predictive power was 90.10%, and overall classification accuracy reached 88.46%.

Ventricular arrhythmias

There were three variables that showed difference between dogs with ventricular arrhythmias: RPT measured in V1, V3 and V6 leads (Table 16). Indeed, all of them also presented AUC > 0.7 for the identification of dogs with this type of rhythm disturbance (Table 17).

The final logistic regression model for identifying ventricular arrhythmias included the indices V1 and V3 (Table 18). The model showed a high discriminative ability, with an AUC of 0.9434 (95% CI: 0.8697 to 1.000, p = 0.0026). V3 demonstrated a strong association (OR = 2.284; 95% CI: 1.315 to 6.155), while V1 also contributed significantly (OR = 1.670; 95% CI: 1.047 to 3.469). The model achieved excellent overall accuracy (97.52%), specificity (100.00%), and NPV (97.50%), but sensitivity

was limited (25.00%). These findings indicate that the combined use of these indices is effective in distinguishing dogs with ventricular arrhythmias from those without.

Correlations between markers of ventricular activation time *vs.* each other, or other variables

Although we observed correlation results between the echocardiographic and electrocardiographic variables of ventricular activation time, no moderately strong or very strong correlation was found between them (supplementary material tables A and B).

Intra-observer analyses

Measurements of ventricular activation time were repeated to access intra-observer variability. They did not differ from the first measurement. The lowest bias was observed in IDI and the highest bias was observed in Inter-Vb, as shown in Table 19.

DISCUSSION

We evaluated electrocardiographic and echocardiographic indices of ventricular conduction heterogeneity in dogs and investigated their behavior in different stages of MMVD. Our hypothesis that these indices change with the progression of the disease, and that they behave differently in dogs with arrhythmias, cardiac remodeling or HF was confirmed, with the exception of electrical interventricular dyssynchrony (assessed by IDI), that did not show differences between groups studied.

R-peak time (RPT) is an easily measurable ECG variable that plays a key role in diagnosing, treating, and predicting the prognosis of various cardiovascular and infectious diseases (Aiken et al., 2022; Battaia et al., 2022; Cinier et al., 2021; Estes,

2017; Sivri et al., 2023). Prolonged RPT is linked to pathophysiological mechanisms such as impaired cellular calcium and potassium conduction, increased cardiac myocyte size, and interstitial fibrosis. Studies indicate that prolonged RPT is associated with sudden cardiac death, a higher risk of HF, subclinical myocardial dysfunction, and the severity of coronary artery disease in people (Bayam et al., 2021; Cekirdekci et al., 2019; Darouian et al., 2016; O'Neal et al., 2016). Additionally, RPT is an independent risk factor for mortality in COVID-19 patients (Sivri et al., 2023).

At the time of this writing, the only pathological condition in which RPT has been studied in veterinary medicine is in dogs with BBB (Battaia et al., 2022). As this index reflects the electrical activation time that occurs from the endocardium to the epicardium (Pérez-Riera, de Abreu, Barbosa-Barros, Nikus, et al., 2016), this analysis in precordial leads can be used to differentiate RBBB from left BBB (Surawicz et al., 2009). In healthy dogs, right ventricle RPT (V1) should be < 18 ms, while LV RPT (V2-V6) should be < 35 ms (Mateos Pañero et al., 2021). RPT > 28 ms in lead V1 and >36 ms in lead V5 in dogs indicate the presence of RBBB and left BBB, respectively (Battaia et al., 2022). In our study, healthy dogs presented RPT values similar to the results published previously (Mateos Pañero et al., 2021). None of our groups presented mean RPT above the cut-off point for identifying BBB (Table 2), as only one dog presented RBBB (and RPT V1 36.67 ms). Even so, RPT was higher in dogs with arrhythmias. As MMVD advances, progressive left cardiac chamber dilation and heightened sympathetic tone significantly elevate the risk of electrical disturbances (Crosara et al., 2010; Vila et al., 2021). Since the left chambers are best studied using left precordial leads, prolongation of the RPT in MMVD dogs is expected to occur specially in them. Indeed, we found that an RPT V3 exceeding 30.3 ms demonstrated a 94.4% accuracy in identifying dogs with ventricular arrhythmias, highlighting its

potential as a reliable diagnostic marker (Table 17). Furthermore, in addition to RPT values measured in V3 and V6, our analyses identified RPT V1 as a robust predictor of ventricular arrhythmias, a result supported by the logistic regression model, which identified RPT V1 and V3 as independent predictors. This suggests that electrical disturbances in MMVD dogs may extend beyond the left heart, involving the right ventricular conduction system. These findings underscore the importance of evaluating multiple precordial leads when assessing the risk of ventricular arrhythmias in this population. Further research is needed to clarify the clinical implications and guide potential management strategies.

RPT measured in the left precordial leads increased with progression of MMVD, and were more prolonged in dogs with dilated hearts and HF. This finding indicates that the time that electrical impulse takes to travel from the endocardium to the epicardium in the LV increases with the dilation of left cardiac chambers and the HF. An association between delayed RPT and risk for HF events is also shown in people (O'Neal et al., 2016). For every 10 ms increase in RPT, there was a 1.42 times greater risk of HF events, and that risk increased significantly when RPT was >45 ms (O'Neal et al., 2016). In another study, RPT of >50 ms in leads V5 and V6 was a strong predictor of HF events in people (HR 2.81) (O'Neal et al., 2017). From an electrophysiological point of view, the RPT coincides with the upstroke velocity (phase 0) of the ventricular myocyte action potential, and it is characterized by the rapid inflow of sodium ions in the ventricular cardiomyocytes. Normally, the duration of this phase is of a few milliseconds, but in dilated or hypertrophied hearts it is associated with electrical myocardial remodeling, an increase in action potential duration and its temporal inhomogeneity, as well as with an increase in RPT. The neurohumoral activation in decompensated congestive HF could probably play the lead role in the prolongation of

RPT. High catecholamine levels, inducing a downregulation of β-adrenergic myocardial receptors, could reduce chrono/dromo/inotropy, also causing an increase in the RPT (Piccirillo et al., 2023).

During normal ventricular activation, the difference between RPT V5 and RPT V1 is quite small, but not zero. In healthy dogs, IDI was previously reported as 23 (16-29)%, which is similar to the value obtained in our control group 19.1 (±8.2) %. Although we observed an increase in LV electrical activation times in advanced stages of MMVD, IDI did not exceed the reference values in any group of any test performed, indicating that electrical ventricular dyssynchrony is not relevant with the worsening of MMVD, nor with the presence of arrhythmias, congestive HF or cardiac remodeling. This finding may be associated with the fact that MMVD is not a disease originating in the electrical system, but rather a disease that causes cardiovascular damage due to volume overload. On the other hand, variables assessing both intra-LV and interventricular electromechanical and electrosystolic dyssynchrony increased with progression of MMVD, and differed between dogs with cardiac remodeling and dogs with normal-sized hearts. We found that dogs with inter-Vb <-9.3 ms are 10.6 times more prone to have remodeled left chambers, with 80% sensitivity, and 72.5% specificity (Table 5). This increase in mechanical interventricular conduction delay in dogs with cardiac dilation is mainly due to the electromechanical and electrosystolic delays measured in the LV lateral wall (L-RSb and L-RSp, respectively). Dogs with dilated cardiomyopathy also present more prolonged L-RSb, L-RSp, S-RSb and S-RSp than healthy dogs, and their LV free wall activation time is more delayed than of the interventricular septum (Simpson et al., 2008). As these measurements indicate the time that the electrical impulse takes to travel through the left ventricle walls, the volume overload and dilation of this chamber associated with tissue fibrosis eventually

results in a longer time for electrical propagation.

Interventricular mechanical dyssynchrony assessed by aortic and pulmonic flows also changed with the worsening of MMVD (Table 3), and resulted in differences when looking to dogs with remodeled hearts or HF. We observed that RAo, which corresponds to the LV pre-ejection period, is more delayed in healthy dogs than RPulm, which corresponds to the RV pre-ejection period. This pattern has already been reported in healthy dogs, people and primates (Trikhun et al., 2020; Zhu et al., 2021). In dogs with HF or remodeled hearts, we found an inversion of this pattern, with a predominance of right ventricular mechanical delay. This finding has also been previously noted in people with HF (Zhu et al., 2021).

The application of logistic regression in this study was instrumental in distinguishing the independent contributions of echocardiographic and ECG variables to cardiac remodeling, HF and arrhythmias. While ROC analysis demonstrated diagnostic performance for individual variables, regression models allowed us to evaluate their predictive power after adjusting for the influence of other factors. For example, even among multiple indices with significant ROC values, logistic regression identified L-RSp, RPT V4 and RPT V6 as the most robust predictors of cardiac remodeling (Table 6), as well as L-RSp and P V6 as arrhythmia predictors (Table 12), highlighting their independent association with structural and electrical heart changes in MMVD. These findings emphasize the significant role of atrial conduction disturbances in reflecting structural heart changes.

Although we observed significant changes in ventricular mechanical and electrical activation indices in dogs with cardiac structural, hemodynamic or electrical abnormalities, we did not find a strong correlation between these variables. Myocardial excitation and conduction are electrical activities, and electrical dyssynchrony is best

assessed by electrocardiogram. The excitation and conduction of the myocardium result in contraction and relaxation, and mechanical dyssynchrony is better studied by echocardiogram. Given the nexus between temporal electrical activation and mechanical function, mechanical dyssynchrony is expected to be the result of an abnormal electrical activation pattern. However, both mechanical and electrical dyssynchrony can exist alone or in combination with each other (Perry et al., 2011; Risum, 2014). We found that although MMVD causes a greater delay in left ventricular electrical activation times, this is not significant enough to result in interventricular electrical dyssynchrony. On the other hand, mechanical dyssynchrony increased along the progression of MMVD, indicating that cardiac remodeling and HF in this disease cause more impairment of mechanical performance than electrical heterogeneity. These findings suggest that RPT and mechanical dyssynchrony indices could serve as practical markers for early detection of arrhythmias and heart failure in MMVD, aiding clinical decision-making.

LIMITATIONS

As MMVD is a degenerative disease that is mainly seen in older dogs, group differences related to age are the main limitations of this study. Although there was no correlation between the indices studied and age, we do not know whether this difference between the groups may have influenced the investigation. Although we used the same protocol, the dogs were evaluated in two different locations, with different echocardiogram and electrocardiogram equipment. Therefore, we suggest that future studies be carried out standardizing only one piece of equipment for performing the echocardiogram and one piece of equipment for performing the electrocardiogram. Radiographic examination was not included in the standard protocol and therefore not performed in all dogs. Not using 24-hour Holter analysis for

the exclusion of AF and other arrhythmias is another limitation. It was a cross-sectional study, without case follow-up, which implies the loss of information about the prognostic power of the evaluated indices. Future research should include longitudinal analyses to assess the prognostic value of ventricular activation indices.

CONCLUSION

Both electrical and mechanical ventricular activation times were prolonged, with mechanical dyssynchrony significantly increasing alongside MMVD progression, underlining their diagnostic and prognostic value in this condition. Some ventricular activation times obtained by ECG and by echocardiography proved to be adequate arrhythmogenic markers, and identified dilated hearts or HF with adequate specificity and sensitivity. These findings emphasize the importance of integrating electrocardiographic and echocardiographic markers into routine evaluations for early detection and management of MMVD-related complications. Furthermore, this is the first paper evaluating RPT and IDI in dogs with MMVD.

Footnotes

[a] - Philips Affiniti 50 ultrasound system equipped with 2-4, 3-8 and 4-12 MHz phased-array transducers, Andover, MA, USA.

[b] – Siemens Acuson P500 ultrasound system equipped with 2-4 and 4-8 MHz phased-array transducers, Issaquah, Washington, USA.

[c] - RadiAnt DICOM Viewer - Poznan, Wielkopolskie , Poland.

[d] – INPulse – INCardio ICV2.1 - Florianópolis, Santa Catarina, Brazil

[e] - TEB ECG PC - Tecnologia Eletrônica Brasileira, São Paulo, São Paulo, Brazil.

[f] - Graphpad prism 5.0 Software

REFERENCES

Abdellah, A. T., & El-Nagary, M. (2018). Prevalence of P wave dispersion and interatrial block in patients with systolic heart failure and their relationship with functional status, hospitalization and one year mortality. *The Egyptian Heart Journal*, *70*(3), 181–187. https://doi.org/10.1016/j.ehj.2018.02.006

Aiken, A. V., Goldhaber, J. I., & Chugh, S. S. (2022). Delayed intrinsicoid deflection: Electrocardiographic harbinger of heart disease. *Annals of Noninvasive Electrocardiology*, *27*(3). https://doi.org/10.1111/anec.12940

Akamatsu, K., Ito, T., Miyamura, M., Kanzaki, Y., Sohmiya, K., & Hoshiga, M. (2020). Usefulness of tissue Doppler-derived atrial electromechanical delay for identifying patients with paroxysmal atrial fibrillation. *Cardiovascular Ultrasound*, *18*(1), 22. https://doi.org/10.1186/s12947-020-00205-2

Bader, H., Garrigue, S., Lafitte, S., Reuter, S., Jaïs, P., Haïssaguerre, M., Bonnet, J., Clementy, J., & Roudaut, R. (2004). Intra-left ventricular electromechanical asynchrony. *Journal of the American College of Cardiology*, *43*(2), 248–256. https://doi.org/10.1016/j.jacc.2003.08.038

BaronToaldo, M., Guglielmini, C., Diana, A., Sarcinella, F., & Cipone, M. (2014). Feasibility and reproducibility of echocardiographic assessment of regional left atrial deformation and synchrony by tissue Doppler ultrasonographic imaging in healthy dogs. *American Journal of Veterinary Research*, *75*(1), 59–66. https://doi.org/10.2460/ajvr.75.1.59

Battaia, S., Perego, M., Perciballi, C., Cavallini, D., & Santilli, R. (2022). Noninvasive electrocardiographic parameters to assess interventricular dyssynchrony in dogs with bundle branch blocks. *Journal of Veterinary Cardiology*, *41*, 134–144. https://doi.org/10.1016/j.jvc.2022.02.005

Bax, J. J., Ansalone, G., Breithardt, O. A., Derumeaux, G., Leclercq, C., Schalij, M. J., Sogaard, P., St. John Sutton, M., & Nihoyannopoulos, P. (2004). Echocardiographic evaluation of cardiac resynchronization therapy: ready for routine clinical use? *Journal of the American College of Cardiology*, *44*(1), 1–9. https://doi.org/10.1016/j.jacc.2004.02.055

Bax, J. J., Molhoek, S. G., van Erven, L., Voogd, P. J., Somer, S., Boersma, E., Steendijk, P., Schalij, M. J., & Van der Wall, E. E. (2003). Usefulness of myocardial tissue Doppler echocardiography to evaluate left ventricular dyssynchrony before and after biventricular pacing in patients with idiopathic dilated cardiomyopathy. *The American Journal of Cardiology*, *91*(1), 94–97. https://doi.org/10.1016/S0002-9149(02)03009-6

Bayam, E., Yıldırım, E., Kalçık, M., Karaduman, A., Kalkan, S., Güner, A., Küp, A., Kahyaoğlu, M., Yılmaz, Y., Selcuk, M., & Uyan, C. (2021). Relationship between P wave peak time and coronary artery disease severity in non-ST elevation acute coronary syndrome. *Herz*, *46*(2), 188–194. https://doi.org/10.1007/s00059-019-04859-1

Bleeker, G. B., Schalij, M. J., Molhoek, S. G., Holman, E. R., Verwey, H. F., Steendijk, P., van der Wall, E. E., & Bax, J. J. (2005). Frequency of left ventricular dyssynchrony in patients with heart failure and a narrow QRS complex. *The American Journal of Cardiology*, *95*(1), 140–142. https://doi.org/10.1016/j.amjcard.2004.08.082

Bleeker, G. B., Schalij, M. J., Molhoek, S. G., Verwey, H. F., HOLMAN, E. R., BOERSMA, E., STEENDIJK, P., VAN DER WALL, E. E., & BAX, J. J. (2004). Relationship Between QRS Duration and Left Ventricular Dyssynchrony in Patients with End-Stage Heart Failure. *Journal of Cardiovascular Electrophysiology*, *15*(5), 544–549. https://doi.org/10.1046/j.1540-8167.2004.03604.x

Boon, J. A. (2011). *Veterinary echocardiography* (J. A. Boon, Ed.). Wiley-Blackwell.

Bristow, M. R., Saxon, L. A., Boehmer, J., Krueger, S., Kass, D. A., De Marco, T., Carson, P., DiCarlo, L., DeMets, D., White, B. G., DeVries, D. W., & Feldman, A. M. (2004). Cardiac-Resynchronization Therapy with or without an Implantable Defibrillator in Advanced Chronic Heart Failure. *New England Journal of Medicine*, *350*(21), 2140–2150. https://doi.org/10.1056/NEJMoa032423

Cekirdekci, E. I., Unal Evren, E., Evren, H., & Bugan, B. (2019). R-peak time: A novel marker

606 of depolarization in patients with Human Immunodeficiency Virus. *Journal of*
607 *Electrocardiology*, *55*, 133–137. https://doi.org/10.1016/j.jelectrocard.2019.05.016
608 Celik, Y., Yıldırım, N., Demir, V., Alp, C., Sahin, O., & Tolga Doğru, M. (2021). Atrial
609 electromechanical delay and p wave dispersion associated with severity of chronic
610 obstructive pulmonary disease. *African Health Sciences*, *21*(1), 140–149.
611 https://doi.org/10.4314/ahs.v21i1.19
612 Chan, Y. H. (2003). Biostatistics 104: correlational analysis. *Singapore Medical Journal*,
613 *44*(12), 614–619.
614 Cheng, A., Helm, R. H., & Abraham, T. P. (2009). Pathophysiological mechanisms underlying
615 ventricular dyssynchrony. *Europace*, *11*(Supplement 5), v10–v14.
616 https://doi.org/10.1093/europace/eup272
617 Cinier, G., Yilmaz, A. S., Tekkesin, A. I., & Cetin, M. (2021). Predictors for the prolonged R
618 wave peak time among patients with arterial hypertension. *Turk Kardiyoloji Dernegi*
619 *Arsivi-Archives of the Turkish Society of Cardiology*, *49*(5), 387–394.
620 https://doi.org/10.5543/tkda.2021.80540
621 Cornell, C. C., Kittleson, M. D., Della Torre, P., Häggström, J., Lombard, C. W., Pedersen, H.
622 D., Vollmar, A., & Wey, A. (2004). Allometric scaling of M-mode cardiac measurements
623 in normal adult dogs. *Journal of Veterinary Internal Medicine*, *18*(3), 311–321.
624 https://doi.org/10.1892/0891-6640(2004)18<311:asomcm>2.0.co;2
625 Crosara, S., Borgarelli, M., Perego, M., Häggström, J., La Rosa, G., Tarducci, A., & Santilli,
626 R. A. (2010). Holter monitoring in 36 dogs with myxomatous mitral valve disease.
627 *Australian Veterinary Journal*, *88*(10), 386–392. https://doi.org/10.1111/j.1751-
628 0813.2010.00628.x
629 Darouian, N., Narayanan, K., Aro, A. L., Reinier, K., Uy-Evanado, A., Teodorescu, C.,
630 Gunson, K., Jui, J., & Chugh, S. S. (2016). Delayed intrinsicoid deflection of the QRS
631 complex is associated with sudden cardiac arrest. *Heart Rhythm*, *13*(4), 927–932.
632 https://doi.org/10.1016/j.hrthm.2015.12.022
633 De Vos, C. B., Weijs, B., Crijns, H. J. G. M., Cheriex, E. C., Palmans, A., Habets, J., Prins,
634 M. H., Pisters, R., Nieuwlaat, R., & Tieleman, R. G. (2009). Atrial tissue Doppler imaging
635 for prediction of new-onset atrial fibrillation. *Heart*, *95*(10), 835–840.
636 https://doi.org/10.1136/hrt.2008.148528
637 Dhingra, R., Pencina, M. J., Wang, T. J., Nam, B.-H., Benjamin, E. J., Levy, D., Larson, M.
638 G., Kannel, W. B., D'Agostino, R. B., & Vasan, R. S. (2006). Electrocardiographic QRS
639 Duration and the Risk of Congestive Heart Failure. *Hypertension*, *47*(5), 861–867.
640 https://doi.org/10.1161/01.HYP.0000217141.20163.23
641 Dilaveris, P. E., & Gialafos, J. E. (2001). P-Wave Dispersion: A Novel Predictor of
642 Paroxysmal Atrial Fibrillation. *Annals of Noninvasive Electrocardiology*, *6*(2), 159–165.
643 https://doi.org/10.1111/j.1542-474X.2001.tb00101.x
644 Dittrich, G., Campos, G. M. V. der B., Sousa, M. G., & Oliveira, S. T. (2018). P wave
645 dispersion in obese dogs with and without mitral valve disease. *Ciência Rural*, *48*(10).
646 https://doi.org/10.1590/0103-8478cr20180047
647 Duru, M., Seyfeli, E., Kuvandik, G., Kaya, H., & Yalcin, F. (2006). Effect of Weight Loss on P
648 Wave Dispersion in Obese Subjects*. *Obesity*, *14*(8), 1378–1382.
649 https://doi.org/10.1038/oby.2006.156
650 Erbay, A. R., Turhan, H., Yasar, A. S., Bicer, A., Senen, K., Sasmaz, H., Sabah, I., & Yetkin,
651 E. (2005). Effects of long-term beta-blocker therapy on P-wave duration and dispersion
652 in patients with rheumatic mitral stenosis. *International Journal of Cardiology*, *102*(1),
653 33–37. https://doi.org/10.1016/j.ijcard.2004.03.079
654 Estes, E. H. (2017). Commentary on Electrocardiographic Time to Intrinsicoid Deflection and
655 Heart Failure: the Multi-Ethnic Study of Atherosclerosis. *Clinical Cardiology*, *40*(1), 53–
656 53. https://doi.org/10.1002/clc.22629
657 Falchi, A. G., Grecchi, I., Muggia, C., & Tinelli, C. (2014). Weight loss and P wave dispersion:
658 a preliminary study. *Obesity Research & Clinical Practice*, *8*(6), e614–e617.
659 https://doi.org/10.1016/j.orcp.2014.08.005
660 Glikson, M., Nielsen, J. C., Kronborg, M. B., Michowitz, Y., Auricchio, A., Barbash, I. M.,

Barrabés, J. A., Boriani, G., Braunschweig, F., Brignole, M., Burri, H., Coats, A. J. S., Deharo, J. C., Delgado, V., DIller, G. P., Israel, C. W., Keren, A., Knops, R. E., Kotecha, Di., … Tolosana, J. M. (2021). 2021 ESC Guidelines on cardiac pacing and cardiac resynchronization therapy. In *European Heart Journal* (Vol. 42, Issue 35, pp. 3427–3520). Oxford University Press. https://doi.org/10.1093/eurheartj/ehab364

Gorcsan, J., Marek, J. J., & Onishi, T. (2012). The Contemporary Role of Echocardiography in Improving Patient Response to Cardiac Resynchronization Therapy. In *Current Cardiovascular Imaging Reports* (Vol. 5, Issue 6, pp. 462–472). Current Medicine Group LLC 1. https://doi.org/10.1007/s12410-012-9172-2

Gorcsan, J., & Tayal, B. (2015). Newer Echocardiographic Techniques in Cardiac Resynchronization Therapy. In *Cardiac Electrophysiology Clinics* (Vol. 7, Issue 4, pp. 609–618). W.B. Saunders. https://doi.org/10.1016/j.ccep.2015.08.013

Griffiths, L. G., Fransioli, J. R., & Chigerwe, M. (2011). Echocardiographic assessment of interventricular and intraventricular mechanical synchrony in normal dogs. *Journal of Veterinary Cardiology*, *13*(2), 115–126. https://doi.org/10.1016/j.jvc.2011.02.001

Guglielmini, C., Goncalves Sousa, M., Baron Toaldo, M., Valente, C., Bentivoglio, V., Mazzoldi, C., Bergamin, I., Drigo, M., & Poser, H. (2020). Prevalence and risk factors for atrial fibrillation in dogs with myxomatous mitral valve disease. *Journal of Veterinary Internal Medicine*, *34*(6), 2223–2231. https://doi.org/10.1111/jvim.15927

Guntekin, U., Gunes, Y., Tuncer, M., Gunes, A., Sahin, M., & Simsek, H. (2008). Long-term Follow-up of P-wave Duration and Dispersion in Patients with Mitral Stenosis. *Pacing and Clinical Electrophysiology*, *31*(12), 1620–1624. https://doi.org/10.1111/j.1540-8159.2008.01235.x

Haghjoo, M., Bagherzadeh, A., Fazelifar, A. F., Haghighi, Z. O., Esmaielzadeh, M., Alizadeh, A., Emkanjoo, Z., Sadeghpour, A., Samiei, N., Farahani, M. M., Sadr-Ameli, M. A., Maleki, M., & Noohi, F. (2007). Prevalence of Mechanical Dyssynchrony in Heart Failure Patients with Different QRS Durations. *Pacing and Clinical Electrophysiology*, *30*(5), 616–622. https://doi.org/10.1111/j.1540-8159.2007.00722.x

Hansson, K., Häggström, J., Kvart, C., & Lord, P. (2002). LEFT ATRIAL TO AORTIC ROOT INDICES USING TWO-DIMENSIONAL AND M-MODE ECHOCARDIOGRAPHY IN CAVALIER KING CHARLES SPANIELS WITH AND WITHOUT LEFT ATRIAL ENLARGEMENT. *Veterinary Radiology & Ultrasound*, *43*(6), 568–575. https://doi.org/10.1111/j.1740-8261.2002.tb01051.x

Irdem, A., Aydın Sahin, D., Kervancioglu, M., Baspinar, O., Sucu, M., Keskin, M., & Kilinc, M. (2016). Evaluation of P-Wave Dispersion, Diastolic Function, and Atrial Electromechanical Conduction in Pediatric Patients with Subclinical Hypothyroidism. *Echocardiography*, *33*(9), 1397–1401. https://doi.org/10.1111/echo.13255

Jagannatha, G. N. P., Antara, I. M. P. S., Kosasih, A. M., Kamardi, S., & Pradnyana, I. W. A. S. (2024). P-wave peak time and P-wave dispersion in surface electrocardiography as initial predictors of new-onset atrial fibrillation in early-onset hypertension. *Hypertension Research*, *47*(1), 137–148. https://doi.org/10.1038/s41440-023-01357-0

Janus, I., Noszczyk-Nowak, A., Nowak, M., Ciaputa, R., Kandefer-Gola, M., & Pasławska, U. (2016). A comparison of the histopathologic pattern of the left atrium in canine dilated cardiomyopathy and chronic mitral valve disease. *BMC Veterinary Research*, *12*(1), 3. https://doi.org/10.1186/s12917-015-0626-z

Keene, B. W., Atkins, C. E., Bonagura, J. D., Fox, P. R., Häggström, J., Fuentes, V. L., Oyama, M. A., Rush, J. E., Stepien, R., & Uechi, M. (2019). ACVIM consensus guidelines for the diagnosis and treatment of myxomatous mitral valve disease in dogs. *Journal of Veterinary Internal Medicine*, *33*(3), 1127–1140. https://doi.org/10.1111/jvim.15488

Kirk, J. A., & Kass, D. A. (2013). Electromechanical Dyssynchrony and Resynchronization of the Failing Heart. *Circulation Research*, *113*(6), 765–776. https://doi.org/10.1161/CIRCRESAHA.113.300270

Koo, T. K., & Li, M. Y. (2016). A Guideline of Selecting and Reporting Intraclass Correlation Coefficients for Reliability Research. *Journal of Chiropractic Medicine*, *15*(2), 155–163.

https://doi.org/10.1016/j.jcm.2016.02.012
Korovesis, T. G., Koutrolou-Sotiropoulou, P., & Katritsis, D. G. (2022). Arrhythmogenic Mitral Valve Prolapse. *Arrhythmia & Electrophysiology Review*, *11*. https://doi.org/10.15420/aer.2021.28
Kosar, F., Aksoy, Y., Ari, F., Keskin, L., & Sahin, I. (2008). P-Wave Duration and Dispersion in Obese Subjects. *Annals of Noninvasive Electrocardiology*, *13*(1), 3–7. https://doi.org/10.1111/j.1542-474X.2007.00194.x
Lafitte, S., Garrigue, S., Perron, J.-M., Bordachar, P., Reuter, S., Jaïs, P., Haïssaguerre, M., Clementy, J., & Roudaut, R. (2004). Improvement of left ventricular wall synchronization with multisite ventricular pacing in heart failure: a prospective study using Doppler tissue imaging. *European Journal of Heart Failure*, *6*(2), 203–212. https://doi.org/10.1016/j.ejheart.2003.10.008
Lane, R. E. (2004). Selection and optimisation of biventricular pacing: the role of echocardiography. *Heart*, *90*(suppl_6), vi10–vi16. https://doi.org/10.1136/hrt.2004.043000
Lee, J., Mizuno, M., Mizuno, T., Harada, K., & Uechi, M. (2015). Pathologic Manifestations on Surgical Biopsy and Their Correlation with Clinical Indices in Dogs with Degenerative Mitral Valve Disease. *Journal of Veterinary Internal Medicine*, *29*(5), 1313–1321. https://doi.org/10.1111/jvim.13587
LL, T., SG, T., & KK, P. (2013). ECG P wave abnormalities. *Singapore Medical Journal*, *54*(1), 4–5. https://doi.org/10.11622/smedj.2013002
Mano, H., Okumura, Y., Watanabe, I., Ohta, M., Kogawa, R., Sasaki, N., Nakai, T., Ohkubo, K., Kofune, M., Nagashima, K., Sonoda, K., Haruta, H., & Hirayama, A. (2014). Changes over time in echocardiographic variables and atrial electromechanical intervals after ablation for atrial fibrillation. *Journal of Arrhythmia*, *30*(6), 466–472. https://doi.org/10.1016/j.joa.2014.01.005
Mateos Pañero, M., Battaia, S., Ramera, L., Perego, M., & Santilli, R. A. (2021). R-peak time in clinically healthy dogs with different thoracic conformations. *Veterinary Journal*, *268*. https://doi.org/10.1016/j.tvjl.2020.105592
Müller, P., Weijs, B., Bemelmans, N. M. A. A., Mügge, A., Eckardt, L., Crijns, H. J. G. M., Bax, J. J., Linz, D., & den Uijl, D. W. (2021). Echocardiography-derived total atrial conduction time (PA-TDI duration): risk stratification and guidance in atrial fibrillation management. *Clinical Research in Cardiology*, *110*(11), 1734–1742. https://doi.org/10.1007/s00392-021-01917-9
Ndrepepa, G., Zrenner, B., Deisenhofer, I., Karch, M., Schneider, M., Schreieck, J., & Schmitt, C. (2000). Relationship between surface electrocardiogram characteristics and endocardial activation sequence in patients with typical atrial flutter. *Zeitschrift Für Kardiologie*, *89*(6), 527–537. https://doi.org/10.1007/s003920070225
Neves, J., Pedro, B., Christley, R., & Dukes-McEwan, J. (2018). Usefulness of pulsed-wave tissue Doppler imaging at the mitral annulus for prediction of new-onset atrial fibrillation in dogs. *Journal of Veterinary Cardiology*, *20*(6), 425–437. https://doi.org/10.1016/j.jvc.2018.10.002
Noszczyk-Nowak, A. (2012). P-Wave Dispersion in Prediction of Maintenance of Sinus Rhythm After an Electrical Cardioversion of Atrial Fibrillation in Dogs. *Bulletin of the Veterinary Institute in Pulawy*, *56*(1), 99–102. https://doi.org/10.2478/v10213-012-0018-0
Noszczyk-Nowak, A., Paslawska, U., Szalas, A., & Nicpon, J. (2008). P-WAVE DISPERSION IN HEALTHY DOGS. A PRELIMINARY STUDY. *Bulletin of the Veterinary Institute in Pulawy*, *52*, 683–688.
Noszczyk-Nowak, A., Szałas, A., Pasławska, U., & Nicpoń, J. (2011). Comparison of P-wave dispersion in healthy dogs, dogs with chronic valvular disease and dogs with disturbances of supraventricular conduction. *Acta Veterinaria Scandinavica*, *53*(1), 18. https://doi.org/10.1186/1751-0147-53-18
Ogawa, M., Ogi, H., Miyakawa, H., Hsu, H.-H., Miyagawa, Y., & Takemura, N. (2022). Evaluation of the association between electrocardiogram parameters and left cardiac

remodeling in dogs with myxomatous mitral valve disease. *Veterinary World*, 2072–2083. https://doi.org/10.14202/vetworld.2022.2072-2083

Okutucu, S., Aytemir, K., & Oto, A. (2016). P-wave dispersion: What we know till now? *JRSM Cardiovascular Disease*, *5*, 204800401663944. https://doi.org/10.1177/2048004016639443

O'Neal, W. T., Mazur, M., Bertoni, A. G., Bluemke, D. A., Al-Mallah, M. H., Lima, J. A. C., Kitzman, D., & Soliman, E. Z. (2017). Electrocardiographic Predictors of Heart Failure With Reduced Versus Preserved Ejection Fraction: The Multi-Ethnic Study of Atherosclerosis. *Journal of the American Heart Association*, *6*(6). https://doi.org/10.1161/JAHA.117.006023

O'Neal, W. T., Qureshi, W. T., Nazarian, S., Kawel-Boehm, N., Bluemke, D. A., Lima, J. A. C., & Soliman, E. Z. (2016). Electrocardiographic Time to Intrinsicoid Deflection and Heart Failure: The Multi-Ethnic Study of Atherosclerosis. *Clinical Cardiology*, *39*(9), 531–536. https://doi.org/10.1002/clc.22561

Özer, N., Aytemir, K., Atalar, E., Sade, E., Aksöyek, S., Övünç, K., Açýl, T., Nazlý, N., Özmen, F., Oto, A., & Kes, S. (2000). P Wave Dispersion in Hypertensive Patients with Paroxysmal Atrial Fibrillation. *Pacing and Clinical Electrophysiology*, *23*(11P2), 1859–1862. https://doi.org/10.1111/j.1540-8159.2000.tb07038.x

Özer, N., Yavuz, B., Can, I., Atalar, E., Aksöyek, S., Övünç, K., Özmen, F., & Kes, S. (2005). Doppler tissue evaluation of intra-atrial and interatrial electromechanical delay and comparison with P-wave dispersion in patients with mitral stenosis. *Journal of the American Society of Echocardiography*, *18*(9), 945–948. https://doi.org/10.1016/j.echo.2005.01.015

Pedro, B. M., Alves, J. V., Cripps, P. J., Stafford Johnson, M. J., & Martin, M. W. S. (2011). Association of QRS duration and survival in dogs with dilated cardiomyopathy: A retrospective study of 266 clinical cases. *Journal of Veterinary Cardiology*, *13*(4), 243–249. https://doi.org/10.1016/j.jvc.2011.09.003

Pérez-Riera, A. R., de Abreu, L. C., Barbosa-Barros, R., Grindler, J., Fernandes-Cardoso, A., & Baranchuk, A. (2016). P-wave dispersion: an update. *Indian Pacing and Electrophysiology Journal*, *16*(4), 126–133. https://doi.org/10.1016/j.ipej.2016.10.002

Pérez-Riera, A. R., de Abreu, L. C., Barbosa-Barros, R., Nikus, K. C., & Baranchuk, A. (2016). R-Peak Time: An Electrocardiographic Parameter with Multiple Clinical Applications. *Annals of Noninvasive Electrocardiology*, *21*(1), 10–19. https://doi.org/10.1111/anec.12323

Perry, R., De Pasquale, C. G., Chew, D. P., McGavigan, A. D., & Joseph, M. X. (2011). Tissue Doppler Derived Mechanical Dyssynchrony Does Not Change after Cardiac Resynchronization Therapy. *Echocardiography*, *28*(9), 961–967. https://doi.org/10.1111/j.1540-8175.2011.01498.x

Pessoa, R. B. (2019). *Mensuração do Tempo de Condução Atrial Total por meio da ecocardiografia tecidual em cães normais e em cães com Valvopatia Mitral Mixomatosa* [Universidade de São Paulo]. https://doi.org/10.11606/D.10.2019.tde-21112018-122807

Piccirillo, G., Moscucci, F., Mezzadri, M., Caltabiano, C., Di Diego, I., Carnovale, M., Corrao, A., Stefano, S., Scinicariello, C., Giuffrè, M., De Santis, V., Sciomer, S., Rossi, P., & Magrì, D. (2023). Electrocardiographic and other Noninvasive Hemodynamic Markers in Decompensated CHF Patients. *Journal of Cardiovascular Development and Disease*, *10*(3), 125. https://doi.org/10.3390/jcdd10030125

Ponikowski, P., Voors, A. A., Anker, S. D., Bueno, H., Cleland, J. G. F., Coats, A. J. S., Falk, V., González-Juanatey, J. R., Harjola, V.-P., Jankowska, E. A., Jessup, M., Linde, C., Nihoyannopoulos, P., Parissis, J. T., Pieske, B., Riley, J. P., Rosano, G. M. C., Ruilope, L. M., Ruschitzka, F., … van der Meer, P. (2016). 2016 ESC Guidelines for the diagnosis and treatment of acute and chronic heart failure. *European Heart Journal*, *37*(27), 2129–2200. https://doi.org/10.1093/eurheartj/ehw128

Pozios, I., Vouliotis, A. I., Dilaveris, P., & Tsioufis, C. (2023). Electro-Mechanical Alterations in Atrial Fibrillation: Structural, Electrical, and Functional Correlates. *Journal of Cardiovascular Development and Disease*, *10*(4), 149.

826 https://doi.org/10.3390/jcdd10040149
827 Risum, N. (2014). Assessment of mechanical dyssynchrony in cardiac resynchronization
828 therapy. *Dan Med J* , *61*(12), B4981.
829 Rodrigues, A. C. T., Tsutsui, J. M., & Mathias Jr, W. (2006). Avaliação de dissincronia
830 cardíaca pelo ecocardiograma: estratégias para um resultado adequado Cardiac
831 dyssynchrony in patients with heart failure: strategies for an adequate
832 echocardiographic assessment. *Revista Brasileira de Ecocardiografia*, *19*(3), 46–51.
833 Rudski, L. G., Lai, W. W., Afilalo, J., Hua, L., Handschumacher, M. D., Chandrasekaran, K.,
834 Solomon, S. D., Louie, E. K., & Schiller, N. B. (2010). Guidelines for the
835 Echocardiographic Assessment of the Right Heart in Adults: A Report from the
836 American Society of Echocardiography. *Journal of the American Society of*
837 *Echocardiography*, *23*(7), 685–713. https://doi.org/10.1016/j.echo.2010.05.010
838 Russo, V., Rago, A., Di Meo, F., Papa, A. A., Ciardiello, C., Cristiano, A., Calabrò, R., Russo,
839 M. G., & Nigro, G. (2015). Atrial Septal Aneurysms and Supraventricular Arrhythmias:
840 The Role of Atrial Electromechanical Delay. *Echocardiography*, *32*(10), 1504–1514.
841 https://doi.org/10.1111/echo.12908
842 Salem, A. S., Abazeed, S. H., Elhawary, A., & Abdelmonem, A. H. (2021). Correlation
843 Between Left Ventricular Electromechanical Delay and Body Mass Index. *European*
844 *Heart Journal Supplements*, *23*(Supplement_D).
845 https://doi.org/10.1093/eurheartj/suab069.004
846 Santilli, R. A., Moïse, N. S., Pariaut, R., & Perego, M. (2019). *Electrocardiography of the dog*
847 *and cat: diagnosis of arrhythmias* (R. A. Santilli, N. S. Moïse, R. Pariaut, & M. Perego,
848 Eds.). Edra.
849 Santilli, R. A., Porteiro Vázquez, D. M., Gerou-Ferriani, M., Lombardo, S. F., & Perego, M.
850 (2019). Development and assessment of a novel precordial lead system for accurate
851 detection of right atrial and ventricular depolarization in dogs with various thoracic
852 conformations. *American Journal of Veterinary Research*, *80*(4), 358–368.
853 https://doi.org/10.2460/ajvr.80.4.358
854 Seyfeli, E., Duru, M., Kuvandık, G., Kaya, H., & Yalcin, F. (2006). Effect of obesity on P-wave
855 dispersion and QT dispersion in women. *International Journal of Obesity*, *30*(6), 957–
856 961. https://doi.org/10.1038/sj.ijo.0803233
857 Simpson, K. E., Devine, B. C., Woolley, R., Corcoran, BrendamM., & French, A. T. (2008).
858 TIMING OF LEFT HEART BASE DESCENT IN DOGS WITH DILATED
859 CARDIOMYOPATHY AND NORMAL DOGS. *Veterinary Radiology & Ultrasound*, *49*(3),
860 287–294. https://doi.org/10.1111/j.1740-8261.2008.00359.x
861 Sivri, F., Şencan, M., Ceyhan, B. Ö., Içen, Y. K., Coskun, M., & Aksoy, F. (2023). Prognostic
862 value of R wave peak time in COVID-19 pneumonia. *Journal of Electrocardiology*, *80*,
863 91–95. https://doi.org/10.1016/j.jelectrocard.2023.05.005
864 Spach, M. S., Miller, W. T., Geselowitz, D. B., Barr, R. C., Kootsey, J. M., & Johnson, E. A.
865 (1981). The discontinuous nature of propagation in normal canine cardiac muscle.
866 Evidence for recurrent discontinuities of intracellular resistance that affect the
867 membrane currents. *Circulation Research*, *48*(1), 39–54.
868 https://doi.org/10.1161/01.RES.48.1.39
869 Spartalis, M., Tzatzaki, E., Spartalis, E., Damaskos, C., Athanasiou, A., Livanis, E., &
870 Voudris, V. (2017). Pathophysiology and Current Evidence for Detection of
871 Dyssynchrony. *Cardiology Research*, *8*(5), 179–183. https://doi.org/10.14740/cr598w
872 Spragg, D. D., & Kass, D. A. (2006). Pathobiology of Left Ventricular Dyssynchrony and
873 Resynchronization. *Progress in Cardiovascular Diseases*, *49*(1), 26–41.
874 https://doi.org/10.1016/j.pcad.2006.05.001
875 Surawicz, B., Childers, R., Deal, B. J., & Gettes, L. S. (2009). AHA/ACCF/HRS
876 Recommendations for the Standardization and Interpretation of the Electrocardiogram.
877 *Journal of the American College of Cardiology*, *53*(11), 976–981.
878 https://doi.org/10.1016/j.jacc.2008.12.013
879 Sweeney, M. O., & Prinzen, F. W. (2006). A New Paradigm for Physiologic Ventricular
880 Pacing. *Journal of the American College of Cardiology*, *47*(2), 282–288.

https://doi.org/10.1016/j.jacc.2005.09.029
Tapia-Orihuela, R. K., Gharacholou, S. M., Asirvatham, S. J., & Munoz, F. D.-C. (2022). Electrocardiographic markers of cardiac resynchronization therapy response: delayed time to intrinsicoid deflection onset in lateral leads. *Journal of Geriatric Cardiology : JGC*, *19*(1), 21–30. https://doi.org/10.11909/j.issn.1671-5411.2022.01.009
Tidholm, A., Ljungvall, I., HÃ¶glund, K., Westling, A. B., & HÃ¤ggstrÃ¶m, J. (2009). Tissue Doppler and Strain Imaging in Dogs with Myxomatous Mitral Valve Disease in Different Stages of Congestive Heart Failure. *Journal of Veterinary Internal Medicine*, *23*(6), 1197–1207. https://doi.org/10.1111/j.1939-1676.2009.0403.x
Trikhun, P., Surachetpong, S. D., Sutayatram, S., & Buranakarl, C. (2020). Left ventricular systolic function in dogs with pulmonic stenosis. *Veterinary World*, *13*(11), 2436–2442. https://doi.org/10.14202/vetworld.2020.2436-2442
Turhan, H., Yetkin, E., Senen, K., Yilmaz, M. B., Ileri, M., Atak, R., Cehreli, S., & Kutuk, E. (2002). Effects of percutaneous mitral balloon valvuloplasty on P-wave dispersion in patients with mitral stenosis. *The American Journal of Cardiology*, *89*(5), 607–609. https://doi.org/10.1016/S0002-9149(01)02307-4
van Everdingen, W. M., Schipper, J. C., Van 'T Sant, J., Misier, K. R., Meine, M., & Cramer, M. J. (2016). Echocardiography and cardiac resynchronisation therapy, friends or foes? In *Netherlands Heart Journal* (Vol. 24, Issue 1, pp. 25–38). Bohn Stafleu van Loghum. https://doi.org/10.1007/s12471-015-0769-3
Vereckei, A., Szelényi, Z., Kutyifa, V., Zima, E., Szénási, G., Kiss, M., Katona, G., Karádi, I., & Merkely, B. (2018). Novel electrocardiographic dyssynchrony criteria improve patient selection for cardiac resynchronization therapy. *EP Europace*, *20*(1), 97–103. https://doi.org/10.1093/europace/euw326
Vernooy, K., Verbeek, X. A. A. M., Paschar, M., & Prinzen, F. W. (2003). Relation Between Abnormal Ventricular Impulse Conduction and Heart Failure. *Journal of Interventional Cardiology*, *16*(6), 557–562. https://doi.org/10.1046/j.1540-8183.2003.01061.x
Vieira, M. L. C., Maddukuri, P. V., Phang, R. S., Pandian, N. G., Mathias Júnior, W., & Ramires, J. A. F. (2005). Demonstração do mecanismo da terapia de ressincronização ventricular com ecocardiografia tridimensional em tempo real em paciente com insuficiência cardíaca. *Arquivos Brasileiros de Cardiologia*, *85*(5). https://doi.org/10.1590/S0066-782X2005001800006
Vila, B. de C. P., Camacho, A. A., & Sousa, M. G. (2021). T-wave peak-end interval and ratio of T-wave peak-end and QT intervals: novel arrhythmogenic and survival markers for dogs with myxomatous mitral valve disease. *Journal of Veterinary Cardiology*, *35*, 25–41. https://doi.org/10.1016/j.jvc.2021.02.004
Villani, G. Q., Piepoli, M., Rosi, A., & Capucci, A. (1996). P-wave dispersion index: a marker of patients with paroxysmal atrial fibrillation. *International Journal of Cardiology*, *55*(2), 169–175. https://doi.org/10.1016/0167-5273(96)02677-0
Wang, J., Kurrelmeyer, K. M., Torre-Amione, G., & Nagueh, S. F. (2007). Systolic and Diastolic Dyssynchrony in Patients With Diastolic Heart Failure and the Effect of Medical Therapy. *Journal of the American College of Cardiology*, *49*(1), 88–96. https://doi.org/10.1016/j.jacc.2006.10.023
Yano, M., Kohno, M., Konishi, M., Takahashi, T., Seki, K., & Matsuzaki, M. (1994). Influence of left ventricular regional nonuniformity on afterload-dependent relaxation in intact dogs. *American Journal of Physiology-Heart and Circulatory Physiology*, *267*(1), H148–H154. https://doi.org/10.1152/ajpheart.1994.267.1.H148
Yu, C.-M. (2003). High prevalence of left ventricular systolic and diastolic asynchrony in patients with congestive heart failure and normal QRS duration. *Heart*, *89*(1), 54–60. https://doi.org/10.1136/heart.89.1.54
Zhu, T., Lei, M., Wang, Z., Zhang, R., Zhang, Y., Jin, W., Yu, C., Huang, C. L.-H., Liu, D., Zheng, W., Liu, Y., Quan, X., Kong, L., Liang, S., & Zhang, X. (2021). A Comparative Study of Systolic and Diastolic Mechanical Synchrony in Canine, Primate, and Healthy and Failing Human Hearts. *Frontiers in Cardiovascular Medicine*, *8*. https://doi.org/10.3389/fcvm.2021.750067

936
937

938

Table 1. Demographic, echocardiographic and electrocardiographic features of healthy dogs and dogs with myxomatous mitral valve disease.

	Control (n=42)	B1 (n=50)	B2 (n=19)	C (n=28)	P
Age (years)	2 (2; 5)[a]	8 (4; 11)[b]	11.2 (±2.4)[bc]	12.2 (±2.3)[c]	<0.0001**
Body weight (kg)	8.5 (±2.9)[a]	7.2 (4.7; 10)[b]	7.3 (5.3; 8;3)[b]	7.5 (±2.8)[b]	0.3172**
Females (N [%])	23 (54.8)	27 (54)	11 (57.9)	14 (50)	0.9589*
HR min (bpm)	97.9 (±26.5)[a]	90.1 (±26.9)[abc]	71.1 (±23.2)[b]	100.6 (±29.6)[c]	0.0073***
HR max (bpm)	154.8 (±30.4)	154 (140; 188)	168.9 (±49.4)	186.1 (±52.8)	0.1106**
HR med (bpm)	133 (±30.7)[ab]	122.7 (±25.3)[a]	127.8 (±35.4)[ab]	150.7 (±28.6)[b]	0.0034**
PQ interval (ms)	80 (70; 87)[a]	83 (76; 93.8)[ac]	95.7 (±16.6)[bc]	97.5 (±18.7)[b]	<0.0001**
QRS complex (ms)	54 (50; 60)[a]	55(±5.1)[a]	57.3 (±5.5)[ab]	62.5 (54; 70)[b]	<0.0001**
LA (mm)	1.9 (±0.3)[a]	1.9 (±0.3)[a]	2.6 (2.4; 3)[b]	3 (±0.5)[b]	<0.0001**
LA:Ao	1.3 (±0.1)[a]	1.3 (1.2; 1.4)[a]	2 (±0.3)[b]	2.4 (±0.4)[c]	<0.0001**
LVIDd (mm)	2.5 (±0.5)[a]	2.4 (2.2; 3)[a]	3.2 (3.1; 3.5)[b]	3.7 (3.4; 3.8)[c]	<0.0001**
LVIDs (mm)	1.5 (1.3; 1.8)[ab]	1.5 (±0.4)[a]	1.7 (±0.4)[ab]	1.8 (±0.4)[b]	0.0153**
LVIDdN	1.3 (1.2; 1.5)[a]	1.5 (±0.2)[b]	1.9 (±0.2)[c]	2 (±0.3)[d]	<0.0001***
LVIDsN	0.8 (0.7; 0.9)	0.8 (±0.1)	0.9 (±0.2)	0.9 (±0.2)	0.3796**
FS (%)	40 (±8.3)[a]	43.1 (±8.1)[a]	50 (±6.7)[b]	51.2 (±7.8)[b]	<0.0001***
E (cm/s)	71.2 (±14)[a]	64.1 (±14.2)[a]	98 (±20.2)[b]	132.9 (±23.8)[c]	<0.0001***
E:A	1.3 (1.1; 1.7)[a]	1.1 (0.8; 1.4)[b]	1.1(±0.4)[ab]	1.3 (1.1; 2.1)[a]	0.0012**
E:IVRT	1.2 (±0.4)[a]	0.9 (±0.3)[b]	1.5 (±0.6)[ac]	2.2 (1.9; 2.5)[c]	<0.0001**
E:E'	7.4 (±2.1)[ab]	6.8 (5.7; 7.8)[a]	8.9 (±3)[bc]	10.8 (8.4; 13.2)[c]	<0.0001**

Results are presented as mean ± standard deviation for normally distributed data or median (interquartile range) for non-normally distributed data, based on the normality test outcomes. Values followed by the same letter do not differ from each other by Dunn's test or Tukey's multiple comparison test (P>0.05).

*: Chi-square test; **: Kruskal-Wallis test and Dunn test; ***: Tukey's multiple comparison test; E: Peak velocity of early diastolic transmitral flow; E:A: Ratio of early-to-late transmitral flow peak velocities; E:IVRT: ratio of early transmitral flow to isovolumetric

relaxation time; E:E': Ratio of early transmitral flow peak velocity to the early mitral annulus tissue peak velocity; FS: Fractional shortening; LA:Ao: Ratio of the left atrial dimensions to the aortic annulus dimension; LVIDdN: left ventricular end diastolic diameter normalized for body weight; LVIDsN: left ventricular end systolic diameter normalized for body weight.

Table 2. Electrical ventricular activation times and dyssynchrony in healthy dogs and dogs with myxomatous mitral valve disease.

	Control	B1	B2	C	P
RPT V1 (ms)	17.3 (±3.3)	20 (15.7; 22)	22.3 (14.8; 23.8) (15.2; 23.5)	22.7 (14.8; 23.3)	0.0674*
RPT V2 (ms)	22.5 (±3) [a]	24.3 (22; 26.7) [ab]	26.7 (26; 28) [b]	27.3 (22.5; 29.3) [b]	0.0001*
RPT V3 (ms)	22.9 (±3)[a]	25.2 (±2.9)[b]	27 (26; 28)[bc]	27.9 (±4.)[c]	<0.0001*
RPT V4 (ms)	25.3 (±3.1)[ab]	25.7 (±3.4)[a]	27.7 (26.7;28.5)[ab]	29 (28; 31.3)[b]	<0.0001*
RPT V5 (ms)	28.1 (±3.1)[a]	28 (26.3; 30)[a]	28.8 (28; 29.3)[ab]	30.9 (±2.6)[b]	0.0004*
RPT V6 (ms)	30.2 (±3.3)[a]	28.7 (27.3; 30)[a]	30.3 (±1.4)[ab]	32 (30.2; 35)[b]	<0.0001*
IDI (%)	19.1 (±8.2)	13.5 (9; 21.3)	10 (7.3; 24.8)	11.5 (10; 28.5)	0.1953*

Results are presented as mean ± standard deviation for normally distributed data or median (interquartile range) for non-normally distributed data, based on the normality test outcomes. Values followed by the same letter do not differ from each other by Dunn's test or Tukey's multiple comparison test (P>0.05).

*Kruskal-Wallis test and Dunn test; RPT: R-peak Time; IDI: interventricular dyssynchrony index.

Table 3. Mechanical ventricular activation times and dyssynchrony in healthy dogs and dogs with myxomatous mitral valve disease.

	Control	B1	B2	C	P
L-RSb (ms)	37.8 (31.8; 49.1)[a]	42.6 (±10.2)[ab]	48.7 (37.2; 59.3)[ab]	47.9 (±11.2)[b]	0.0085*
L-RSp (ms)	62.7 (52.4; 74.2)[a]	66.2 (±15.7)[a]	88.8 (75.9; 105.8)[b]	75.9 (±17.9)[b]	<0.0001*
S-RSb (ms)	40.7 (33.7; 49)	42 (±10.9)	44.6 (±10.6)	42.2 (38.9; 52.5)	0.7054*
S-RSp (ms)	64.7 (53.3; 77.8)	62.7 (50; 76.5)	66 (54.7; 78)	68.3 (58; 80.5)	0.3733*
R-RSb (ms)	39 (30.7; 53.7)[a]	38.4 (±14.8)[ab]	28.4 (±16.8)[b]	33.3 (17; 39.2)[ab]	0.0302*
R-RSp (ms)	70 (59.2; 90.6)	66.5 (53.3; 84.9)	67.9 (±25.4)	63 (54.4; 117)	0.5157*
Rpulm (ms)	21 (14; 29.3)[a]	25.8 (±9.3)[a]	28.2 (±8.9)[ab]	37.8 (±13.9)[b]	<0.0001*
RAo (ms)	31.9 (±14.5)	32.5 (24.5; 40.8)	29.1 (±11.9)	33.2 (±12.4)	0.5709*
Pulm-Ao (ms)	-8 (±10.3)[a]	-5.2 (±13.3)[a]	1.2 (±11.5)[ab]	4.7 (±15.7)[b]	0.0004**
Intra-LVb (ms)	0.4 (±5.6) [a]	0.1 (±10.2) [a]	-8.4 (±15.2) [b]	-6.3 (±13.9) [ab]	0.0070**
Intra-LVp (ms)	2 (-6.7; 6.7)[a]	-0.9 (±19.1)[a]	-29.3 (±25.1)[b]	-45. (±25.5)[a]	0.0001*
Inter-Vb (ms)	-2.2 (-9.9; 7.3)[a]	-3.9 (±13.6)[a]	-26.8 (±18.6)[b]	-16.7 (-27; -2.8)[ab]	<0.0001*
Inter-Vp (ms)	4.2 (-1.3; 18.6)[a]	5.8 (±26.7)[a]	-31 (±30.2)[b]	-0.2 (±42.6)[a]	0.0001*

Results are presented as mean ± standard deviation for normally distributed data or median (interquartile range) for non-normally distributed data, based on the normality test outcomes. Values followed by the same letter do not differ from each other by Dunn's test or Tukey's multiple comparison test (P>0.05).

*Kruskal-Wallis test and Dunn test; **Tukey's multiple comparison test; Inter-Vb: Mechanical interventricular conduction delay using the beginning of the S' wave; Inter-Vp: Mechanical interventricular conduction delay using the peak of the S' wave; Intra-LVb: Mechanical intra-left ventricle conduction delay using the beginning of the S' wave; Intra-LVb: Mechanical intra-left ventricle conduction delay using the peak of the S' wave; L-RSb: Electromechanical delay measured in lateral mitral annulus; L-RSp: Electrosystolic delay measured in lateral mitral annulus; Pulm-Ao : Mechanical interventricular dyssynchrony; Rao: Time intervals from the start of the QRS complex to the beginning of the aortic flow; RPulm: Time intervals from the start of the QRS complex to the beginning of the pulmonic flow; R-RSb: Electromechanical delay measured in lateral tricuspid annulus; R-RSp: Electrosystolic delay measured in lateral tricuspid annulus; S-RSb: Electromechanical delay measured septal mitral annulus; S-RSp: Electrosystolic delay

measured septal mitral annulus Inter-Vb

Table 4. Markers of ventricular activation times and dyssynchrony in dogs with normal size hearts and in dogs with dilated hearts.

	Normal size hearts	Dilated hearts	P
RPT V1 (ms)	20.3 (15.5; 22.1)	22.7 (15; 23.3)	0.0928*
RPT V2 (ms)	24.3 (22; 26.7)	26.7 (24.2; 28.7)	0.0033*
RPT V3 (ms)	25 (±2.8)	27.3 (26; 29)	0.0004*
RPT V4 (ms)	25.5 (±3.4)	28 (27.3; 29.8)	<0.0001*
RPT V5 (ms)	28 (26.2; 29.7)	29.3 (28.7; 30.9)	0.0005*
RPT V6 (ms)	28.7 (26.3; 30)	30.8 (30; 32.7)	<0.0001*
IDI	13 (9; 21)	11 (8.3; 25.8)	0.9878*
L-RSb (ms)	40.3 (± 8.7)	48 (39.2; 57.3)	0.0006*
L-RSp (ms)	64.2 (±16.1)	27.2 (65.6; 92.9)	<0.0001*
S-RSb (ms)	40.3 (±10.6)	42.2 (36; 50)	0.2956*
S-RSp (ms)	55.3 (48.5; 75.4)	67 (55.5; 77.7)	0.0294*
R-RSb (ms)	37.1 (±13.9)	25 (17; 39.2)	0.0432*
R-RSp (ms)	63.8 (49.4; 84.8)	62.8 (53.9; 84.2)	0.9947*
Rpulm (ms)	26 (±9.9)	34.2 (±12.9)	0.0008**
RAo (ms)	31.4 (±11.9)	30.8 (±12.2)	0.8109**
Pulm-Ao (ms)	-5.3 (±13.4)	3.4 (±14.2)	0.0032**
Intra-LVb (ms)	0 (±10.2)	-7.3 (±14.3)	0.0107**
Intra-LVp (ms)	-1.9 (±18.3)	-15.4 (±27.9)	0.0107**
Inter-Vb (ms)	-4.1 (±13.7)	-19.3 (-37.7; -10.7)	0.0002*
Inter-Vp (ms)	5.6 (±27)	-14 (±40.2)	0.0119**

Results are presented as mean ± standard deviation for normally distributed data or median (interquartile range) for non-normally distributed data, based on the normality test outcomes.

*Mann-Whitney test; **Unpaired t test; Inter-Vb: Mechanical interventricular conduction delay using the beginning of the S' wave; Inter-Vp: Mechanical interventricular conduction delay using the peak of the S' wave; Intra-LVb: Mechanical intra-left ventricle conduction delay using the beginning of the S' wave; Intra-LVb: Mechanical intra-left ventricle conduction delay using the peak of the S' wave; L-RSb: Electromechanical delay measured in lateral mitral annulus; L-RSp: Electrosystolic delay measured in lateral mitral annulus; Pulm-Ao : Mechanical interventricular dyssynchrony; Rao: Time intervals from the start of the QRS complex to the beginning of the aortic flow; RPulm: Time intervals from the start of the QRS complex to the beginning of the pulmonic flow; R-RSb: Electromechanical delay measured in lateral tricuspid annulus; R-RSp: Electrosystolic delay measured in lateral tricuspid annulus; S-RSb: Electromechanical delay measured septal mitral annulus; S-RSp: Electrosystolic delay measured septal mitral annulus Inter-Vb; RPT: R-peak Time; IDI: interventricular dyssynchrony index.

Table 5. Cut-off values for each marker of ventricular conduction time and its respective AUC value, P value, sensitivity, specificity, PPV, NPV, accuracy and odds ratio for detecting cardiac remodeling

Index	AUC	p	Cutoff (ms)	Sensitivity (%)	95% CI	Specificity (%)	95% CI	Positive likelihood ratio	PPV	NPV	Accuracy (%)	Odds Ratio
RPT V6	0.81	<0.0001	> 28.8	92.5	80.14% to 97.42%	63.0	48.60% to 75.48%	2.5	0.69	0.91	76.7	21.0
Inter-Vb	0.74	0.0003	< -10.8	74.3	57.93% to 85.84%	77.5	62.50% to 87.68%	3.3	0.74	0.78	76.0	10.0
Inter-Vb	0.74	0.0003	< -9.3	80.0	64.11% to 89.96%	72.5	57.17% to 83.89%	2.9	0.72	0.81	76.0	10.6
RPT V4	0.77	<0.0001	> 27.7	70.0	54.57% to 81.93%	75.5	61.91% to 85.40%	2.9	0.70	0.76	73.0	7.2
L-RSp	0.76	<0.0001	> 77.7	59.1	44.41% to 72.31%	84.1	70.63% to 92.07%	3.7	0.79	0.67	71.6	7.6
RPT V4	0.77	<0.0001	> 26.8	82.5	68.05% to 91.25%	61.2	47.25% to 73.57%	2.1	0.63	0.81	70.8	7.4
RPT V6	0.81	<0.0001	> 30.2	60.0	44.60% to 73.65%	78.3	64.43% to 87.74%	2.8	0.71	0.69	69.8	5.4
L-RSp	0.76	<0.0001	> 72.2	70.5	55.78% to 81.84%	68.2	53.44% to 80.00%	2.2	0.69	0.70	69.3	5.1
L-RSb	0.71	0.0008	> 46.7	57.1	42.21% to 70.88%	79.6	65.50% to 88.85%	2.8	0.73	0.66	68.6	5.2
RPT V3	0.71	0.0006	> 27	58.5	43.37% to 72.24%	75.0	61.22% to 85.08%	2.3	0.67	0.68	67.4	4.2
RPT V5	0.71	0.0007	> 28.8	70.0	54.57% to 81.93%	65.3	51.31% to 77.08%	2.0	0.62	0.73	67.4	4.4
RPT V5	0.71	0.0007	> 29.2	67.5	52.02% to 79.92%	65.3	51.31% to 77.08%	1.9	0.61	0.71	66.3	3.9
L-RSb	0.71	0.0008	> 43.8	66.7	51.55% to 78.99%	65.9	51.14% to 78.12%	2.0	0.65	0.67	66.3	3.9
RPT V3	0.71	0.0006	> 25.8	80.5	65.99% to 89.77%	52.1	38.33% to 65.53%	1.7	0.59	0.76	65.2	4.5

AUC: area under the curve; Inter-Vb: Mechanical interventricular conduction delay using the beginning of the S' wave; L-RSb: Electromechanical delay measured in lateral mitral annulus; L-RSp: Electrosystolic delay measured in lateral mitral annulus; RPT: R-peak Time; PPV: Positive predictive value; NPV: Negative predictive value

Table 6. Logistic regression model for cardiac remodeling prediction in dogs with MMVD

Variable	Estimate (β)	Standard Error	95% CI	Odds Ratio (95% CI)
Intercept	-19.53	4.295	-29.15 to -12.13	—
L-RSp	0.0655	0.01569	0.03707 to 0.09915	1.068 (1.038 to 1.104)
RPT V4	0.1992	0.09456	0.03086 to 0.4085	1.220 (1.031 to 1.504)
RPT V6	0.2889	0.1123	0.08052 to 0.5265	1.335 (1.084 to 1.693)

L-RSp: Electrosystolic delay measured in lateral mitral annulus; RPT: R-peak Time

Table 7. Markers of ventricular activation times and dyssynchrony in dogs with heart failure and dogs without heart failure.

	No HF	HF	P
RPT V1 (ms)	20.8 (15.3; 22.8)	22.7 (14.8; 23.3)	0.2561*
RPT V2 (ms)	25.3 (22; 26.7)	27.3 (22.5; 29.3)	0.0928*
RPT V3 (ms)	26 (24.1; 27.3)	27.9 (±4.5)	0.0044*
RPT V4 (ms)	26.7 (24.3; 28)	29 (28; 31.3)	<0.0001*
RPT V5 (ms)	28 (26.7; 29.3)	30.9 (±2.6)	<0.0001*
RPT V6 (ms)	28.8 (28; 30.4)	32 (30.2; 35)	<0.0001*
IDI	12 (9; 22.5)	11.5 (10; 28.5)	0.4497*
L-RSb (ms)	41.7 (35; 50)	47.9 (±11.2)	0.0431*
L-RSp (ms)	71.3 (55.7; 86)	75.9 (±17.9)	0.3032*
S-RSb (ms)	41.3 (±10.7)	44 (30.5; 49.87)	0.9448*
S-RSp (ms)	57.7 (50; 75)	68.3 (58; 80.5)	0.0367*
R-RSb (ms)	34.3 (±15.6)	33.3 (17; 39.2)	0.6503*
R-RSp (ms)	63 (50; 84.3)	63 (54.4; 117)	0.6098*
Rpulm (ms)	26.8 (±9.7)	37.8 (±13.9)	<0.0001**
RAo (ms)	30.3 (±11.8)	33.2 (±12.4)	0.2968**
Pulm-Ao (ms)	-3.6 (±13.2)	4.7 (±15.7)	0.0108**
Intra-LVb (ms)	0 (-6.7; 5.3)	-6.3 (±13.9)	0.3103*
Intra-LVp (ms)	-10.1 (±23.9)	-4.5 (±25.5)	0.4345*
Inter-Vb (ms)	-5.8 (-19.9; 4)	-16.7 (-27; -2.8)	0.3548*
Inter-Vp (ms)	-5 (±32.4)	-0.2 (±42.6)	0.5991**

Results are presented as mean ± standard deviation or median (interquartile interval).

*Mann-Whitney test; **Unpaired t test; HF: heart failure; Inter-Vb: Mechanical interventricular conduction delay using the beginning of the S' wave; Inter-Vp: Mechanical interventricular conduction delay using the peak of the S' wave; Intra-LVb: Mechanical intra-left ventricle conduction delay using the beginning of the S' wave; Intra-LVb: Mechanical intra-left ventricle conduction delay using the beginning of the S' wave; L-RSb: Electromechanical delay measured in lateral mitral annulus; L-RSp: Electrosystolic delay measured in lateral mitral annulus; Pulm-Ao : Mechanical interventricular dyssynchrony; Rao: Time intervals from the start of the QRS complex to the beginning of the aortic flow; RPulm: Time intervals from the start of the QRS complex to the beginning of the pulmonic flow; R-RSb: Electromechanical delay measured in lateral tricuspid annulus; R-RSp: Electrosystolic delay measured in lateral tricuspid annulus; S-RSb: Electromechanical delay measured septal mitral annulus; S-RSp: Electrosystolic delay measured septal mitral annulus Inter-Vb; RPT: R-peak Time; IDI: interventricular dyssynchrony index.

Table 8. Cut-off values for each marker of ventricular conduction time and its respective AUC value, P value, sensitivity, specificity, PPV, NPV, accuracy and odds ratio for detecting heart failure.

Index	AUC	p	Cutoff (ms)	Sensitivity (%)	95% CI	Specificity (%)	95% CI	Positive likelihood ratio	PPV	NPV	Accuracy (%)	Odds Ratio
RPT V4	0.82	<0.0001	> 29.2	50.0	31.43% to 68.57%	95.4	87.29% to 98.74%	10.8	0.80	0.84	83.2	20.7
RPT V6	0.83	<0.0001	> 30.5	75.0	55.10% to 88.00%	75.8	63.85% to 84.75%	3.1	0.55	0.89	75.6	9.4
Rpulm (ms)	0.73	0.0005	> 34.8	63.0	44.23% to 78.47%	79.1	67.93% to 87.12%	3.0	0.55	0.84	74.5	6.4
RPT V4	0.82	<0.0001	> 27.7	83.3	64.15% to 93.32%	69.2	57.20% to 79.11%	2.7	0.50	0.92	73.0	11.3
RPT V5	0.79	<0.0001	> 29.7	62.5	42.71% to 78.84%	76.9	65.36% to 85.49%	2.7	0.50	0.85	73.0	5.6
RPT V5	0.79	<0.0001	> 29.2	83.3	64.15% to 93.32%	63.1	50.92% to 73.77%	2.3	0.45	0.91	68.5	8.5
RPT V6	0.83	<0.0001	> 29.7	91.7	74.15% to 98.52%	58.1	45.67% to 69.52%	2.2	0.46	0.95	67.4	15.2
Rpulm (ms)	0.73	0.0005	> 30.8	70.4	51.52% to 84.15%	64.2	52.22% to 74.60%	2.0	0.44	0.84	66.0	4.3

AUC: area under the curve; RPulm: Time intervals from the start of the QRS complex to the beginning of the pulmonic flow; RPT: R-peak Time; PPV: Positive predictive value; NPV: Negative predictive value

Table 9. Logistic regression model for HF prediction in dogs with MMVD

Variable	Estimate (β)	Standard Error	95% CI (Profile Likelihood)	Odds Ratio (95% CI)
Intercept	-16.51	3.748	-24.83 to -9.989	—
RPT V4	0.3072	0.1098	0.1239 to 0.5613	1.360 (1.132 to 1.753)
RPT V6	0.2169	0.1103	0.0002395 to 0.4383	1.242 (1.000 to 1.550)

RPT: R-peak Time

Table 10. Markers of ventricular activation times and dyssynchrony in dogs with arrhythmias and dogs with sinus rhythms.

	No arrhytmia	Arrhytmia	P
RPT V1 (ms)	18 (14.9; 22.1)	22.4 (±6)	0.0034*
RPT V2 (ms)	24.3 (21 ; 26.7)	27.3 (24.3; 32.2)	0.0039*
RPT V3 (ms)	25.3 (22; 26.7)	28.5 (±5.1)	0.0023*
RPT V4 (ms)	26.7 (24.3; 28)	28.7 (±6)	0.0255*
RPT V5 (ms)	28.7 (26.7; 30)	29.6 (±3.7)	0.0887*
RPT V6 (ms)	30 (28; 31)	33 (±3)	0.0002*
IDI (%)	15 (9; 25)	11 (6; 18)	0.1029*
L-RSb (ms)	39.3 (32.3; 47.3)	51.3 (±13.9)	0.0016*
L-RSp (ms)	62.8 (50.6; 76.1)	82.2 (±21.4)	0.0026*
S-RSb (ms)	38.7 (±10.4)	45.7 (±15.9)	0.0295**
S-RSp (ms)	57.7 (49.2; 70.3)	67 (54; 81.3)	0.0478*
R-RSb (ms)	35.5 (21.8; 44.1)	27.7 (16.5; 38.7)	0.2408*
R-RSp (ms)	61.7 (51; 78.7)	61.8; 51.9; 77.6)	0.9851*
Rpulm (ms)	24 (16.1; 33.3)	32.9 (±13.5)	0.0172*
RAo (ms)	29.5 (±11)	30.3 (±17.2)	0.7922**
Pulm-Ao (ms)	-4.2 (±12)	2.6 (±20)	0.0511**
Intra-LVb (ms)	-0.3 (-6; 4.7)	-6.7 (±14.2)	0.2112*
Intra-LVp (ms)	0.5 (-15.4; 7.2)	-11.4 (±27.6)	0.2254*
Inter-Vb (ms)	-4.7 (-17.3; 5.2)	-18 (±26.4)	0.0151*
Inter-Vp (ms)	2.3 (±29.8)	-16.9 (±39.7)	0.0335**

Results are presented as mean ± standard deviation for normally distributed data or median (interquartile range) for non-normally distributed data, based on the normality test outcomes.(P>0.05).

*Mann-Whitney test; **Unpaired t test; HF: heart failure; Inter-Vb: Mechanical interventricular conduction delay using the beginning of the S' wave; Inter-Vp: Mechanical interventricular conduction delay using the peak of the S' wave; Intra-LVb: Mechanical intra-left ventricle conduction delay using the beginning of the S' wave; Intra-LVb: Mechanical intra-left ventricle conduction delay using the beginning of the S' wave; L-RSb: Electromechanical delay measured in lateral mitral annulus; L-RSp: Electrosystolic delay measured in lateral mitral annulus; Pulm-Ao : Mechanical interventricular dyssynchrony; Rao: Time intervals from the start of the QRS complex to the beginning of the aortic flow; RPulm: Time intervals from the start of the QRS complex to the beginning of the pulmonic flow; R-RSb: Electromechanical delay measured in lateral tricuspid annulus; R-RSp: Electrosystolic delay measured in lateral tricuspid annulus; S-RSb: Electromechanical delay measured septal mitral annulus; S-RSp: Electrosystolic delay measured septal mitral annulus; RPT: R-peak Time; IDI: interventricular dyssynchrony index.

Table 11. Cut-off values for each marker of ventricular conduction time and its respective AUC value, P value, sensitivity, specificity, PPV, NPV, accuracy and odds ratio for arrhythmias.

Index	AUC	p	Cutoff (ms)	Sensitivity (%)	95% CI	Specificity (%)	95% CI	Likelihood ratio	PPV	NPV	Accuracy (%)	Odds Ratio
L-RSp	0.73	0.0032	> 81.2	75.0	50.50% to 89.82%	83.0	74.75% to 88.98%	4.4	0.39	0.96	81.6	14.2
RPT V1	0.73	0.0041	> 23.2	53.3	30.12% to 75.19%	84.9	76.88% to 90.49%	3.5	0.33	0.93	81.0	6.4
L-RSb	0.75	0.002	> 48.5	73.3	48.05% to 89.10%	79.4	70.57% to 86.12%	3.6	0.33	0.95	78.3	10.4
RPT V3	0.75	0.003	> 27	71.4	45.35% to 88.28%	76.4	67.62% to 83.33%	3.0	0.28	0.95	75.8	8.1
RPT V6	0.79	0.0003	> 31.2	73.3	48.05% to 89.10%	76.0	66.92% to 83.15%	3.1	0.31	0.95	75.6	8.7
RPT V2	0.73	0.0047	> 26.3	64.3	38.76% to 83.66%	74.8	65.96% to 81.93%	2.5	0.24	0.94	73.6	5.3
RPT V6	0.79	0.0003	> 30.8	73.3	48.05% to 89.10%	70.2	60.81% to 78.14%	2.5	0.26	0.95	70.6	6.5
L-RSp	0.73	0.0032	> 72.2	81.3	56.99% to 93.41%	66.0	56.60% to 74.35%	2.4	0.25	0.96	67.2	8.1
RPT V2	0.73	0.0047	> 25.8	71.4	45.35% to 88.28%	66.7	57.47% to 74.75%	2.1	0.21	0.95	67.2	5.0
Inter-Vb	0.71	0.0163	< -14.7	69.2	42.37% to 87.32%	71.7	61.81% to 79.92%	2.5	0.13	0.87	67.0	1.1
RPT V1	0.73	0.0041	> 21.8	73.3	48.05% to 89.10%	65.1	55.64% to 73.50%	2.1	0.23	0.95	66.1	5.1
Inter-Vb	0.71	0.0163	< -11.8	76.9	49.74% to 91.82%	68.5	58.41% to 77.07%	2.4	0.15	0.88	65.1	1.3
L-RSb	0.75	0.002	> 43.2	80.0	54.81% to 92.95%	63.7	54.05% to 72.40%	2.2	0.23	0.96	64.2	6.5
RPT V3	0.75	0.003	> 26.3	71.4	45.35% to 88.28%	60.9	51.57% to 69.51%	1.8	0.19	0.94	62.1	3.9

Inter-Vb: Mechanical interventricular conduction delay using the beginning of the S' wave; L-RSb: Electromechanical delay measured in lateral mitral annulus; L-RSp: Electrosystolic delay measured in lateral mitral annulus; RPulm: Time intervals from the start of the QRS complex to the beginning of the pulmonic flow; RPT: R-peak Time; IDI: interventricular dyssynchrony index; AUC: area under the curve; PPV: Positive predictive value; NPV: Negative predictive value.

Table 12. Logistic regression model for arrhythmia prediction in dogs with MMVD

Variable	Estimate (β)	Standard Error	95% CI (Profile Likelihood)	Odds Ratio	95% CI (Odds Ratio)
Intercept (β_0)	-14.51	3.446	-21.98 to -8.335	-	-
L-RSp	0.02197	0.01138	0.00110 to 0.04669	1.022	1.001 to 1.048
RPT V6	0.3714	0.09838	0.1919 to 0.5811	1.450	1.212 to 1.788

RPT: R-peak Time; L-RSp: Electrosystolic delay measured in lateral mitral annulus.

Table 13. Markers of ventricular activation times and dyssynchrony in dogs with supraventricular arrhythmias and dogs without it.

	No arrhythmia	Arrhythmia	P
RPT V1 (ms)	18 (15; 22)	22.7 (18; 24.7)	0.0318*
RPT V2 (ms)	24.3 (21; 26.7)	27.3 (24.7; 32.7)	0.0064*
RPT V3 (ms)	25.3 (22; 27.2)	28.1 (±5.7)	0.0345*
RPT V4 (ms)	26.7 (24.3; 28)	29.5 (±6)	0.025*
RPT V5 (ms)	28.7 (29.6; 30)	30.3 (±2.8)	0.0584*
RPT V6 (ms)	30 (28; 31.3)	32.9 (±3.1)	0.0023*
IDI (%)	15 (9.8; 25)	14.5 (±9.2)	0.2750*
L-RSb (ms)	41 (33.3; 50)	53 (±12.9)	0.0023*
L-RSp (ms)	65.7 (53.9; 77.5)	89 (±17.2)	<0.0001*
S-RSb (ms)	41.6 (±12.1)	49.7 (±17.5)	0.1049*
S-RSp (ms)	64 (51.3; 76.5)	79.4 (±23.3)	0.0137*
R-RSb (ms)	38 (27.7; 49.3)	33.3 (16; 54)	0.5157*
R-RSp (ms)	66.8 (56; 85)	63.7 (49; 110.8)	0.8723*
Rpulm (ms)	23.7 (17; 31.7)	35.4 (±12.6)	0.0026*
RAo (ms)	32.2 (24.3; 39)	34.5 (±17.4)	0.5040*
Pulm-Ao (ms)	-6.7 (±12.7)	0.2 (±21.7)	0.0691**
Intra-LVb (ms)	0 (-5.3; 5.3)	-5 (±15.1)	0.4847*
Intra-LVp (ms)	0.67 (-9; 7.3)	-10.5 (±29.9)	0.2052*
Inter-Vb (ms)	-3.8 (-15; 5.9)	-12.9 (±28.4)	0.0992*
Inter-Vp (ms)	3.2 (-6.5; 14.6)	-13.2 (±46.2)	0.1371*

Results are presented as mean ± standard deviation for normally distributed data or median (interquartile range) for non-normally distributed data, based on the normality test outcomes.(P>0.05).

*Mann-Whitney test; **Unpaired t test; HF: heart failure; Inter-Vb: Mechanical interventricular conduction delay using the beginning of the S' wave; Inter-Vp: Mechanical interventricular conduction delay using the peak of the S' wave; Intra-LVb: Mechanical intra-left ventricle conduction delay using the beginning of the S' wave; Intra-LVb: Mechanical intra-left ventricle conduction delay using the beginning of the S' wave; L-RSb: Electromechanical delay measured in lateral mitral annulus; L-RSp: Electrosystolic delay measured in lateral mitral annulus; Pulm-Ao : Mechanical interventricular dyssynchrony; Rao: Time intervals from the start of the QRS complex to the beginning of the aortic flow; RPulm: Time intervals from the start of the QRS complex to the beginning of the pulmonic flow; R-RSb: Electromechanical delay measured in lateral tricuspid annulus; R-RSp: Electrosystolic delay measured in lateral tricuspid annulus; S-RSb: Electromechanical delay measured septal mitral annulus; S-RSp: Electrosystolic delay measured septal mitral annulus Inter-Vb; RPT: R-peak Time; IDI: interventricular dyssynchrony index.

Table 14. Cut-off values for each marker of ventricular conduction time and its respective AUC value, P value, sensitivity, specificity, PPV, NPV, accuracy and odds ratio for supraventricular arrhythmias.

Index	AUC	p	Cutoff (ms)	Sensitivity (%)	95% CI	Specificity (%)	95% CI	Positive likelihood ratio	PPV	NPV	Accuracy (%)	Odds Ratio
RPTV4	0.70	0.0266	> 29.2	45.5	21.27% to 71.99%	89.2	82.05% to 93.71%	4.2	0.29	0.94	85.7	7.2
S-RSp	0.70	0.0148	> 77.9	53.9	29.14% to 76.79%	81.7	74.88% to 86.91%	2.9	0.29	0.94	85.0	6.7
RPTV6	0.77	0.0033	> 32.3	63.6	35.38% to 84.83%	86.8	79.04% to 91.97%	4.8	0.32	0.96	84.3	11.1
L-RSb	0.75	0.0029	> 52.3	61.5	35.52% to 82.29%	81.3	74.42% to 86.65%	3.3	0.33	0.95	83.5	8.9
L-RSp	0.81	0.0002	> 81.2	84.6	57.77% to 97.27%	80.9	74.12% to 86.18%	4.4	0.32	0.97	81.8	14.2
L-RSb	0.75	0.0029	> 48.5	84.6	57.77% to 97.27%	70.3	62.71% to 76.95%	2.9	0.31	0.98	79.1	18.4
Rpulm	0.73	0.0032	> 33.3	66.7	41.71% to 84.82%	77.0	69.98% to 82.74%	2.9	0.23	0.96	73.4	6.4
RPTV1	0.70	0.0333	> 22.5	54.6	28.01% to 78.73%	76.9	68.06% to 83.80%	2.4	0.18	0.94	73.2	3.6
RPTV2	0.74	0.0076	> 26.3	63.6	35.38% to 84.83%	73.5	64.64% to 80.72%	2.4	0.18	0.96	72.4	4.8
S-RSp	0.70	0.0148	> 66.8	76.9	49.74% to 91.82%	58.2	50.43% to 65.63%	1.8	0.20	0.96	70.0	6.1
RPTV6	0.77	0.0033	> 30.8	72.7	43.44% to 90.25%	68.9	59.52% to 76.89%	2.3	0.19	0.96	68.6	5.7
RPTV4	0.70	0.0266	> 27.7	72.7	43.44% to 90.25%	66.7	57.47% to 74.75%	2.2	0.17	0.96	66.7	5.2
RPTV2	0.74	0.0076	> 25.8	72.7	43.44% to 90.25%	65.5	56.34% to 73.61%	2.1	0.17	0.96	66.1	5.1
RPTV1	0.70	0.0333	> 21.8	72.7	43.44% to 90.25%	65.7	56.39% to 74.01%	2.1	0.17	0.96	65.0	4.8

L-RSp	0.81	0.0002	> 83.2	76.9	49.74% to 91.82%	83.3	76.84% to 88.29%	4.6	0.19	0.97	64.6	7.8
Rpulm	0.73	0.0032	> 24.8	80.0	54.81% to 92.95%	53.9	46.33% to 61.37%	1.7	0.16	0.97	54.7	5.8

AUC: area under the curve; L-RSb: Electromechanical delay measured in lateral mitral annulus; L-RSp: Electrosystolic delay measured in lateral mitral annulus; S-RSp: Electrosystolic delay measured septal mitral annulus; RPulm: Time intervals from the start of the QRS complex to the beginning of the pulmonic flow; PPV: Positive predictive value; NPV: Negative predictive value.

Table 15. Logistic regression model for supraventricular arrhythmia prediction in dogs with MMVD

Parameter	Estimate (β)	95% CI (β)	Odds Ratio	95% CI (OR)
Intercept	-18.49	-29.89 to -9.580	-	-
L-RSb (ms)	0.05529	0.01022 to 0.1144	1.057	1.010 to 1.121
RPT V6 (ms)	0.4407	0.1893 to 0.7426	1.554	1.208 to 2.101

RPT: R-peak Time; L-RSb: Electromechanical delay measured in lateral mitral annulus.

Table 16. Markers of ventricular activation times and dyssynchrony in dogs with ventricular arrhythmias and dogs without it.

	No arrhytmia	Arrhytmia	P
RPT V1 (ms)	18 (15.7; 22.7)	25.3 (±7.2)	0.0011*
RPT V2 (ms)	24.3 (21; 26.7)	27.8 (±5.3)	0.1078*
RPT V3 (ms)	25.5 (22.8; 27.3)	31.8 (±4.5)	0.0010**
RPT V4 (ms)	27 (24.3; 28)	29.6 (±8.6)	0.2539*
RPT V5 (ms)	29.3 (27; 30)	28.1 (±4.9)	0.8041*
RPT V6 (ms)	30 (28; 31.8)	33.5 (±2.9)	0.0178*
IDI (%)	15 (9; 25)	4.4 (±19.2)	0.0557*
L-RSb (ms)	40.7(33; 49)	51.1 (±18.1)	0.2854*
L-RSp (ms)	64.3 (52.2; 80.3)	85 (43.5; 86.3)	0.8871
S-RSb (ms)	38 (32; 48)	41.1 (±9.2)	0.7615*
S-RSp (ms)	59 (50; 74)	58.1 (±9.2)	0.6808*
R-RSb (ms)	35.3 (21; 44.3)	26.3 (22.8; 86.2)	0.7846*
R-RSp (ms)	62.3 (51.5; 81.8)	84.8 (±43.5)	0.4617*
Rpulm (ms)	25 (17.3; 34.7)	31.5 (±21.3)	0.6519*
RAo (ms)	30.3 (±11.9)	23.5 (±13.5)	0.2135**
Pulm-Ao (ms)	-3.7 (±13)	8.1 (±21.9)	0.0554**
Intra-LVb (ms)	0 (-6; 5.3)	-10 (±9.5)	0.1144*
Intra-LVp (ms)	-0.7 (±-17.9; 7.5)	-10.9 (±17.4)	0.5607*
Inter-Vb (ms)	-7.7 (±18.9)	-6 (±42.6)	0.8655**
Inter-Vp (ms)	0.3 (±32)	8.7 (±41.3)	0.6118**

Results are presented as mean ± standard deviation for normally distributed data or median (interquartile range) for non-normally distributed data, based on the normality test outcomes.(P>0.05).

*Mann-Whitney test; **Unpaired t test; HF: heart failure; Inter-Vb: Mechanical interventricular conduction delay using the beginning of the S' wave; Inter-Vp: Mechanical interventricular conduction delay using the peak of the S' wave; Intra-LVb: Mechanical intra-left ventricle conduction delay using the beginning of the S' wave; Intra-LVb: Mechanical intra-left ventricle conduction delay using the beginning of the S' wave; L-RSb: Electromechanical delay measured in lateral mitral annulus; L-RSp: Electrosystolic delay measured in lateral mitral annulus; Pulm-Ao : Mechanical interventricular dyssynchrony; Rao: Time intervals from the start of the QRS complex to the beginning of the aortic flow; RPulm: Time intervals from the start of the QRS complex to the beginning of the pulmonic flow; R-RSb: Electromechanical delay measured in lateral tricuspid annulus; R-RSp: Electrosystolic delay measured in lateral tricuspid annulus; S-RSb: Electromechanical delay measured septal mitral annulus; S-RSp: Electrosystolic delay measured septal mitral annulus Inter-Vb; RPT: R-peak Time; IDI: interventricular dyssynchrony index.

Table 17. Cut-off values for each marker of ventricular conduction time and its respective AUC value, P value, sensitivity, specificity, PPV, NPV, accuracy and odds ratio for ventricular arrhythmias.

Index	AUC	p	Cutoff (ms)	Sensitivity (%)	95% CI	Specificity (%)	95% CI	Positive likelihood ratio	PPV	NPV	Accuracy (%)	Odds Ratio
RPT V3	0.92	0.004	> 30.3	75.0	30.06% to 98.72%	95.1	89.68% to 97.73%	15.3	0.33	0.99	94.4	58.0
RPT V3	0.92	0.004	> 28.3	75.0	30.06% to 98.72%	87.7	80.70% to 92.41%	6.1	0.13	0.98	87.4	7.8
RPT V1	0.83	0.0134	> 23.2	80.0	37.55% to 98.97%	83.1	75.27% to 88.75%	4.7	0.17	0.99	87.3	21.4
RTP V6	0.80	0.0215	> 33.7	60.0	23.07% to 92.89%	87.9	80.76% to 92.67%	5.0	0.18	0.98	86.8	10.9
RTP V6	0.80	0.0215	> 31.7	80.0	37.55% to 98.97%	75.0	66.40% to 81.99%	3.2	0.12	0.99	75.2	12.0
RPT V1	0.83	0.0134	> 22.5	80.0	37.55% to 98.97%	74.6	66.03% to 81.57%	3.1	0.12	0.99	74.8	11.7

AUC: area under the curve; RPT: R-Peak Time; PPV: Positive predictive value; NPV: Negative predictive value.

Table 18. Logistic regression model for ventricular arrhythmia prediction in dogs with MMVD

Variable	Estimate	Standard Error	95% CI (Profile Likelihood)	Odds Ratio	95% CI (Odds Ratio)
Intercept	-37.89	17.73	-82.62 to -14.03	-	-
V1	0.5129	0.3087	0.04630 to 1.244	1.670	1.047 to 3.469
V3	0.8259	0.3954	0.2736 to 1.817	2.284	1.315 to 6.155

RPT: R-peak Time.

Table 19. Intra-observer bias and difference in markers of ventricular conduction times in dogs.

		Bias	SD of Bias	95% Limits of Agreement	P
Intra-observer	Pulm-Ao (ms)	-3.397	11	-25.74 to 18.94	0.2735**
	Intra-LVb (ms)	1.897	6.12	-10.1 to 13.89	0.1235**
	Intra-LVp (ms)	1.6	8.78	-15.61 to 18.81	0.6516*
	Inter-Vb (ms)	5.283	18	-30 to 40.57	0.404*
	Inter-Vp (ms)	4.563	13.19	-21.29 to 30.42	0.1496*
	IDI (%)	1.103	5.747	-10.16 to 12.37	0.8325*

*Mann-Whitney test; **Unpaired t test; Inter-Vb: Mechanical interventricular conduction delay using the beginning of the S' wave; Inter-Vp: Mechanical interventricular conduction delay using the peak of the S' wave; Intra-LVb: Mechanical intra-left ventricle conduction delay using the beginning of the S' wave; Intra-LVb: Mechanical intra-left ventricle conduction delay using the beginning of the S' wave; Pulm-Ao : Mechanical interventricular dyssynchrony; IDI: interventricular dyssynchrony index; SD: standard deviation

FIGURE LEGENDS

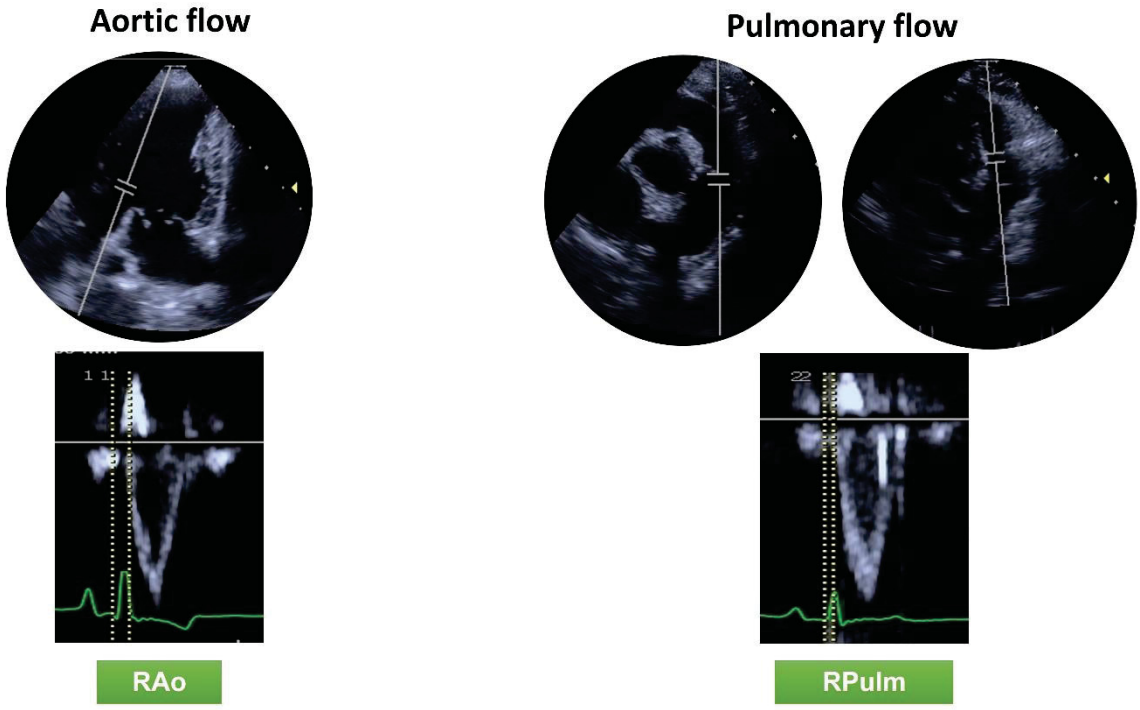

Figure 1. Mechanical interventricular dyssynchrony was defined as the difference between RPulm (the time intervals in milliseconds from the start of the QRS complex on the simultaneously acquired ECG to the beginning of the pulmonic flow acquired using pulsed-wave Doppler) and RAo (the time intervals in milliseconds from the start of the QRS complex on the simultaneously acquired ECG to the beginning of the aortic flow acquired using pulsed-wave Doppler). Rao: Time intervals from the start of the QRS complex to the beginning of the aortic flow; RPulm: Time intervals from the start of the QRS complex to the beginning of the pulmonic flow.

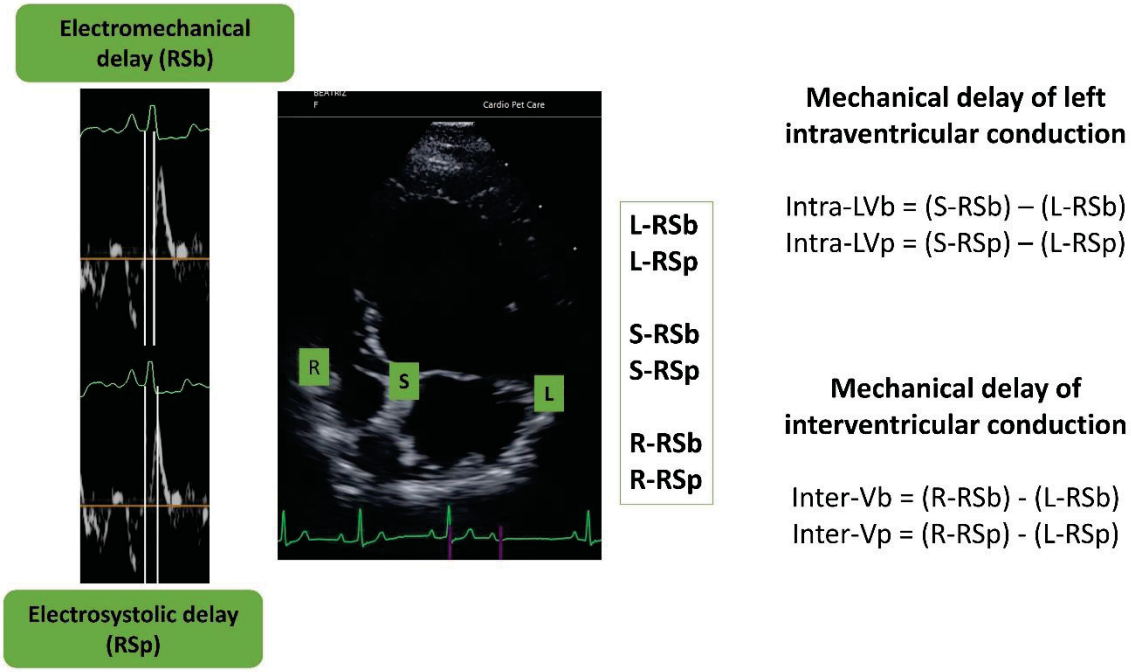

Figure 2. The time between the beginning of the QRS complex in ECG and the beginning of S' wave in tissue Doppler traces was defined as the electromechanical delay (RSb). The time between the beginning of the QRS complex in ECG and the peak of S' wave in tissue Doppler traces was defined as the electrosystolic delay (RSp). Both RSb and RSp were measured in three points: lateral mitral anulus (L-RSb, L-RSp), septal mitral anulus (S-RSb, S-RSp), and lateral tricuspid annulus (R-RSb, R-RSp). The difference between the S-RSb and L-RSb times, and between S-RSp and L-RSp times was defined as the mechanical intra-left ventricle conduction delay (Intra-LVb and Intra-LVp, respectively). The difference between the R-RSb and L-RSb times, and between R-RSp and L-RSp times was defined as the mechanical interventricular conduction delay (Inter-Vb and Inter-Vp, respectively). RSb: the electromechanical delay; RSp: the electrosystolic delay; L-RSb: electromechanical delay measured in lateral mitral annulus; L-RSp: electrosystolic delay measured in lateral mitral annulus; R-RSb: electromechanical delay measured in lateral tricuspid annulus; R-RSp: electrosystolic delay measured in lateral tricuspid annulus; S-RSb: electromechanical delay measured in septal mitral annulus; S-RSp: electrosystolic delay measured in septal mitral annulus; Intra-LVb: Mechanical intra-left ventricle conduction delay using the beginning of the S' wave; Intra-LVp: Mechanical intra-left ventricle conduction delay using the peak of the S' wave; Inter-Vb: Mechanical interventricular conduction delay using the beginning of the S' wave; Inter-Vp: Mechanical interventricular conduction delay using the peak of the S' wave

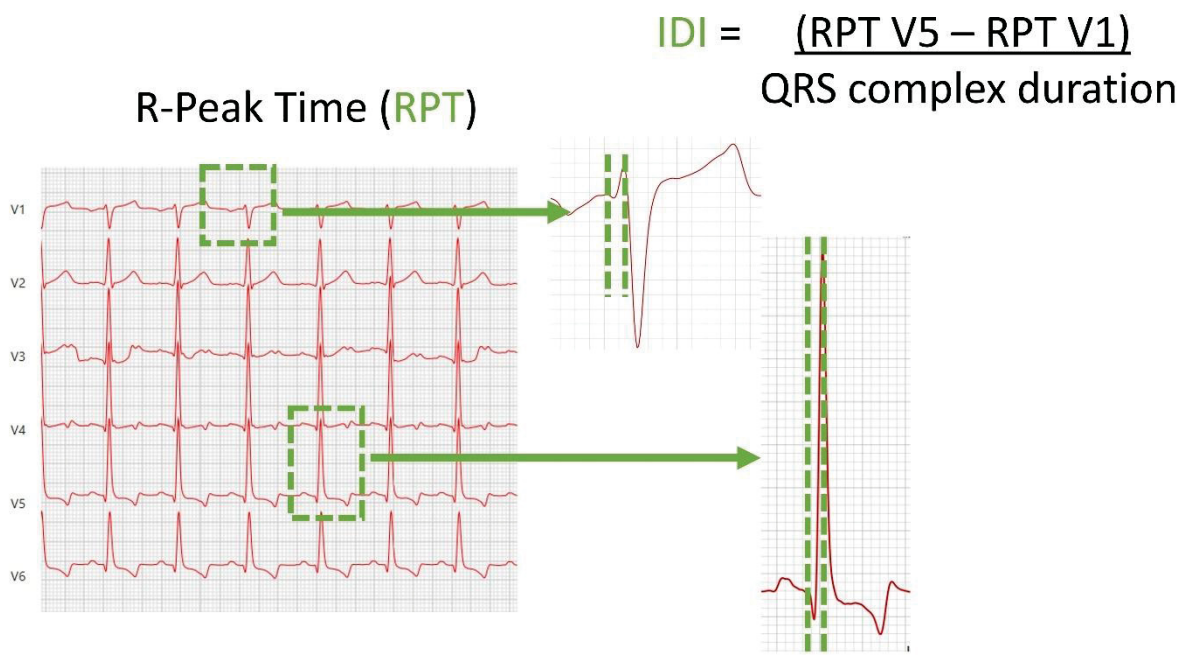

Figure 3. R-peak time (RPT) was measured in each precordial lead from the earliest onset of the QRS complex to the peak of the R wave or, if present, R' wave. The IDI was determined, by calculating the absolute value of the difference between RPT in leads V5 and V1, reflecting left and right ventricular electrical potentials, divided by the QRS duration. RPT: R-peak time; IDI: the interventricular dyssynchrony index.

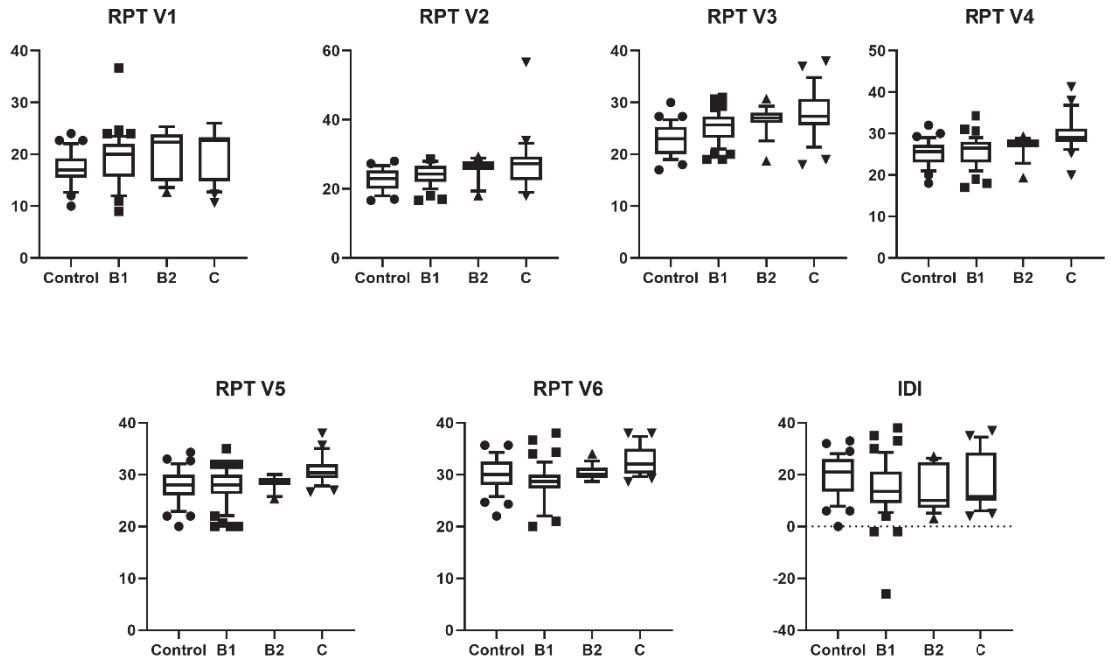

Figure 4. Electrocardiographic indices of ventricular activation times in healthy dogs and dogs with different stages of myxomatous mitral valve disease. Results are presented in milliseconds. RPT: R-peak Time; IDI: interventricular dyssynchrony index.

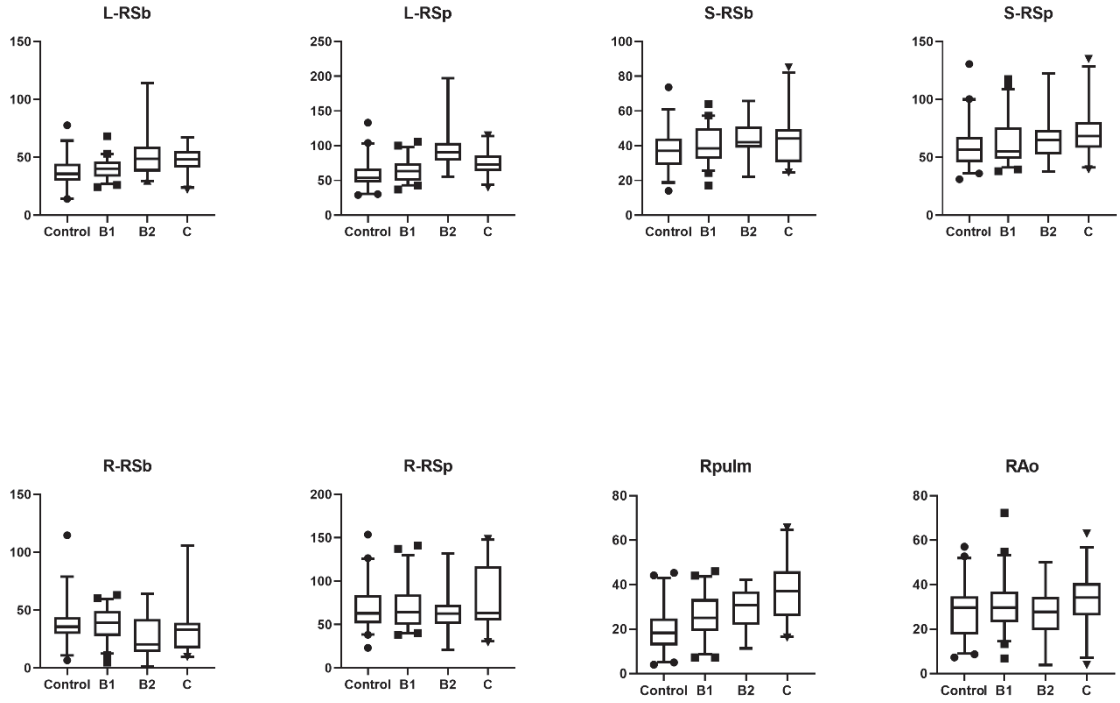

Figure 5. Echocardiographic indices of ventricular activation times in healthy dogs and dogs with different stages of myxomatous mitral valve disease. Results are presented in milliseconds. L-RSb: Electromechanical delay measured in lateral mitral annulus; L-RSp: Electrosystolic delay measured in lateral mitral annulus; Rao: Time intervals from the start of the QRS complex to the beginning of the aortic flow; RPulm: Time intervals from the start of the QRS complex to the beginning of the pulmonic flow; R-RSb: Electromechanical delay measured in lateral tricuspid annulus; R-RSp: Electrosystolic delay measured in lateral tricuspid annulus; S-RSb: Electromechanical delay measured septal mitral annulus; S-RSp: Electrosystolic delay measured septal mitral annulus Inter-Vb

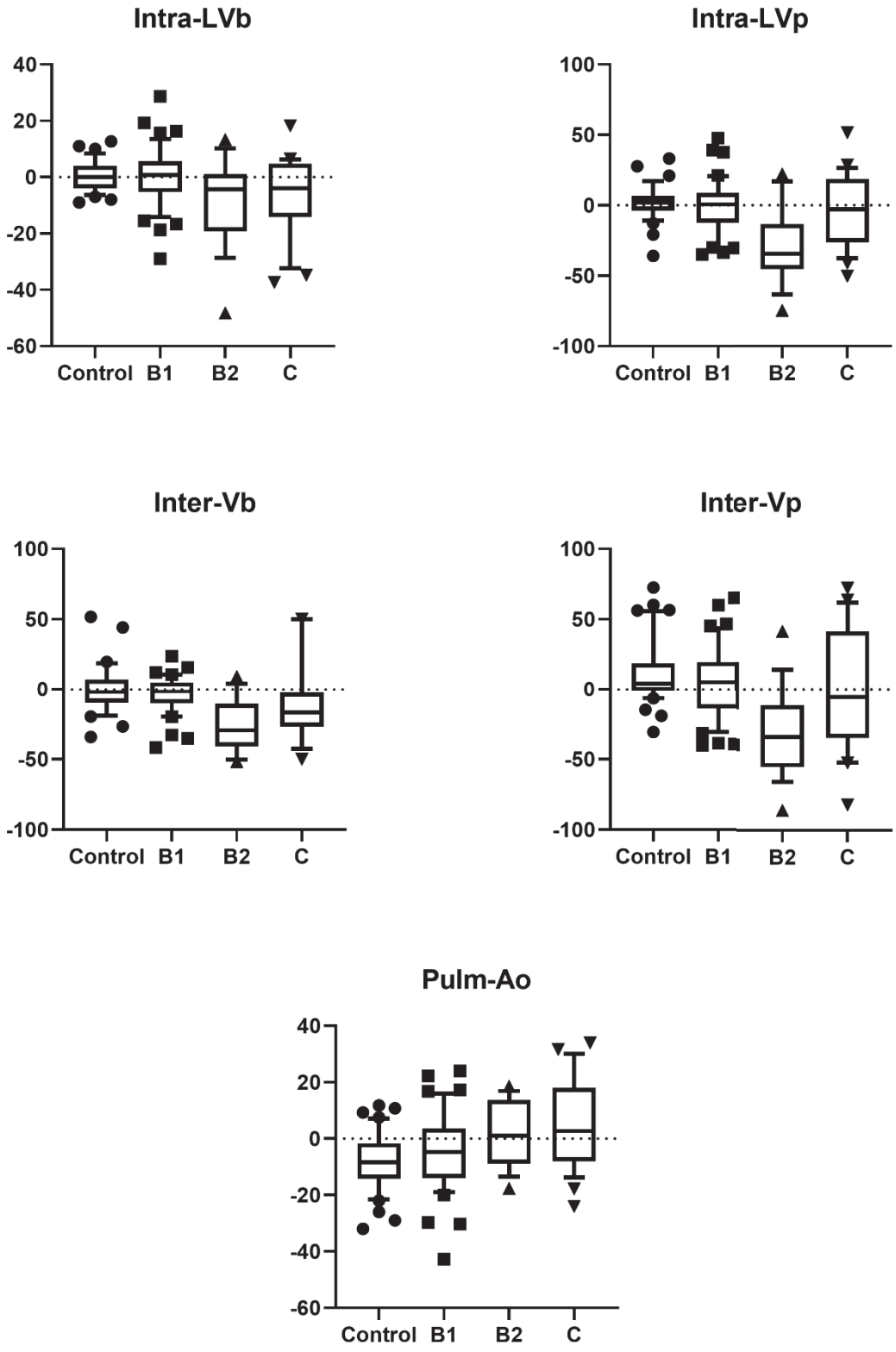

Figure 6. Indices of mechanical ventricular dyssynchrony in healthy dogs and dogs with different stages of myxomatous mitral valve disease. Results are presented in milliseconds. Inter-Vb: Mechanical interventricular conduction delay using the beginning of the S' wave; Inter-Vp: Mechanical interventricular conduction delay using

the peak of the S' wave; Intra-LVb: Mechanical intra-left ventricle conduction delay using the beginning of the S' wave; Intra-LVp: Mechanical intra-left ventricle conduction delay using the peak of the S' wave; Pulm-Ao : Mechanical interventricular dyssynchrony.

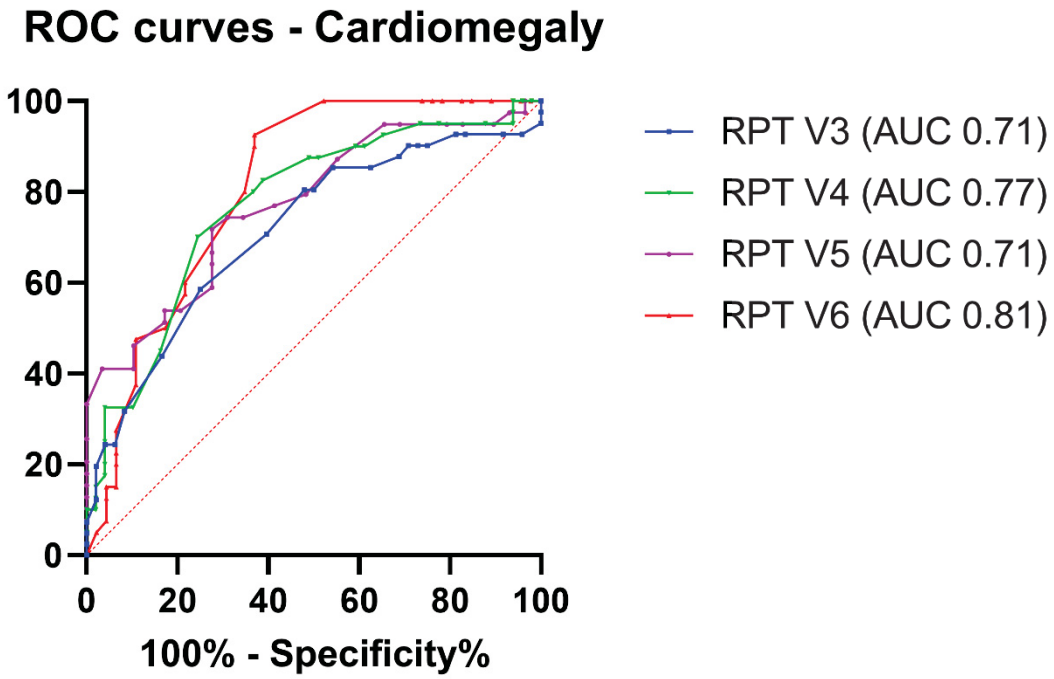

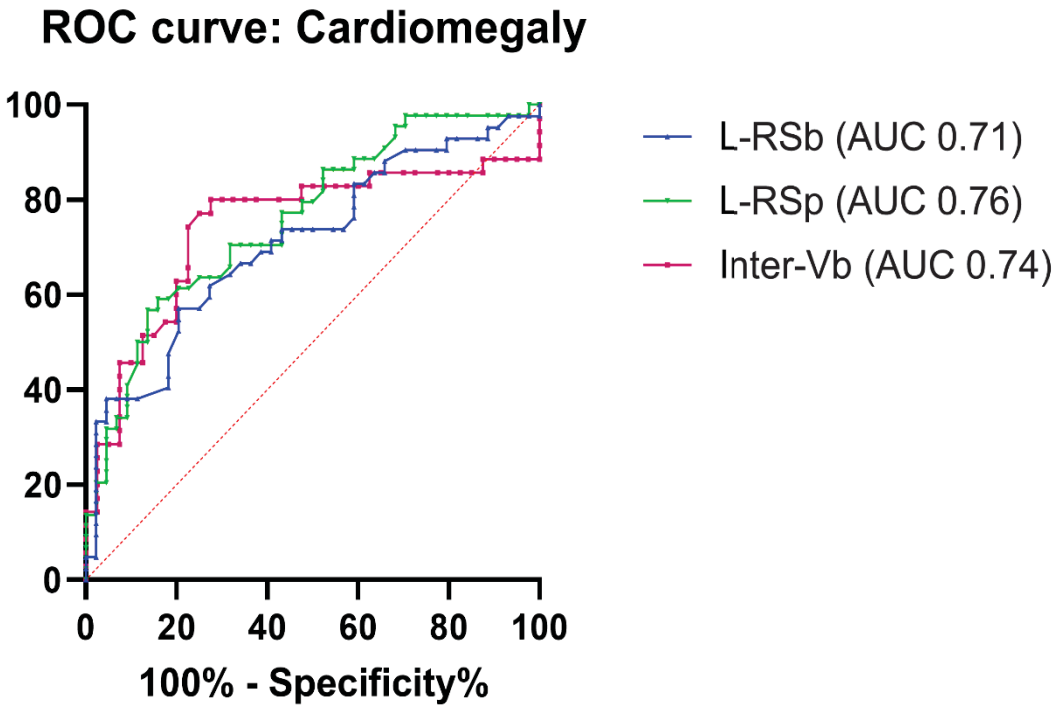

Figure 7. Receiver operating characteristic curves constructed to assess sensitivity and specificity of echocardiographic and electrocardiographic markers of ventricular activation for differentiation of dogs presenting cardiomegaly and dogs with normal cardiac size. ROC: Receiver operating characteristic curve; L-RSb: Electromechanical delay measured in lateral mitral annulus; L-RSp: Electrosystolic delay measured in lateral mitral annulus; Inter-Vb: Mechanical interventricular

conduction delay using the beginning of the S’ wave.

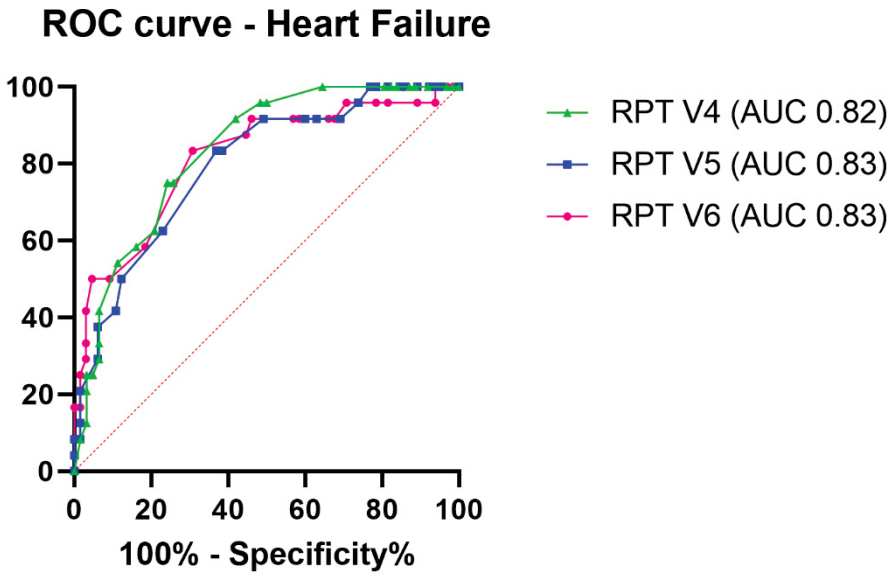

Figure 8. Receiver operating characteristic curves constructed to assess sensitivity and specificity of echocardiographic and electrocardiographic markers of ventricular activation for differentiation of dogs presenting heart failure and asymptomatic dogs. ROC: Receiver operating characteristic curve; RPT: R-peak Time.

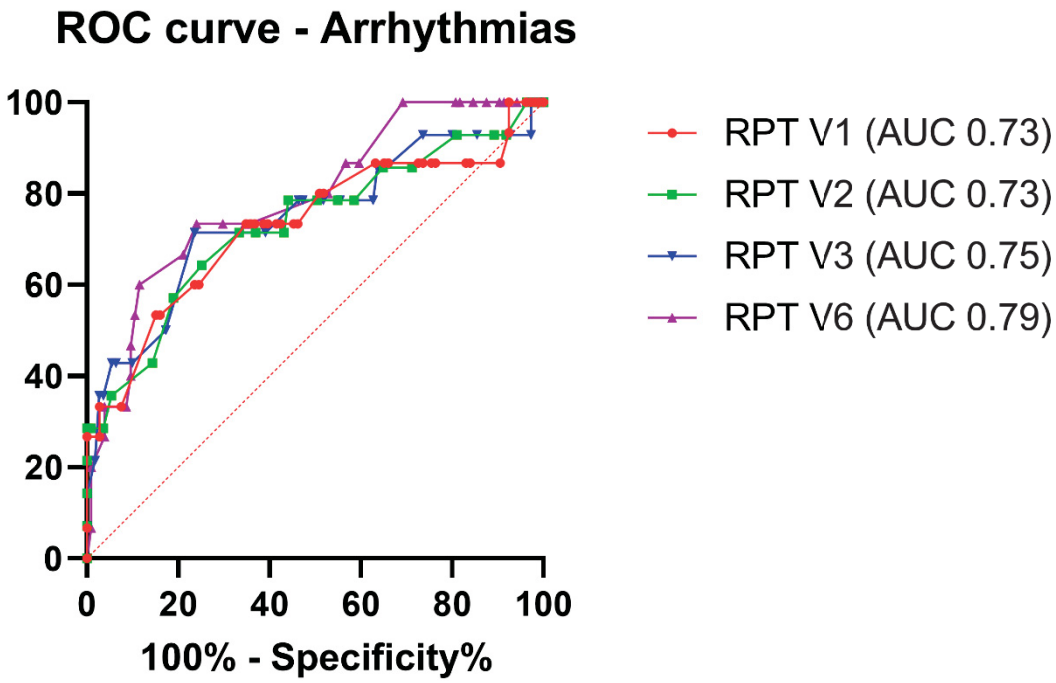

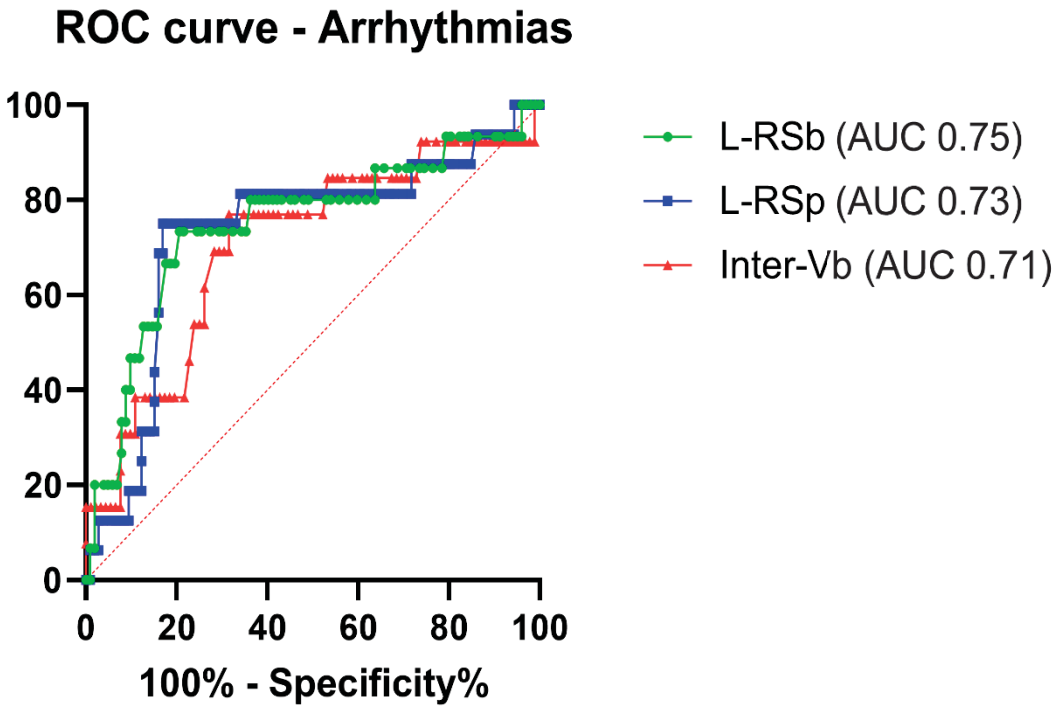

Figure 9. Receiver operating characteristic curves constructed to assess sensitivity and specificity of echocardiographic markers of ventricular activation for differentiation of dogs presenting arrhythmias and dogs without it. ROC: Receiver operating characteristic curve; L-RSb: Electromechanical delay measured in lateral mitral annulus; L-RSp: Electrosystolic delay measured in lateral mitral annulus; Inter-Vb: Mechanical interventricular conduction delay using the beginning of the S' wave; ;

RPT: R-peak Time.

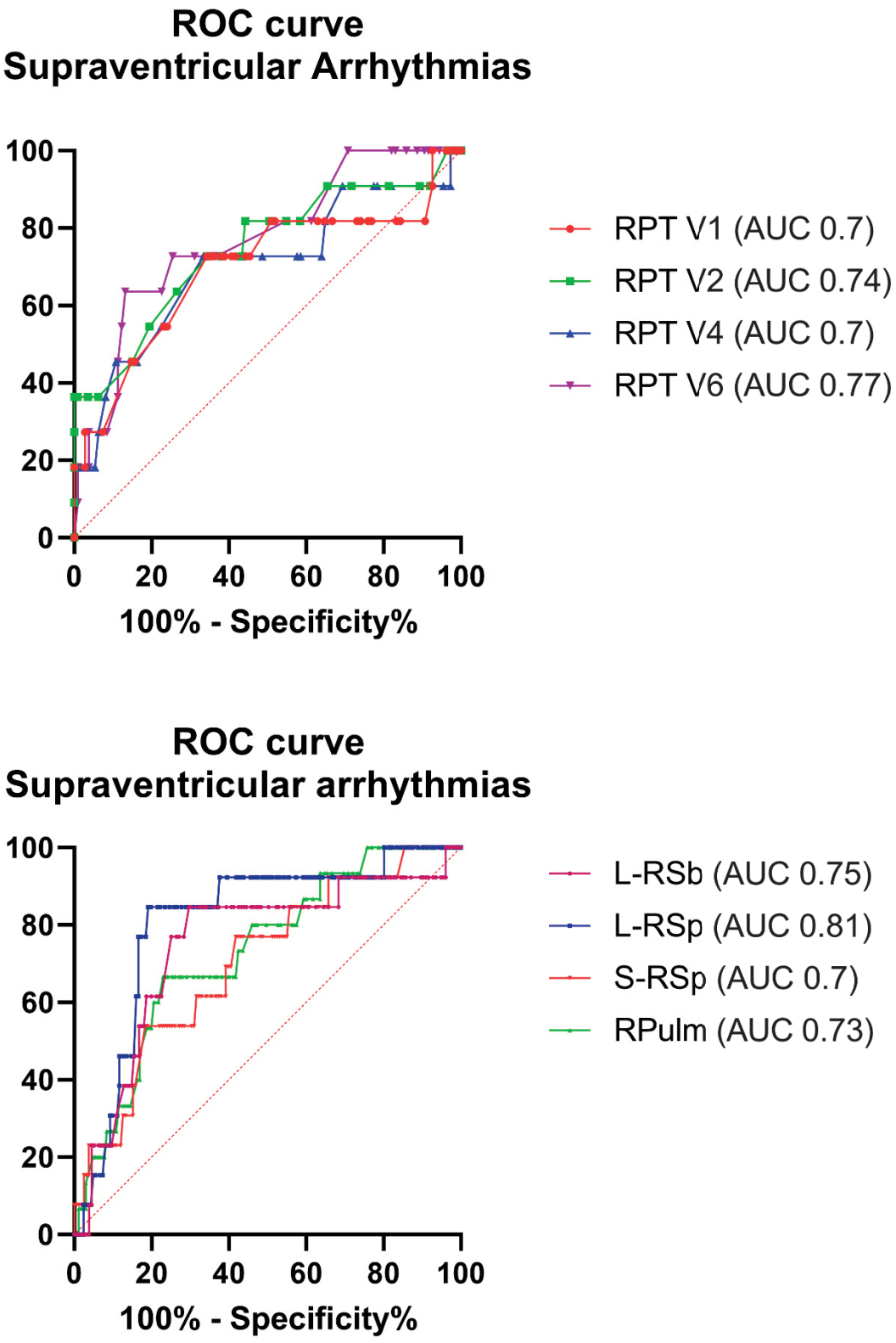

Figure 10. Receiver operating characteristic curves constructed to assess sensitivity and specificity of echocardiographic and electrocardiographic markers of ventricular activation for differentiation of dogs presenting supraventricular arrhythmias

and dogs without it. ROC: Receiver operating characteristic curve; L-RSb: Electromechanical delay measured in lateral mitral annulus; L-RSp: Electrosystolic delay measured in lateral mitral annulus; RPulm: Time intervals from the start of the QRS complex to the beginning of the pulmonic flow; RPT: R-peak Time.

SUPPLEMENTARY MATERIAL TABLES

Supplementary material table A. P-values obtained by Spearman's test to investigate correlations between markers ECG and echocardiographic of ventricle conduction times, as well as to check correlation with epidemiological, electrocardiographic and echocardiographic variables.

	L-RSb	L-RSp	S-RSb	S-RSp	R-RSb	R-RSp	Rpulm	Rao	Intra-LVb	Intra-LVp	Pulm-Ao	Inter-Vb	Inter-Vp	V1	V2	V3	V4	V5	V6	IDI
Age (years	2.8E-06	3.06E-07	0.007764	0.066963	0.794298	0.496913	2.51E-14	0.009936	0.100014	0.002055	4.42E-05	0.00403	0.004047	0.026832	1.24E-07	4.22E-11	1.36E-06	0.004641	0.439203	0.441521
Weight	0.332418	0.245177	0.040654	0.007131	0.1794	0.027299	0.568292	0.146189	0.717558	0.292598	0.041484	0.833898	0.319676	0.401276	0.220086	0.444322	0.191189	0.011643	3.06E-05	0.056507
LA	4.44E-06	1.4E-09	0.002182	2.52E-06	0.651154	0.333017	3.66E-07	0.04073	0.066027	0.026347	0.02259	0.000281	0.005132	0.111144	0.009155	0.000191	3E-07	7.18E-07	4.88E-08	0.650399
Ao	0.377327	0.366325	0.052526	0.056978	0.513248	0.386304	0.195384	0.970967	0.373404	0.295145	0.119313	0.562568	0.691969	0.009627	0.018927	0.066485	0.587609	0.34742	0.023792	0.022815
LA/Ao	0.001969	2.27E-05	0.543195	0.10832	0.252537	0.881691	1.41E-08	0.360122	0.017457	0.002449	1.67E-05	0.019846	0.009178	0.000368	7.86E-07	3.99E-08	3.38E-06	0.002028	0.034058	0.118596
LVIDd	0.000119	4.97E-08	0.0028	2.63E-07	0.732273	0.047238	1.26E-05	0.011567	0.212065	0.144906	0.179827	0.003293	0.07638	0.106619	0.034224	0.007888	5.9E-07	3.27E-05	2.49E-07	0.845566
LVIDs	0.058897	0.007775	0.003493	3.15E-07	0.266751	0.02688	0.189951	0.007425	0.486173	0.224266	0.168634	0.354298	0.681038	0.750221	0.628165	0.772028	0.03709	0.009313	9.05E-05	0.425114
LVIDdN	0.000587	1.1E-07	0.071753	0.000294	0.624626	0.201525	1.22E-06	0.117812	0.081574	0.014387	0.008137	0.001471	0.030906	0.035125	0.000852	0.000307	9.1E-07	0.002181	0.00112	0.510261
LVIDsN	0.045852	0.002716	0.007787	1.24E-06	0.378696	0.036257	0.064982	0.010198	0.476549	0.40364	0.473455	0.378466	0.512589	0.328833	0.878121	0.786632	0.034927	0.070615	0.018296	0.874438
FS	0.501088	0.065686	0.038483	0.012532	0.005731	0.026937	0.002531	0.051406	0.001342	1.55E-06	1.81E-06	0.004636	0.009476	0.060939	1.11E-05	9.46E-07	0.001021	0.024372	0.392427	0.424305
E	0.018937	0.005608	0.673596	0.058188	0.393763	0.896644	0.000701	0.91405	0.056717	0.283255	0.000765	0.051968	0.316934	0.127958	0.035706	0.006063	0.000408	0.000456	0.00017	0.902514
A	0.002005	0.000491	0.303067	0.650615	0.248947	0.254134	1.19E-07	0.584815	0.154726	0.003252	1.84E-06	0.002 68	0.000336	0.038866	0.001324	1.62E-05	0.000732	0.266483	0.680616	0.243315
E/A	0.436366	0.438679	0.174582	0.282457	0.799624	0.352751	0.035163	0.716578	0.545912	0.085739	0.07729	0.35026	0.02782	0.312073	0.13307	0.024884	0.747204	0.097555	8.21E-05	0.161416
IVRT	0.001873	0.02986	5.61E-05	0.003084	0.033438	0.016915	0.009212	0.000202	0.512265	0.83245	0.198778	0.660359	0.755305	0.109385	0.548551	0.123799	0.227066	0.338736	0.418976	0.458201

E/IVRT	0.720016	0.245267	0.031606	0.971504	0.08319	0.201306	0.285601	0.211029	0.098714	0.342086	0.003947	0.048813	0.287238	0.778623	0.34992	0.346883	0.109293	0.103219	0.007308	0.690514
E/E'lat	0.217585	0.191197	0.515224	0.534529	0.326837	0.990735	0.052112	0.375818	0.186215	0.857924	0.287079	0.063887	0.363172	0.716155	0.730111	0.427809	0.263282	0.008428	0.000425	0.136947
E/E'sep	0.78492	0.969192	0.552997	0.480919	0.83212	0.845773	0.632681	0.28469	0.888464	0.683106	0.501433	0.895123	0.864446	0.027049	2.35E-05	0.013382	0.37978	0.100131	0.031594	0.006838
E'	0.087811	0.030873	0.601238	0.116523	0.719644	0.670785	0.016885	0.479625	0.302126	0.099033	0.047354	0.31385	0.61754	9.7E-05	0.002258	0.001965	0.000358	0.080748	0.422982	0.017298
A'	0.0025	2.93E-05	0.077318	0.187512	0.134188	0.281908	4.2E-07	0.961624	0.689737	0.001008	9.55E-08	0.002047	6.61E-05	1.09E-08	2.57E-08	1E-07	0.002069	0.940105	0.030447	8.61E-07
E'/A'	0.142295	0.009361	0.265001	0.945976	0.085268	0.167858	0.000696	0.836028	0.746018	0.023775	0.000366	0.005604	0.000162	0.000185	0.001158	0.003569	0.443372	0.301279	0.00427	6.54E-05
S'	0.203352	0.005118	0.197261	0.087844	0.368963	0.288668	3.1E-07	0.918681	0.377723	0.073435	3.14E-07	0.07745	0.005447	2.13E-05	7.53E-07	2.8E-07	2.4E-08	0.019984	0.539201	0.068184
L-RSb		1.54E-20	1.58E-11	4.06E-10	0.01135	0.001382	2.95E-09	2.79E-07	4.58E-07	0.000635	0.33808	0.000223	0.001085	0.000303	0.017839	0.001029	0.0131	0.10804	0.47671	0.022914
L-RSp	1.54E-20		1.54E-06	2.32E-09	0.270752	0.016448	3.61E-07	0.000965	4.35E-05	3.12E-12	0.154762	0.000425	1.79E-09	0.007905	0.014362	0.007227	0.001741	0.143659	0.771285	0.029369
S-RSb	1.58E-11	1.54E-06		3.52E-28	5.4E-10	1.77E-09	4.23E-05	2.2E-06	8.26E-05	0.021095	0.683295	0.22084	0.601866	0.063883	0.099829	0.00383	0.028469	0.297416	0.659379	0.320712
S-RSp	4.06E-10	2.32E-09	3.52E-28		4.68E-07	3.38E-11	1.76E-05	6.6E-08	0.006155	0.000448	0.324282	0.31531	0.51579	0.012213	0.0471	0.037282	0.017038	0.057582	0.576435	0.170824
R-RSb	0.01135	0.270752	5.4E-10	4.68E-07		2.37E-21	0.029072	0.004488	0.001436	0.000295	0.706988	3.31E-21	3.43E-09	0.175594	0.716289	0.467085	0.55199	0.333598	0.051724	0.380855
R-RSp	0.001382	0.016448	1.77E-09	3.38E-11	2.37E-21		0.058403	0.00128	0.030294	0.001879	0.242856	3.67E-09	2.32E-14	0.770488	0.966667	0.784648	0.748466	0.821981	0.26363	0.928649
Rpulm	2.95E-09	3.61E-07	4.23E-05	1.76E-05	0.029072	0.058403		1.51E-07	0.239918	0.19379	3.34E-10	0.411234	0.121106	2.64E-06	1.16E-06	2.42E-09	2.22E-06	0.007543	0.568369	0.008038
Rao	2.79E-07	0.000965	2.2E-06	6.6E-08	0.004488	0.00128	1.51E-07		0.420436	0.906726	3.49E-09	0.60699	0.924968	0.021566	0.103023	0.021071	0.002819	0.027832	0.538002	0.431966
Intra-LVb	4.58E-07	4.35E-05	8.26E-05	0.006155	0.001436	0.030294	0.239918	0.420436		9.26E-16	0.666402	7.95E-10	2.91E-06	0.190114	0.54683	0.556835	0.359187	0.581044	0.093771	0.215458
Intra-LVp	0.000635	3.12E-12	0.021095	0.000448	0.000295	0.001879	0.19379	0.906726	9.26E-16		0.173456	2.93E-09	1.84E-16	0.294246	0.283484	0.171575	0.089362	0.627212	0.821973	0.282674
Pulm-Ao	0.33808	0.154762	0.683295	0.324282	0.706988	0.242856	3.34E-10	3.49E-09	0.666402	0.173456		0.809891	0.146099	0.012801	0.004699	0.001312	0.068725	0.519135	0.145273	0.04609
Inter-Vb	0.000223	0.000425	0.22084	0.31531	3.31E-21	3.67E-09	0.411234	0.60699	7.95E-10	2.93E-09	0.809891		8.28E-21	0.02177	0.201324	0.365979	0.040051	0.13606	0.043236	0.148694

Inter-Vp	0.001085	1.79E-09	0.601866	0.51579	3.43E-09	2.32E-14	0.121106	0.924968	2.91E-06	1.84E-16	0.146099	8.28E-21		0.05154	0.264497	0.105125	0.036368	0.272328	0.531579	0.079443
HR min	0.117572	0.019278	0.001629	0.04345	0.100498	0.013028	0.041341	0.606467	0.348131	0.695067	0.255199	0.505241	0.884269	0.000818	0.00228	0.003585	0.702777	0.175494	0.823818	0.000142
HR max	0.010413	0.130419	0.92753	0.886806	0.988245	0.352099	1.05E-05	0.427491	0.0241	0.096831	0.000444	0.235238	0.110463	0.009573	0.015592	0.002776	0.08598	0.349547	0.180846	0.146645
HR med	0.849873	0.809169	0.009399	0.340738	0.042333	0.008028	0.454716	0.433237	0.330462	0.728751	0.04055	0.25886	0.071022	0.280994	0.677996	0.886348	0.568637	0.03731	0.797894	0.032805
QRS axis	0.776545	0.268214	0.54358	0.973092	0.781656	0.425144	0.243526	0.867081	0.626085	0.644199	0.420029	0.827741	0.187859	0.444495	0.575583	0.246687	0.045686	0.058345	0.957243	0.013648
P (mV)	0.140027	0.11209	0.478162	0.75574	0.253431	0.078556	1.69E-06	0.400982	0.099472	0.047736	1.6E-05	0.124648	0.08977	0.009307	0.047766	0.003068	0.009597	0.123971	0.032234	0.138866
P (ms)	0.133557	0.031152	0.472951	0.139448	0.560417	0.763634	0.040622	0.431172	0.232933	0.107586	0.191091	0.115815	0.216178	0.695211	0.410825	0.070456	0.000724	1.22E-07	7.84E-05	0.069095
P-R (ms)	0.000873	0.003463	6.96E-05	8.78E-05	0.405616	0.031315	0.024491	0.001545	0.800334	0.947594	0.244389	0.085196	0.600878	0.123995	0.327792	0.043918	0.070604	0.023063	0.000206	0.57329
QRS (mV)	0.008326	0.004506	0.080462	0.031305	0.110625	0.33726	7.41E-06	0.137533	0.414953	0.184872	0.002652	0.005388	0.020382	0.004263	4.24E-06	7.54E-06	0.00012	0.010397	0.069531	0.146712
QRS (ms)	0.206013	0.074468	0.830362	0.167638	0.055479	0.416905	0.897559	0.543931	0.028916	0.152991	0.879226	0.029922	0.107828	0.073709	0.133076	0.059022	0.004069	0.000216	1.63E-05	0.866782
S-T	0.893244	0.102075	0.764651	0.43012	0.426692	0.760462	0.108783	0.044371	0.184828	0.007073	0.726 16	0.999819	0.412029	0.30067	0.635188	0.245293	0.832367	0.405056	0.333571	0.958693
QT (ms)	0.208119	0.01314	0.004913	0.006974	0.584898	0.008327	0.523484	0.029494	0.883925	0.486084	0.180892	0.627752	0.704034	0.183144	0.162986	0.219089	0.155933	0.408394	0.051793	0.266473
T (mV)	0.154396	0.064905	0.056356	0.030251	0.932645	0.154177	0.002096	0.071972	0.25533	0.737753	0.126471	0.694861	0.043074	0.012801	0.001919	0.014173	0.003653	0.099403	0.847 21	0.101362
V1	0.000303	0.007905	0.063883	0.012213	0.175594	0.770488	2.64E-06	0.021566	0.190114	0.294246	0.012801	0.021 77	0.05154		7.95E-09	2.53E-06	0.009672	0.808244	0.794 88	1.2E-31
V2	0.017839	0.014362	0.099829	0.0471	0.716289	0.966667	1.16E-06	0.103023	0.546 83	0.283484	0.004699	0.201324	0.264497	7.95E-09		1.88E-29	1.85E-12	0.002153	0.244915	0.000275
V3	0.001029	0.007227	0.00383	0.037282	0.467085	0.784648	2.42E-09	0.021071	0.556835	0.171575	0.001312	0.365979	0.105125	2.53E-06	1.88E-29		2.01E-23	8.79E-07	0.032814	0.080695
V4	0.0131	0.001741	0.028469	0.017038	0.55199	0.748466	2.22E-06	0.002819	0.359187	0.089362	0.068725	0.040051	0.036368	0.009672	1.85E-12	2.01E-23		1.06E-15	1.45E-05	0.266136
V5	0.10804	0.143659	0.297416	0.057582	0.333598	0.821981	0.007543	0.027832	0.581044	0.627212	0.519135	0.136 06	0.272328	0.808244	0.002153	8.79E-07	1.06E-15		1.31E-13	4.68E-08
V6	0.47671	0.771285	0.659379	0.576435	0.051724	0.263 63	0.568369	0.538002	0.093771	0.821973	0.145273	0.043236	0.531579	0.794 88	0.244915	0.032814	1.45E-05	1.31E-13		0.002712

IDI	0.022914	0.029369	0.320712	0.170824	0.380855	0.928649	0.008038	0.431966	0.215458	0.282674	0.04609	0.148694	0.079443	1.2E-31	0.000275	0.080695	0.266136	4.68E-08	0.002712

Inter-Vb: Mechanical interventricular conduction delay using the beginning of the S' wave; Inter-Vp: Mechanical interventricular conduction delay using the peak of the S' wave; Intra-LVb: Mechanical intra-left ventricle conduction delay using the beginning of the S' wave; Intra-LVb: Mechanical intra-left ventricle conduction delay using the beginning of the S' wave; L-RSb: Electromechanical delay measured in lateral mitral annulus; L-RSp: Electrosystolic delay measured in lateral mitral annulus; Pulm-Ao : Mechanical interventricular dyssynchrony; Rao: Time intervals from the start of the QRS complex to the beginning of the aortic flow; RPulm: Time intervals from the start of the QRS complex to the beginning of the pulmonic flow; R-RSb: Electromechanical delay measured in lateral tricuspid annulus; R-RSp: Electrosystolic delay measured in lateral tricuspid annulus; S-RSb: Electromechanical delay measured septal mitral annulus; S-RSp: Electrosystolic delay measured septal mitral annulus Inter-Vb; E: Peak velocity of early diastolic transmitral flow; E:A: Ratio of early-to-late transmitral flow peak velocities; E:IVRT: ratio of early transmitral flow to isovolumetric relaxation time; E:E': Ratio of early transmitral flow peak velocity to the early mitral annulus tissue peak velocity; FS: Fractional shortening; LA:Ao: Ratio of the left atrial dimensions to the aortic annulus dimension; LVIDdN: left ventricular end diastolic diameter normalized for body weight; LVIDsN: left ventricular end systolic diameter normalized for body weight.

Supplementary material table B. Rho-values obtained by Spearman's test to investigate correlations between markers ECG and echocardiographic of ventricle conduction times, as well as to check correlation with epidemiological, electrocardiographic and echocardiographic variables.

	L-RSb	L-RSp	S-RSb	S-RSp	R-RSb	R-RSp	Rpulm	Rao	V1	V2	V3	V4	V5	V6	IDI
Age (years	0.412786	0.437304	0.243955	0.16438 7	0.024913	0.062347	0.599319	0.223667	0.200467	0.450097	0.546733	0.416455	0.25265	0.07127	-0.07091
Weight	0.088862	0.103871	0.18796	0.23861	0.127202	0.199869	-0.04972	0.126689	-0.07635	-0.10957	-0.06875	0.117209	0.22500 3	0.36933 9	0.173855
LA	0.405095	0.50685	0.279417	0.40673 3	-0.04319	0.088752	0.425484	0.178371	0.146175	0.23317	0.330225	0.442424	0.43105 7	0.47659 8	0.042151
Ao	0.081309	0.081155	0.178942	0.17071 5	0.062417	0.07945 8	-0.11341	-0.0032	-0.23547	-0.21053	-0.16601	-0.04937	0.08579 4	0.20802 6	0.209469
LA/Ao	0.279791	0.367762	0.056527	0.14432 3	-0.10902	-0.01367	0.469046	0.080287	0.31992	0.426465	0.470497	0.404984	0.27677 6	0.19530 1	-0.14446
LVIDd	0.344088	0.462501	0.272818	0.44107 6	0.032684	0.180766	0.370016	0.219186	0.148035	0.190336	0.238526	0.432408	0.36663 5	0.45362	0.018122
LVIDs	0.172946	0.236111	0.266812	0.43845 1	0.105832	0.201231	0.114798	0.232033	0.029362	-0.04392	-0.02639	0.188215	0.23454 4	0.35249 4	0.074111
LVIDdN	0.309293	0.451679	0.16638	0.31853 7	-0.04673	0.116926	0.407665	0.136791	0.192546	0.295772	0.32012	0.425812	0.27490 5	0.29635 3	-0.06121
LVIDsN	0.182653	0.264954	0.243867	0.41786 4	0.083976	0.190596	0.161101	0.222905	0.089899	0.013912	0.024655	0.190382	0.16426 1	0.21693 3	-0.0147
FS	0.062811	0.166497	-0.19329	-0.22545	-0.26298	-0.2037	0.263708	-0.17191	0.173048	0.386257	0.428448	0.294988	0.20545 9	0.08014 6	-0.07489
E	0.213098	0.24446	-0.03901	0.16922 3	-0.08099	0.011883	0.290251	0.009448	0.139152	0.188063	0.245159	0.312611	0.31136 6	0.33806	0.011348
A	0.279314	0.306064	0.095608	0.04090 3	-0.10984	-0.10447	0.441212	0.047984	0.188839	0.285202	0.378148	0.300519	0.10138 7	-0.03829	-0.10824
E/A	-0.07171	-0.0696	-0.12582	0.09688 1	0.024254	0.085209	-0.18353	-0.03189	-0.09305	-0.13564	-0.20223	-0.02936	0.15069 5	0.35447 1	0.129746
IVRT	0.288218	0.199205	0.369576	0.27020 6	0.205815	0.222367	0.231142	0.325285	0.152793	0.056517	0.144978	0.114022	0.09081 9	-0.07819	-0.07179
E/IVRT	0.033935	0.107338	-0.20235	0.00332 4	-0.16826	-0.12004	0.095865	-0.11219	0.026983	0.087957	0.088905	0.150786	0.15408 2	0.25560 1	0.038567
E/E'lat	0.113861	0.117681	-0.06076	0.05630 3	-0.09392	-0.00107	0.171402	0.07862	-0.03368	-0.03155	0.072745	0.102493	0.23948 6	0.32190 7	0.13832
E/E'sep	-0.02669	-0.00371	-0.05827	-0.06759	-0.02136	-0.01894	-0.04586	-0.10244	-0.22223	-0.40557	-0.2454	-0.08832	0.16536 7	0.21731 9	0.272916

E'	0.157171	0.193198	0.048812	0.141671	-0.03445	0.039199	0.21005	0.062789	0.349678	0.274009	0.278697	0.31926	0.160066	0.075103	-0.21972
A'	0.275837	0.365855	0.164674	0.119632	-0.14371	-0.09945	0.42955	-0.00429	0.496396	0.479794	0.463111	0.27851	0.006961	-0.20194	-0.43831
E'/A'	-0.13589	-0.23251	-0.10434	-0.00617	0.16484	0.127252	-0.29589	0.018474	-0.33766	-0.29194	-0.26403	-0.07062	0.09555	0.264589	0.361954
S'	0.123371	0.266356	0.128724	0.168212	-0.09174	-0.10503	0.46496	-0.00985	0.415216	0.471145	0.489078	0.52282	0.23356	0.063777	-0.18597
L-RSb	1	0.71917	0.580603	0.543738	0.241675	0.297351	0.51072	0.450186	0.342677	0.225529	0.310199	0.236978	0.155507	0.070544	-0.22189
L-RSp	0.71917	1	0.434265	0.511759	0.105922	0.220451	0.436465	0.291698	0.248691	0.226785	0.249245	0.288895	0.137821	0.028031	-0.20687
S-RSb	0.580603	0.434265	1	0.805961	0.546683	0.526566	0.369031	0.421589	0.181502	0.158457	0.276054	0.210884	0.101666	-0.04352	-0.09881
S-RSp	0.543738	0.511759	0.805961	1	0.454912	0.558564	0.375149	0.462027	0.23608	0.184751	0.194475	0.222126	0.178382	0.053343	-0.13152
R-RSb	0.241675	0.105922	0.546683	0.454912	1	0.746361	0.207245	0.267802	-0.13722	-0.03624	0.072808	-0.05928	-0.0967	-0.19611	0.089492
R-RSp	0.297351	0.220451	0.526566	0.558564	0.746361	1	0.17328	0.290652	0.028397	-0.00399	0.026233	-0.03064	-0.0216	-0.10851	0.008759
Rpulm	0.510724	0.436465	0.369031	0.375149	0.207245	0.17328	1	0.43795	0.416972	0.423666	0.509408	0.414969	0.242788	-0.05351	-0.24498
Rao	0.450186	0.291698	0.421589	0.462027	0.267802	0.290652	0.43795	1	0.212295	0.148934	0.210413	0.270389	0.201693	0.058012	-0.07399
Intra-LVb	-0.45341	-0.37463	0.361742	0.25736	0.302974	0.206667	-0.11246	-0.07723	-0.13211	-0.06005	-0.05885	-0.09173	-0.05556	-0.16936	0.126246
Intra-LVp	-0.31523	-0.58203	0.217744	0.315491	0.340229	0.285697	-0.12047	-0.0109	-0.10233	-0.10317	-0.1319	-0.1635	-0.04726	-0.02211	0.105816
Pulm-Ao	0.08896	0.128552	-0.03828	-0.08961	-0.03624	-0.10789	0.512521	-0.48596	0.230497	0.25642	0.291238	0.167447	0.059932	-0.13727	-0.18722
Inter-Vb	-0.34654	-0.33176	0.118773	0.097528	0.753466	0.527886	-0.08025	-0.05029	-0.23397	-0.12953	-0.09231	-0.20675	-0.15165	-0.20787	0.149312
Inter-Vp	-0.30346	-0.51859	0.050287	0.060941	0.526639	0.629261	-0.14474	-0.00884	-0.19054	-0.10831	-0.15753	-0.20165	-0.10707	-0.06204	0.172779
HR min	-0.15995	-0.23487	-0.31577	-0.20239	-0.17137	-0.25131	-0.2024	-0.05161	-0.32782	-0.29602	-0.2845	-0.03786	0.134523	0.022661	0.371369
HR max	0.259013	0.153054	0.009356	0.014415	0.001549	-0.0955	0.421032	0.079422	0.256662	0.236619	0.291882	0.169194	0.09311	-0.13559	-0.14621

HR med	-0.02035	-0.02511	-0.27089	-0.09726	-0.22207	-0.27333	0.07484	-0.07884	-0.10942	-0.04119	0.014186	0.056818	0.206501	0.025667	0.215834
QRS axis	-0.02712	0.102748	0.058263	-0.00314	-0.02737	-0.07542	-0.10508	-0.01518	0.069571	-0.05014	-0.10396	-0.17837	-0.1698	-0.00493	-0.22369
P (mV)	0.140323	0.147036	-0.06801	-0.02894	-0.11245	-0.16544	0.413037	0.076084	0.234566	0.176714	0.262798	0.230841	0.138881	-0.19565	-0.1359
P (ms)	0.141992	0.197692	0.068504	0.13628	-0.05718	0.028346	0.182677	0.071033	0.03568	0.073609	0.161705	0.297257	0.451911	0.351154	0.16583
P-R (ms)	0.308862	0.265949	0.366793	0.3517	0.081608	0.200916	0.200347	0.280295	0.139442	0.087533	0.179826	0.161621	0.203165	0.331244	-0.0517
QRS (mV)	0.2471	0.25866	0.165886	0.197517	-0.15586	-0.09029	0.387403	0.133572	0.256003	0.395293	0.38712	0.335905	0.228438	0.165574	-0.13272
QRS (ms)	0.119867	0.164136	0.020471	0.127318	-0.18659	-0.07643	0.011585	0.054791	0.161844	0.134011	0.168673	0.25424	0.32512	0.380946	0.015409
S-T	0.012766	-0.1506	0.028604	0.073	-0.07801	-0.02874	0.143558	0.180166	0.094076	0.042501	0.104263	0.019045	0.075122	0.088651	-0.00476
QT (ms)	0.119317	0.22676	0.264005	0.246113	0.053654	0.244958	0.057361	0.194789	0.120818	0.124544	0.110249	0.127158	0.074591	0.177242	-0.10181
T (mV)	-0.13486	-0.16978	-0.18085	-0.19874	0.008307	0.133739	-0.27159	-0.1615	-0.22388	0.27276	0.21805	0.25714	-0.14805	-0.0177	0.149649
V1	0.342677	0.248691	0.181502	0.23608	-0.13722	0.028397	0.416972	0.212295	1	0.493048	0.412834	0.23436	0.022292	0.024292	-0.82776
V2	0.225529	0.226785	0.158457	0.184751	-0.03624	-0.00399	0.423666	0.148934	0.493048	1	0.801374	0.577163	0.273052	0.106962	-0.32633
V3	0.310199	0.249245	0.276054	0.194475	0.072808	0.02623	0.509408	0.210413	0.412834	0.801374	1	0.745557	0.424764	0.195005	-0.16009
V4	0.236978	0.288895	0.210884	0.222126	-0.05928	-0.03064	0.414969	0.270389	0.23436	0.577163	0.745557	1	0.639069	0.383031	0.101886
V5	0.155507	0.137821	0.101666	0.178382	-0.0967	-0.0216	0.242788	0.201693	0.022292	0.273052	0.424764	0.639069	1	0.608576	0.471844
V6	0.070544	0.028031	-0.04352	0.053343	-0.19611	-0.10851	-0.05351	0.058012	0.024292	0.106962	0.195005	0.383031	0.608576	1	0.274811
IDI	-0.22189	-0.20687	-0.09881	-0.13152	0.089492	0.008759	-0.24498	-0.07399	-0.82776	-0.32633	-0.16009	0.101886	0.471844	0.274811	1

Inter-Vb: Mechanical interventricular conduction delay using the beginning of the S' wave; Inter-Vp: Mechanical interventricular conduction delay using the peak of the S' wave; Intra-LVb: Mechanical intra-left ventricle conduction delay using the beginning of the S' wave; Intra-LVb: Mechanical intra-left ventricle conduction delay using the beginning of the S' wave; L-RSb: Electromechanical

delay measured in lateral mitral annulus; L-RSp: Electrosystolic delay measured in lateral mitral annulus; Pulm-Ao : Mechanical interventricular dyssynchrony; Rao: Time intervals from the start of the QRS complex to the beginning of the aortic flow; RPulm: Time intervals from the start of the QRS complex to the beginning of the pulmonic flow; R-RSb: Electromechanical delay measured in lateral tricuspid annulus; R-RSp: Electrosystolic delay measured in lateral tricuspid annulus; S-RSb: Electromechanical delay measured septal mitral annulus; S-RSp: Electrosystolic delay measured septal mitral annulus Inter-Vb; E: Peak velocity of early diastolic transmitral flow; E:A: Ratio of early-to-late transmitral flow peak velocities; E:IVRT: ratio of early transmitral flow to isovolumetric relaxation time; E:E': Ratio of early transmitral flow peak velocity to the early mitral annulus tissue peak velocity; FS: Fractional shortening; LA:Ao: Ratio of the left atrial dimensions to the aortic annulus dimension; LVIDdN: left ventricular end diastolic diameter normalized for body weight; LVIDsN: left ventricular end systolic diameter normalized for body weight.

FINAL CONSIDERATIONS

Summary of Key Findings

The two papers address complementary aspects of cardiac activation heterogeneity in dogs with Myxomatous Mitral Valve Disease (MMVD). The first paper focused on atrial activation markers, while the second investigated ventricular activation markers. Both studies demonstrated that indices of electrical and mechanical activation can provide valuable insights into the progression of MMVD and its clinical implications.

In the first paper, atrial activation indices, such as P DII, S-PAp, and Pmax, proved useful in identifying cardiac changes and heart failure (HF). Although some indices showed high areas under the curve (AUC), the variation in clinical relevance of others highlights the need for a more detailed analysis of markers in different clinical contexts. In the second paper, ventricular activation times revealed an increase with disease progression and associated mechanical heterogeneity. These data were valuable for understanding how changes in ventricular activation correlate with disease stages and HF.

Additional Discussion and Critical Observations

While the findings of the papers are promising, it is important to consider some limitations and areas for future research. The methodology used, including electrocardiography and echocardiography, proved effective for assessing activation indices, but data interpretation may be influenced by variables such as variability between dogs and the complexity of MMVD. Integrating other diagnostic techniques, such as cardiac magnetic resonance imaging or long-term monitoring, could provide a more comprehensive view.

Additionally, the clinical application of the indices identified in the papers needs validation across different dog populations and clinical conditions. The accuracy and sensitivity of the markers should be tested in further studies to confirm their utility and effectiveness in veterinary clinical practice.

Clinical Implications and Future Directions

The findings of this thesis have significant implications for the management of MMVD in dogs. The identification of non-invasive cardiac activation markers may enhance the evaluation of disease progression and assist in monitoring cardiac remodeling. The potential to use these markers to predict arrhythmias and other

complications offers a valuable tool for veterinary clinicians.

Future studies are recommended to focus on validating the identified indices, exploring their applicability in various stages of the disease and in diverse dog populations. Furthermore, investigating other activation parameters and their integration with clinical data could provide a more comprehensive understanding of MMVD and improve treatment strategies.

Conclusion

In summary, the studies conducted provide a significant contribution to understanding cardiac activation heterogeneity in MMVD in dogs. Integrating electrocardiographic and echocardiographic markers has proven to be a promising approach for monitoring and managing the disease. Continued research in this area is crucial to improving diagnostic accuracy and expanding therapeutic options available for MMVD in dogs.

VITA

Médica veterinária graduada pela Universidade Estadual Paulista (UNESP) “Júlio de Mesquita Filho”, Faculdade de Ciências Agrárias e Veterinárias (FCAV), Campus Jaboticabal (2011-2015).

Foi trainee e diretora de Projetos de medicina veterinária na empresa Consultoria Agropecuária Júnior (CAP Jr.) da UNESP Jaboticabal (2012-2014).

Realizou iniciação científica na área de Patologia Animal, com ênfase em carcinoma de células escamosas em cães e gatos e imunohistoquímica de p53 e HER2 (2014-2015).

Realizou estágio curricular na área de clínica médica de pequenos animais nas instituições UNESP Jaboticabal, Universidade Federal do Paraná (UFPR), UNESP Câmpus Botucatu e Universidade de São Paulo (USP) (2015).

Concluiu o programa de Aprimoramento Profissional em Medicina Veterinária e Saúde Pública na área de Clínica Médica de Pequenos Animais na UNESP Jaboticabal (2016-2018), com o trabalho de conclusão na área de cardiologia veterinária.

Acompanhou o serviço de cardiologia veterinária do Cornell University Hospital for Animals em 2017 através do Visiting Veterinarian.

Mestre em Medicina Veterinária, com foco em cardiologia veterinária, pela UNESP Jaboticabal (2018-2020).

Participou da tradução do livro "Eletrocardiografia De Cães E Gatos - Diagnóstico De Arritmias" dos autores Santilli R, Moise NS, Pariaut R, e Perego M (2019).

Cursou o Doutorado no Programa de Pós-graduação em Ciências Veterinárias da Universidade Federal do Paraná (UFPR), com a linha de pesquisa Medicina Experimental e Comparada (2020-2024).

REFERENCES

ABDELLAH, A. T.; EL-NAGARY, M. Prevalence of P wave dispersion and interatrial block in patients with systolic heart failure and their relationship with functional status, hospitalization and one year mortality. *The Egyptian Heart Journal*, v. 70, n. 3, p. 181–187, set. 2018.

AIKEN, A. V.; GOLDHABER, J. I.; CHUGH, S. S. Delayed intrinsicoid deflection: Electrocardiographic harbinger of heart disease. *Annals of Noninvasive Electrocardiology*, v. 27, n. 3, 17 maio 2022.

AKAMATSU, K. et al. Usefulness of tissue Doppler-derived atrial electromechanical delay for identifying patients with paroxysmal atrial fibrillation. *Cardiovascular Ultrasound*, v. 18, n. 1, p. 22, 22 dez. 2020.

BADER, H. et al. Intra-left ventricular electromechanical asynchrony. *Journal of the American College of Cardiology*, v. 43, n. 2, p. 248–256, jan. 2004.

BARONTOALDO, M. et al. Feasibility and reproducibility of echocardiographic assessment of regional left atrial deformation and synchrony by tissue Doppler ultrasonographic imaging in healthy dogs. *American Journal of Veterinary Research*, v. 75, n. 1, p. 59–66, jan. 2014.

BATTAIA, S. et al. Noninvasive electrocardiographic parameters to assess interventricular dyssynchrony in dogs with bundle branch blocks. *Journal of Veterinary Cardiology*, v. 41, p. 134–144, jun. 2022.

BAX, J. J. et al. Usefulness of myocardial tissue Doppler echocardiography to evaluate left ventricular dyssynchrony before and after biventricular pacing in patients with idiopathic dilated cardiomyopathy. *The American Journal of Cardiology*, v. 91, n. 1, p. 94–97, jan. 2003.

BAX, J. J. et al. Echocardiographic evaluation of cardiac resynchronization therapy: ready for routine clinical use? *Journal of the American College of Cardiology*, v. 44, n. 1, p. 1–9, jul. 2004.

BAYAM, E. et al. Relationship between P wave peak time and coronary artery disease severity in non-ST elevation acute coronary syndrome. *Herz*, v. 46, n. 2, p. 188–194, 2 mar. 2021.

BLEEKER, G. B. et al. Relationship Between QRS Duration and Left Ventricular Dyssynchrony in Patients with End-Stage Heart Failure. *Journal of Cardiovascular Electrophysiology*, v. 15, n. 5, p. 544–549, 30 abr. 2004.

BLEEKER, G. B. et al. Frequency of left ventricular dyssynchrony in patients with heart failure and a narrow QRS complex. *The American Journal of Cardiology*, v. 95, n. 1, p. 140–142, jan. 2005.

BOON, J. A. *Veterinary echocardiography*. Ames: Wiley-Blackwell, 2011.

BRISTOW, M. R. et al. Cardiac-Resynchronization Therapy with or without an Implantable Defibrillator in Advanced Chronic Heart Failure. *New England Journal of Medicine*, v. 350, n. 21, p. 2140–2150, 20 maio 2004.

CEKIRDEKCI, E. I. et al. R-peak time: A novel marker of depolarization in patients with Human Immunodeficiency Virus. *Journal of Electrocardiology*, v. 55, p. 133–137, jul. 2019.

CELIK, Y. et al. Atrial electromechanical delay and p wave dispersion associated with severity of chronic obstructive pulmonary disease. *African Health Sciences*, v. 21, n. 1, p. 140–9, 16 abr. 2021.

CHAN, Y. H. Biostatistics 104: Correlational Analysis. *Singapore medical journal*, v. 44, n. 12, p. 614–619, dez. 2003.

CHENG, A.; HELM, R. H.; ABRAHAM, T. P. Pathophysiological mechanisms

underlying ventricular dyssynchrony. *Europace*, v. 11, n. Supplement 5, p. v10–v14, 1 nov. 2009.
CINIER, G. et al. Predictors for the prolonged R wave peak time among patients with arterial hypertension. *Turk Kardiyoloji Dernegi Arsivi-Archives of the Turkish Society of Cardiology*, v. 49, n. 5, p. 387–394, 2 jul. 2021.
CORNELL, C. C. et al. Allometric Scaling of M-Mode Cardiac Measurements in Normal Adult Dogs. *Journal of veterinary internal medicine*, v. 18, n. 3, p. 311–321, 2004.
CROSARA, S. et al. Holter Monitoring in 36 Dogs with Myxomatous Mitral Valve Disease. *Australian veterinary journal*, v. 88, n. 10, p. 386–392, out. 2010.
DAROUIAN, N. et al. Delayed intrinsicoid deflection of the QRS complex is associated with sudden cardiac arrest. *Heart Rhythm*, v. 13, n. 4, p. 927–932, abr. 2016.
DE VOS, C. B. et al. Atrial tissue Doppler imaging for prediction of new-onset atrial fibrillation. *Heart*, v. 95, n. 10, p. 835–840, 1 maio 2009.
DHINGRA, R. et al. Electrocardiographic QRS Duration and the Risk of Congestive Heart Failure. *Hypertension*, v. 47, n. 5, p. 861–867, maio 2006.
DILAVERIS, P. E.; GIALAFOS, J. E. P-Wave Dispersion: A Novel Predictor of Paroxysmal Atrial Fibrillation. *Annals of Noninvasive Electrocardiology*, v. 6, n. 2, p. 159–165, abr. 2001.
DITTRICH, G. et al. P wave dispersion in obese dogs with and without mitral valve disease. *Ciência Rural*, v. 48, n. 10, 11 out. 2018.
DURU, M. et al. Effect of Weight Loss on P Wave Dispersion in Obese Subjects*. *Obesity*, v. 14, n. 8, p. 1378–1382, ago. 2006.
ERBAY, A. R. et al. Effects of long-term beta-blocker therapy on P-wave duration and dispersion in patients with rheumatic mitral stenosis. *International Journal of Cardiology*, v. 102, n. 1, p. 33–37, jun. 2005.
ESTES, E. H. Commentary on Electrocardiographic Time to Intrinsicoid Deflection and Heart Failure: the Multi-Ethnic Study of Atherosclerosis. *Clinical Cardiology*, v. 40, n. 1, p. 53–53, jan. 2017.
FALCHI, A. G. et al. Weight loss and P wave dispersion: a preliminary study. *Obesity Research & Clinical Practice*, v. 8, n. 6, p. e614–e617, nov. 2014.
GLIKSON, M. et al. *2021 ESC Guidelines on cardiac pacing and cardiac resynchronization therapyEuropean Heart Journal*Oxford University Press, , 14 set. 2021. .
GORCSAN, J.; MAREK, J. J.; ONISHI, T. *The Contemporary Role of Echocardiography in Improving Patient Response to Cardiac Resynchronization TherapyCurrent Cardiovascular Imaging Reports*Current Medicine Group LLC 1, , 1 dez. 2012. .
GORCSAN, J.; TAYAL, B. *Newer Echocardiographic Techniques in Cardiac Resynchronization TherapyCardiac Electrophysiology Clinics*W.B. Saunders, , 2015. .
GRIFFITHS, L. G.; FRANSIOLI, J. R.; CHIGERWE, M. Echocardiographic assessment of interventricular and intraventricular mechanical synchrony in normal dogs. *Journal of Veterinary Cardiology*, v. 13, n. 2, p. 115–126, jun. 2011.
GUGLIELMINI, C. et al. Prevalence and risk factors for atrial fibrillation in dogs with myxomatous mitral valve disease. *Journal of Veterinary Internal Medicine*, v. 34, n. 6, p. 2223–2231, 8 nov. 2020.
GUNTEKIN, U. et al. Long-term Follow-up of P-wave Duration and Dispersion in Patients with Mitral Stenosis. *Pacing and Clinical Electrophysiology*, v. 31, n. 12, p.

1620–1624, 11 dez. 2008.
HAGHJOO, M. et al. Prevalence of Mechanical Dyssynchrony in Heart Failure Patients with Different QRS Durations. *Pacing and Clinical Electrophysiology*, v. 30, n. 5, p. 616–622, maio 2007.
HANSSON, K. et al. LEFT ATRIAL TO AORTIC ROOT INDICES USING TWO-DIMENSIONAL AND M-MODE ECHOCARDIOGRAPHY IN CAVALIER KING CHARLES SPANIELS WITH AND WITHOUT LEFT ATRIAL ENLARGEMENT. *Veterinary Radiology & Ultrasound*, v. 43, n. 6, p. 568–575, 19 nov. 2002.
IRDEM, A. et al. Evaluation of P-Wave Dispersion, Diastolic Function, and Atrial Electromechanical Conduction in Pediatric Patients with Subclinical Hypothyroidism. *Echocardiography*, v. 33, n. 9, p. 1397–1401, set. 2016.
JAGANNATHA, G. N. P. et al. P-wave peak time and P-wave dispersion in surface electrocardiography as initial predictors of new-onset atrial fibrillation in early-onset hypertension. *Hypertension Research*, v. 47, n. 1, p. 137–148, 28 jan. 2024.
JANUS, I. et al. A comparison of the histopathologic pattern of the left atrium in canine dilated cardiomyopathy and chronic mitral valve disease. *BMC Veterinary Research*, v. 12, n. 1, p. 3, 5 dez. 2016.
KEENE, B. W. et al. ACVIM consensus guidelines for the diagnosis and treatment of myxomatous mitral valve disease in dogs. *Journal of Veterinary Internal Medicine*, v. 33, n. 3, p. 1127–1140, 2019.
KIRK, J. A.; KASS, D. A. Electromechanical Dyssynchrony and Resynchronization of the Failing Heart. *Circulation Research*, v. 113, n. 6, p. 765–776, 30 ago. 2013.
KOO, T. K.; LI, M. Y. A Guideline of Selecting and Reporting Intraclass Correlation Coefficients for Reliability Research. *Journal of Chiropractic Medicine*, v. 15, n. 2, p. 155–163, 2016. Disponível em: <http://dx.doi.org/10.1016/j.jcm.2016.02.012>.
KOROVESIS, T. G.; KOUTROLOU-SOTIROPOULOU, P.; KATRITSIS, D. G. Arrhythmogenic Mitral Valve Prolapse. *Arrhythmia & Electrophysiology Review*, v. 11, 28 jul. 2022.
KOSAR, F. et al. P-Wave Duration and Dispersion in Obese Subjects. *Annals of Noninvasive Electrocardiology*, v. 13, n. 1, p. 3–7, 23 jan. 2008.
LAFITTE, S. et al. Improvement of left ventricular wall synchronization with multisite ventricular pacing in heart failure: a prospective study using Doppler tissue imaging. *European Journal of Heart Failure*, v. 6, n. 2, p. 203–212, mar. 2004.
LANE, R. E. Selection and optimisation of biventricular pacing: the role of echocardiography. *Heart*, v. 90, n. suppl_6, p. vi10–vi16, 1 dez. 2004.
LEE, J. et al. Pathologic Manifestations on Surgical Biopsy and Their Correlation with Clinical Indices in Dogs with Degenerative Mitral Valve Disease. *Journal of Veterinary Internal Medicine*, v. 29, n. 5, p. 1313–1321, 27 set. 2015.
LL, T.; SG, T.; KK, P. ECG P wave abnormalities. *Singapore Medical Journal*, v. 54, n. 1, p. 4–5, 15 jan. 2013.
MANO, H. et al. Changes over time in echocardiographic variables and atrial electromechanical intervals after ablation for atrial fibrillation. *Journal of Arrhythmia*, v. 30, n. 6, p. 466–472, 18 dez. 2014.
MATEOS PAÑERO, M. et al. R-peak time in clinically healthy dogs with different thoracic conformations. *Veterinary Journal*, v. 268, 1 fev. 2021.
MÜLLER, P. et al. Echocardiography-derived total atrial conduction time (PA-TDI duration): risk stratification and guidance in atrial fibrillation management. *Clinical Research in Cardiology*, v. 110, n. 11, p. 1734–1742, 28 nov. 2021.
NDREPEPA, G. et al. Relationship between surface electrocardiogram characteristics and endocardial activation sequence in patients with typical atrial

flutter. *Zeitschrift für Kardiologie*, v. 89, n. 6, p. 527–537, jun. 2000.
NEVES, J. et al. Usefulness of pulsed-wave tissue Doppler imaging at the mitral annulus for prediction of new-onset atrial fibrillation in dogs. *Journal of Veterinary Cardiology*, v. 20, n. 6, p. 425–437, dez. 2018.
NOSZCZYK-NOWAK, A. et al. P-WAVE DISPERSION IN HEALTHY DOGS. A PRELIMINARY STUDY. *Bulletin of the Veterinary Institute in Pulawy*, v. 52, p. 683–688, 2008.
NOSZCZYK-NOWAK, A. et al. Comparison of P-wave dispersion in healthy dogs, dogs with chronic valvular disease and dogs with disturbances of supraventricular conduction. *Acta Veterinaria Scandinavica*, v. 53, n. 1, p. 18, 11 dez. 2011.
NOSZCZYK-NOWAK, A. P-Wave Dispersion in Prediction of Maintenance of Sinus Rhythm After an Electrical Cardioversion of Atrial Fibrillation in Dogs. *Bulletin of the Veterinary Institute in Pulawy*, v. 56, n. 1, p. 99–102, 1 mar. 2012.
OGAWA, M. et al. Evaluation of the association between electrocardiogram parameters and left cardiac remodeling in dogs with myxomatous mitral valve disease. *Veterinary World*, p. 2072–2083, 27 ago. 2022.
OKUTUCU, S.; AYTEMIR, K.; OTO, A. P-wave dispersion: What we know till now? *JRSM Cardiovascular Disease*, v. 5, p. 204800401663944, 1 jan. 2016.
O'NEAL, W. T. et al. Electrocardiographic Time to Intrinsicoid Deflection and Heart Failure: The Multi-Ethnic Study of Atherosclerosis. *Clinical Cardiology*, v. 39, n. 9, p. 531–536, 23 set. 2016.
O'NEAL, W. T. et al. Electrocardiographic Predictors of Heart Failure With Reduced Versus Preserved Ejection Fraction: The Multi-Ethnic Study of Atherosclerosis. *Journal of the American Heart Association*, v. 6, n. 6, 6 nov. 2017.
ÖZER, N. et al. P Wave Dispersion in Hypertensive Patients with Paroxysmal Atrial Fibrillation. *Pacing and Clinical Electrophysiology*, v. 23, n. 11P2, p. 1859–1862, nov. 2000.
ÖZER, N. et al. Doppler tissue evaluation of intra-atrial and interatrial electromechanical delay and comparison with P-wave dispersion in patients with mitral stenosis. *Journal of the American Society of Echocardiography*, v. 18, n. 9, p. 945–948, set. 2005.
PEDRO, B. M. et al. Association of QRS duration and survival in dogs with dilated cardiomyopathy: A retrospective study of 266 clinical cases. *Journal of Veterinary Cardiology*, v. 13, n. 4, p. 243–249, dez. 2011.
PÉREZ-RIERA, A. R. et al. R-Peak Time: An Electrocardiographic Parameter with Multiple Clinical Applications. *Annals of Noninvasive Electrocardiology*, v. 21, n. 1, p. 10–19, jan. 2016a.
PÉREZ-RIERA, A. R. et al. P-wave dispersion: an update. *Indian Pacing and Electrophysiology Journal*, v. 16, n. 4, p. 126–133, jul. 2016b.
PERRY, R. et al. Tissue Doppler Derived Mechanical Dyssynchrony Does Not Change after Cardiac Resynchronization Therapy. *Echocardiography*, v. 28, n. 9, p. 961–967, out. 2011.
PESSOA, R. B. *Mensuração do Tempo de Condução Atrial Total por meio da ecocardiografia tecidual em cães normais e em cães com Valvopatia Mitral Mixomatosa*. 2019. Universidade de São Paulo, São Paulo, 2019.
PICCIRILLO, G. et al. Electrocardiographic and other Noninvasive Hemodynamic Markers in Decompensated CHF Patients. *Journal of Cardiovascular Development and Disease*, v. 10, n. 3, p. 125, 15 mar. 2023.
PONIKOWSKI, P. et al. 2016 ESC Guidelines for the diagnosis and treatment of acute and chronic heart failure. *European Heart Journal*, v. 37, n. 27, p. 2129–2200,

14 jul. 2016.
POZIOS, I. et al. Electro-Mechanical Alterations in Atrial Fibrillation: Structural, Electrical, and Functional Correlates. *Journal of Cardiovascular Development and Disease*, v. 10, n. 4, p. 149, 31 mar. 2023.
RISUM, N. Assessment of mechanical dyssynchrony in cardiac resynchronization therapy. *Dan Med J* , v. 61, n. 12, p. B4981, dez. 2014.
RODRIGUES, A. C. T.; TSUTSUI, J. M.; MATHIAS JR, W. Avaliação de dissincronia cardíaca pelo ecocardiograma: estratégias para um resultado adequado Cardiac dyssynchrony in patients with heart failure: strategies for an adequate echocardiographic assessment. *Revista Brasileira de Ecocardiografia*, v. 19, n. 3, p. 46–51, 2006.
RUDSKI, L. G. et al. Guidelines for the Echocardiographic Assessment of the Right Heart in Adults: A Report from the American Society of Echocardiography. *Journal of the American Society of Echocardiography*, v. 23, n. 7, p. 685–713, jul. 2010.
RUSSO, V. et al. Atrial Septal Aneurysms and Supraventricular Arrhythmias: The Role of Atrial Electromechanical Delay. *Echocardiography*, v. 32, n. 10, p. 1504–1514, 1 out. 2015.
SALEM, A. S. et al. Correlation Between Left Ventricular Electromechanical Delay and Body Mass Index. *European Heart Journal Supplements*, v. 23, n. Supplement_D, 8 out. 2021.
SANTILLI, R. A. et al. *Electrocardiography of the dog and cat: diagnosis of arrhythmias*. Trento: Edra, 2019a.
SANTILLI, R. A. et al. Development and assessment of a novel precordial lead system for accurate detection of right atrial and ventricular depolarization in dogs with various thoracic conformations. *American Journal of Veterinary Research*, v. 80, n. 4, p. 358–368, abr. 2019b.
SEYFELI, E. et al. Effect of obesity on P-wave dispersion and QT dispersion in women. *International Journal of Obesity*, v. 30, n. 6, p. 957–961, 24 jun. 2006.
SIMPSON, K. E. et al. TIMING OF LEFT HEART BASE DESCENT IN DOGS WITH DILATED CARDIOMYOPATHY AND NORMAL DOGS. *Veterinary Radiology & Ultrasound*, v. 49, n. 3, p. 287–294, 2 maio 2008.
SIVRI, F. et al. Prognostic value of R wave peak time in COVID-19 pneumonia. *Journal of Electrocardiology*, v. 80, p. 91–95, set. 2023.
SPACH, M. S. et al. The discontinuous nature of propagation in normal canine cardiac muscle. Evidence for recurrent discontinuities of intracellular resistance that affect the membrane currents. *Circulation Research*, v. 48, n. 1, p. 39–54, jan. 1981.
SPARTALIS, M. et al. Pathophysiology and Current Evidence for Detection of Dyssynchrony. *Cardiology Research*, v. 8, n. 5, p. 179–183, 2017.
SPRAGG, D. D.; KASS, D. A. Pathobiology of Left Ventricular Dyssynchrony and Resynchronization. *Progress in Cardiovascular Diseases*, v. 49, n. 1, p. 26–41, jul. 2006.
SURAWICZ, B. et al. AHA/ACCF/HRS Recommendations for the Standardization and Interpretation of the Electrocardiogram. *Journal of the American College of Cardiology*, v. 53, n. 11, p. 976–981, mar. 2009.
SWEENEY, M. O.; PRINZEN, F. W. A New Paradigm for Physiologic Ventricular Pacing. *Journal of the American College of Cardiology*, v. 47, n. 2, p. 282–288, jan. 2006.
TAPIA-ORIHUELA, R. K. et al. Electrocardiographic markers of cardiac resynchronization therapy response: delayed time to intrinsicoid deflection onset in lateral leads. *Journal of geriatric cardiology : JGC*, v. 19, n. 1, p. 21–30, 28 jan. 2022.

TIDHOLM, A. et al. Tissue Doppler and Strain Imaging in Dogs with Myxomatous Mitral Valve Disease in Different Stages of Congestive Heart Failure. *Journal of Veterinary Internal Medicine*, v. 23, n. 6, p. 1197–1207, nov. 2009.
TRIKHUN, P. et al. Left ventricular systolic function in dogs with pulmonic stenosis. *Veterinary World*, v. 13, n. 11, p. 2436–2442, 14 nov. 2020.
TURHAN, H. et al. Effects of percutaneous mitral balloon valvuloplasty on P-wave dispersion in patients with mitral stenosis. *The American Journal of Cardiology*, v. 89, n. 5, p. 607–609, mar. 2002.
VAN EVERDINGEN, W. M. et al. *Echocardiography and cardiac resynchronisation therapy, friends or foes?Netherlands Heart Journal*Bohn Stafleu van Loghum, , 1 jan. 2016. .
VERECKEI, A. et al. Novel electrocardiographic dyssynchrony criteria improve patient selection for cardiac resynchronization therapy. *EP Europace*, v. 20, n. 1, p. 97–103, 1 jan. 2018.
VERNOOY, K. et al. Relation Between Abnormal Ventricular Impulse Conduction and Heart Failure. *Journal of Interventional Cardiology*, v. 16, n. 6, p. 557–562, dez. 2003.
VIEIRA, M. L. C. et al. Demonstração do mecanismo da terapia de ressincronização ventricular com ecocardiografia tridimensional em tempo real em paciente com insuficiência cardíaca. *Arquivos Brasileiros de Cardiologia*, v. 85, n. 5, nov. 2005.
VILA, B. de C. P.; CAMACHO, A. A.; SOUSA, M. G. T-wave peak-end interval and ratio of T-wave peak-end and QT intervals: novel arrhythmogenic and survival markers for dogs with myxomatous mitral valve disease. *Journal of Veterinary Cardiology*, v. 35, p. 25–41, 2021.
VILLANI, G. Q. et al. P-wave dispersion index: a marker of patients with paroxysmal atrial fibrillation. *International Journal of Cardiology*, v. 55, n. 2, p. 169–175, jul. 1996.
WANG, J. et al. Systolic and Diastolic Dyssynchrony in Patients With Diastolic Heart Failure and the Effect of Medical Therapy. *Journal of the American College of Cardiology*, v. 49, n. 1, p. 88–96, jan. 2007.
YANO, M. et al. Influence of left ventricular regional nonuniformity on afterload-dependent relaxation in intact dogs. *American Journal of Physiology-Heart and Circulatory Physiology*, v. 267, n. 1, p. H148–H154, 1 jul. 1994.
YU, C.-M. High prevalence of left ventricular systolic and diastolic asynchrony in patients with congestive heart failure and normal QRS duration. *Heart*, v. 89, n. 1, p. 54–60, 1 jan. 2003.
ZHU, T. et al. A Comparative Study of Systolic and Diastolic Mechanical Synchrony in Canine, Primate, and Healthy and Failing Human Hearts. *Frontiers in Cardiovascular Medicine*, v. 8, 28 out. 2021.

ANNEX 1 – CERTIFICATE FROM THE COMMITTEE ON ETHICS IN THE USE AND EXPERIMENTATION OF ANIMALS

UNIVERSIDADE FEDERAL DO PARANÁ
SETOR DE CIÊNCIAS AGRÁRIAS
COMISSÃO DE ÉTICA NO USO DE ANIMAIS

CERTIFICADO

Certificamos que o protocolo número 047/2022, referente ao programa de pesquisa **"Avaliação de índices dissociação cardíaca em cães com doença mixomatosa da valva mitral e em cães saudáveis",** sob a responsabilidade de **Marlos Gonçalves Sousa** – que envolve a produção, manutenção e/ou utilização de animais pertencentes ao filo Chordata, subfilo Vertebrata (exceto o homem), para fins de pesquisa científica ou ensino – encontra-se de acordo com os preceitos da Lei nº 11.794, de 8 de Outubro de 2008, do Decreto nº 6.899, de 15 de julho de 2009, e com as normas editadas pelo Conselho Nacional de Controle da Experimentação Animal (CONCEA), e foi aprovado pela COMISSÃO DE ÉTICA NO USO DE ANIMAIS (CEUA) DO SETOR DE CIÊNCIAS AGRÁRIAS DA UNIVERSIDADE FEDERAL DO PARANÁ - BRASIL, com grau 2 de invasividade, em 07/12/2022.

Finalidade	Pesquisa
Vigência da autorização	Dezembro/2022 até Novembro/2024
Espécie/Linhagem	*Canis lupus familiaris* (canino)
Número de animais	200
Peso/Idade	3 a 25kg/Adultos
Sexo	Macho e fêmea
Origem	Hospital Veterinário da UFPR e Centro de Diagnóstico Veterinário Diagvet em Curitiba, Paraná, Brasil

*A autorização para início da aula se torna válida a partir da data de emissão deste certificado.

CERTIFICATE

We certify that the protocol number 047/2022, regarding the research program **"Evaluation of cardiac dissociation indices in dogs with myxomatous mitral valve disease and in healthy dogs"** under **Marlos Gonçalves Sousa** – which includes the production, maintenance and/or utilization of animals from Chordata phylum, Vertebrata subphylum (except Humans), for scientific or teaching purposes – is in accordance with the precepts of Law nº 11.794, of 8 October 2008, of Decree nº 6.899, of 15 July 2009, and with the edited rules from Conselho Nacional de Controle da Experimentação Animal (CONCEA), and it was approved by the ANIMAL USE ETHICS COMMITTEE OF THE AGRICULTURAL SCIENCES CAMPUS OF THE UNIVERSIDADE FEDERAL DO PARANÁ (Federal University of Paraná, Brazil), with degree 2 of invasiveness, on 2022, December 7th.

Purpose	Research
Validity	2022 November until 2024 November
Specie/Line	*Canis lupus familiaris* (canine)
Number of animals	200
Weight/Age	From 6.614lb up to 55.12lb/Adults
Sex	Male and female
Origin	UFPR Veterinary Hospital and Diagvet Veterinary Diagnostic Center in Curitiba, Paraná, Brazil

*The authorization to start the research becomes valid from the date of issue of this certificate.

Curitiba, 07 de dezembro de 2022

gov.br Documento assinado digitalmente
ALEX MAIORKA
Data: 09/12/2022 18:30:55-0300
Verifique em https://verificador.iti.br

Alex Maiorka
Coordenador
Comissão de Ética no Uso de Animais
AG - UFPR